

Role of Cellulose Synthase-Like (Csl) genes in barley root growth and differentiation

Haoyu Lou



A thesis submitted to The University of Adelaide in fulfilment of the
requirements for the degree of Doctor of Philosophy

The University of Adelaide / The University of Nottingham

Faculty of Sciences

School of Agriculture, Food and Wine (UA) / School of Bioscience (UoN)



THE UNIVERSITY
of ADELAIDE

February 2020

Contents

Declaration	iii
Acknowledgments	iv
List of publications and expected publications	vii
Thesis Abstract.....	viii
Chapter 1 – Introduction and Literature Review.....	1
Abstract.....	2
Introduction.....	3
Plant root structure.....	4
Root anatomy and cellular organisation.....	5
Root hair growth.....	9
Plant cell walls and their components.....	10
Cell wall polysaccharides.....	11
Cell wall composition in barley.....	13
Genes involved in barley root tip cell wall synthesis.....	15
<i>CsIF6</i> is the main <i>CsIF</i> gene in barley but roles for family members remain unclear.....	17
Arabidopsis <i>CsID</i> and barley <i>CsIF</i> genes are closely related	19
Use of transgenic approaches to identify plant gene function.....	20
Summary.....	22
Research questions.....	23
Main Aims and Objectives	23
Figures.....	25
Tables	31
Reference.....	32
Chapter 2 - Genetic and compositional analysis of cell wall polysaccharides in barley root tips	40
Statement of Authorship	41
Abstract.....	43
Introduction.....	44
Materials and methods	46
Results	50
Discussion.....	56
Figures.....	66
Tables	73
References	76
Chapter 3 - <i>Cellulose synthase-like F (CsIF)</i> genes control barley root growth and differentiation by mediating cell wall polysaccharide synthesis.....	81
Statement of Authorship	82
Abstract.....	85
Materials and methods	90
Results	96
Figures.....	113
Tables	127
Supplementary materials	129
Reference.....	131
Chapter 4 - <i>HvCsIF3</i> affects root epidermal cell proliferation and root hair elongation	137
Statement of Authorship	138
Abstract.....	140
Introduction.....	141
Materials and methods	144
Results	149
Discussion.....	154
Figures.....	163
Tables	174

Supplementary materials	177
Reference	178
Chapter 5 - Knock-down of <i>HvCsIF3</i> and <i>HvCsIF9</i> gene expressions in barley is predicted to increase plant tolerance to low nutrient stresses over the vegetative stage	182
Statement of Authorship	183
Abstract	185
Introduction	186
Materials and methods	188
Results	192
Discussion	199
Figures	209
Tables	226
Supplementary materials	229
References	235
Chapter 6 - Summary and Future Directions	239
Thesis Summary	240
Future directions	244
Appendix 1 - Exploring the Role of Cell Wall-Related Genes and Polysaccharides during Plant Development.....	250
Appendix 2 – Candidature Milestones.....	271

Declaration

I certify that this work contains no material which has been accepted for the award of any other degree or diploma in my name, in any university or other tertiary institution and, to the best of my knowledge and belief, contains no material previously published or written by another person, except where due reference has been made in the text. In addition, I certify that no part of this work will, in the future, be used in a submission in my name, for any other degree or diploma in any university or other tertiary institution without the prior approval of the University of Adelaide and where applicable, any partner institution responsible for the joint-award of this degree.

I give permission for the digital version of my thesis to be made available on the web, via the University's digital research repository, the Library Search and also through web search engines, unless permission has been granted by the University to restrict access for a period of time.

Haoyu Lou

28/02/2020

Acknowledgments

Firstly, I would like to express my appreciation to my supervisors Prof. Vincent Bulone (UA), A/Prof. Matthew Tucker (UA), Prof. Malcolm Bennett (UN), and Dr. Leah Band (UN). Your endless assistance and support during my candidature has been beyond helpful. Especially during the exchange experience between Adelaide and Nottingham. We kept regular skype meetings for my entire candidature and overcame the difficulties in time zones and travelling. I felt extra support from all of you, not only academically, but also for personal developments. I was very lucky to have you as my supervisors.

I would like to say special thank you to Stav Manafis and Jennifer Dewick, for their guidance and assistance with administration and communication between the two Universities. Also great thanks to Chao Ma who arranged material transfer between the two Universities, and Ian Fisk, the coordinator of the Adelaide-Nottingham program, for his support to students that undertake the joint PhD like me.

I wish to express my sincere thanks to the following researchers in University of Adelaide: Dr. Neil Shirley for his help with qPCR experiments and gene expression analysis; Dr. Jelle Lahnstein and Dr. Long Yu for their assistance with HPLC and linkage analysis; Dr. Julian Schwerdt for his great help on phylogenetic studies; Dr. Xiujuan Yang and Chao Ma for teaching me RNA hybridisation, and special thanks to Xiujuan who helped me with sample embedding and sectioning; Caterina Selva and Dr. Xiujuan Yang for their help with the BiFC experiments; Dayton Bird and Kylie Neumann for taking care of my plants while I was away.

I would also like to express my appreciation to following wonderful people at the University of Nottingham, without them, my visit in Nottingham would have been much tougher: Dr. Kamal Swarup, Dr. Rahul Bhosale and Dr. Nicky Lefty for their patience and guidance in the lab and expertise in construct design and plant transformation; Jingyi Han for taking care of my plants and bacteria cultures when I was unable to go to the lab; Dr. Brian Atkinson for his help with

WinRhizo root scanner; Dr. Daniel von Wangenheim and Jason Banda for their great assistance on microscopy work; Mark Meacham for his help with arranging the glasshouse experiments and taking care of my plants; Dr. Jayalath De Silva for assisting with Licor photosynthesis experiments. Miaoyuan Hua for his kindness help with barley transformation and building reporter lines.

This part is especially dedicated to Dr. Ishan Ajmera, the best computer modelling person that I know. Thanks to Ishan, we planned entire glasshouse and phenotyping experiments together. We also spent many Saturday afternoons together at the library to dig out the parameters for the OpenSimRoot model. He helped to optimize the Australian barley OSR model in this thesis, with the parameters collected by either us or himself. He also ran the final *in silico* experiments with his HPC resources and gave me back the extracted data for me to analyse. He was also very supportive for the thesis writing, giving valuable comments on the last chapter. Without him, I would have never been able to do mathematical modelling, and Chapter 5 would have not been completed without his great help and support.

Special shout out goes to the Tucker Lab and MJB Lab members! Matthew Aubert, Laura Wilkinson, Dayton Bird, Cindy Callens, Caterina Selva, Chao Ma, Weng Leong, Kum (Maple) Ang, Rosanna Petrella, Sara Pinto, Xiujuan Yang, and Ghazwan Karem. Each of you have contributed to my PhD in some way, whether through helping with my project, developing ideas during our brain storming sessions, or hanging out for food and bubble teas, or simply non-sense chatting about everything. And to Azad Kilic, Bipin Pandey, Britta Kuempers, Daniela Dietrich, Elina Chrysanthou, Emily Morris, Jason Banda, Jingyi Han, John Vaughan-hirsch and Umar Mohammed. Thank you for all the great times we've had together, and for creating a warm, supportive, inspiring and motivating work environment.

Here goes another special thanks to my dearest cousin, Xiao Tang. She was there when I first came to Nottingham. We spent so many weekends and holidays together in Nottingham and Coventry. Since I left home for my studies in 2011, I haven't got the chance to spend time with

families until we reunited in the UK. She was also very supportive and helpful. Together we set up the pots for my glasshouse experiment. She also helped with many of the image post-processing with her expertise in the use of Adobe photoshop and illustrator. She is expecting a baby this year, and she named her little one with the nick name Da Mai (means barley). Big big thank you to my dearest cousin, loves to both of you.

Al mio caro Riccardo Fusi, thank you for being such a supportive boyfriend during this special period. You were always on call in the lab, helping with all the little but important details. Especially for your help with the cross sections and glasshouse work, with all the root washing and we both end up getting covered in mud at the end of the day. Despite the lab work, we also spent so much time together exploring and travelling. Thank you for surviving this journey with me.

To my loving family, Chunhua Tang and Fasheng Lou, for your unconditional love and support like always. Thank you for being there for me through all my failures and successes, I hope I can continue to make you proud with whatever comes next! 非常感谢爸爸妈妈一直以来的鼓励支持和理解。拥有你们是我最大的财富。希望我也能一直让你们骄傲和开心。同时也很感谢外公外婆和奶奶，以及所有的家里人。谢谢大家。

To all of you, thank you.

List of publications

1. Tucker MR, **Lou H**, Aubert MK, Wilkinson LG, Little A, Houston K, Pinto SC and Shirley NJ (2018) Exploring the role of cell wall-related genes and polysaccharides during plant development. **Plants** 7(2):42 (May 2018)
2. **Lou H**, Tucker MR, Shirley NJ, Yu L, Band L, Bennett MJ and Bulone V. Genetic and cell wall compositional analysis of barley root tips. (to be published)
3. **Lou H**, Tucker MR, Shirley NJ, Lahnstein J, Yu L, Yang X, Ma C, Schwerdt J, Fusi R, Burton RA, Band L, Bennett MJ and Bulone V. *Cellulose synthase-like F (CslF)* genes affect root growth and differentiation by mediating cell wall polysaccharide biosynthesis in barley and Arabidopsis. (to be published)
4. **Lou H**, Ajmera I, Band L, Tucker MR, Bennett MJ and Bulone V. Knock-down of *HvCslF3* and *HvCslF9* gene expressions in barley is predicted to increase plant tolerance to low nutrient stresses over the vegetative stage. (to be published)
5. Fusi R, Milner SG, Rosignoli S, Bovina R, Vieira C, **Lou H**, Atkinson B, York L, Sturrock C, Stein N, Mascher M, Tuberosa R, Bishopp A, Bennett MJ, Bhosale R and Salvi S. The auxin efflux carrier PIN1a plays a key role in vascular patterning in cereal roots. (to be published)
6. Fusi R, Bhosale R, Rosignoli S, Milner SG, Bovina R, Kirshner G, Pandey B, **Lou H**, Borkar A, Vieira C, Tassinari A, York L, Atkinson B, Sturrock C, Lynch JP, Mooney S, Tucker MR, Mascher M, Moulia B, Tuberosa R, Hochholdinger F, Bennett MJ and Salvi S. Mutations in the TUBBY Protein EGT1 confers enhanced root gravitropic responsiveness. (to be published)

Thesis Abstract

Barley is a commercial important crop with multiple utilisations. It is widely used in the malting and brewing industries, and with rising attention as super food for its high dietary fibre content. Intensive studies have focused on grain development to improve grain quality to benefit agricultural practices. Less attention has been given to root development. Roots are important plant organs that provide mechanical strength to anchor plants to soil substrates. Roots are also responsible for water and nutrients capture and transportation to aerial organs to support plant development. From the root apical meristem, cells undergo rapid division to form different tissues in the meristem zone, followed by longitudinal expansion to enlarge cell size in the elongation zone, and complete final differentiation in the maturation zone to form fully functional root cells. During this process, cell wall biosynthesis and assembly are critical determinants because the rapidly enlarging cells require strength to resist internal pressure, and also flexibility to allow unidirectional cell expansion. Plant cell walls are composed of various polymers, including cellulose, hemicelluloses, and pectins, which confer distinct chemical and mechanical properties. Cell wall polysaccharide heterogeneity has been described in various tissues and species including *Arabidopsis* roots and barley developing grains. However, very limited knowledge on the relationships between the composition of root tip cell walls and the development of barley roots has been reported due to the complexity and heterogeneity of the roots. The work presented in this thesis aimed to identify the roles of two cell wall related genes belonging to the *Cellulose Synthase-Like (Csl)* family during root tip development.

To gain a better understanding of gene regulation and polysaccharide composition in the barley root tip, we first analysed the expression of the *Csl* genes in different root regions and showed predominate expression of *HvCslF3* and *HvCslF9* genes in the meristem and elongation zones. Cell wall polysaccharide composition of barley root tips was determined by immunohistochemistry and glycosidic linkage analysis.

To further understand the functions of the *HvCsIF3* and *HvCsIF9* genes in the barley root tip, we employed RNAi to generate knock-down mutants, and analysed the morphological and dynamic differences between the mutants and the wild-type cultivar Golden Promise. These genes are essential in maintaining seminal root elongation and cortical radial patterning of seedlings. The potential functions of *HvCsIF3* and *HvCsIF9* genes in regulating the synthesis of cell wall polysaccharides, (1,4)- β -linked glucoxytan and (1,3;1,4)- β -glucan, respectively, were revealed. This indicates that cell wall composition affects root development as a smaller root system was observed in the mutant barley seedlings.

Notably, the restrictions on root development were not limited to seedlings. Indeed, we also show the reduction in the root systems and aerial tissue development in the glasshouse grown mutant plants throughout the vegetative growth. The smaller root systems resulted in limitation on water and nutrient uptake. Transportation may be the main reason behind the decreased development of aerial organs. To support this hypothesis, mathematical modelling was used to predict the difference in water and nutrients capture between the genotypes. The simulations also highlighted the variations on plant performance in response to nutrient stresses. Interestingly, the mutant root systems contain certain traits that are beneficial for the plant to tolerate low nutrient availabilities. These findings suggested a new direction in plant breeding to generate plants with more efficient root traits based on cell wall related gene expression and regulation.

A phylogenetic study indicated the close relationship between the *CsIF* and *CsID* gene families. The Arabidopsis genome lacks *CsIF* genes and the plant therefore provides an excellent heterologous expression system to study the functions of *HvCsIF* genes. By introducing the *HvCsIF3* gene into wild-type Arabidopsis (Col-0) plants and root hair mutants deficient in *AtCsID3* and *AtCsID5*, we demonstrated the functional redundancy between the *CsID* and *CsIF* gene families and identified a role for *HvCsIF3* in root hair cell file specification and root hair elongation.

Chapter 1

Introduction and Literature Review



Abstract

From a global perspective, barley is the fourth most important cereal crop. It is utilised in many sectors, including the human food, animal feed and malting and brewing industries. Barley growth and development have been extensively studied from an agronomic perspective, but the genetic basis for root developmental events is not well understood compared to other plants such as *Arabidopsis*, rice and maize. Despite being an essential organ that supplies water and nutrients for plant growth, improving adaptability and productivity under abiotic and biotic stresses, little is known about formation and differentiation of barley root tissues. Investigating barley root development has the potential to contribute new knowledge for plant breeding and agricultural practices. The role of cell walls during root growth is particularly important in this context, since root function is dependent upon cell wall structure and composition. Cell wall synthesis is a complex process involving many hundreds of genes. Previous studies in barley characterised the *Cellulose Synthase-like F (CslF)* family, of which *CslF6* is implicated in 1,3;1,4- β -glucan biosynthesis. The same studies indicated that additional *CslF* family members, including *CslF3* and *CslF9*, exhibit specific expression in root tips, yet it remains unclear what function they might play in these tissues. Therefore, the aims of this project were to investigate and characterise the function of *CslF* family genes in barley root development, to determine the biochemical function of their products and investigate effects of the genes on plant growth under different environment stresses *in silico*. Successful completion of this project will provide a fundamental understanding of cell wall synthesis in barley roots as well as specific knowledge on the role of the *CslF* gene family in this process.

Introduction

Barley is one of the most highly adapted cereal grains with >8000 years of cultivation and production in a wide range of climates and environments. It is the fourth most important cereal crop in the world, with an annual global production of nearly 142.3 million tonnes in 2017/2018 (USDA, 2019). Nearly 6% of which was contributed by Australia as the fourth largest producer of barley, behind the European Union, Former Soviet Union and Canada (USDA, 2019). In Australia, barley is the second most produced cereal crop after wheat. It produces food for humans, for animal feed and as a source of biomass for the malting and brewing industries.

Barley is a self-pollinating, diploid monocot species that contains 7 pairs of chromosomes (1H-7H). Considerable attention has been dedicated to the understanding of barley grain development over the past decades with the aim of improving yield and quality. However, fewer efforts have been made towards understanding the molecular and genetic events that control the development of barley roots, despite this organ's importance for plant growth. Its primary function is to anchor the plant to its soil substrate and support plant growth by absorbing water, dissolving minerals and transporting these nutrients to other tissues (Witcombe et al., 2008; Imani et al., 2011). In some cases, roots act as a storage tissue and play a role in pathogen resistance (Cook, 2006; Fuller et al., 2008; Imani et al., 2011). As shown by studies in other systems such as *Arabidopsis*, much can be learned from this single organ as it is simple, easily accessible and has all developmental stages present at all times (Schiefelbein and Benfey, 1991).

Cell walls of plants are important extracellular structures that contribute to many aspects of plant growth and development in addition to providing strength and support for apical growth. Cell walls comprise a matrix of complex cellulosic and non-cellulosic polysaccharides, phenolic compounds and proteins (Fincher, 2009). In root cells, the synthesis and properties of

cell walls are particularly crucial as the cell wall is involved in the determination of root architecture, water and nutrient uptake and transport, intercellular communication, resistance to pathogens and other stresses (Farrokhi et al., 2006). In barley, similar to other plant species, the biosynthesis and modification of cell wall polysaccharides is determined by the action of diverse enzyme families including glycosyltransferases (GTs), transglycosidases, and glycoside hydrolases (GHs). The enzymes and genes that encode them are grouped based on functional domains and predicted biochemical functions (Lombard et al., 2014). One large group of GTs is represented by the *Cellulose synthase (CesA)* and *Cellulose Synthase Like (Csl)* gene families, which are members of the GT2 family. Specific members are responsible for the synthesis of polysaccharides including cellulose, (1,3;1,4)- β -glucan, mannan and xyloglucan (Cantarel et al., 2009; Doblin et al., 2009). The role of these genes has been examined in many systems, although the majority of data has been derived from Arabidopsis, poplar, barley and rice. In general, the detailed molecular and biochemical function of GT2 members during cell wall biosynthesis remains unclear in the root, particularly in the case of barley.

In this literature review, current knowledge about root structure and development is presented, with a focus on Arabidopsis and barley. This review also addresses evidence that putative GT genes exert cell and zone-specific roles during root growth, and considers the opportunities for combining studies of GT activity, cell wall biosynthesis and plant development to understand the fundamental details of barley root growth.

Plant root structure

During germination, the root is the first organ to emerge from the seed. A root can be divided into three zones based on distinct biological events along its longitudinal axes (Figure 1-1). The root apical meristematic (RAM) zone is located at the tip and protected by a specialised cap tissue. The RAM contains stem cells that repeatedly divide to produce daughter cells. The region above the RAM is termed the elongation zone. Within this region, cells with

determined fate cease division activity and expand longitudinally instead. The maturation zone lies above the elongation zone and is demarked by the cessation of cell expansion and the appearance of root hairs. Cells complete their differentiation within this region to form fully functional mature root cells. Later in the maturation zone, lateral root emergence takes place in the pericycle layer of the root to generate branches and enlarge the root system area.

The root system structure and cellular radial organisation differs between species (Figure 1-2). Barley has a fibrous root system, in which primary and seminal roots differentiate from the embryo during germination and are associated with young seedlings (Figure 1-2 A, B) (Hochholdinger and Zimmermann, 2008). The primary and seminal roots of barley are difficult to distinguish as they are classified based on their emerging position on the embryo during germination (Knipfer and Fricke, 2010; Kirschner et al., 2017). Post-embryonic (adventitious) root (Figure 1-2 F) development is dependent on the extensive shoot-borne root system (Feldman, 1994; Hochholdinger and Zimmermann, 2008). The development of post-embryonic roots is important to support water and nutrient foraging required for plant growth later in development. In contrast to barley, *Arabidopsis* has a tap root system (Figure 1-2 C) which develops from an embryonic primary root whose origin can be tracked back to the first cells within the embryo (Jürgens, 1992). The root system is enlarged mainly through lateral root branching rather than emergence of post-embryonic roots. Even though the root system architecture can differ between different species (Table 1-1), root morphology is surprisingly similar between flowering plants.

Root anatomy and cellular organisation

Arabidopsis has a very simple root anatomy that allows the investigation of root morphology changes during development (Malamy and Benfey, 1997), whereas the structure of root tissues in other species like barley is often more complex (Figure 1-1 C, 1-2 E, F). Like *Arabidopsis*, barley root tissues are organised in a radial-symmetric pattern, which is

established in the root apical meristem. Barley root tissues are composed of one layer of epidermis, four to six layers of cortex, one layer of endodermis, one layer of pericycle and a series of central vascular tissues (Kirschner et al., 2017). The thickness of the cortex varies between different cultivars (Chimungu et al., 2014). Similar variation in cortical cell layers was observed in maize and may influence the ability of different genotypes to adapt to changing soil environment (Jaramillo et al., 2013; Chimungu et al., 2014). The cellular organisation of the *Arabidopsis* root is similar to barley, except that it contains only one cortical cell layer (Somssich et al., 2016). In general, *Arabidopsis* root cellular structure is very simple with predictable numbers of cells in each tissue layer (Dolan et al., 1993; Salazar-Henao et al., 2016). The other main difference between barley and *Arabidopsis* is the organization of the central stele. Barley root vascular tissues comprise one large central metaxylem surrounded by eight small peripheral xylem vessels (Kirschner et al., 2017). In contrast, the stele in *Arabidopsis* contains two protophloems and protoxylem poles positioned in perpendicular directions (Dolan et al., 1993).

The cellular organisation of the individual root growth zones also differs between *Arabidopsis* and barley. A model of the *Arabidopsis* root tip is presented in Figure 1-1 B. Within the central region of the root meristematic zone, a single layer of stem cells surrounds a group of cells with little mitotic activity, termed the quiescent centre (QC), collectively comprising the stem cell niche (Sablowski, 2007; Aichinger et al., 2012). The number of cells within the QC varies between species (Schiefelbein et al., 1997; Hochholdinger and Zimmermann, 2008). There are approximately 2 to 4 cells in the QC region of *Arabidopsis*, while 800 to 1200 QC cells occur in the rice and maize QC regions (Hochholdinger and Zimmermann, 2008). Kirschner et al. (2017) recently characterised the barley meristem region and reported approximately 30 QC cells in the barley stem cell niche. When the QC cells in *Arabidopsis* roots are ablated using a laser, the stem cells directly in contact with the QC lose their capacity to divide, suggesting the QC regulates the maintenance of stem cell identity by short range or

contact based signalling (Van den Berg et al., 1997; Nystul and Spradling, 2006; Tucker and Laux, 2007). In order to differentiate, stem cells undergo anticlinal and/or periclinal divisions to produce a daughter cell that is adjacent to the QC that remains undifferentiated, and another daughter cell that escapes the root stem cell niche, but continues to divide a finite number of times, then differentiates into specific root tissues (Tucker and Laux, 2007). These tissues include the columella (distal), lateral root cap and epidermis (lateral), ground tissues consisting of the cortex and endodermis, and vascular bundle (proximal) cell types (Tucker and Laux, 2007).

The elongation zone represents the region where rapid cell expansion takes place (Dolan and Davies, 2004). Cells that undergo elongation initially expand rapidly, then the growth rate decreases and eventually stops at the end of the elongation zone (van der Weele et al., 2003). Cell elongation in roots is regulated by hormones like gibberellic acid (GA) (Fu and Harberd, 2003). GA promotes cell elongation by negatively regulating the stability of DELLA growth regulatory proteins Gibberellic Acid Insensitive (GAI) and Repressor of Ga1-3 (RGA) (Fu and Harberd, 2003; Dolan and Davies, 2004). The cell wall is a critical determinant during this period because the rapidly enlarging cells require strength to resist internal pressure, and also flexibility to allow unidirectional cell expansion (Dolan and Davies, 2004). Arabidopsis *CesA* proteins are responsible for cellulose biosynthesis and mutants deficient in the corresponding genes show abnormal cell expansion in roots, suggesting cellulose is involved in the control of root cell expansion (Arioli et al., 1998). Many studies have shown that *CesAs* function in different tissues and at different stages of development. In Arabidopsis, the *CesA1*, *CesA3* and *CesA6* genes participate in primary cell wall cellulose synthesis, whereas *CesA4*, *CesA7* and *CesA8* are involved in cellulose synthesis in secondary cell walls, and there is evidence suggesting that other *CesA* members are involved in more tissue specific pathways with redundant functions to each other (Gardiner et al., 2003; Taylor et al., 2003; Persson et al., 2007; Hill et al., 2014). Another family of cell wall related proteins, the arabinogalactan proteins

(AGPs), plays a role in cell elongation (Ding and Zhu, 1997; Seifert et al., 2002). AGPs have diverse roles during plant growth and development, but their specific function in root development is unclear (Gaspar et al., 2001; Popper, 2008). Additionally, cell wall flexibility in elongating cells is thought to be regulated by modification of pectin structure. Dolan et al. (1997) reported that uniformly distributed esterified pectins are found in the walls of cells present within the elongation zone. In non-growing cells, non-esterified pectins are present uniformly in the cell walls, which are rigid (McCartney et al., 2003).

Despite hormonal control and cell wall flexibility, other factors including cortical microtubules, polysaccharide assembly pathways, and transcriptional regulators also affect root cell elongation. Cortical microtubules are mainly composed of horizontally orientated cellulosic microfibrils on the root cells (Petricka et al., 2012). These cellulosic microfibrils provide force and track to allow longitudinal cell expansion (Petricka et al., 2012). Mutants with defective cortical microtubule development and regulation showed disrupted cell expansion and irregular root growth, including *Arabidopsis* mutants *bot1*, *fra2*, *mor1*, and *ton2* (Bichet et al., 2001; Burk et al., 2001; Whittington et al., 2001; Camilleri et al., 2002). Cortical microtubule-determined cell elongation is completed with directional polysaccharide deposition which provides the material on arranged tracks during cell wall modification and remodelling (Petricka et al., 2012). These processes involve the activity of cell wall polysaccharide synthases, hydrolases and transporters (Petricka et al., 2012).

In the root maturation zone, cell growth ceases and tissues begin to fully differentiate and adopt more specialised functions, such as xylem, phloem and cortex. A key biomarker for the onset of the maturation zone is the formation of root hairs. Root hairs function to increase the root surface area in contact with soil, favouring water absorption and nutrient uptake. Another feature is the development of secondary cell walls in xylem and endodermal tissues, which requires lignin deposition. Cell walls within this region become stronger in order to

provide structural support and serve as a primary protective barrier (McCartney et al., 2003). Lateral roots also emerge from root pericycle cells. Lateral root branching is crucial for the adaptation of the roots to heterogeneous environments and to increase root surface area for nutrient uptake. Lateral root founder cells are specified in the basal meristem region, whereas initiation of lateral root formation takes place in the maturation zone. The process of lateral root emergence has been studied mostly in *Arabidopsis* due to the simple cellular structure (Banda et al., 2019). When lateral roots initiate, the founder cells undergo asymmetric division to form the lateral root primordium which eventually form a new lateral root branch (Casimiro et al., 2001; Moreno-Risueno et al., 2010; Goh et al., 2012).

As root tissues become older after maturation, ground tissues can undergo programmed cell death (PCD). In older *Arabidopsis* roots, epidermal and cortical cell layers undergo PCD as central vascular tissues divide and enlarge. In older maize roots, cortical cells undergo PCD to form aerenchyma. The development of aerenchyma favours the transportation of oxygen, water and nutrients. Aerenchyma serve as airspaces within roots to assist adaptation to different soil environments. For example, wetland species suffering from waterlogging form aerenchyma to favour water and nutrient acquisition through the reduced living root cortex (Evans, 2004). Aerenchyma-like spaces have been described in mature barley roots due to root cortical senescence, but they become obvious only in mature root tissues at least 16 cm from tips (Evans, 2004; Schneider et al., 2017). Genetic variation has been described between species, and a negative association between root cortical senescence and respiration, radial water and nutrient transportation are proposed to be an important aspect of plant adaptation for soil resource acquisition (Schneider et al., 2017).

Root hair growth

Root hairs form from differentiated epidermal cells, also known as trichoblasts, when in the maturation zone (Schiefelbein and Somerville, 1990; Dolan et al., 1994; Bibikova and

Gilroy, 2002). Root hairs are tubular extensions to enlarge surface area that function in water and nutrient uptake, in anchoring of the plant and as interaction sites with symbiotic microorganisms like rhizobium (Gilroy and Jones, 2000). The formation of Arabidopsis root hairs follows a linear pattern on the root surface, where hairs only emerge from epidermal cells in direct contact with two cortical cells. In contrast, the formation of root hairs in many other species follows either an asymmetric cell division pattern (e.g. Brachypodium) or random patterns (e.g. barley, rice) (Pemberton et al., 2001; Salazar-Henao et al., 2016). Root hair initiation is followed by tip growth until the mature root hair forms (Bibikova and Gilroy, 2002).

In Arabidopsis, the initiation of root hair is regulated by the RHD6 bHLH transcription factor which is activated by R3-type MYB transcription factors (CPC, TRY, and ETC1) interacting with the WER-GL3-TTG1 complex. The WER-GL3-TTG1 complex also functions in the maintenance of non-hair cell properties by inducing the R2R3-type MYB transcription factor GL2 (Salazar-Henao et al., 2016; Shibata and Sugimoto, 2019). In contrast to Arabidopsis, the genetic and molecular controls of monocot root hair formation is yet to be revealed in detail. In many monocot species, asymmetric cell division of epidermal cells creates a large daughter cell that maintains normal epidermal cell fate, and a small daughter cell which becomes a root hair cell (Sinnott and Bloch, 1939; Cutter and Feldman, 1970; Schiefelbein et al., 1997). To date, a few genes responsible for cell wall polysaccharide synthesis have been shown to participate in cereal root hair formation in maize (*Zmrth1*, *Zmrth3*) (Wen et al., 2005; Hochholdinger et al., 2008), rice (*OsCslD1*, *OsCslD4*) (Kim et al., 2007; Ding et al., 2009; Yuo et al., 2009) and barley (*HvEXPI*) (Kwasniewski and Szarejko, 2006; Kwasniewski et al., 2010). However, the regulatory machinery for the cell wall related genes affecting root hair development remains under investigation.

Plant cell walls and their components

The cell walls provide the protective coat that surround the protoplast and supports cell

structure and shape. Cell walls function in intercellular communication, directional cell growth and expansion, transportation regulation, defence against pathogen infection, and as carbohydrate sinks to support plant development, especially in seeds (Albersheim et al., 2010; Keegstra, 2010). Recently, studies of cell walls have gained increasing interest because of the potential for the production of liquid fuels and as a source of health promoting dietary carbohydrates (Pettolino et al., 2012). In general, cell walls are a cellulose microfibril matrix coated with diverse non-cellulosic polysaccharides and various proteins and glycoproteins including structural proteins and enzymes (Albersheim et al., 2010; Keegstra, 2010). There are two main types of cell walls: the thin dynamic primary cell walls synthesised surround young cells that undergo division and expansion, and the lignified secondary cell walls that are synthesised around mature cells. The secondary cell walls provide further mechanical support to the plant tissues in which they occur (Pettolino et al., 2012; Tucker et al., 2018).

Cell wall polysaccharides

Polysaccharides are the main components that make up approximately 90% and 60% of the dry weight of primary and secondary cell walls, respectively (Bacic et al., 1988). Other components include proteins, silica, phenolics and polyphenolics (Bacic et al., 1988). One of the most abundant cell wall polysaccharides is cellulose, which made up to 10-14% of the primary cell wall dry weight and 40-60% of the secondary cell wall dry weight (Hématy and Höfte, 2006). It is a large linear molecule composed of β -1,4 linked glycosyl units. Parallel aligned cellulose microfibrils are linked by hydrogen bonds to form the matrix of cell wall structure (Hématy and Höfte, 2006). The synthesis of cellulose involves multiple genes from the *CesA* family to form the rosettes for the cellulose synthesis complex, and studies have shown different *CesA* members are responsible for the cellulose synthesis in different plant tissues (Doblin et al., 2002). Other important polysaccharides found in cell walls are pectin and hemicellulose. Pectin is structural polysaccharide that includes three major groups

(homogalacturonan, rhamnogalacturonan I, and rhamnogalacturonan II). Approximately 60-70% of pectin found in plant cell walls is homogalacturonan (Willats et al., 2001; Atmodjo et al., 2013). Pectin is the most dynamic polysaccharide with distinct functions during plant development. It provides structure support and intercellular adhesion, regulates signalling molecule movement, affects secondary cell wall formation, and functions as hydration polymer to support plant growth (Atmodjo et al., 2013). Due to the complexity of pectin structure, the synthesis of pectin is yet to be fully understood. Similar to cellulose, increasing evidence suggests that pectin synthesis may involve multiple proteins to form a biosynthetic complex (Atmodjo et al., 2013). In addition to pectin, hemicellulose, the other non-cellulosic polysaccharide group, is more diverse. The hemicellulosic polysaccharides contain β -1,4 linked backbones with or without side chain substitutions (Scheller and Ulvskov, 2010). The major hemicelluloses include xyloglucans, mannans, xylans, and (1,3;1,4)- β -glucans. Hemicellulose structure and abundance varies between species and tissue types, and they are known to be significant in cell wall strengthening and flexibility by interacting with cellulose (Scheller and Ulvskov, 2010; Tucker et al., 2018). Because of the heterogeneity of hemicellulose, the biosynthesis machinery is diverse and remains under study. Efforts had been made to address the genetic regulation of hemicellulose in different species, and to date, numerous genes from the glycosylhydrolases (GH) and glycosyltransferases (GT) families have been identified to participate in different hemicellulose synthesis individually or cooperatively (Tucker et al., 2018).

Cell wall composition varies in different species, organs, and even under different environmental conditions. The molecular basis for cell wall formation in barley has been relatively well characterised during grain development, mainly because of the economic value of grains for malting, brewing and feed. However, less research has focused on the cell walls of vegetative tissues or organs such as the root (Smith and Harris, 1999). In the primary cell walls of dicot plants, a cellulosic network is embedded in a complex polysaccharide matrix,

which is rich in xyloglucans and pectins (Bacic et al., 1988; Farrokhi et al., 2006). However, in monocots such as barley, the matrix is dominated by arabinoxylans and (1,3;1,4)- β -glucans, also called mixed-linkage glucans. The amount of other polysaccharides, including callose, mannans and pectin's, is relatively low (Bacic et al., 1988; Farrokhi et al., 2006). (1,3;1,4)- β -Glucan is known to present in the Poaceae, which comprise the grasses and cereal species (Trethewey and Harris, 2002). More recently Little et al. (2018) reported the discovery of minor amount of (1,3;1,4)- β -glucan in commelinid, non-commelinid and distantly related non-commelinids species, however, (1,3;1,4)- β -glucan was not able to be quantified using enzymatic assays. (1,3;1,4)- β -glucan is one of several polymers that shows structural and quantitative variation between species and tissues. For example, 70% of the barley endosperm cell walls consist of (1,3;1,4)- β -glucan, while the aleurone cell walls contain only 25% of this polymer (Fincher, 1975). The relative abundance of (1,3;1,4)- β -glucan in the cell walls of wheat endosperm and aleurone cells shows the opposite trend compared to barley (Bacic and Stone, 1981).

Cell wall composition in barley

Barley coleoptiles have previously been used as a model to study cell wall metabolism, because cell division, elongation and maturation are easily distinguished in these tissues (Gibeaut et al., 2005). Compositional analyses indicated that the content of (1,3;1,4)- β -glucan in cell walls increased during elongation and rapidly declined during maturation. A similar pattern has been found in maize (Kim et al., 2000; Thomas et al., 2000), and several endo- and exo-hydrolases are thought to be responsible for the observed decreases during maturation (Thomas et al., 2000; Roulin et al., 2002). (1,3;1,4)- β -glucan also acts as a source of energy during maturation through its hydrolytic conversion to glucose (Roulin et al., 2002). However, in the developing barley grain, (1,3;1,4)- β -glucan accumulates throughout development and remains at high levels in the cell walls of the starchy endosperm, suggesting a different role for

(1,3;1,4)- β -glucan in the grain compare to other vegetative tissues (Wilson et al., 2006).

Gibeaut et al. (2005) also reported the proportions of other major cell wall polysaccharides in developing barley coleoptiles, with steady contents of cellulose (35-40%), arabinoxylans (25-30%) and xyloglucans (8-12%) throughout growth. Pectic polysaccharides content is high in dividing cells (30%) and gradually decreases to 10% when growth ceases (Gibeaut et al., 2005). Alterations in polysaccharide structure were found in the arabinoxylans. Indeed, this class of polymers becomes less substituted with arabinose residues when cells mature (Gibeaut et al., 2005; McCartney et al., 2005; Wilson et al., 2012).

Callose is another well-known polysaccharide found in cell wall-related structures, including the cell plate formation during cell division and plasmodesmata regulation. (Trethewey and Harris, 2002; Piršelová and Matušíková, 2013). It is also synthesised in response to various stresses, e.g., wounding, pathogen infection, and incompatible pollination (Trethewey and Harris, 2002; Piršelová and Matušíková, 2013; Douchkov et al., 2016). In barley root tips, callose is present in minor amounts at the plasmodesmata region of the primary cell walls (Trethewey and Harris, 2002). Similar distributions have been found in maize and bean (Northcote et al., 1989; Turner et al., 1994). In the developing barley grain, callose only appears during the syncytial and cellularization stages (Wilson et al., 2006). The highest abundance of callose was found in the walls of dividing cells and cell plates, and it decreases progressively towards the end of cellularization and only found in the region of plasmodesmata (Wilson et al., 2006). Similar distribution patterns of callose in barley root cell walls were also reported by Trethewey and Harris (2002). Callose is also known to be significant in intercellular communication as it regulates the movement of molecules between cells through plasmodesmata. The deposition and degradation of callose at plasmodesmata is controlled via multiple callose synthases and (1,3)- β -glucanases. Accumulation of callose at plasmodesmata constricts the transportation channel, whereas callose degradation opens plasmodesmata and

allows molecule movement between cells (Ruan et al., 2001; Chen and Kim, 2009). Studies in birch revealed the synthesis and degradation of callose can be influenced by change of photoperiod and temperature, which also correspond to plasmodesmata regulated symplasmic continuity (Rinne and van der Schoot, 1998; Rinne et al., 2001).

The distribution of (1,3;1,4)- β -glucan in the cell walls of barley seedlings has been studied using immunogold labelling. Trethewey and Harris (2002) reported that (1,3;1,4)- β -glucan is present in most of the walls of the root, including the stem cell niche, except for the outer root cap. However, the amount of (1,3;1,4)- β -glucan was minor compared to the leaves and coleoptile, and immunogold labelling showed concentrated (1,3;1,4)- β -glucan in the cell walls adjacent to the plasma membrane and the newly formed cell plate. In epidermal and columella cell walls, the distribution decreases toward the root tip with no (1,3;1,4)- β -glucan found in the lateral root cap cell walls (Trethewey and Harris, 2002). Even though the distribution of (1,3;1,4)- β -glucan in barley root elongation and maturation zones were not described, the examination of (1,3;1,4)- β -glucan in elongating coleoptile and leaf tissues suggested the low concentration of (1,3;1,4)- β -glucan in the meristematic regions, whereas the concentration increases rapidly in elongating cells, indicating more active (1,3;1,4)- β -glucan accumulation in cells undergo expansion (Trethewey and Harris, 2002).

Genes involved in barley root tip cell wall synthesis

The synthesis of cell wall polysaccharides is a complex process that involves many genes. The *Glucan-synthase-like (Gsl)*, *CesA* and *Csl* gene families play an important role in callose, cellulose and non-cellulosic β -linked polysaccharide biosynthesis, respectively (Delmer, 1999; Richmond and Somerville, 2001; Li et al., 2003; Farrokhi et al., 2006; Brownfield et al., 2007). Members from the *Csl /CesA* gene families are responsible for the synthesis of different cell wall polysaccharides in various tissues (Figure 1-3) (Farrokhi et al., 2006; Schreiber et al., 2014; Schwerdt, 2017). One of the key *Csl* genes in cereals is *CsIF6*

which is involved in (1,3;1,4)- β -glucan biosynthesis and has been studied in many species (Burton et al., 2006; Nemeth et al., 2010; Cseh et al., 2013). Gene expression analysis revealed the expression of *CsIF6* in different barley tissues, and functional analysis suggests *CsIF6* is a key component in the regulation of (1,3;1,4)- β -glucan synthesis in barley (Burton et al., 2008; Burton et al., 2011). Silencing of *CsIF6* in barley resulted in complete removal of (1,3;1,4)- β -glucan in various barley tissues (Taketa et al., 2012). More recently, genes from the *CsIH* and *CsIJ* families were also found to participate in the regulation of the proportion of (1,3;1,4)- β -glucan (Doblin et al., 2009; Little et al., 2018). The ability of *CsIF6* to catalyse the formation of (1,3) and (1,4)- β -glucosidic linkages has been well studied in (1,3;1,4)- β -glucan synthesis, however, Little et al. (2019) recently demonstrated that other *CsIF* members also involved in the synthesis of two new linkages, namely (1,4)- β -glucosidic and (1,4)- β -xylosidic linkages. *HvCsIF3* and *HvCsIF10* contribute to the synthesis of a new cell wall polysaccharide named (1,4)- β -linked glucoxytan, a linear molecule consisting of β -(1,4) linked glucose and xylose residues. A similar structure was previously reported in the cell walls of green marine alga *Ulvalrs* (Ray and Lahaye, 1995), which hydrolyses into Xylp-(1,4)- β -Glc p and Glcp-(1,4)- β -Xylp disaccharides after treatment with cellulase (E-CELTR) (Little et al., 2019). Other *CsI* genes also contribute to the formation of different polysaccharides. For example, *CsIA* and *CsIC* are involved in mannan/glucomannan and xyloglucan synthesis, respectively (Dhugga et al., 2004; Liepman et al., 2005; Cocuron et al., 2007). The role of *CsIDs* in the synthesis of cellulose (Park et al., 2011) and mannan (Yin et al., 2011) was proposed but the conflicting results are still debated and need to be clarified. Interestingly, in barley, *CsID2* has been proposed to participate in pathogen defence as the expression of *CsID2* was significantly upregulated in the powdery mildew attacked leaves, and alterations in leaf cell wall composition, especially the cellulose and arabinoxytan concentration, were found in the *CsID2* downregulated transgenic barleys (Douchkov et al., 2016).

In the case of root hair formation, Kwasniewski and Szarejko (2006) reported that the

initiation of root hair from epidermal cells is most influenced by *HvEXB1* in barley. The Arabidopsis orthologs *AtEXP7* and *AtEXP18* are also involved in root hair initiation (Cho and Cosgrove, 2002). In addition, Kwasniewski et al. (2010) characterised a barley *root hair less* (*rhl 1.a*) mutant and found ten new candidate genes involved in root hair morphogenesis. Interestingly, most of the candidate genes encode proteins that are related to cell walls, including xyloglucan endotransglycosylases, arabinogalactan proteins and extensin (Kwasniewski et al., 2010). In addition, evidence suggests that the *CsID* gene family is involved in the elongation of root hair, in both dicot and monocot plants (Favery et al., 2001; Wang et al., 2001) (Figure 1-4, 1-5). In Arabidopsis, the *csld2/3/5* mutants showed root hair defects at variable levels, with either abnormal or aborted root hairs found (Yin et al., 2011). Similar phenotypes were also observed in the rice *csld1* (Kim et al., 2007) and poplar *csld5* mutants, of which, the root hair development of poplar *csld5* was successfully restored by introducing Arabidopsis *CsID3* gene (Peng et al., 2019). In the case of barley, no evidence to date has shown the association between the *CsID* genes and root hair development.

***CsIF6* is the main *CsIF* gene in barley but roles for family members remain unclear**

CsIF and *CsIH* gene families are present in grass species only (Richmond and Somerville, 2000; Hazen et al., 2002; Farrokhi et al., 2006; Doblin et al., 2009). There are at least 9 *CsIF* genes and 1 *CsIH* gene in the barley genome. Overexpression of barley *CsIH1* and rice *CsIF2*, *CsIF4* and *CsIF9* genes in transgenic Arabidopsis plants led to the formation of mixed-linkage glucans in this species, which is normally devoid of (1,3;1,4)- β -glucan (Burton et al., 2006; Doblin et al., 2009). Transcriptional profiles of individual genes were examined in barley (Burton et al., 2008; Doblin et al., 2009), and the expression level of some members in different regions of roots are shown in Figure 1-6. The gene expression analysis revealed that transcription levels of the genes are not correlated across barley tissues, suggesting their action may be independent from each other (Doblin et al., 2009). However, another theory suggests

that the biosynthesis of cell wall polysaccharides requires the cooperation of multiple enzymes from the same or different *Csl* subfamily to form a protein complex (Buckeridge et al., 2004; Farrokhi et al., 2006). This was shown for cellulose biosynthesis that requires multiple CesA members (Doblin et al., 2002), and Arabidopsis xyloglucan biosynthesis that involves a multi-GT enzyme complex (Chou et al., 2012; Zabolina, 2012). Potential interactions between *CsIF* and *CsIH* members have not been reported, and in general, functional roles for most *CsIF/H* members remains unclear. The exception is *CsIF6*, which has been well characterised during the past decade (Burton et al., 2008; Doblin et al., 2009; Burton et al., 2011).

One possibility is that *CsIF6* is the only functional member of this family *in planta*. In barley, *CsIF6* is generally highly expressed and the most predominant member of the *CsIF* gene family in the studied tissues. Taketa et al. (2012) reported that the *CsIF6* locus in the barley genome is exclusively responsible for (1,3;1,4)- β -glucan accumulation, although this study only analysed a subset of tissues including the whole grain, the de-embryoed grain, the endosperm, leaf blades and leaf sheaths. Burton et al. (2011) showed that the overexpression of *CsIF6* in barley grain results in up to 80% increase in (1,3;1,4)- β -glucan content. *CsIF6* function has also been confirmed in rice by overexpressing the rice *CsIF6* gene in tobacco and generating *cslf6* knockout rice mutants (Vega-Sánchez et al., 2012). The data indicated that the gene is involved in (1,3;1,4)- β -glucan deposition, cell wall mechanical properties and defence responses in vegetative tissues (Vega-Sánchez et al., 2012). In wheat, a *CsIF6* RNAi line also exhibited decreased levels of (1,3;1,4)- β -glucan (Nemeth et al., 2010). In all studies of *cslf6* mutants reported to date, plants show a severe reduction in (1,3;1,4)- β -glucan levels and stunted growth but remain viable and capable of producing seeds. No similar results have been reported for other *CsIF* genes; hence it is unclear what role they play in cell wall biosynthesis, growth and development. Only indirect evidence provides support for a functional role. Notably, a genome-wide association scan of 2-row spring and winter barley indicated that *CsIF* members (*CsIF3*, 4, 8, 10, 12) and *CsIH1* collocate with QTL that influence grain (1,3;1,4)- β -glucan

content (Houston et al., 2014). However, further investigations are required to reveal the function of each of the genes. To date, double mutants of *CsIF* genes have not been reported in any species.

The expression profiles of *CsIF* genes in different regions of barley root (Figure 1.6) indicated that higher expressions of *CsIF4* and *CsIF6* occur in the maturation region, which points toward a role in mature cell wall synthesis (Burton et al., 2008). In contrast, *CsIF3* and *CsIF9* are expressed at higher levels at the tip of the root compared to other root tissues, suggesting a potential role in cell elongation (Burton et al., 2008). Barley has only one *CsIH* gene, which is transcribed at very low levels in the many tissues analysed. Doblin et al. (2009) proposed that the barley *CsIH1* gene mediates the biosynthesis of (1,3;1,4)- β -glucan independently and functions in both primary and secondary cell wall development.

Arabidopsis *CsID* and barley *CsIF* genes are closely related

The *CsIF* genes are monocot-specific but closely related to the *CsID* genes that are present in both monocot and dicot species (Schwerdt et al., 2015). The function of *CsIDs* in barley remains largely unclear, except for *CsID2*, which has recently been shown to participate in pathogen defence and callose synthesis (Douchkov et al., 2016). *CsID2* mediates the formation of cell wall papillae in the epidermal layer when barley is attacked by the powdery mildew pathogen (Douchkov et al., 2016). Research on *CsID* genes from other plants highlighted a role for *CsIDs* in tip growth, including root hair morphogenesis and pollen tube development (Doblin et al., 2001; Kim et al., 2007; Bernal et al., 2008; Yin et al., 2011; Peng et al., 2019).

For example, in Arabidopsis, plants lacking functional *CsID* genes show defects in root growth (Figure 1-3), as revealed by the analysis of mutant seedlings five days post germination (Yin et al., 2011). *CsID2*, *CsID3* and *CsID5* appear to function in root elongation as mutants

have reduced root length, especially the double and triple mutant lines. The single mutants are root hair deficient (*csld2* and *csld3*) and show reduced stem growth (*csld5*) (Yin et al., 2011). *CsLD3* encodes a protein that is only found in the tip of the root hairs. This protein locates in the endoplasmic reticulum and is involved in the synthesis of cellulose in rapidly expanding primary cell walls. The *CsLD3* gene is required for the elongation of root hairs (Favery et al., 2001). Park et al. (2011) demonstrated that the Arabidopsis root hair deficient mutant *csld3* could be rescued by complementation with *CesA6*, a gene involved in cellulose synthesis. Furthermore, *CsLD1* and *CsLD4* regulate pollen tube development in Arabidopsis by participating in cellulose synthesis in pollen tube walls. This was concluded from the observation that the pollen tube wall layer becomes disordered in *csld1* and *csld4* single and double mutants, with deficiencies in male transmission (Wang et al., 2011). However, the biochemical characterisation of the proteins and their regulation requires more efforts.

Additionally, the rice *CsLD1* gene, which is the orthologue of the Arabidopsis *CsLD2* and *CsLD3* genes, plays an important role in root hair morphogenesis, especially during elongation (Kim et al., 2007; Yin et al., 2011). The rice *csld1* mutants develop similar number of root hairs to WT but these are shorter (Figure 1-5 C, D). Conversely, the overexpression of *CsLD1* in rice leads to longer root hairs (Figure 1-5 E, F) (Kim et al., 2007). The rice *CsLD4* mutant shows similar phenotypic changes to the Arabidopsis *csld5* mutants (Li et al., 2009; Yin et al., 2011). Peng et al. (2019) complemented poplar *csld5* mutant with Arabidopsis *CsLD3* gene to further confirm the significance of *CsLD* family in root hair development across species. However, direct evidence to reveal the protein activity of CslDs in poplar remain absent. Mannan synthase activity has also been attributed to CslD proteins in Arabidopsis (Verhertbruggen et al., 2011; Yin et al., 2011). Previous findings on *CsLDs* in other species may assist the elucidation of the function of the barley *CsIFs* genes based on their common origin.

Use of transgenic approaches to identify plant gene function

Loss-of-function approaches are widely used in genetic studies. RNA interference (RNAi) and CRISPR-based mutagenesis screening methods are now well-established in the field of plant science. RNAi, also known as post-transcriptional gene silencing, is a commonly used technology in genetic studies that can assist in production of a pseudo-allelic series to characterise gene function. Transformation of plants with target-specific RNAi constructs produces double-stranded RNAs, and these are processed into siRNAs by the Dicer enzymes (Matthew, 2004). The siRNAs then form RNA-induced silencing complexes with Argonaute proteins to knockdown the expression of the targeted endogenous gene, at either the mRNA or genomic DNA level. Individual transgenic events typically exhibit stable but different levels of gene down regulation, which provide an excellent resource to study the effects of the target gene during plant development under different expression levels (Matthew, 2004). The RNAi method cannot create the gene knockout event, which can be particularly useful when studying potentially embryo-lethal genes, but also limits the application of this method in research. To date, the studies of barley *Csl* genes have largely been dependent on over-expression in barley or heterologous expression system (Doblin et al., 2009; Burton et al., 2011). The exception is *HvCslF6*, for which a loss-of-function mutant was generated via gamma radiation (Tonooka et al., 2009).

In addition to RNAi, the recent development of precise gene editing and modification tools of user-specific sequences is rapidly changing the landscape of plant genomic research (Lozano-Juste and Cutler, 2014). CRISPR systems originate from prokaryotic immune systems and protect bacteria from external nucleic acids, including viral DNA and external plasmids (Barrangou et al., 2007; Wiedenheft et al., 2012). Feng et al. (2013) were the first to demonstrate the application of the CRISPR/Cas9 system in genome editing in plants on Arabidopsis. The CRISPR/Cas9 system requires only a single guide RNA and a 20 bp binding site in the genomic DNA to generate target specificity (Sander and Joung, 2014). It allows multiplex genome modifications by inducing more than one guide RNA in one transformation experiment (Belhaj

et al., 2015). Compared with traditional mutation methods, the frequencies of genome alteration via CRISPR/Cas9 are generally high. For example, 50-89% and 21-67% mutation frequencies have been observed in *Arabidopsis* and rice, respectively (Mao et al., 2013; Zhang et al., 2014), compared to average transformation efficiencies of 1%, 10% and 11% for floral dip, *Agrobacterium*-mediated transformation and particle bombardment, respectively (Gao and Nielsen, 2013). Furthermore, first generation homozygous mutations were reported in *Arabidopsis*, rice and tomato, which highlighted the efficiency of the CRISPR/Cas9 system in plant genome editing (Feng et al., 2013; Brooks et al., 2014; Sander and Joung, 2014; Zhang et al., 2014). In recent years, this technique has been applied to other plant species including barley (Gasparis et al., 2018; Lawrenson and Harwood, 2019), rice (Jiang et al., 2013; Shan et al., 2013), wheat (Shan et al., 2013), sorghum (Jiang et al., 2013), tobacco (Jiang et al., 2013), maize (Liang et al., 2014), tomato (Brooks et al., 2014; Ron et al., 2014), and sweet orange (Jia and Wang, 2014).

Summary

The root is a vital organ that affects the growth of the whole plant. Cell wall biosynthesis plays an important role in root growth and is regulated by a large number of cell wall genes, such as the *CsID* genes in *Arabidopsis*. In barley, the functional characterisation of the *CsID*-related *CsIF* gene family has been dominated by the *CsIF6* gene which is the major determinant of (1,3;1,4)- β -glucan biosynthesis. Several other *CsIF* genes show distinct transcriptional profiles in the root tip, but their function remains unclear. In general, limited research has been conducted to characterise the specific details of barley root development and genetic regulation. Therefore, understanding the genetic and molecular regulation of cell wall biosynthesis in barley roots will be useful to improve our understanding of cell wall biosynthetic enzymes, root morphogenesis and possibly for the improvement of future agricultural practises.

In this work, a combination of bioinformatics, microscopy, genetics, transgenic analysis, cell

wall characterisation, CRISPR/Cas9 gene editing, RNAi silencing, complementation studies in *Arabidopsis* and computer modelling were used to investigate and characterise the expression and function of *HvCsIF3* and *HvCsIF9* in cell wall biosynthesis in developing barley roots. Gene expression profiling from region-specific tissue samples and RNA in situ hybridisation were used to determine the site of *CsIF* gene expression in wild-type and mutant barley roots during plant development. In collaboration with Dr Kelly Houston and Dr Guillermo Garcia (James Hutton Institute, Scotland), the CRISPR/Cas9 system was used to generate loss of function alleles for *CsIF3* and *CsIF9* genes. This occurred in parallel with the analysis of *CsIF3* and *CsIF9* RNAi lines to study the phenotypic alterations associated with loss of *CsIF* gene function in barley. In addition, *Arabidopsis csld* mutants were employed as heterologous systems to determine whether barley *CsIF* genes have retained *CsID*-like functions in tip-growth. The outcomes of these studies provide a comprehensive understanding of the genetic and molecular function of barley *CsIF* genes in root development.

Research questions

The *CsIF* gene family of barley contains nine identified genes, for which only one (*CsIF6*) has an assigned function in (1,3;1,4)- β -glucan biosynthesis. Several *CsIF* genes including *CsIF3* and *CsIF9* are expressed in defined regions of the barley root, but it remains unknown whether they have a specific role in cell wall biosynthesis, growth or development. It is also unclear whether these genes function as part of a large network of cell wall genes that might act co-ordinately during different stages or in different zones of the root. Therefore, specific research questions include: what phenotype will be obtained in barley *CsIF* loss of function mutants, can the barley *CsIF* genes rescue the *Arabidopsis csld* tip-growth defected mutants, and what cell wall components do barley *CsIF* genes make in a heterologous system?

Main Aims and Objectives

This project is divided into three major aims:

Aim 1: Create temporal and spatial expression profiles of cell wall genes during barley root growth and development. And identify the composition of cell wall polysaccharides in barley root tips

Aim 2: Define the roles of barley *CsLF3* and *CsLF9* genes in root development and infer their functions in cell wall formation and polysaccharide synthesis.

Aim 3: Analyse the plant development *in silico* using OpenSimRoot and predict the effects of Csl proteins on plant performance and root-soil interactions under different nutrient stresses.

Figures

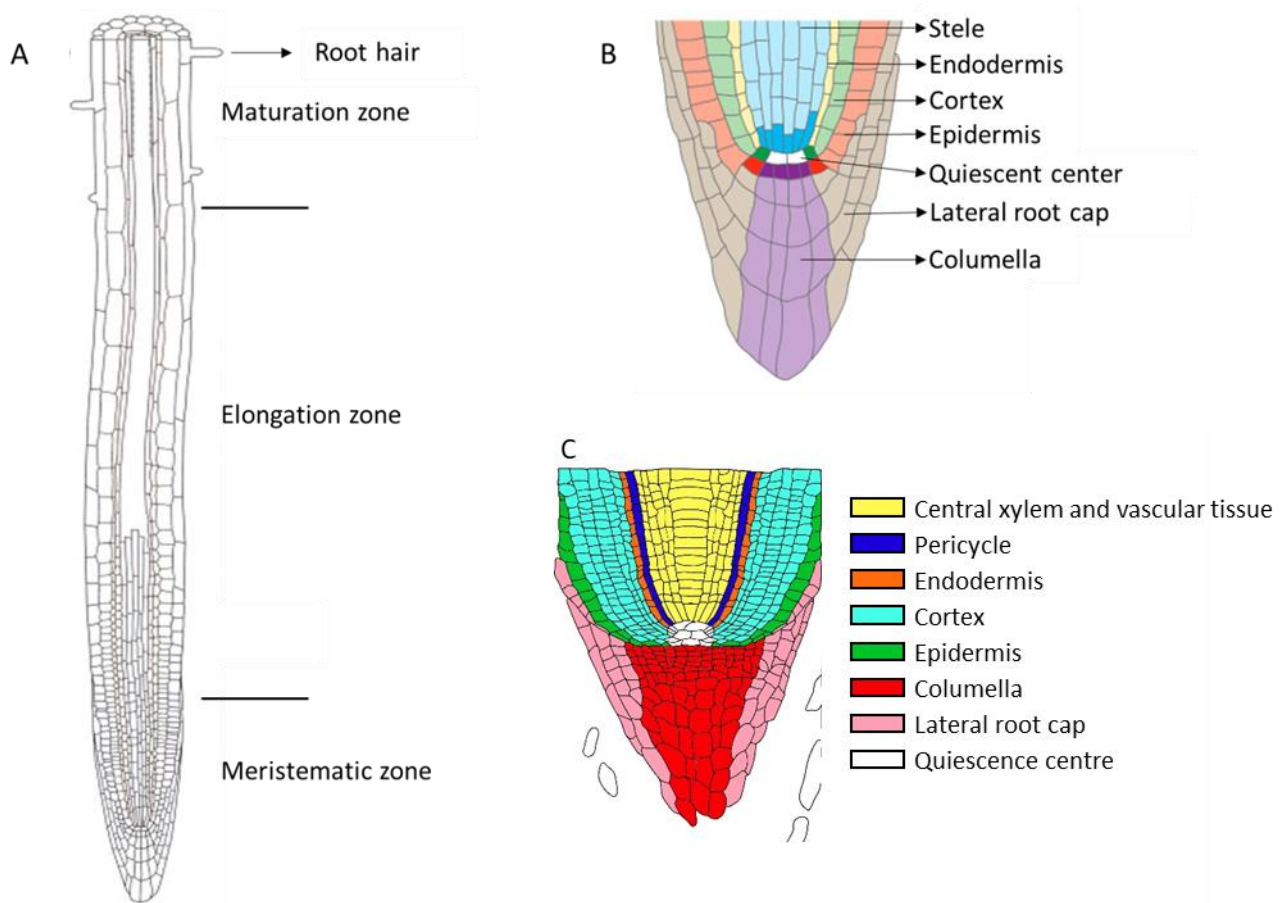


Figure 1-1. Plant root structure. A, Structure of the Arabidopsis root with its meristematic, elongation and maturation zones and a root hair. B, Structure of the Arabidopsis root tip and stem cell niche. Stem cells surround the quiescent center (white) and are indicated by different colours to distinguish the different cell types. Green: cortex and endodermis stem cells; red: epidermis and lateral root cap stem cells; purple: columella stem cells; blue: vascular tissue stem cells. C, Barley root tip schematic longitudinal section. Tissues are colour coded as indicated in legend. A and B adapted from Briggs (1978); Aichinger et al. (2012) .

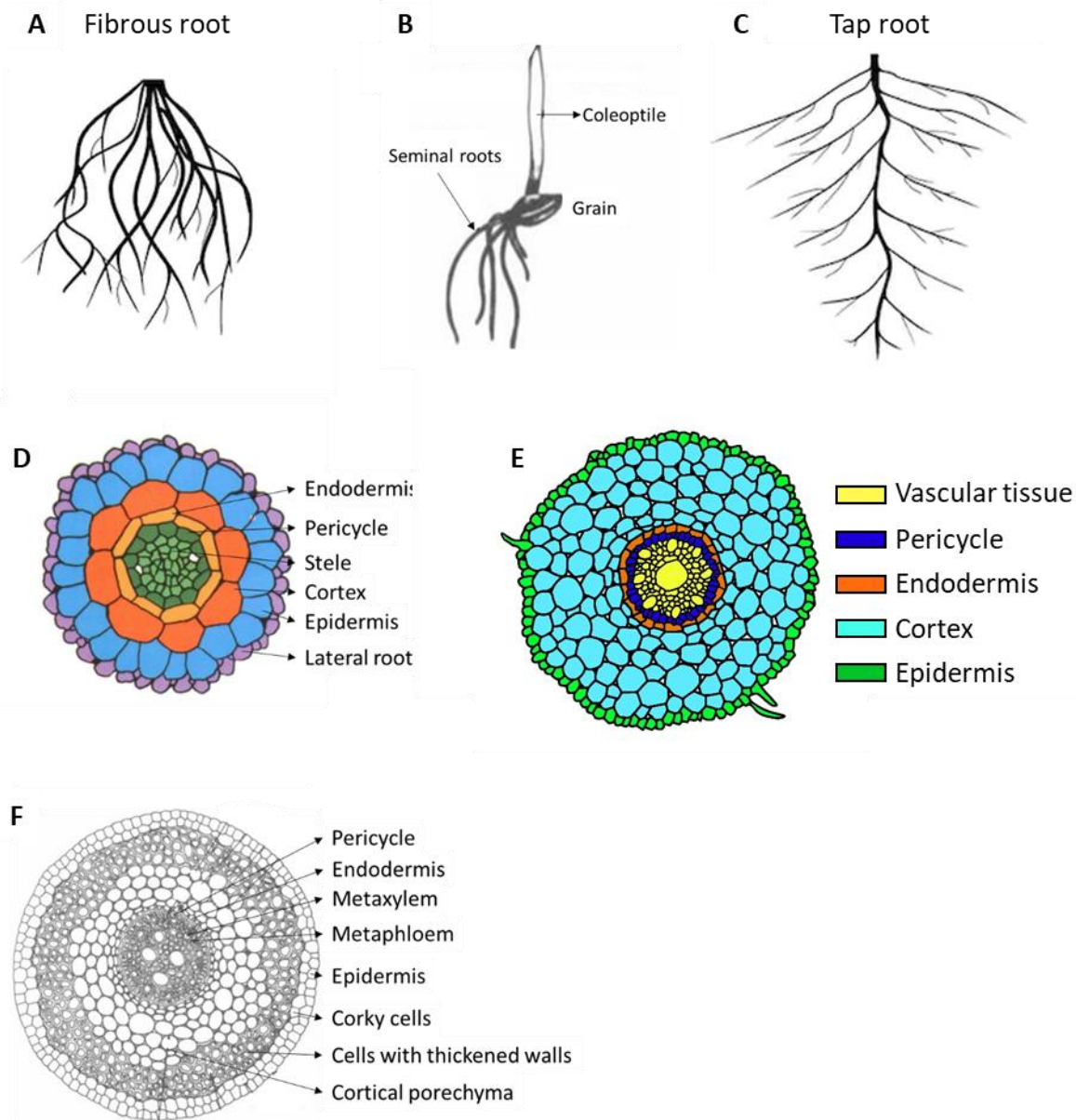


Figure 1-2. Root system architectures and anatomy. A, a fibrous root system (barley). B, barley seedling showing coleoptile and seminal roots emerging from grain. C, a tap root system (Arabidopsis). D, a transverse section of Arabidopsis root from the late meristem zone. E, a barley root transverse section of young seminal root. F, a transverse section of a mature barley adventitious root. E, D and F adapted from Schiefelbein et al. (1997) and Briggs (1978).

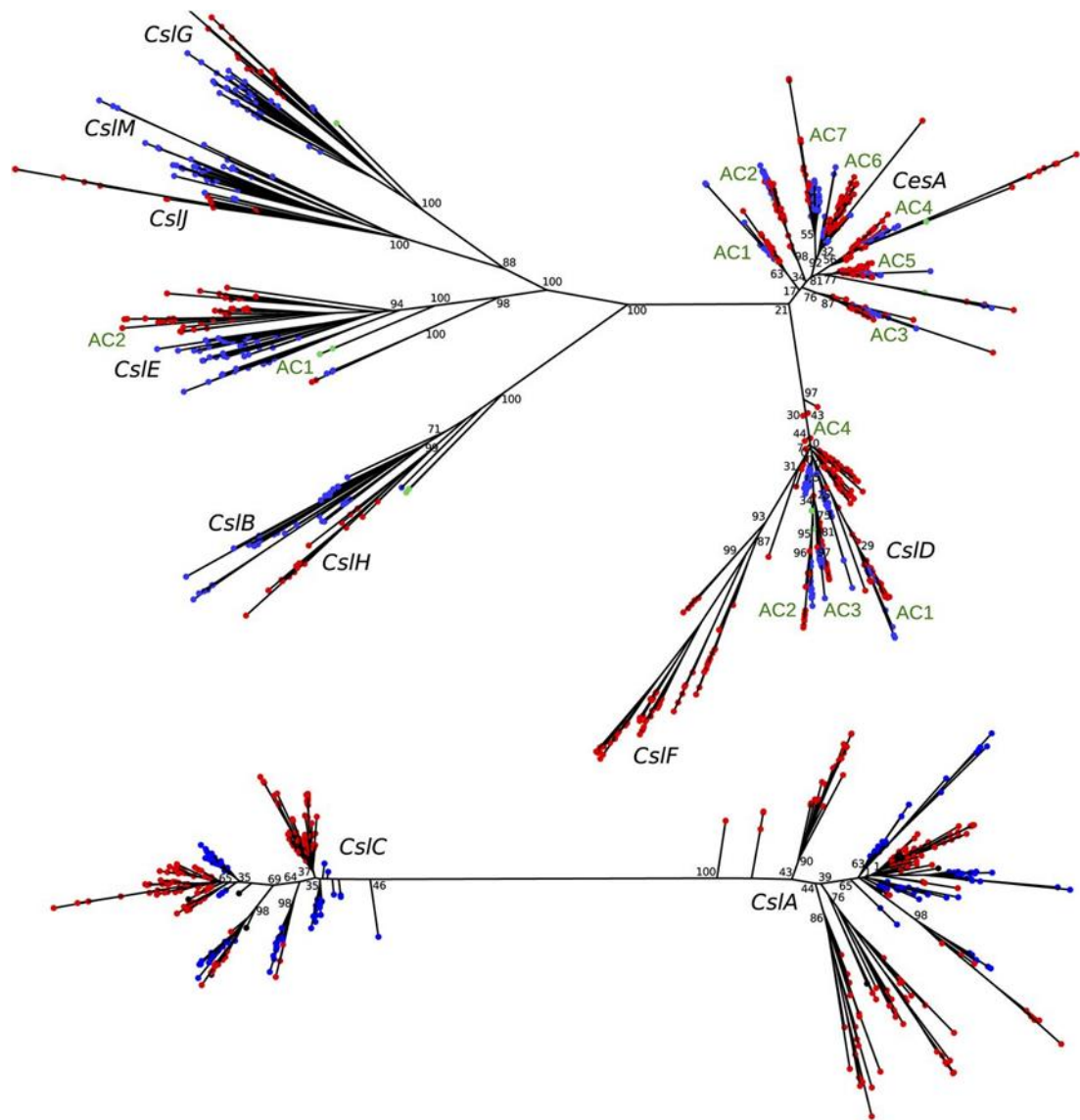


Figure 1-3. Cellulose synthase and cellulose synthase-like gene families in higher plants.

Best-known ML trees constructed using RAxML of the cellulose synthase superfamily in 46 angiosperm species, including monocots (red nodes), eudicots (blue nodes), and the basal angiosperm *Amborella trichopoda* (green nodes). Bootstrap values are indicated in black for deep nodes. 11 gene families identified, *CesaA*, *CslA*, *CslB*, *CslC*, *CslD*, *CslE*, *CslF*, *CslG*, *CslH*, *CslJ*, *CslM*. *CslD* is most close related to the *CesaA*, and *CslF* is branched out from *CslD*. Figure adapted from Little et al. (2018).

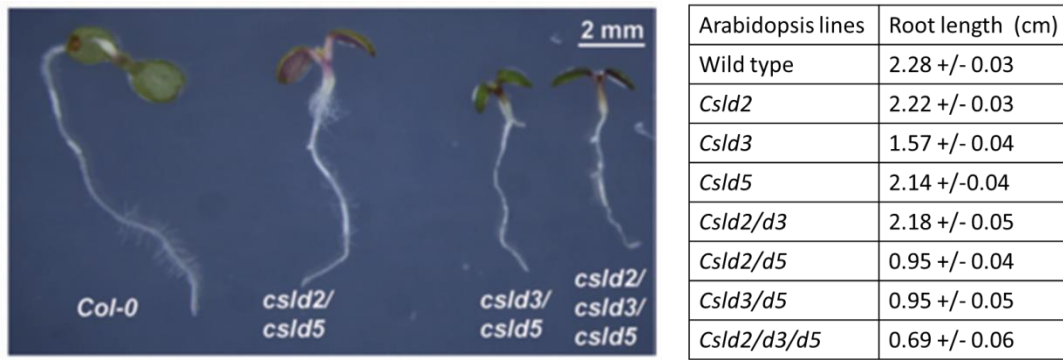


Figure 1-4. Arabidopsis *cslD2*, *cslD3* and *cslD5* single/double/triple mutants display restricted growth phenotypes compared to Col-0 (wild type). Figure and data adapted from Yin et al. (2011).

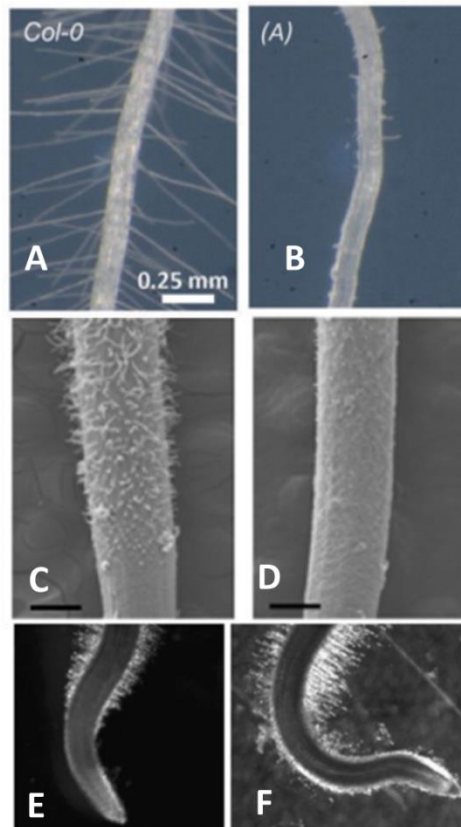


Figure 1-5. Arabidopsis and rice root hair mutant phenotypes. A, Arabidopsis wild type root. B, Arabidopsis *cslD3* mutant root. C, SEM image of wild type rice root. D, SEM image of *CslD1* down-regulated rice root. E, Wild type rice root. F, Rice root overexpressing *CslD1*. Figure adapted from Kim et al. (2007); Yin et al. (2011).

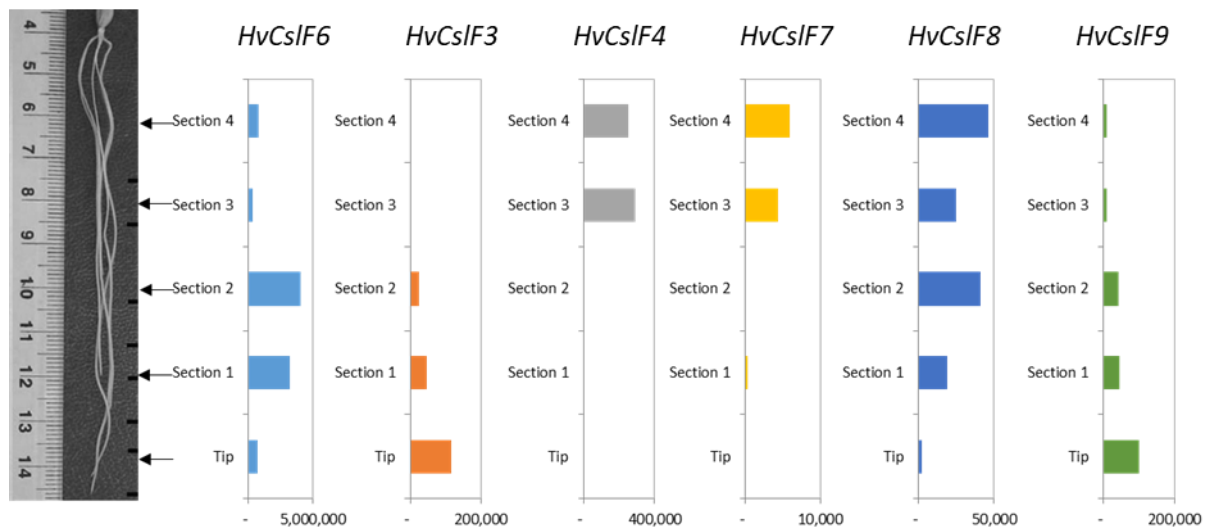


Figure 1-6. The expression profiles of 6 *CsIF* genes in different regions of barley root. Data shown high expression of *HvCsIF3* and *HvCsIF9* in the root tips. *HvCsIF6* showed highest expression in section 1 and 3. The levels of expression of *HvCsIF4*, *HvCsIF7*, and *HvCsIF8* were higher in mature roots. Data extracted from Burton et al. (2008).

Tables

Table 1-1. Differences in root architecture, structure and cellular organization in monocot and dicot species (Hochholdinger and Zimmermann, 2008).

	Monocot	Dicot (Arabidopsis)
Root architecture		
Root system	Fibrous root	Tap root
Shoot-borne root system	Extensive	Absent
Root structure		
Secondary growth	None	From cell divisions in the cambia or lateral meristem
Pith	Large, well developed	None, or little
Vascular bundle	8 to more	4 to 6
Xylem vessel shape	Oval	Angular or polygonal
Pericycle	Multilayered	Single layered
Cortex	Wide	Narrow
Root cellular organization		
Primary root initiation	Endogenous	Exogenous
Epidermal cells that form root hairs	Unpredictable	Predictable
Lateral root formation	Pericycle and endodermis, at phloem poles	Pericycle, at xylem poles
Cortex cell layers	10-15	1
Quiescent center cells	800-1200 (maize and rice)	4

Reference

- Aichinger E, Kornet N, Friedrich T, Laux T** (2012) Plant stem cell niches. *Annual Review of Plant Biology* **63**: 615-636
- Albersheim P, Darvill A, Roberts K, Sederoff R, Staehelin A** (2010) Plant cell walls. Garland Science
- Arioli T, Peng L, Betzner AS, Burn J, Wittke W, Herth W, Camilleri C, Höfte H, Plazinski J, Birch R** (1998) Molecular analysis of cellulose biosynthesis in Arabidopsis. *Science* **279**: 717-720
- Atmodjo MA, Hao Z, Mohnen D** (2013) Evolving views of pectin biosynthesis. *Annual Review of Plant Biology* **64**: 747-779
- Bacic A, Harris PJ, Stone BA** (1988) Structure and function of plant cell walls. *The Biochemistry of Plants* **14**: 297-371
- Bacic A, Stone B** (1981) Isolation and ultrastructure of aleurone cell walls from wheat and barley. *Functional Plant Biology* **8**: 453-474
- Banda J, Bellande K, von Wangenheim D, Goh T, Guyomarc'h S, Laplaze L, Bennett MJ** (2019) Lateral root formation in Arabidopsis: a well-ordered L-Rexit. *Trends in Plant Science* **24**: 826-839
- Barrangou R, Fremaux C, Deveau H, Richards M, Boyaval P, Moineau S, Romero DA, Horvath P** (2007) CRISPR provides acquired resistance against viruses in prokaryotes. *Science* **315**: 1709-1712
- Belhaj K, Chaparro-Garcia A, Kamoun S, Patron NJ, Nekrasov V** (2015) Editing plant genomes with CRISPR/Cas9. *Current Opinion in Biotechnology* **32**: 76-84
- Bernal A, Yoo C-M, Mutwil M, Jensen J, Hou G, Blaukopf C, Sørensen I, Blancaflor E, Scheller H, Willats W** (2008) Functional analysis of the cellulose synthase-like genes CSLD1, CSLD2, and CSLD4 in tip-growing Arabidopsis cells. *Plant Physiology* **148**: 1238-1253
- Bibikova T, Gilroy S** (2002) Root hair development. *Journal of Plant Growth Regulation* **21**: 383-415
- Bichet A, Desnos T, Turner S, Grandjean O, Höfte H** (2001) BOTERO1 is required for normal orientation of cortical microtubules and anisotropic cell expansion in Arabidopsis. *The Plant Journal* **25**: 137-148
- Briggs DE** (1978) Barley. Chapman & Hall
- Brooks C, Nekrasov V, Lippman ZB, Van Eck J** (2014) Efficient gene editing in tomato in the first generation using the clustered regularly interspaced short palindromic repeats/CRISPR-associated 9 system. *Plant Physiology* **166**: 1292-1297
- Brownfield L, Ford K, Doblin MS, Newbigin E, Read S, Bacic A** (2007) Proteomic and biochemical evidence links the callose synthase in *Nicotiana glauca* pollen tubes to the product of the *NaGSLI* gene. *The Plant Journal* **52**: 147-156
- Buckeridge MS, Rayon C, Urbanowicz B, Tiné MAS, Carpita NC** (2004) Mixed linkage (1-3),(1-4)- β -D-glucans of grasses. *Cereal Chemistry* **81**: 115-127
- Burk DH, Liu B, Zhong R, Morrison WH, Ye Z-H** (2001) A Katanin-like protein regulates normal cell wall biosynthesis and cell elongation. *The Plant Cell* **13**: 807-827
- Burton RA, Collins HM, Kibble NA, Smith JA, Shirley NJ, Jobling SA, Henderson M, Singh RR, Pettolino F, Wilson SM** (2011) Over-expression of specific *HvCslF* cellulose synthase-like genes in transgenic barley increases the levels of cell wall (1, 3; 1, 4)- β -D-glucans and alters their fine structure. *Plant Biotechnology Journal* **9**: 117-135
- Burton RA, Collins HM, Kibble NAJ, Smith JA, Shirley NJ, Jobling SA, Henderson M, Singh RR, Pettolino F, Wilson SM, Bird AR, Topping DL, Bacic A, Fincher GB** (2011) Over-expression of specific *HvCslF* cellulose synthase-like genes in transgenic barley increases the levels of cell wall (1,3;1,4)- β -D-glucans and alters their fine

- structure. *Plant Biotechnology Journal* **9**: 117-135
- Burton RA, Jobling SA, Harvey AJ, Shirley NJ, Mather DE, Bacic A, Fincher GB** (2008) The genetics and transcriptional profiles of the cellulose synthase-like HvCslF gene family in barley. *Plant Physiology* **146**: 1821-1833
- Burton RA, Wilson SM, Hrmova M, Harvey AJ, Shirley NJ, Medhurst A, Stone BA, Newbigin EJ, Bacic A, Fincher GB** (2006) Cellulose synthase-like CslF genes mediate the synthesis of cell wall (1, 3; 1, 4)- β -D-glucans. *Science* **311**: 1940-1942
- Camilleri C, Azimzadeh J, Pastuglia M, Bellini C, Grandjean O, Bouchez D** (2002) The Arabidopsis TONNEAU2 gene encodes a putative novel protein phosphatase 2A regulatory subunit essential for the control of the cortical cytoskeleton. *The Plant Cell* **14**: 833-845
- Cantarel BL, Coutinho PM, Rancurel C, Bernard T, Lombard V, Henrissat B** (2009) The Carbohydrate-Active EnZymes database (CAZy): an expert resource for glycogenomics. *Nucleic Acids Research* **37**: D233-D238
- Casimiro I, Marchant A, Bhalerao RP, Beeckman T, Dhooge S, Swarup R, Graham N, Inzé D, Sandberg G, Casero PJ** (2001) Auxin transport promotes Arabidopsis lateral root initiation. *The Plant Cell* **13**: 843-852
- Chen XY, Kim JY** (2009) Callose synthesis in higher plants. *Plant Signaling & Behavior* **4**: 489-492
- Chimungu JG, Brown KM, Lynch JP** (2014) Reduced root cortical cell file number improves drought tolerance in maize. *Plant Physiology* **166**: 1943-1955
- Cho HT, Cosgrove DJ** (2002) Regulation of root hair initiation and expansin gene expression in *Arabidopsis*. *The Plant Cell* **14**: 3237-3253
- Chou Y-H, Pogorelko G, Zobotina OA** (2012) Xyloglucan xylosyltransferases XXT1, XXT2, and XXT5 and the glucan synthase CSLC4 form Golgi-localized multiprotein complexes. *Plant Physiology* **159**: 1355-1366
- Cocuron J-C, Lerouxel O, Drakakaki G, Alonso AP, Liepman AH, Keegstra K, Raikhel N, Wilkerson CG** (2007) A gene from the cellulose synthase-like C family encodes a β -1, 4 glucan synthase. *Proceedings of the National Academy of Sciences of the United States of America* **104**: 8550-8555
- Cook RJ** (2006) Toward cropping systems that enhance productivity and sustainability. *Proceedings of the National Academy of Sciences of the United States of America* **103**: 18389-18394
- Cseh A, Soós V, Rakszegi M, Türkösi E, Balázs E, Molnár-Láng M** (2013) Expression of HvCslF9 and HvCslF6 barley genes in the genetic background of wheat and their influence on the wheat β -glucan content. *Annals of Applied Biology* **163**: 142-150
- Cutter EG, Feldman LJ** (1970) Trichoblasts in hydrocharis. I. origin, differentiation, dimensions and growth. *American Journal of Botany* **57(2)**: 190-201
- Delmer DP** (1999) Cellulose biosynthesis: exciting times for a difficult field of study. *Annual Review of Plant Biology* **50**: 245-276
- Dhugga KS, Barreiro R, Whitten B, Stecca K, Hazebroek J, Randhawa GS, Dolan M, Kinney AJ, Tomes D, Nichols S** (2004) Guar seed β -mannan synthase is a member of the cellulose synthase super gene family. *Science* **303**: 363-366
- Ding L, Zhu JK** (1997) A role for arabinogalactan-proteins in root epidermal cell expansion. *Planta* **203**: 289-294
- Ding W, Yu Z, Tong Y, Huang W, Chen H, Wu P** (2009) A transcription factor with a bHLH domain regulates root hair development in rice. *Cell Research* **19**: 1309-1311
- Doblin MS, De Melis L, Newbigin E, Bacic A, Read SM** (2001) Pollen tubes of *Nicotiana glauca* express two genes from different β -glucan synthase families. *Plant Physiology* **125**: 2040-2052
- Doblin MS, Kurek I, Jacob-Wilk D, Delmer DP** (2002) Cellulose biosynthesis in plants: from genes to rosettes. *Plant and Cell Physiology* **43**: 1407-1420

- Doblin MS, Pettolino FA, Wilson SM, Campbell R, Burton RA, Fincher GB, Newbiggin E, Bacic A** (2009) A barley cellulose synthase-like CslH gene mediates (1, 3; 1, 4)- β -D-glucan synthesis in transgenic *Arabidopsis*. *Proceedings of the National Academy of Sciences of the United States of America* **106**: 5996-6001
- Dolan L, Davies J** (2004) Cell expansion in roots. *Current Opinion in Plant Biology* **7**: 33-39
- Dolan L, Duckett CM, Grierson C, Linstead P, Schneider K, Lawson E, Dean C, Poethig S, Roberts K** (1994) Clonal relationships and cell patterning in the root epidermis of *Arabidopsis*. *Development* **120**: 2465-2465
- Dolan L, Janmaat K, Willemsen V, Linstead P, Poethig S, Roberts K, Scheres B** (1993) Cellular organisation of the *Arabidopsis thaliana* root. *Development* **119**: 71-84
- Dolan L, Linstead P, Roberts K** (1997) Developmental regulation of pectic polysaccharides in the root meristem of *Arabidopsis*. *Journal of Experimental Botany* **48**: 713-720
- Douchkov D, Lueck S, Hensel G, Kumlehn J, Rajaraman J, Johrde A, Doblin MS, Beahan CT, Kopischke M, Fuchs R** (2016) The barley (*Hordeum vulgare*) cellulose synthase-like D2 gene (*HvCslD2*) mediates penetration resistance to host-adapted and nonhost isolates of the powdery mildew fungus. *New Phytologist* **212**: 421-433
- Douchkov D, Lueck S, Hensel G, Kumlehn J, Rajaraman J, Johrde A, Doblin MS, Beahan CT, Kopischke M, Fuchs R, Lipka V, Niks RE, Bulone V, Chowdhury J, Little A, Burton RA, Bacic A, Fincher GB, Schweizer P** (2016) The barley (*Hordeum vulgare*) cellulose synthase-like D2 gene (*HvCslD2*) mediates penetration resistance to host-adapted and nonhost isolates of the powdery mildew fungus. *New Phytologist* **212**: 421-433
- Evans DE** (2004) Aerenchyma formation. *New Phytologist* **161**: 35-49
- Farrokhi N, Burton RA, Brownfield L, Hrmova M, Wilson SM, Bacic A, Fincher GB** (2006) Plant cell wall biosynthesis: genetic, biochemical and functional genomics approaches to the identification of key genes. *Plant Biotechnology Journal* **4**: 145-167
- Favery B, Ryan E, Foreman J, Linstead P, Boudonck K, Steer M, Shaw P, Dolan L** (2001) *KOJAK* encodes a cellulose synthase-like protein required for root hair cell morphogenesis in *Arabidopsis*. *Genes & Development* **15**: 79-89
- Feldman L** (1994) The maize root. *In* The maize handbook. Springer, pp 29-37
- Feng Z, Zhang B, Ding W, Liu X, Yang D, Wei P, Cao F, Zhu S, Zhang F, Mao Y** (2013) Efficient genome editing in plants using a CRISPR/Cas system. *Cell Research* **23**: 1229
- Fincher G** (1975) Morphology and chemical composition of barley endosperm cell walls. *Journal of the Institute of Brewing* **81**: 116-122
- Fincher GB** (2009) Revolutionary times in our understanding of cell wall biosynthesis and remodeling in the grasses. *Plant Physiology* **149**: 27-37
- Fu X, Harberd NP** (2003) Auxin promotes *Arabidopsis* root growth by modulating gibberellin response. *Nature* **421**: 740-743
- Fuller VL, Lilley CJ, Urwin PE** (2008) Nematode resistance. *New Phytologist* **180**: 27-44
- Gao C, Nielsen KK** (2013) Comparison between *Agrobacterium*-mediated and direct gene transfer using the gene gun. *Biolistic DNA Delivery: Methods and Protocols* **940**: 3-16
- Gardiner JC, Taylor NG, Turner SR** (2003) Control of cellulose synthase complex localization in developing xylem. *The Plant Cell* **15**: 1740-1748
- Gaspar Y, Johnson KL, McKenna JA, Bacic A, Schultz CJ** (2001) The complex structures of arabinogalactan-proteins and the journey towards understanding function. *Plant Molecular Biology* **47**: 161-176
- Gasparis S, Kała M, Przyborowski M, Łyżnik LA, Orczyk W, Nadolska-Orczyk A** (2018) A simple and efficient CRISPR/Cas9 platform for induction of single and multiple, heritable mutations in barley (*Hordeum vulgare* L.). *Plant Methods* **14**: 111-124
- Gibeaut DM, Pauly M, Bacic A, Fincher GB** (2005) Changes in cell wall polysaccharides in developing barley (*Hordeum vulgare*) coleoptiles. *Planta* **221**: 729-738
- Gilroy S, Jones DL** (2000) Through form to function: root hair development and nutrient

- uptake. *Trends in Plant Science* **5**: 56-60
- Goh T, Joi S, Mimura T, Fukaki H** (2012) The establishment of asymmetry in *Arabidopsis* lateral root founder cells is regulated by LBD16/ASL18 and related LBD/ASL proteins. *Development* **139**: 883-893
- Hazen SP, Scott-Craig JS, Walton JD** (2002) Cellulose synthase-like genes of rice. *Plant Physiology* **128**: 336-340
- Hématy K, Höfte H** (2006) Cellulose and cell elongation. *In* *The Expanding Cell*. Springer, pp 33-56
- Hill JL, Hammudi MB, Tien M** (2014) The *Arabidopsis* cellulose synthase complex: a proposed hexamer of CESA trimers in an equimolar stoichiometry. *The Plant Cell* **26**: 4834-4842
- Hochholdinger F, Wen TJ, Zimmermann R, Chimot-Marolle P, Da Costa e Silva O, Bruce W, Lamkey KR, Wienand U, Schnable PS** (2008) The maize (*Zea mays* L.) *roothairless3* gene encodes a putative GPI-anchored, monocot-specific, COBRA-like protein that significantly affects grain yield. *The Plant Journal* **54**: 888-898
- Hochholdinger F, Zimmermann R** (2008) Conserved and diverse mechanisms in root development. *Current Opinion in Plant Biology* **11**: 70-74
- Houston K, Russell J, Schreiber M, Halpin C, Oakey H, Washington JM, Booth A, Shirley N, Burton RA, Fincher GB** (2014) A genome wide association scan for (1, 3; 1, 4)- β -glucan content in the grain of contemporary 2-row spring and winter barleys. *BMC Genomics* **15**: 907-921
- Imani J, Li L, Schaefer P, Kogel KH** (2011) STARTS—A stable root transformation system for rapid functional analyses of proteins of the monocot model plant barley. *The Plant Journal* **67**: 726-735
- Jaramillo RE, Nord EA, Chimungu JG, Brown KM, Lynch JP** (2013) Root cortical burden influences drought tolerance in maize. *Annals of Botany* **112**: 429-437
- Jia H, Wang N** (2014) Targeted genome editing of sweet orange using Cas9/sgRNA. *Plos One* **9**: e93806
- Jiang W, Zhou H, Bi H, Fromm M, Yang B, Weeks DP** (2013) Demonstration of CRISPR/Cas9/sgRNA-mediated targeted gene modification in *Arabidopsis*, tobacco, sorghum and rice. *Nucleic Acids Research* **41**: e188
- Jürgens G** (1992) Pattern formation in the flowering plant embryo. *Current Opinion in Genetics & Development* **2**: 567-570
- Keegstra K** (2010) Plant Cell Walls. *Plant Physiology* **154**: 483-486
- Kim CM, Park S, Je BI, Park S, Park S, Piao H-L, Eun M, Dolan L, Han C-d** (2007) *OsCSLD1*, a Cellulose Synthase-Like D1 gene, is required for root hair morphogenesis in rice. *Plant Physiology* **143**: 1220-1230
- Kim CM, Park SH, Je BI, Park SH, Park SJ, Piao HL, Eun MY, Dolan L, Han C-d** (2007) *OsCSLD1*, a cellulose synthase-like D1 gene, is required for root hair morphogenesis in rice. *Plant Physiology* **143**: 1220-1230
- Kim J-B, Olek AT, Carpita NC** (2000) Cell wall and membrane-associated exo- β -D-glucanases from developing maize seedlings. *Plant Physiology* **123**: 471-486
- Kirschner GK, Stahl Y, Von Korff M, Simon R** (2017) Unique and conserved features of the barley root meristem. *Frontiers in Plant Science* **8**: 1240-1240
- Knipfer T, Fricke W** (2010) Water uptake by seminal and adventitious roots in relation to whole-plant water flow in barley (*Hordeum vulgare* L.). *Journal of Experimental Botany* **62**: 717-733
- Kwasniewski M, Janiak A, Mueller-Roeber B, Szarejko I** (2010) Global analysis of the root hair morphogenesis transcriptome reveals new candidate genes involved in root hair formation in barley. *Journal of Plant Physiology* **167**: 1076-1083
- Kwasniewski M, Szarejko I** (2006) Molecular cloning and characterization of *β -expansin* gene related to root hair formation in barley. *Plant Physiology* **141**: 1149-1158

- Lawrenson T, Harwood WA** (2019) Creating targeted gene knockouts in barley using CRISPR/Cas9. *In* Barley. Springer, pp 217-232
- Li J, Burton RA, Harvey AJ, Hrmova M, Wardak AZ, Stone BA, Fincher GB** (2003) Biochemical evidence linking a putative callose synthase gene with (1-3)- β -D-glucan biosynthesis in barley. *Plant Molecular Biology* **53**: 213-225
- Li M, Xiong G, Li R, Cui J, Tang D, Zhang B, Pauly M, Cheng Z, Zhou Y** (2009) Rice *cellulose synthase-like D4* is essential for normal cell-wall biosynthesis and plant growth. *The Plant Journal* **60**: 1055-1069
- Liang Z, Zhang K, Chen K, Gao C** (2014) Targeted mutagenesis in *Zea mays* using TALENs and the CRISPR/Cas system. *Journal of Genetics and Genomics* **41**: 63-68
- Liepman AH, Wilkerson CG, Keegstra K** (2005) Expression of cellulose synthase-like (Csl) genes in insect cells reveals that CslA family members encode mannan synthases. *Proceedings of the National Academy of Sciences of the United States of America* **102**: 2221-2226
- Little A, Lahnstein J, Jeffery DW, Khor SF, Schwerdt JG, Shirley NJ, Hooi M, Xing X, Burton RA, Bulone V** (2019) A novel (1, 4)- β -linked glucoxytan is synthesized by members of the Cellulose Synthase-Like F gene family in land plants. *ACS Central Science* **5**: 73-84
- Little A, Schwerdt JG, Shirley NJ, Khor SF, Neumann K, O'Donovan LA, Lahnstein J, Collins HM, Henderson M, Fincher GB, Burton RA** (2018) Revised phylogeny of the Cellulose Synthase Genes Superfamily: insights into cell wall evolution. *Plant Physiology* **177**: 1124-1141
- Lombard V, Ramulu HG, Drula E, Coutinho PM, Henrissat B** (2014) The carbohydrate-active enzymes database (CAZy) in 2013. *Nucleic Acids Research* **42**: D490-D495
- Lozano-Juste J, Cutler SR** (2014) Plant genome engineering in full bloom. *Trends in Plant Science* **19**: 284-287
- Malamy JE, Benfey PN** (1997) Organization and cell differentiation in lateral roots of *Arabidopsis thaliana*. *Development* **124**: 33-44
- Mao Y, Zhang H, Xu N, Zhang B, Gou F, Zhu JK** (2013) Application of the CRISPR-Cas system for efficient genome engineering in plants. *Molecular Plant* **6**: 2008-2011
- Matthew L** (2004) RNAi for plant functional genomics. *International Journal of Genomics* **5**: 240-244
- McCartney L, Marcus SE, Knox JP** (2005) Monoclonal antibodies to plant cell wall xylans and arabinoxylans. *Journal of Histochemistry & Cytochemistry* **53**: 543-546
- McCartney L, Steele-King CG, Jordan E, Knox JP** (2003) Cell wall pectic (1-4)- β -D-galactan marks the acceleration of cell elongation in the *Arabidopsis* seedling root meristem. *The Plant Journal* **33**: 447-454
- Moreno-Risueno MA, Van Norman JM, Moreno A, Zhang J, Ahnert SE, Benfey PN** (2010) Oscillating gene expression determines competence for periodic *Arabidopsis* root branching. *Science* **329**: 1306-1311
- Nemeth C, Freeman J, Jones HD, Sparks C, Pellny TK, Wilkinson MD, Dunwell J, Andersson AA, Åman P, Guillon F** (2010) Down-regulation of the *CSLF6* gene results in decreased (1, 3; 1, 4)- β -D-glucan in endosperm of wheat. *Plant Physiology* **152**: 1209-1218
- Northcote D, Davey R, Lay J** (1989) Use of antisera to localize callose, xylan and arabinogalactan in the cell-plate, primary and secondary walls of plant cells. *Planta* **178**: 353-366
- Nystul TG, Spradling AC** (2006) Breaking out of the mold: diversity within adult stem cells and their niches. *Current Opinion in Genetics & Development* **16**: 463-468
- Park S, Szumlanski AL, Gu F, Guo F, Nielsen E** (2011) A role for *CSLD3* during cell-wall synthesis in apical plasma membranes of tip-growing root-hair cells. *Nature Cell Biology* **13**: 973-980

- Pemberton LM, Tsai S-L, Lovell PH, Harris PJ** (2001) Epidermal patterning in seedling roots of eudicotyledons. *Annals of Botany* **87**: 649-654
- Peng X, Pang H, Abbas M, Yan X, Dai X, Li Y, Li Q** (2019) Characterization of Cellulose synthase-like D (CSLD) family revealed the involvement of PtrCslD5 in root hair formation in *Populus trichocarpa*. *Scientific Reports* **9**: 1452-1460
- Persson S, Paredes A, Carroll A, Palsdottir H, Doblin M, Poindexter P, Khitrov N, Auer M, Somerville CR** (2007) Genetic evidence for three unique components in primary cell-wall cellulose synthase complexes in *Arabidopsis*. *Proceedings of the National Academy of Sciences of the United States of America* **104**: 15566-15571
- Petricka JJ, Winter CM, Benfey PN** (2012) Control of *Arabidopsis* root development. *Annual Review of Plant Biology* **63**: 563-590
- Pettolino FA, Walsh C, Fincher GB, Bacic A** (2012) Determining the polysaccharide composition of plant cell walls. *Nature Protocols* **7**: 1590-1607
- Piršelová B, Matušíková I** (2013) Callose: the plant cell wall polysaccharide with multiple biological functions. *Acta Physiologiae Plantarum* **35**: 635-644
- Popper ZA** (2008) Evolution and diversity of green plant cell walls. *Current Opinion in Plant Biology* **11**: 286-292
- Ray B, Lahaye M** (1995) Cell-wall polysaccharides from the marine green alga *Ulva "rigida"* (Ulvales, Chlorophyta). Extraction and chemical composition. *Carbohydrate Research* **274**: 251-261
- Richmond TA, Somerville CR** (2000) The cellulose synthase superfamily. *Plant Physiology* **124**: 495-498
- Richmond TA, Somerville CR** (2001) Integrative approaches to determining Csl function. *In* Plant cell walls. Springer, pp 131-143
- Rinne PL, Kaikuranta PM, van der Schoot C** (2001) The shoot apical meristem restores its symplasmic organization during chilling-induced release from dormancy. *The Plant Journal* **26**: 249-264
- Rinne PL, van der Schoot C** (1998) Symplasmic fields in the tunica of the shoot apical meristem coordinate morphogenetic events. *Development* **125**: 1477-1485
- Ron M, Kajala K, Pauluzzi G, Wang D, Reynoso MA, Zumstein K, Garcha J, Winte S, Masson H, Inagaki S** (2014) Hairy root transformation using *Agrobacterium rhizogenes* as a tool for exploring cell type-specific gene expression and function using tomato as a model. *Plant Physiology* **166**: 455-469
- Roulin S, Buchala AJ, Fincher GB** (2002) Induction of (1-3, 1-4)- β -D-glucan hydrolases in leaves of dark-incubated barley seedlings. *Planta* **215**: 51-59
- Ruan YL, Llewellyn DJ, Furbank RT** (2001) The control of single-celled cotton fiber elongation by developmentally reversible gating of plasmodesmata and coordinated expression of sucrose and K⁺ transporters and expansin. *The Plant Cell* **13**: 47-60
- Sablowski R** (2007) The dynamic plant stem cell niches. *Current Opinion in Plant Biology* **10**: 639-644
- Salazar-Henao JE, Vélez-Bermúdez IC, Schmidt W** (2016) The regulation and plasticity of root hair patterning and morphogenesis. *Development* **143**: 1848-1858
- Sander JD, Joung JK** (2014) CRISPR-Cas systems for editing, regulating and targeting genomes. *Nature Biotechnology* **32**: 347-355
- Scheller HV, Ulvskov P** (2010) Hemicelluloses. *Annual Review of Plant Biology* **61**: 263-289
- Schiefelbein JW, Benfey PN** (1991) The development of plant roots: new approaches to underground problems. *The Plant Cell* **3**: 1147
- Schiefelbein JW, Masucci JD, Wang H** (1997) Building a root: the control of patterning and morphogenesis during root development. *The Plant Cell* **9**: 1089-1098
- Schiefelbein JW, Somerville C** (1990) Genetic control of root hair development in *Arabidopsis thaliana*. *The Plant Cell* **2**: 235-243
- Schneider HM, Wojciechowski T, Postma JA, Brown KM, Lücke A, Zeisler V, Schreiber**

- L, Lynch JP** (2017) Root cortical senescence decreases root respiration, nutrient content and radial water and nutrient transport in barley. *Plant, Cell & Environment* **40**: 1392-1408
- Schreiber M, Wright F, MacKenzie K, Hedley PE, Schwerdt JG, Little A, Burton RA, Fincher GB, Marshall D, Waugh R, Halpin C** (2014) The barley genome sequence assembly reveals three additional members of the CslF (1,3;1,4)- β -glucan synthase gene family. *Plos One* **9**: e90888
- Schwerdt JG** (2017) The evolutionary history and dynamics of the cellulose synthase superfamily. University of Adelaide
- Schwerdt JG, MacKenzie K, Wright F, Oehme D, Wagner JM, Harvey AJ, Shirley NJ, Burton RA, Schreiber M, Halpin C, Zimmer J, Marshall DF, Waugh R, Fincher GB** (2015) Evolutionary dynamics of the Cellulose Synthase gene superfamily in grasses. *Plant Physiology* **168**: 968-983
- Seifert GJ, Barber C, Wells B, Dolan L, Roberts K** (2002) Galactose biosynthesis in *Arabidopsis*: genetic evidence for substrate channeling from UDP-D-galactose into cell wall polymers. *Current Biology* **12**: 1840-1845
- Shan Q, Wang Y, Li J, Zhang Y, Chen K, Liang Z, Zhang K, Liu J, Xi JJ, Qiu JL** (2013) Targeted genome modification of crop plants using a CRISPR-Cas system. *Nature Biotechnology* **31**: 686-688
- Shibata M, Sugimoto K** (2019) A gene regulatory network for root hair development. *Journal of Plant Research* **132**: 301-309
- Sinnott EW, Bloch R** (1939) Cell polarity and the differentiation of root hairs. *Proceedings of the National Academy of Sciences of the United States of America* **25**: 248-252
- Smith BG, Harris PJ** (1999) The polysaccharide composition of Poales cell walls: Poaceae cell walls are not unique. *Biochemical Systematics and Ecology* **27**: 33-53
- Somssich M, Khan GA, Persson S** (2016) Cell wall heterogeneity in root development of *Arabidopsis*. *Frontiers in Plant Science* **7**: 1242-1252
- Taketa S, Yuo T, Tonooka T, Tsumuraya Y, Inagaki Y, Haruyama N, Larroque O, Jobling SA** (2012) Functional characterization of barley betaglucanless mutants demonstrates a unique role for *CsIF6* in (1, 3; 1, 4)- β -D-glucan biosynthesis. *Journal of Experimental Botany* **63**: 381-392
- Taylor NG, Howells RM, Huttly AK, Vickers K, Turner SR** (2003) Interactions among three distinct CesA proteins essential for cellulose synthesis. *Proceedings of the National Academy of Sciences of the United States of America* **100**: 1450-1455
- Thomas BR, Inouhe M, Simmons CR, Nevins DJ** (2000) Endo-1, 3; 1, 4- β -glucanase from coleoptiles of rice and maize: role in the regulation of plant growth. *International Journal of Biological Macromolecules* **27**: 145-149
- Tonooka T, Aoki E, Yoshioka T, Taketa S** (2009) A novel mutant gene for (1-3, 1-4)- β -D-glucanless grain on barley (*Hordeum vulgare* L.) chromosome 7H. *Breeding Science* **59**: 47-54
- Trethewey JA, Harris PJ** (2002) Location of (1-3)-and (1-3),(1-4)- β -D-glucans in vegetative cell walls of barley (*Hordeum vulgare*) using immunogold labelling. *New Phytologist* **154**: 347-358
- Tucker MR, Laux T** (2007) Connecting the paths in plant stem cell regulation. *Trends in Cell Biology* **17**: 403-410
- Tucker MR, Lou H, Aubert MK, Wilkinson LG, Little A, Houston K, Pinto SC, Shirley NJ** (2018) Exploring the role of cell wall-related genes and polysaccharides during plant development. *Plants* **7**: 42-58
- Turner A, Wells B, Roberts K** (1994) Plasmodesmata of maize root tips: structure and composition. *Journal of Cell Science* **107**: 3351-3361
- USDA** (2019) World agricultural production. *In*. Foreign Agricultural Service/ Office of Global Analysis, United States Department of Agriculture, p 28

- Van den Berg C, Willemsen V, Hendriks G, Weisbeek P, Scheres B** (1997) Short-range control of cell differentiation in the *Arabidopsis* root meristem. *Nature* **390**: 287-289
- van der Weele CM, Jiang HS, Palaniappan KK, Ivanov VB, Palaniappan K, Baskin TI** (2003) A new algorithm for computational image analysis of deformable motion at high spatial and temporal resolution applied to root growth. Roughly uniform elongation in the meristem and also, after an abrupt acceleration, in the elongation zone. *Plant Physiology* **132**: 1138-1148
- Vega-Sánchez ME, Verherbruggen Y, Christensen U, Chen X, Sharma V, Varanasi P, Jobling SA, Talbot M, White RG, Joo M** (2012) Loss of *cellulose synthase-like F6* function affects mixed-linkage glucan deposition, cell wall mechanical properties, and defense responses in vegetative tissues of rice. *Plant Physiology* **159**: 56-69
- Verherbruggen Y, Yin L, Oikawa A, Scheller HV** (2011) Mannan synthase activity in the *CSLD* family. *Plant Signaling & Behavior* **6**: 1620-1623
- Wang W, Wang L, Chen C, Xiong G, Tan X-Y, Yang K-Z, Wang Z-C, Zhou Y, Ye D, Chen L-Q** (2011) *Arabidopsis CSLD1* and *CSLD4* are required for cellulose deposition and normal growth of pollen tubes. *Journal of Experimental Botany* **62**: 5161-5177
- Wang X, Cnops G, Vanderhaeghen R, De Block S, Van Montagu M, Van Lijsebettens M** (2001) *AtCSLD3*, a *cellulose synthase-like* gene important for root hair growth in *Arabidopsis*. *Plant Physiology* **126**: 575-586
- Wen T-J, Hochholdinger F, Sauer M, Bruce W, Schnable PS** (2005) The *roothairless1* gene of maize encodes a homolog of *sec3*, which is involved in polar exocytosis. *Plant Physiology* **138**: 1637-1643
- Whittington AT, Vugrek O, Wei KJ, Hasenbein NG, Sugimoto K, Rashbrooke MC, Wasteney GO** (2001) MOR1 is essential for organizing cortical microtubules in plants. *Nature* **411**: 610-613
- Wiedenheft B, Sternberg SH, Doudna JA** (2012) RNA-guided genetic silencing systems in bacteria and archaea. *Nature* **482**: 331-338
- Willats WGT, McCartney L, Mackie W, Knox JP** (2001) Pectin: cell biology and prospects for functional analysis. *Plant Molecular Biology* **47**: 9-27
- Wilson SM, Burton RA, Collins HM, Doblin MS, Pettolino FA, Shirley N, Fincher GB, Bacic A** (2012) Pattern of deposition of cell wall polysaccharides and transcript abundance of related cell wall synthesis genes during differentiation in barley endosperm. *Plant Physiology* **159**: 655-670
- Wilson SM, Burton RA, Doblin MS, Stone BA, Newbigin EJ, Fincher GB, Bacic A** (2006) Temporal and spatial appearance of wall polysaccharides during cellularization of barley (*Hordeum vulgare*) endosperm. *Planta* **224**: 655-667
- Witcombe J, Hollington P, Howarth C, Reader S, Steele K** (2008) Breeding for abiotic stresses for sustainable agriculture. *Philosophical Transactions of the Royal Society of London B: Biological Sciences* **363**: 703-716
- Yin L, Verherbruggen Y, Oikawa A, Manisseri C, Knierim B, Prak L, Jensen JK, Knox JP, Auer M, Willats WGT, Scheller HV** (2011) The cooperative activities of *CSLD2*, *CSLD3*, and *CSLD5* are required for normal *Arabidopsis* development. *Molecular Plant* **4**: 1024-1037
- Yuo T, Toyota M, Ichii M, Taketa S** (2009) Molecular cloning of a root hairless gene *rth1* in rice. *Breeding Science* **59**: 13-20
- Zabotina OA** (2012) Xyloglucan and its biosynthesis. *Frontiers in Plant Science* **3**: 134-138
- Zhang H, Zhang J, Wei P, Zhang B, Gou F, Feng Z, Mao Y, Yang L, Zhang H, Xu N, Zhu J-K** (2014) The CRISPR/Cas9 system produces specific and homozygous targeted gene editing in rice in one generation. *Plant Biotechnology Journal* **12**: 797-807

Chapter 2

Genetic and compositional analysis of cell wall polysaccharides in barley root tips



Statement of Authorship

Title of Paper	Genetic analysis of cell wall polysaccharide biosynthesis in barley root tips and cell wall compositional analysis
Publication Status	<input type="checkbox"/> Published <input type="checkbox"/> Accepted for Publication <input type="checkbox"/> Submitted for Publication <input checked="" type="checkbox"/> Unpublished and Unsubmitted work written in manuscript style
Publication Details	Genetic analysis of cell wall polysaccharide biosynthesis in barley root tips and cell wall compositional analysis Haoyu Lou, Neil Shirley, Long Yu, Leah Band, Malcolm Bennett, Matthew Tucker, Vincent Bulone

Principal Author

Name of Principal Author (Candidate)	Haoyu Lou		
Contribution to the Paper	Performed experiments and analysed data. Wrote the manuscript.		
Overall percentage (%)	70%		
Certification:	This paper reports on original research I conducted during the period of my Higher Degree by Research candidature and is not subject to any obligations or contractual agreements with a third party that would constrain its inclusion in this thesis. I am the primary author of this paper.		
Signature		Date	24/02/2020

Co-Author Contributions

By signing the Statement of Authorship, each author certifies that:
 the candidate's stated contribution to the publication is accurate (as detailed above);
 permission is granted for the candidate to include the publication in the thesis; and
 the sum of all co-author contributions is equal to 100% less the candidate's stated contribution.

Name of Co-Author	Vincent Bulone		
Contribution to the Paper	Principle supervisor. Conceived the project and designed experiments. Assisted with writing of the manuscript. I hereby certify that the statement of authorship is accurate.		
Signature		Date	24/02/2020

Name of Co-Author	Matthew Tucker		
-------------------	----------------	--	--

Chapter 2 – Genetic and compositional analysis of cell wall polysaccharides in barley root tips

Contribution to the Paper	Co-supervisor. Conceived the project and designed experiments. Assisted with writing of the manuscript. I hereby certify that the statement of authorship is accurate.		
Signature		Date	24/02/2020

Name of Co-Author	Malcolm Bennett		
Contribution to the Paper	Co-supervisor at University of Nottingham. Conceived the project and designed experiments. Assisted with writing of the manuscript. I hereby certify that the statement of authorship is accurate.		
Signature		Date	24/2/20

Name of Co-Author	Leah Band		
Contribution to the Paper	Co-supervisor at University of Nottingham. Conceived the project and designed experiments. Assisted with writing of the manuscript. I hereby certify that the statement of authorship is accurate.		
Signature		Date	25/02/2020

Name of Co-Author	Neil Shirley		
Contribution to the Paper	Assisted with experiment and data analysis. I hereby certify that the statement of authorship is accurate.		
Signature		Date	25/2/2020

Name of Co-Author	Long Yu		
Contribution to the Paper	Assisted with experiment and data analysis and editing of the manuscript. I hereby certify that the statement of authorship is accurate.		
Signature		Date	24/02/2020

Abstract

The development of plant roots provides mechanical strength and the capacity to absorb water and nutrients to support the growth of aerial organs. Understanding root development is therefore important to enable the manipulation of root growth to benefit agricultural practices. During root growth, cell walls provide protective barriers and the strength and flexibility required for cell division and elongation. These characteristics are determined by a range of different polymers located within the wall. The genetic control of plant cell wall biosynthesis is complex. Studies have shown roles for a number of genes, including related members of the *Cellulose Synthase (CesA)* and *Cellulose Synthase-like (Csl)* gene families, in the synthesis of different cell wall polysaccharides, but it is unclear which members contribute to root growth. In this study we examined the expression of several *Csl* genes from the *CslD* and *CslF* families in barley root tips. We discovered the high abundance of transcripts of *HvCslD1*, *HvCslD4*, *HvCslF3*, and *HvCslF9* in the meristem and elongation zones. In contrast, the *HvCslD2* and *HvCslF6* showed higher expression in the maturation zone. To assess how these genes might respond to loss of an important cell wall polysaccharide, we employed the *betaglucanless (bgl)* *Hvclsf6* mutant and detected up-regulation of other *CslF* genes in different zones. We also analysed the cell wall composition of root tips using immunolabelling and glycosidic linkage analysis. The presence and distribution of major cell wall polysaccharides were mapped on longitudinal root sections, which confirmed that the composition of cell walls is highly variable, depends on the cell types, and varies in the meristem, elongation, and maturation zones. Moreover, linkage analysis confirmed the amount of different glycosidic linkages in the root tips. The present study revealed the heterogeneity of barley root tip cell walls, and suggested a potential role of *HvCslF3* and *HvCslF9* in the development of barley root tips.

Introduction

Plant roots are important underground organs that support the development of the entire plant. Roots provide mechanical strength to anchor plants, they participate in the uptake and transport of water and nutrients, act as storage tissue, and function in defence against pathogens (Schiefelbein and Benfey, 1991; Bates and Lynch, 2000; Marzec et al., 2014). Roots can be used as a model to study the stages of plant development as they display a simple gradient of developmental stages in different tissues along the longitudinal axis (Schiefelbein and Benfey, 1991; Somssich et al., 2016). Barley develops a fibrous root system with primary and seminal roots that become highly branched with lateral roots. Unlike other cereal crops, the primary and seminal roots of barley are difficult to distinguish, as they are classified only by the position from which they emerge from the embryo (Knipfer and Fricke, 2010; Kirschner et al., 2017). Along the radial axis, barley roots are arranged in a fixed pattern with epidermis (1 layer), cortex cells (4 or more layers), endodermis (1 layer), pericycle (1 layer), and a central stele (1 large metaxylem and 8 small xylem vessels) (Somssich et al., 2016; Kirschner et al., 2017). On the vertical axis, roots can be divided into three zones, namely the meristem, elongation and maturation zones (Schiefelbein and Benfey, 1991). Cells in different zones represent different developmental stages, and have different cellular activities, and cell wall properties. The formation of the different cell types is dependent upon a group of stem cells in the root tip, which surround a group of slow-dividing cells called the quiescent centre (QC).

Cell walls are complex structures that form a protective barrier and provide stability and flexibility for plant development. Cellulose, hemicelluloses and pectins are the main components of the cell wall matrix and comprise nearly 90% of primary cell walls in grass species (Albersheim et al., 2010; Scheller and Ulvskov, 2010). The composition of the primary cell wall is complex, and varies between cell types and different stages of development (Houston et al., 2016). For example, the young barley coleoptile cell walls are made up of pectins (30 mol%), cellulose (25 mol%), arabinoxylan (25 mol%), xyloglucan (6 mol%), and

minor amounts of (1,3;1,4)- β -glucan (Gibeaut et al., 2005). However, after 5 days of coleoptile growth, the proportion of (1,3;1,4)- β -glucan increases to 10%, while pectins decrease to about 9% (Gibeaut et al., 2005). In the developing barley grain, (1,3;1,4)- β -glucan and arabinoxylan are the major components in endosperm and aleurone cell walls, respectively (Fincher, 1975; Wilson et al., 2006). However, the cell wall composition of barley root tips remains unclear. This contrasts with other species such as *Arabidopsis*, where compositional studies have confirmed the heterogeneity of root cell walls during cell development and under stress (Somssich et al., 2016).

The synthesis of cell wall polysaccharides involves genes from multiple families. The *Cellulose synthase genes (CesAs)* are a well characterised gene family responsible for the biosynthesis of cellulose in many plant species. The regulation and expression of genes in the *HvCesA* family was reported by Burton et al. (2004) who confirmed the high expression of *HvCesA1*, *HvCesA2*, and *HvCesA6* in barley root tips. Moreover, phylogenetic studies revealed two families closely related to the *CesAs*: the *CsID* and *CsIF* families. Members of these gene families play an important role in the synthesis of hemicelluloses, including (1,3;1,4)- β -glucan and mannan in many cereal species (Burton et al., 2006; Tonooka et al., 2009; Yin et al., 2011). A specific role was proposed for the *HvCsIF6* and *HvCsIF9* genes in the control of grain (1,3;1,4)- β -glucan levels, although *in vivo* function has only been verified for *HvCsIF6* (Burton et al., 2008; Taketa et al., 2011). Interestingly, *HvCsIF6* is the most highly expressed *CsIF* gene in all studied barley tissues. Only one study has highlighted the high abundance of *HvCsIF3* and *HvCsIF9* transcripts in the root tips, suggesting a potential role of these genes in root tip development (Burton et al., 2008). In addition to their role in cell wall polysaccharides synthesis, the *CsID* genes also affect root morphology. In rice and *Arabidopsis*, roots exhibit abnormal elongation and root hair morphology in mutants of *OsCsID1* and *OsCsID4* (Kim et al., 2007; Li et al., 2009), and *AtCsID2*, *AtCsID3* and *AtCsID5* (Yin et al., 2011). In barley, the *CsID* genes

were found to be involved in defence against pathogen rather than plant development as they mediated the accumulation of callose on epidermal layers (Douchkov et al., 2016).

There is no doubt that specific members of the *HvCslF* and *HvCslD* gene families are involved in cell wall polysaccharide synthesis, but their role in root development, if any, remains unclear. Members of both families are expressed in roots, but it also remains unclear how this relates to different root zones. There is a significant gap in knowledge of barley root cell wall properties that might be resolved by linking genetic and compositional analysis. In order to gain better understanding of cell wall biosynthesis and composition in the tips of barley roots, we studied four barley genotypes (Golden Promise, WI4330, AKA237 and AKA909) and a β -glucanless (*bgl*) mutant to: 1) examine the expression profile of key *Csl* genes in different zones of root tips, 2) map the presence and deposition of different cell wall polysaccharides on root tip longitudinal sections, and 3) obtain the polysaccharide linkage profile of the cell walls extracted from barley root tips.

Materials and methods

Plant material and preparation

Seeds of wild-type barley genotypes, Golden Promise, WI4330, AKA237 (AGG400237BARLI), AKA909 (AGG407909BARLI), and *bgl* mutant (OUM125 line sourced from Prof Kazuhiro Sato, Okayama University), were surface sterilised in 20% (v/v) sodium hypochlorite for 10 min, then rinsed with MilliQ water. Seeds were soaked in water overnight, then germinated in the dark for 5 d. Root materials were harvested under different conditions depending on the need for each experiment (see below).

Root tip morphology

Barley seeds were placed on 1% agar (pH 5.8) plates and grown vertically in a growth chamber under controlled conditions (24 h light, 21°C). Seminal root tips of 5 days post

Chapter 2 – Genetic and compositional analysis of cell wall polysaccharides in barley root tips

germination (dpg) seedlings were collected using a razor blade and fixed in freshly prepared PFA (4% paraformaldehyde in PBS, w/v, pH 6.9) for 2 h at room temperature under vacuum infiltration. The fixed tissues were washed twice in PBS before being transferred into a ClearSee solution. The protocol for root tissue clearing and staining was adapted from Ursache et al. (2018) with modifications. For clearing, ClearSee solutions were changed every 2 d over at least one week before staining. For staining, roots were stained with Direct Yellow 96 in ClearSee solution (0.1% w/v; excitation 488 nm, emission 519 nm) for 2 h under vacuum infiltration. Cleared and stained specimens were stored in ClearSee solution at room temperature. The root longitudinal images were taken using a Leica SP8 confocal microscope. The centre of root tips was captured by z-stacks from meristem to maturation zones. Images were processed and stitched using Fiji ImageJ and Adobe Photoshop. The data shown are representatives of the average of 10 root tip specimens per barley line.

RNA extraction and cDNA synthesis

Root tips at 5dpg were dissected into 4 sections (0-1 mm, 1-2 mm, 3-5 mm, and 5-10 mm from the tips), representing the meristem, elongation, young maturation and old maturation zones. Fresh samples were frozen in liquid nitrogen and stored at -80°C before further processing. Total RNA extraction was performed using the Spectrum Plant Total RNA Kit (Sigma-Aldrich) according to the manufacturer's instructions. Extracted RNA was treated with the TURBO DNA-free kit (Ambion) to remove residual DNA before being reverse transcribed to synthesize cDNA using the SuperscriptIII Reverse Transcriptase kit (Invitrogen). Only 0.25 µl of enzyme was used for the final extension step. Two independent cDNA synthesis reactions were performed for each sample and the products were combined for qPCR. Once synthesized, the cDNA samples were tested with the *HvGAPDH* (HORVU6Hr1G054520) primers to ensure the quality was sufficient.

Quantitative polymerase chain reaction (qPCR) analysis

Primers were designed to amplify the regions from the end of the coding sequence to the 3' untranslated region (UTR), and the primers used are listed in Table 2-1. qPCR was performed as described in Burton et al. (2008). Each sample includes two biological replicates and three technical replicates. *HvGAPDH* (HORVU6Hr1G054520), *HvTubulin* (HORVU1Hr1G081280), *HvHSP70* (HORVU5Hr1G113180), and *HvCyclophilin* (HORVU6Hr1G012570) were used as housekeeping genes to determine the normalisation factors (Vandesompele et al., 2002; Burton et al., 2004).

Glycosidic linkage analysis

Golden Promise seeds were germinated in germination pouches (Phytoc) for 5 d at room temperature. Seminal root tips (1 cm) were collected in Eppendorf tubes pre-chilled in liquid nitrogen, and freeze-dried overnight. Dried root tissues were ground with a Retsch Mill tissue grinder and kept at room temperature in a dry environment. The alcohol insoluble residues (AIR) were extracted according to Little et al. (2019), except the materials were resuspended and washed in a sequence of 1 ml of 70% ethanol, 100% ethanol, and 100% acetone, and dried on a rotary evaporator. The AIR was de-starched using a thermo-stable α -amylase and amyloglucosidase (Megazyme). The de-starched AIR was then treated with lichenase (Megazyme). The above enzymes were prepared as follows: 1 ml of α -amylase (*Bacillus licheniformis*, E-BLAAM, 3000 U/ml) solution was diluted in 30 ml sodium acetate buffer (100 mM, pH 5.0, containing 5 mM calcium chloride); 30 mg of amyloglucosidase (*Aspergillus niger*, E-AMGDFPD, 36000 U/g) powder was dissolved in 1 ml sodium acetate buffer as above; 1 ml of lichenase (*Bacillus subtilis*, E-LICHN, 1000 U/ml) was diluted in 20 ml sodium phosphate buffer (20 mM, pH 6.5). The dried samples with different enzyme treatments were collected for glycosidic linkage analysis.

Two mg of the above samples (two technical replicates) were methylated according to Ciucanu and Kerek (1984), with the following modifications. Methylation was performed in

Chapter 2 – Genetic and compositional analysis of cell wall polysaccharides in barley root tips

anhydrous dimethyl sulphoxide (DMSO) with 0.3 mL of methyl iodide for 3 h under argon at room temperature with stirring. The reaction mixture was then added to 1 mL of dichloromethane (DCM). The methylated polysaccharides dissolved in DCM were extracted by partitioning against deionized water 3 times and evaporating the organic phase under a stream of argon, followed by extensive hydrolysis at 100°C for 6 h in 0.5 mL of 4 M TFA under argon. The hydrolysate was reduced overnight at room temperature under argon in the presence of NaBD₄ (5 mg) and acetylated with acetic anhydride for 2 h at 100°C while stirring. To recover the partially methylated alditol acetates (PMAAs), the solvent was evaporated under a gentle stream of argon, re-dissolved in DCM before being filtrated through a column filled with anhydrous sodium sulphate powder. The filtrate was transferred to a GC vial and analysed on a Hewlett Packard 6890/5973 GC-MS system fitted with a SP-2380 capillary column (30 m × 0.25 mm i.d., Sigma-Aldrich). Helium was used as the carrier gas. For each sample run, the oven temperature was programmed to increase from 165 °C to 213 °C at 1 °C/min, from 213 °C to 230 °C at 3 °C/min, and from 230 °C to 260 °C at 10 °C/min, followed by a plateau at 260 °C for 10 min (total run time 66.67 min). The mass spectra obtained by electron-impact fragmentation of the different PMAAs were interpreted by comparison with those of reference derivatives and by referring to existing databases (Carpita and Shea, 1988).

Immunolabelling and microscopy

Small sections (5 mm) of fresh 5dpg root tips were collected for fixation and embedding. The procedure of sample preparation was adapted from Burton et al. (2011) with the following modifications. Root samples were fixed in TEM fixative in PBS (0.25% glutaraldehyde, 4% paraformaldehyde, 4% sucrose) overnight with at least one-hour vacuum infiltration. The fixed root tips were rinsed in PBS twice for 8 h. The orientation and angle of each specimen was adjusted according to the purpose of sectioning in 4% agarose gel. The agarose gel with the root tips were then shaped to be “cuboid” using a razor blade. The samples were dehydrated with a serials of ethanol solutions and embedded in LR white resin. Longitudinal sections at 1

µm were cut with a glass knife or diamond knife on a Leica Microtome EM UC6 and mounted onto glass microscope slides. Sections were dried on a hot plate at 60°C for at least 1 h and stored at room temperature for immunolabelling. The antibodies specific to (1,3;1,4)-β-glucan, callose, arabinogalactan protein (AGP), mannan, arabinoxylan and pectin were used for immunolabelling, and the detailed antibody list is recorded in Table 2-2. The immunolabelling was performed as described in Burton et al. (2011). Images were taken and processed by an Axio Imager M2 microscope using an AxioCam MR R3 camera and Zeiss ZEN imaging software.

Results

Root tip anatomy

The anatomy of vertical root tips was obtained from cleared and Direct yellow 96 stained root samples. The cellular organization of the root tips from different genotypes was similar to the description by Kirschner et al. (2017). The meristem was defined as the region from the tip of the root cap to the first cortex cell adjacent to the epidermis that doubled in length, and the elongation zone was marked from the end of the meristem to the position of the first root hair emergence. Figure 2-1 and Table 2-3 show the relative sizes of the meristem zone were similar among the genotypes (approximately 1000-1100 µm), while elongation zone sizes were more variable. AKA237 and OUM125 exhibited shorter elongation zones (745.5 µm and 548.9 µm, respectively) compared with the other genotypes (900-950 µm). AKA237 and AKA909 are the putative parental lines of OUM125. These results indicated a potential natural variation in the length of elongation zone, and a possible association between the *HvCsIF6* gene and root elongation. In the meristem zone, an average of 5 layers of cortex cells was observed, this is one layer more than the barley cultivar Morex (Kirschner et al., 2017) which contains 4 cell layers.

Expression profiling of *CsID* genes in different regions of the root

There are many genes involved in the synthesis of plant cell walls. To understand the expression patterns of cell wall-related genes in different regions of the root, we used qPCR to analyse the abundance of the targeted transcripts in dissected root sections (Figure 2-2).

The *CsID* genes are most close related to the *CesA* genes, which play an important role in cellulose synthesis and deposition in primary and secondary cell walls in both monocots and dicots species (Little et al., 2018). The homologues of the *CsID* genes in *Arabidopsis* and rice participate in tip growth in various tissues (Kim et al., 2007; Bernal et al., 2008; Yin et al., 2011). *HvCsID1* showed the highest transcript levels in different genotypes; the levels were similar in the meristem (zone 1) and elongation (zone 2) zones, and increased gradually from the beginning of the maturation zone (zone 3) (Figure 2-2 B1). There was a notable increase in *HvCsID1* expression in the *bgl* mutant compared to the other lines, mainly in the elongation region of the root, which indicates a possible change in *HvCsID1* expression in response to the lack of HvCslF6 protein during rapid cell expansion (Figure 2-2 B1). Similar to *HvCsID1*, *HvCsID2* was more highly expressed in the mature parts of the root, however, the transcript levels were significantly lower than *HvCsID1*. *HvCsID2* expression in WI4330 increased dramatically in zone 3, but decreased to a similar level as other genotypes in zone 4. Furthermore, no significant change was found in the *bgl* mutant, suggesting no interaction between *HvCsID2* and *HvCslF6* genes. *HvCsID4* was predominantly expressed in the tip of the roots. In Golden Promise and WI4330, *HvCsID4* was expressed at a higher level in the meristem and elongation zones, and the expression decreased in the maturation zones. However, in the parental lines of the *bgl* mutant, the transcript level remained low throughout the different parts of the roots. This suggested a natural variation in gene expression between different cultivars. Relative to the parental lines, *HvCsID4* gene expression increased in the *bgl* mutant in zones 1 and 2.

Expression profiling of *CsIF* and *CsIH* genes in different regions of the root

In contrast to the *CsID* genes that are found in dicots and monocots, two other clusters of *Csl* gene families, *CsIF* and *CsIH*, evolved specifically in the monocots. There are nine *CsIF* genes and one *CsIH* identified in the barley genome, and members of these families mediate the synthesis of (1,3;1,4)- β -glucan (Burton et al., 2006; Doblin et al., 2009; Taketa et al., 2011; Schreiber et al., 2014; Schwerdt et al., 2015). A recent study, however, suggested that different members of the family such as *HvCsIF3* and *HvCsIF10* may be involved in the synthesis of a distinct glucoxytan polymer (Little et al., 2019). Burton et al. (2008) described high levels of expression of *HvCsIF3*, *HvCsIF6*, and *HvCsIF9* in roots, and highlighted the predominant *HvCsIF6* expression. We profiled transcript abundance of these genes and *HvCsIH1* on finely dissected root tips. In zone 1, high transcripts levels of *HvCsIF9* were detected in all genotypes, whereas the expression of *HvCsIF3* and *HvCsIF6* in this region was barely detectable, except for WI4330. When cells started elongating, *HvCsIF3* and *HvCsIF9* expression rapidly increased and peaked in zone 2 (elongation zone). The increase in AKA237 and AKA909 was less obvious due to the generally low transcript levels throughout the different root sections. Notably, in zone 2 and in most genotypes, *HvCsIF6* expression remained at similar levels as in zone 1, which suggests that *HvCsIF3* and *HvCsIF9* are the predominantly expressed *CsIF* genes in the elongation zone (Figure 2-2 B4-B6). Furthermore, the expression of *HvCsIF3* is specific to the elongation and young maturation zones, suggesting a possible role of *HvCsIF3* in cell expansion. In zone 3, high levels of *HvCsIF6* transcripts were detected, more than two-fold higher than *HvCsIF3* and *HvCsIF9*. The expression remained high in zone 4, where *HvCsIF3* and *HvCsIF9* gene expression was almost absent. In summary, our results indicate differences in expression between *HvCsIF* genes in different root regions and in particular, highlight a higher concentration of *HvCsIF3* and *HvCsIF9* transcripts in the root elongation zone. Moreover, the expression of the three analysed *HvCsIF* genes in *bgl* was generally higher compared to both putative parental lines, suggesting a possible regulatory feedback mechanism on gene expression within the *HvCsIF* gene family.

HvCslH1 was reported to mediate the biosynthesis of (1,3;1,4)- β -glucan independent of *HvCslF6*, with the highest expression level found in mature tissues where cell development and cell wall modification cease (Trethewey and Harris, 2002; Trethewey et al., 2005; Doblin et al., 2009). In the barley root tips, *HvCslH1* is barely detected above background in the meristem (Figure 2-2 B7). This suggests that *HvCslH1* is unlikely to have a function during root meristem growth and development.

Mapping of cell wall polysaccharides in barley root tips

To detect the presence of different cell wall polysaccharides, immunolabelling was performed on longitudinal barley root tip sections using antibodies that recognise (1,3;1,4)- β -glucan, callose, arabinogalactan-proteins (AGPs), pectin, mannan and arabinoxylan (Table 2-2; Figure 2-3). Figure 2-4 presents the summary of the cell wall polysaccharide mapping experiments. The distribution of each polysaccharide was consistent in all cultivars, except for (1,3;1,4)- β -glucan and the *bgl* mutant.

(1,3;1,4)- β -Glucan is abundant in the cell walls of most barley organs (Bamforth, 1982; Fincher, 1986; Gibeaut and Carpita, 1991; Tonooka et al., 2009). Consistent with this observation, labelling was detected in the cell walls of all cell types of the wild type genotypes (Figure 2-3 A, B; Figure 2-4 B). In the meristem region, cells from the mature columella and inner layers of the lateral root cap showed less intense labelling in comparison to the other cell types. As cells enter the elongation zone, the labelling intensity became stronger, with the strongest and most evenly distributed signal found in the maturation zone, where the cells finish expanding and start to form fully differentiated cells with different functions. No (1,3;1,4)- β -glucan was found in any parts of the *bgl* mutant root (Figure 2-3 C), consistent with the lack of functional *HvCslF6* protein and previous findings in the grain by Tonooka et al. (2009).

Callose, or (1,3)- β -glucan, is an important polysaccharide that is deposited in the cell plate during cell division. It also regulates plasmodesmata aperture during inter-cellular

communication, and is induced in response to wounding and stresses (Piršelová and Matusšíková, 2013). In the root sections, the labelling intensity for callose was weak at the tip, and increased in mature cells. Figure 2-3 D, E and Figure 2-4 B show that in the younger parts of the root, callose was deposited as even dotted lines in the cell walls of stem cells, cortex, endodermis, pericycle, and phloem. Little or no labelling was observed in highly differentiated or less viable cells, including the lateral root cap, developed columella, and meta-xylem. In more mature cells, the density of callose labelling decreased, but showed stronger fluorescence as punctate dots, possibly representing plasmodesmata.

LM2 antibody recognises the β -linked glucuronic acid in AGPs (Yates et al., 1996). AGP labelling was detected in the centre of the root, evenly distributed along the vertical axis from the QC upwards, in vascular tissues, pericycle, and endodermis (Figure 2-3 F, Figure 2-4 B). Specific signals also accumulated in the most outer cells in the root cap. Labelling was also found in the mature epidermis cells in mature root where cell wall thickening occurs.

Mannan is found in thickened cell walls in some plant species where it may act as carbohydrate storage (Pettolino et al., 2001). Figure 2-3 G indicates that weak mannan labelling was detected in the meristem zone, including the stem cell niche, and the outer layers of the lateral root cap and columella. The signals became stronger in the epidermis, cortex and xylem cells in the elongation and maturation zones (Figure 2-3 H). Notably, the localisation of mannan was not restricted to the cell walls. Especially in the newly formed cells, most of the labelling was observed in punctate foci in the cytoplasm. As the cells develop and the vacuole enlarges, the volume of cytoplasm is reduced, and consequently, the fluorescence signals appeared to be pushed towards the cell walls. In addition, mannan labelling was occasionally found in cell walls of the mature cells.

Arabinoxylan is one of the major hemicelluloses found in barley primary cell walls. It was previously reported in endosperm, aleurone, and vascular tissues (Fincher, 1975; Wilson

Chapter 2 – Genetic and compositional analysis of cell wall polysaccharides in barley root tips et al., 2006). However, no fluorescence signal was found in any root cell types using LM11 antibody (McCartney et al., 2005) in all cultivars examined (Figure 2-3 I).

LM19 antibody (Verhertbruggen et al., 2009) binds to un-esterified homogalacturonan, which represents one form of pectin found in the plant cell wall. LM19 labelling was restricted to the cortex, from newly formed cells to expanding cells in the meristematic and elongation zones (Figure 2-3 J, Figure 2-4 B). In more mature tissues, the labelling decreased, coinciding with the formation of secondary cell walls. Furthermore, unlike other polysaccharides with a universal deposition along the cell walls, LM19 labelling was prominent in the cell wall junctions between the cells. Consistent with other studies of pectins in plant tissues, this suggests a role of un-esterified homogalacturonan in maintaining cell integrity between different layers of cells in the root tip. The above information on the mapping of polysaccharide distribution is summarised in schematic diagrams as shown in Figure 2-4.

Linkage analysis

To complement the immunolabelling studies, we collected the first cm of Golden Promise root tips and analysed cell wall composition by glycosidic linkage analysis. Figure 2-5 shows (1,4)-Glc p was the most abundant glycosidic linkage, corresponding to about 45 mol% in the de-starched Golden Promise root tips. The proportion of (1,4)-Glc p mainly represents the concentration of cellulose, (1,3;1,4)- β -glucan and unhydrolyzed starch. The presence of (4,6)-Glc p also confirmed the presence of remaining starch residues in the sample. The (1,3;1,4)- β -glucan molecules contain the (1,3)-Glc p glycosidic linkage, which was detected at approximately 5.4 mol% in the analysed samples. The second most abundant glycosidic linkage was t-Araf, which represents terminal arabinose residues. Xylosyl residues were detected in three forms, including (1,4)-Xyl p (6.2 mol%), t-Xyl p (4.7 mol%), and (2,3,4)-Xyl p (minor amount). This suggested the presence of a xylosyl backbone and terminal xylosyl residues in the cell walls of Golden Promise root tips. The amount of t-Araf and different forms of Gal p

linkages are likely to reflect the presence of AGP in the root tips. The amount of t-Xylp most likely reflects xyloglucan content together with the (4,6)-Glc p (4.2 mol%). Furthermore, despite the high amount of t-Araf, the arabinose residues are found in many other forms in various proportions. Arabinose exists as a component of biopolymers including hemicelluloses and pectins. Variation in arabinose glycosidic linkage forms indicates the possibility of pectin forms in the barley root tip cell walls. Other glycosidic linkages comprise minor fractions of the profile.

To further quantify the amount of (1,3;1,4)- β -glucan, the de-starched sample was treated with lichenase to hydrolyse the (1,3)- β -links in (1,3;1,4)- β -glucan. Consequently, the concentration of (1,3)-Glc p and (1,4)-Glc p glycosidic linkages decreased to 1.7 mol% and 41 mol%, respectively. Variations in other glucosidic linkages were also observed, particularly in the t-Araf, t-Xylp, and (1,4)-Xlyp levels.

Discussion

The *HvCsID* genes are associated with root elongation in barley

In the present study, we analysed the gene expression profiles of the *HvCsID* and *HvCsIF* genes in different sections of barley root tips. The *CsID* genes encode proteins that share more than one third of amino acid identity with the CesA proteins (Doblin et al., 2001; Richmond and Somerville, 2001). In barley root tissues, *HvCsID1* was the most highly expressed gene analysed in root tips for all genotypes, which is consistent with the previous report of Aditya et al. (2015) on whole root transcript analysis in the Sloop cultivar. The *CsID* genes are highly conserved across different species (Schwerdt, 2017), and the *HvCsID1* homologues in rice (*OsCsID1*, LOC_Os10g42750) and Arabidopsis (*AtCsID3*, At3G03050) play an important role in root hair initiation and elongation (Kim et al., 2007; Yin et al., 2011; Douchkov et al., 2016). Knockouts of these genes result in restricted plant shoot and root development, and aberrant or aborted root hair growth phenotypes (Kim et al., 2007; Bernal et al., 2008; Yin et al., 2011). However, little evidence has been presented to support a similar

Chapter 2 – Genetic and compositional analysis of cell wall polysaccharides in barley root tips

role for *HvCslD1* during root hair development in barley. The generally high expression of *HvCslD1* in roots is similar to *AtCslD3*, which is expressed in multiple tissues but predominantly in roots, whereas *OsCslD1* expression was only found in root hair cells (Kim et al., 2007). The variation in gene expression of close homologues is likely due to rapid evolution in this family, which may result in differences in gene expression pattern and functional diversification (Douchkov et al., 2016). *AtCslD2* and *AtCslD5* are the Arabidopsis homologues of *HvCslD2* and *HvCslD4*. Mutations in both Arabidopsis genes affect root hair development, and the impacts were more severe in the *AtCslD2/D3* and *AtCslD3/D5* double knockouts (Yin et al., 2011), highlighting potential cooperation between CslD proteins in the determination of root hair morphology.

In contrast to *AtCslD2* in Arabidopsis roots, the expression level of *HvCslD2* was relatively low in barley root tips. A significant role of *HvCslD2* in defence against pathogen was reported by Douchkov et al. (2016) who observed upregulation of *HvCslD2* in barley leaves upon powdery mildew infection, and suggested a role of the gene in the modification of the cell wall composition. Unlike the other *HvCslD* genes, *HvCslD4* showed higher expression in the meristem and elongation zones compared to mature roots, suggesting a potential role of *HvCslD4* in root tip development. The rice homologue of *HvCslD4*, *OsCslD4*, is also expressed in root tips. *OscslD4* mutants are dwarf and show altered cell wall composition (Li et al., 2009; Li et al., 2010), including reduced terminal arabinose and increased branching xylose proportion in root tips (Li et al., 2009). The expression dynamics suggests possible roles of the *HvCslD* genes in cell elongation and cell wall biosynthesis. However, the function of individual genes during the development of barley roots is yet to be determined.

(1,3;1,4)- β -Glucan accumulation in developing barley roots correlates with the expression of the *HvCslF* genes

(1,3;1,4)- β -Glucan is an important polysaccharide that supports cellular development and acts as a carbon resource (Meier and Reid, 1982; Buckeridge et al., 2004). Linkage analysis revealed the presence of the (1,3)-glcp glycosidic linkage in Golden Promise barley root tips, indicating the presence of (1,3)- β -linked glucosyl residues, including callose and (1,3;1,4)- β -glucan. After lichenase treatment, the decrease in (1,3)-glcp suggested approximately 4 mol% (1,3;1,4)- β -glucan in the AIR of barley root tips, while the remaining (1,3)-glcp (1.7 mol%) may reflect the proportion of callose concentration. (1,3;1,4)- β -Glucan labelling using the BG1 antibody was detected in the cell walls of many root cell types, with more intense signals in differentiated cells. Our results in 4 different genotypes contrast with the results of Trethewey and Harris (2002) who suggested (1,3;1,4)- β -glucan was absent in the outer root cap. Trethewey and Harris (2002) used immunogold labelling to assess the tissues at very high magnifications. The study verified the presence of very little amounts of (1,3;1,4)- β -glucan in the walls of meristem cells, root cap initial cells and cortical cells, but not in the outer root cap cells. However, based on the immunolabelling with BG1 antibody in the present study (Figure 2-3 A), the fluorescence signals were found in outer root cap cells, but they did not completely surround the cells. This suggested the deposition of (1,3;1,4)- β -glucan content in outer root cap is minimal and not uniform. Hence, immunogold labelling focusing on highly magnified root sections is not the best experimental approach to assess the (1,3;1,4)- β -glucan in outer root caps. In general, the pattern of (1,3;1,4)- β -glucan deposition in roots was similar to the developing starchy endosperm (Wilson et al., 2006). Less (1,3;1,4)- β -glucan was detected in younger cells, but (1,3;1,4)- β -glucan accumulated as cells differentiated and secondary cell walls formed. The gradient of the (1,3;1,4)- β -glucan labelling along the roots was similar to that observed in developing maize and barley seedlings and coleoptiles, where (1,3;1,4)- β -glucan accumulation correlates with cell development, with low concentrations in the meristematic cell walls but synthesis during cell expansion (Kim et al., 2000; Trethewey and Harris, 2002). In vegetative tissues including coleoptiles, mature stem, and leaves, quantitative and immunolabelling studies

show (1,3;1,4)- β -glucan accumulates as the cells grow. Once the tissues reach maturation and cease development, (1,3;1,4)- β -glucan concentration decreases under the action of hydrolytic enzymes (Wilkie, 1979; Carpita and Gibeaut, 1993; Buckeridge et al., 2004; Gibeaut et al., 2005; Trethewey et al., 2005). The expression of genes encoding hydrolytic enzymes was not investigated to determine if they are more abundant in the younger parts of the barley root.

The genes responsible for the synthesis of (1,3;1,4)- β -glucan are members of the *HvCslF* and *HvCslH* families (Burton et al., 2006; Doblin et al., 2009). Burton et al. (2008) reported *HvCslF6* to be predominantly expressed in various tissues and organs including leaf, root, stem and grain. A potential role of *HvCslF6* and *HvCslF9* in the control of (1,3;1,4)- β -glucan content in developing endosperm was also proposed (Burton et al., 2008). Gene expression analysis of *HvCslF3/6/9* and *HvCslH1* in finely dissected root tips revealed the abundance of *HvCslF3* and *HvCslF9* gene transcripts in the young root tips. This was especially obvious in the meristem and elongation zones, where relatively lower levels of *HvCslF6* expression were found. Notably, the transcript level of the *HvCslF6* gene only increased in the maturation zone. *HvCslF6* is the dominant gene involved in (1,3;1,4)- β -glucan synthesis and the spatial gene expression in Golden Promise root tips correlated with the accumulation of the polysaccharide. Similar correlative patterns were reported in developing barley endosperm cell walls (Wilson et al., 2006), maize developing seedlings (Kim et al., 2000), and maize coleoptiles (Carpita et al., 2001).

The gene expression study also confirmed the abundance of *HvCslF3* and *HvCslF9* transcripts in the root tip, as originally reported by Burton et al (2008). In the present study, high transcript levels were detected in the meristem (*HvCslF9*) and elongation zones (*HvCslF3*, *HvCslF9*). The high transcript abundance in the elongation zone may indicate a role of the two genes in cell division and elongation. The cell walls in the meristem and elongation zones are dynamic and flexible due to the high hemicellulose and pectin content, allowing rapid cell division and expansion (Cosgrove, 1997; Somssich et al., 2016). Previous studies suggested

(1,3;1,4)- β -glucan is responsible for the elasticity and expansion of cell walls, allowing them to change cell shape (Kim et al., 2000; Carpita et al., 2001; Buckeridge et al., 2004; Gibeaut et al., 2005; Burton and Fincher, 2009). However, high transcript levels of *HvCslF3* and *HvCslF9* in the meristem and elongation zones do not coincide with the highest accumulation of (1,3;1,4)- β -glucan. A recent study by Little et al. (2019) suggested that *HvCslF3* is capable of producing (1,4)- β -linked glucoxytan in tobacco leaves. Noticeable concentrations of (1,4)- β -linked glucoxytan were also found in barley coleoptiles and roots (Little et al., 2019). Based on our expression data, we speculate that the products of *HvCslF3* and *HvCslF9* may contribute to polysaccharide modifications that are important for root cell division and elongation, and these may not involve (1,3;1,4)- β -glucan.

Gene expression analysis in the *bgl* mutant, which lacks a functional HvCslF6 protein and (1,3;1,4)- β -glucan synthase activity (Taketa et al., 2011), indicated that the *HvCslF3/9* and *HvCslH1* genes were upregulated. This may indicate possible feedback regulation between the *HvCsl* genes in response to changes in protein activity or cell wall composition. However, even though *HvCslF9* and *HvCslH1* have been reported to be involved in the synthesis of (1,3;1,4)- β -glucan in heterologous systems (*Arabidopsis* and tobacco) (Burton et al., 2008; Doblin et al., 2009), no (1,3;1,4)- β -glucan was detected in the tip of the *bgl* roots by immunolabelling. This confirmed the determinant role of HvCslF6 in the synthesis and accumulation of (1,3;1,4)- β -glucan. Although the biological pathway of (1,3;1,4)- β -glucan synthesis remains unclear, a theoretical biosynthesis model by Buckeridge et al. (2004) proposed a cellulose biosynthesis-like model for (1,3;1,4)- β -glucan, which implicates the HvCslF6 protein as the core component as a (1,3;1,4)- β -glucan synthase together with the cooperation of additional (1,3;1,4)- β -glucan glycosyl transferases. Further investigations on *Csl* gene regulation networks and Csl protein interactions are required to solve this gap of knowledge.

Altered forms of deposition revealed multiple functions of callose during cell development

Callose serves multiple functions in plant development. During the early stage of cell division, callose is responsible for cell plate formation via the microtubule-based structure phragmoplast, it also serves the purpose of primary cell wall assembly in newly formed cells (Chen and Kim, 2009; Miart et al., 2014; Drakakaki, 2015; Somssich et al., 2016; Tucker et al., 2018). In the meristem zone of the roots, immunolabelling indicated a high abundance of callose in plate-like shapes surrounding the cells. This was especially obvious in the cell walls of the horizontal cell axes, perhaps indicating that rapid cell division occurred in this region. This is similar to the callose deposition pattern in developing barley endosperm, where callose was found along the entire cell at the stage of anticlinal division (Wilson et al., 2006).

Callose deposition is also found in plasmodesmata in a range of cell types (Tucker et al., 2018). Whether there is a direct correlation between callose deposition and plasmodesmata in the barley meristem zone remains under debate. Such a correlation was reported by Marzec et al. (2014) who found single callose molecules in plasmodesmata using immunogold-labelling in meristem cells of barley. In more mature cells, callose was also found as punctate signals in the cell walls indicating the presence of plasmodesmata. The synthesis and hydrolysis of callose regulates plasmodesmata opening and closing, and is responsible for intercellular communication and symplastic molecule exchanges (Wolf et al., 1991; Somssich et al., 2016; Tucker et al., 2018). Furthermore, plasmodesmata play an important role in the stem cell niche. Studies on *Arabidopsis* and tomato hypothesized that during the root growth, a signal generated from the QC is transmitted to the direct adjacent cells through the plasmodesmata to keep the stem cell status and prevent differentiation (Barclay et al., 1982; van den Berg et al., 1997; Stahl et al., 2013). Similar transportation of transcription factors was also reported in the shoot stem cell niche to maintain the meristem status (Daum et al., 2014; Tucker et al., 2018). Due to difficulties in immunolabelling and sample preparation, our results did not present clear labelling of plasmodesmata in the root stem cell niche area. Future studies are needed to investigate this labelling in greater detail.

Different functions of other major hemicelluloses in barley root tips

Arabinoxylan (AX) is one of the major polysaccharides in barley primary cell walls. It accounts for up to 30% of the cell wall material in coleoptiles (Gibeaut et al., 2005), 70% in aleurone (Bacic and Stone, 1981), and 20% in the endosperm (Fincher, 1975). Unlike the linear structures of (1,3;1,4)- β -glucan and callose, arabinoxylan can be highly substituted. The substitution degree changes during plant growth (Gibeaut et al., 2005). In early stages of development, highly substituted forms of AX are more soluble for molecule transport to the cell wall, while in the mature cell walls, less substituted forms of AX allow the polysaccharides to bond to other cell wall materials more tightly (Gibeaut and Carpita, 1991; Suzuki et al., 2000). Linkage analysis in this study only detected terminal xylose in the Golden Promise root tips, indicating the absence of xylan chains. Hence, relatively high proportion of terminal arabinose were found in the analysed sample. The lack of xylose-based backbone suggests a lack of arabinoxylan in barley root tips, which is consistent with the results of LM11 labelling.

Arabinogalactan proteins (AGPs) were found in the cell walls of cells, from the meristem to the maturation zones. This result differs from the pattern seen in barley endosperm, where AGPs were only found in differentiated tissues (Wilson et al., 2006). Strong labelling with LM2 labelled AGPs (un-esterified homogalacturonan) in the central root steles and the outer root cap, which is in agreement with Marzec et al. (2014) who described AGP deposition on a transverse section of mature root in barley. The same study also highlighted the abundance of AGPs in the root hair cells (Marzec et al., 2014; Milewska-Hendel et al., 2019). However, this was not seen in the present study on young root tips. A role of AGPs in root hair formation and elongation was hypothesised in diverse species including *Arabidopsis*, maize and barley (Ding and Zhu, 1997; Šamaj et al., 1999; Marzec et al., 2014). During this process, certain types of AGPs move towards the hair forming cells and function in intercellular communication and signalling (Marzec et al., 2014). The function of AGPs in the meristem and elongation zones remains unclear. Our results show significant deposition of AGPs in the central stele and

Chapter 2 – Genetic and compositional analysis of cell wall polysaccharides in barley root tips surrounding tissues, highlighting a possible contribution of AGPs to cell wall formation in the vascular tissue along the longitudinal root apex.

Mannans serve a structural and storage role in cell walls (Dhugga et al., 2004; Goubet et al., 2009; Somssich et al., 2016). Mannan accumulation is important in the seed and stem during plant development. Indeed, *Arabidopsis* mutants with altered mannan concentration result in embryogenesis defects and even lethality (Goubet et al., 2009). The deposition of mannan in barley root tips differs from other studied polysaccharides. The (1,4)- β -mannan specific monoclonal antibody (Pettolino et al., 2001) recognised a high abundance of mannan in the cytoplasm of cells in the meristem and elongation zones, and only in the maturation zone was a small proportion of mannan located in the cell walls. The general pattern of deposition was in agreement with González-Calle et al. (2015), who reported the presence of mannan in the root tip and elongation zone of *Brachypodium*. However, the subcellular location was not specified. Mannan is also a bioactive polysaccharide that interacts with plant hormones and affect plant development in various tissues. In *Arabidopsis* roots, the substrate derived from mannan interacts with auxin and causes an enlarged meristem and prolonged elongation zone (Kučerová et al., 2016). Genes from the *CsIA* and *CsID* families have been shown to be involved in the synthesis of mannan in several species (Dhugga et al., 2004; Goubet et al., 2009; Verhertbruggen et al., 2011; He et al., 2015). It is possible that the *HvCsID* genes investigated here contribute to mannan synthesis in the root meristem.

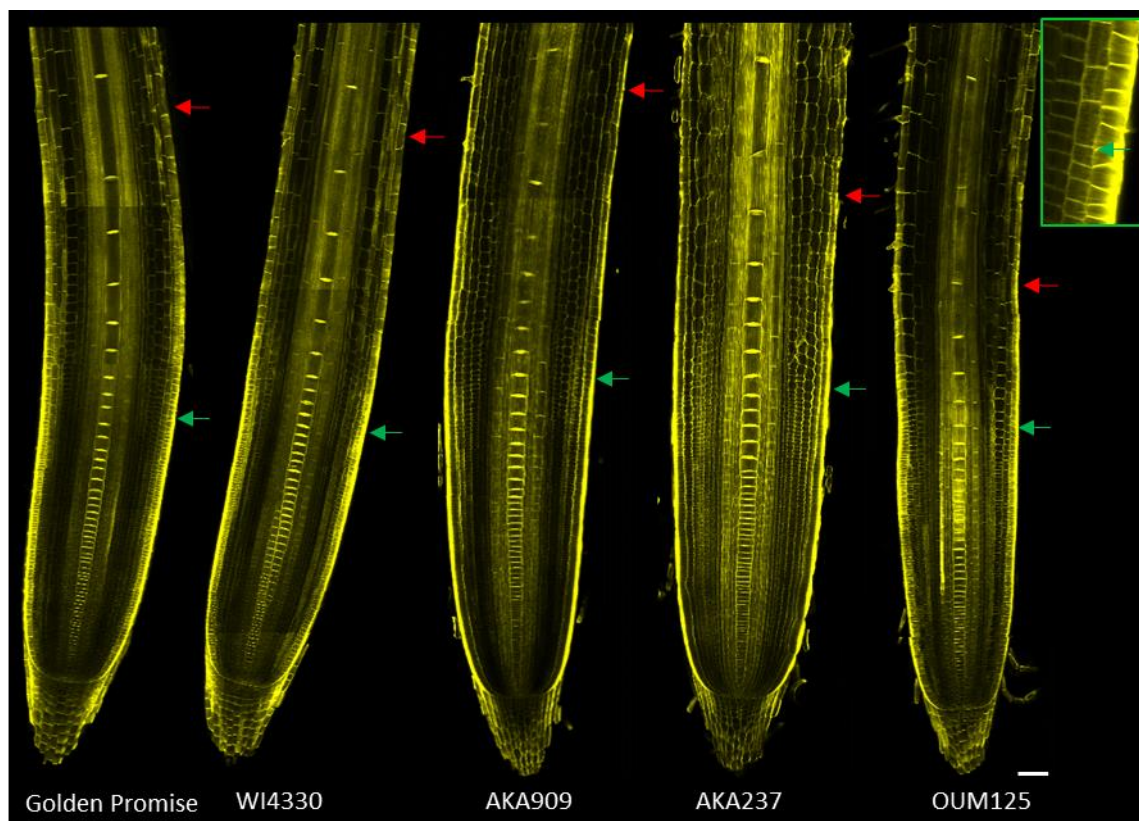
Pectin accumulation is associated with cell expansion

Pectins are heterogeneous polysaccharides that cross-link with other polymers to form a thick aqueous wall matrix that provides support and roles in intercellular signalling (Houston et al., 2016; Tucker et al., 2018). Homogalacturonan, rhamnogalacturonan I, and rhamnogalacturonan II are the three major pectic polysaccharide classes, of which homogalacturonan accounts for up to 65% of cell wall pectins (Atmodjo et al., 2013). The

LM19 antibody detects un-esterified homogalacturonan, which is commonly found in the middle lamella, while the esterified form is typically abundant when pectins are incorporated into young cell walls (Mohnen, 2008; Somssich et al., 2016). In barley root tips, LM19 recognised un-esterified homogalacturonan in cortex cells, similar to that found in the root meristem of wheat, maize, bean, and Arabidopsis, while the content was also particularly high in cell plates during cell cytokinesis in rapidly dividing and growing cells (Northcote et al., 1989; Shevell et al., 1994; Yu et al., 2002; Baluška et al., 2005). The structure of pectins is very complex and variable with typically many side chains and substitutions (Mohnen, 2008). Glycosidic linkage analysis identified many linkages that have been previously described in different forms of pectins, including t-/ (1,2)-/ (1,3)-/ (1,5)-Araf, t-/ (1,3)-/ (1,4)-/ (1,6)-Galp, and t-Glcp. This indicates the presence of various pectin types in the cell walls of barley root tips. The role of pectins in rapid growth are not only restricted to root meristems, but is also important in root hair and pollen tube development, and shoot apical meristems (Höfte et al., 2012; Atmodjo et al., 2013). One theory is that in actively growing tissues, pectins maintain the elasticity and flexibility of the cell walls due to their thick gel-like properties (Mohnen, 2008; Atmodjo et al., 2013). In this study, only the deposition pattern of un-esterified homogalacturonan was mapped on the barley root tips. In order to gain a better understanding of the importance of different forms of pectins, it will be necessary in the future to include other pectin antibodies in similar experiments, such as LM20 to recognise the methyl-esterified forms.

In conclusion, by exploring the expression of *Csl* genes in different regions of barley root tips, we determined that *HvCslF3* and *HvCslF9* are the predominant *CslF* genes expressed in the meristem and elongation zones. This leads to the question of whether *HvCslF3* and *HvCslF9* contribute to barley root tip development. Cell wall compositional analysis revealed the heterogeneity of cell walls in developing barley root tips, but also highlighted the abundance and tissue specificity of (1,3;1,4)- β -glucan, callose, and pectin as key non-cellulosic polysaccharides. Moreover, analysis of the *bgl* mutant suggested that *HvCslF6* is the sole

Chapter 2 – Genetic and compositional analysis of cell wall polysaccharides in barley root tips
determinant of (1,3;1,4)- β -glucan deposition in the OUM/AK genotypes. The variation in cell wall composition between cells and tissues may reflect the unique functional characteristics of different cell types in barley root tips.



Figures

Figure 2-1. ClearSee and Direct Yellow 96 stained root tips. 5 dpg root tips were fixed and cleared, stained, and visualized using a Leica SP8 confocal microscope. Green arrows indicate the first cortical cell that double in length to mark the end of the meristematic zone and the beginning of the elongation zone. The green box represents an example of the start of the cell elongation zone. Red arrows indicate the first root hair to mark the end of elongation zone and the beginning of the maturation zone. Fluorescence signals were detected at 488 nm (excitation) and 519 nm (emission). Z-stacks at the centre of roots were taken at five positions with overlaps. Pictures were stitched using Adobe Illustrator. The photos shown represent the average of 10 root tip specimens per genotype. Photos shown the representative of the images of 10 individual specimens. Scale bar =100 μ m.

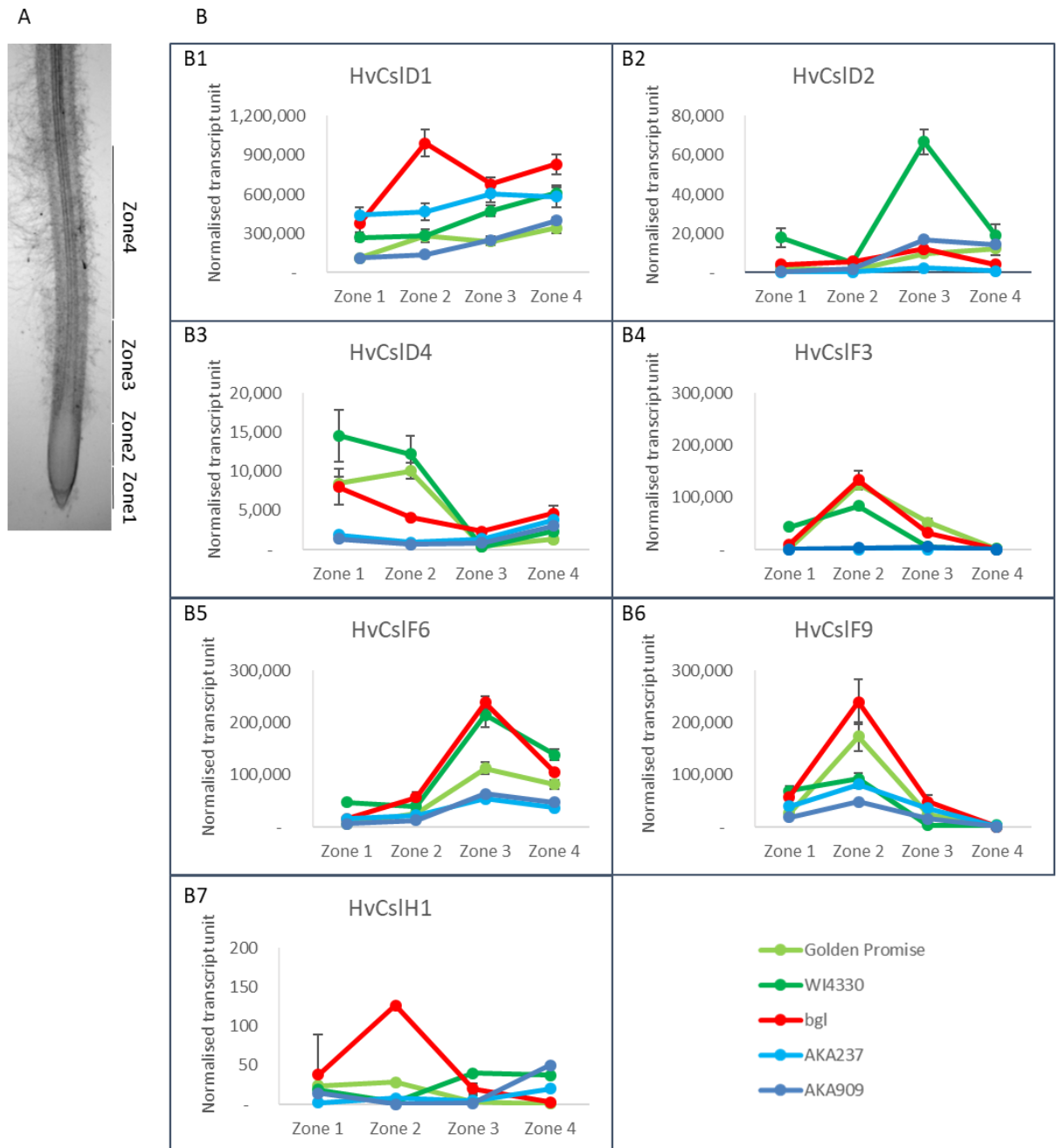


Figure 2-2. Schematic diagram of root tip dissection (A) and qPCR reveal transcript abundance in different root regions (B). A, schematic diagram of the regions used for root tip dissection: zones 1, 2, 3, and 4 represent root meristematic, elongation, young maturation, and old maturation zones, respectively. B, qPCR results showing the normalized transcript abundance in different zones of the root. *HvCsID1* (B1) showed highest expression, and the transcript level increase as root develops. *HvCsID2* (B2) showed similar trend of expression but with lower levels. *HvCsID4* (B3) expressed at high level in zones 1 and 2 and decreased gradually as the root matures. *HvCsIF3* (B4) and *HvCsIF9* (B6) showed highest expression in

zone 2, the expression was barely detectable in zone 4. *HvCslF6* (B5) is mainly expressed in the mature roots (zone 3, 4). *HvCslH1* (B7) showed very low expression, which was consistent with previous studies on aerial tissues. Up-regulation of transcript levels of *HvCslD1*, *HvCslD4*, *HvCslF3*, *HvCslF6*, *HvCslF9*, and *HvCslH1* genes in *bgl* mutant (red) indicate a potential gene coregulation between the *Csl* genes. Error bars indicate standard error.

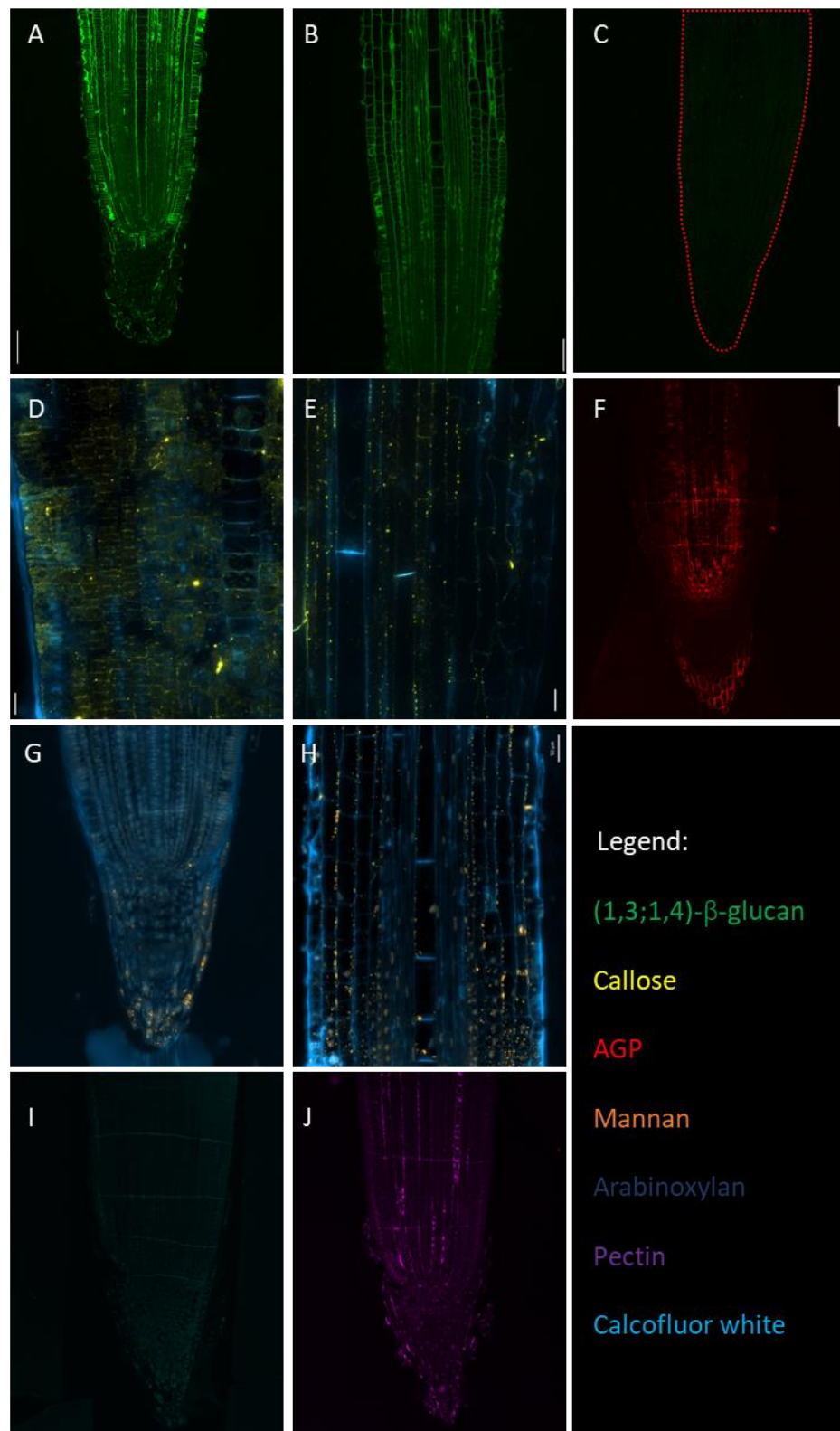


Figure 2-3. immunolabelling of major cell wall polysaccharides in the longitudinal root tip sections. Antibodies specific to (1,3;1,4)-β-glucan (A, wild type; B, wild type; C, *bgl* mutant), callose (D, meristem zone; E, maturation zone), AGP (arabinogalactan proteins) (F), mannan (G, meristem zone with root cap; H, maturation zone), arabinoxylan (I), and pectin (J)

were used to detect the presence of distinct cell wall polysaccharides in the longitudinally sectioned roots. A, weak labelling was observed in all cell types except for mature columella cells, indicating less (1,3;1,4)- β -glucan content in the cell walls of newly formed cells. B, elongation and young maturation root zones. In the wild type barley, strong fluorescence signals are detected in all tissues, with more intensive labelling appearing as cells develop and enter the maturation zone. C, no signal was detected in the cell walls of the *bgl* mutant root tips, suggesting the absence of (1,3;1,4)- β -glucan in the specimens. Callose was found in the cell walls of cells in meristem zone that undergo rapid cell division (D), and as punctate signals on the cell walls, potentially indicating the location of plasmodesmata (E). AGPs (F) were evenly distributed in the cell walls of the central stele and two outer most layers of columella cells. Different from other major cell wall polysaccharides, mannan was not located in the cell walls (G), but in the cytoplasm, especially in the young root cells. As cells develop, the mannan labelling moves towards the cell wall (H). Arabinoxylan (I) was not detected in any cell type. LM19 labelled unesterified homogalacturonan (J) in the cortex area with strong signals detected in the junctions of cortical cells.

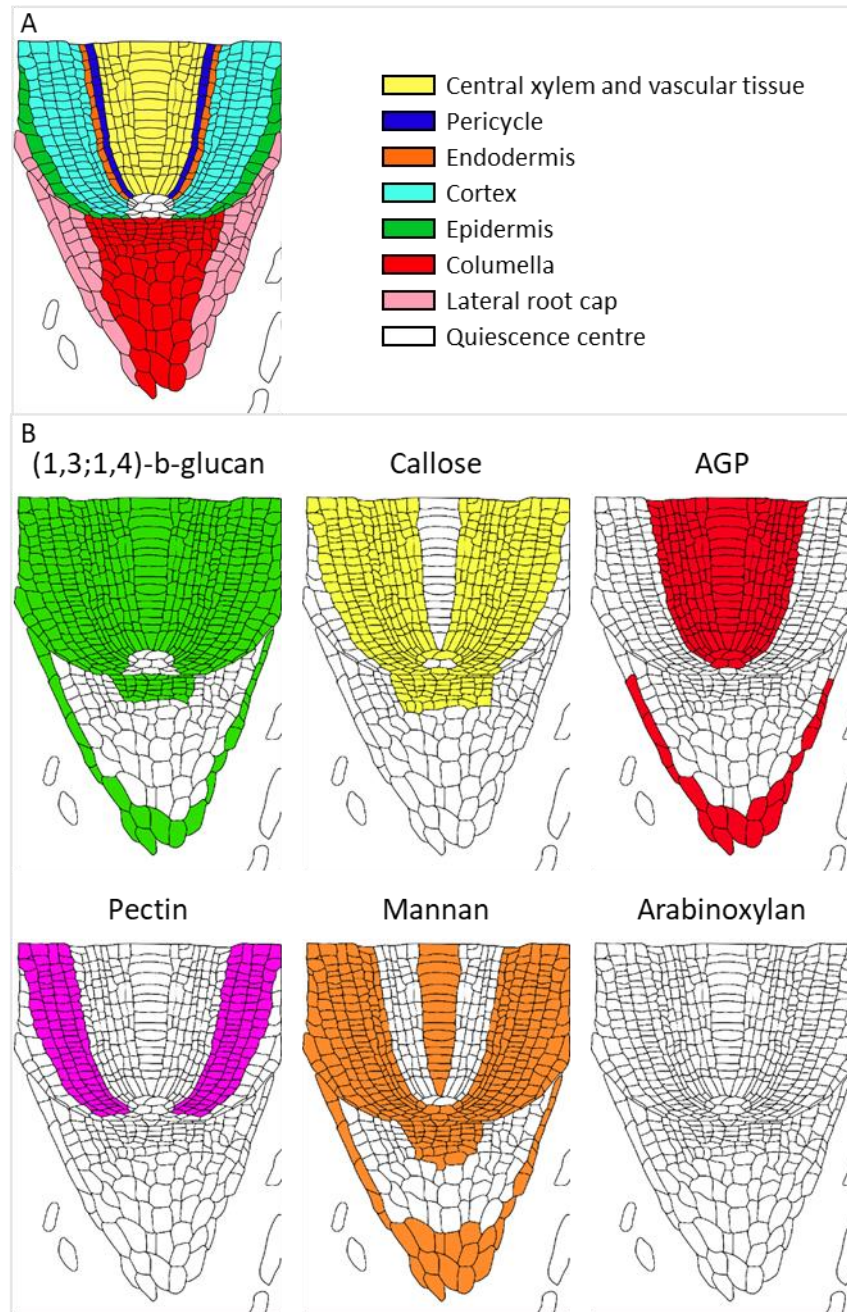


Figure 2-4. Schematic diagram summarising the distribution of cell wall polysaccharides in the meristem zone of root tip. A, the cellular organization of the root tip. B, mapping of different cell wall polysaccharides in the root tips. The Coloured cells indicate the presence of the corresponding polysaccharide in the cell walls.

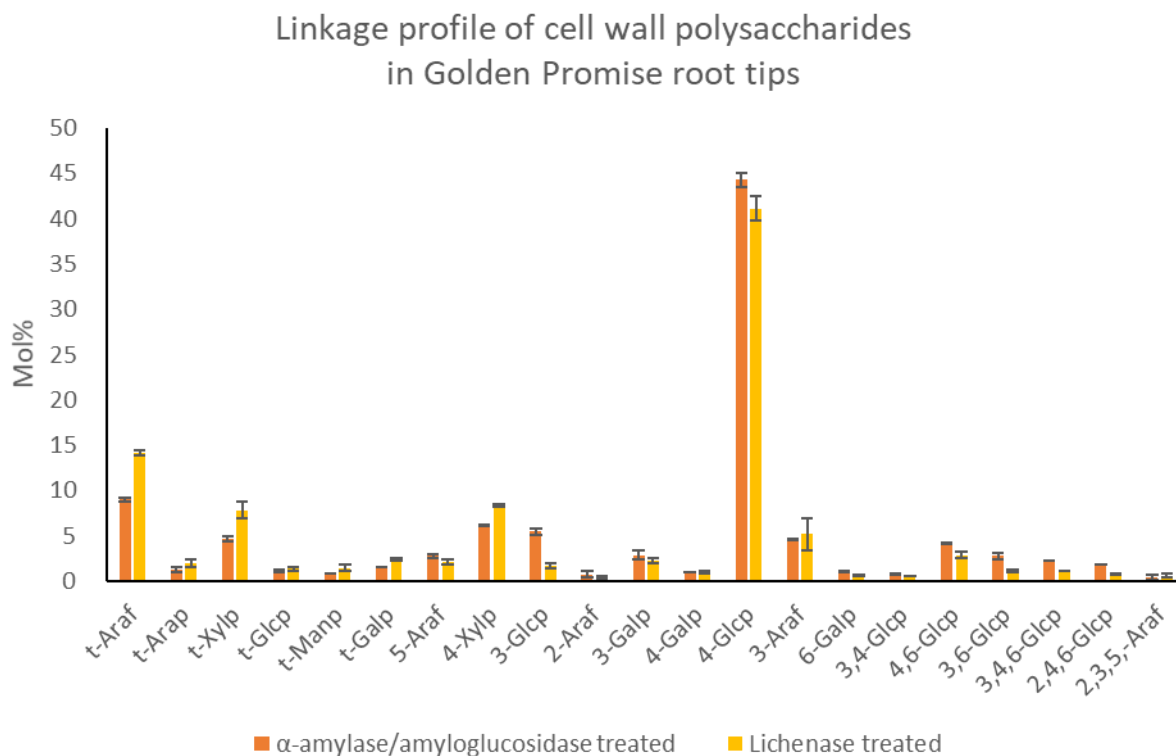


Figure 2-5. Glycosidic linkage analysis of the cell walls of barley root tips. AIR samples were extracted from freeze dried root tips of Golden Promise seedlings. The collected samples were treated with a sequence of α -amylase/amyloglucosidase and lichenase to remove starch and (1,3;1,4)- β -glucan. The products were analysed for their composition in glycosidic linkages. (1,4)-GlcP represent up to 45 mol% of the total glycosidic linkages, followed by arabinose residues. In the lichenase treated samples, reduced (1,3)-GlcP indicate the successful removal of (1,3;1,4)- β -glucan. The remaining (1,3)-GlcP represent the remaining polysaccharides containing (1,3)-linked glucose, including callose. Error bars indicate standard deviations.

Tables**Table 2-1. List of primers used.**

Primer name	Sequence
HvCsIF3_F	CTTGTTGCCGTTGCCTTTACA
HvCsIF3_R	TCAATTGGCTAAAATGGAAGAAAATA
HvCsIF6_F	TGGGCATTACCTTCGTCAT
HvCsIF6_R	TGTCCGGGCAAACATCAA
HvCsIF9_F	CTGCCACCGCGTCCGTGTA
HvCsIF9_R	AGGTTTTGCAGCATTACTTGA
HvCsID1_F	CCGTCCCAGAACTCGCAGAT
HvCsID1_R	CATGACCCACCCACCGTTT
HvCsID2_F	GCCGCACAATTTASCAGCACAA
HvCsID2_R	GCCTGCTAGGGAACCAATA
HvCsID4_F	CGCTGCTCTGGGTCTATATCA
HvCsID4_R	CTGCTTAGGAATCCACCATCA
HvCsIH1_F	TGCTGTGGCTGGATGGTGTT
HvCsIH1_R	GCTTTATTATTGAGAGAGATTGGGAGA
GAPDH_F	GTGAGGCTGGTGCTGATTACG
GAPDH_R	TGGTGCAGCTAGCATTGAGAC
HSP70_F	CGACCAGGGCAACCGCACCAC
HSP70_R	ACGGTGTTGATGGGGTTCATG
α -Tubulin_F	AGTGTCTGTCCACCCACTC
α -Tubulin_R	AGCATGAAGTGGATCCTTGG
Cyclophilin_F	CCTGTCGTGTCGTCGGTCTAAA
Cyclophilin_R	ACGCAGATCCAGCAGCCTAAAG
Hyg_F	GCCGTGGTTGGCTTGTATG
Hyg_R	GGGGCGTCGGTTTCCACTAT

Table 2-2. List of antibodies used.

Epitope	Primary antibody	Type	Secondary antibody	Reference
(1,3;1,4)- β -glucan	BG1	Mouse IgG	Alexa Fluor 488 Goat Anti-mouse IgG	Meikle et al., 1994
Callose	(1,3)- β -glucan	Mouse IgG	Alexa Fluor 488 Goat Anti-mouse IgG	Delmer et al., 1993
Mannan	Anti-mannan	Mouse IgG	Alexa Fluor 488 Goat Anti-mouse IgG	Pettolino et al., 2001
AGP	LM2	Rat IgM	DyLight 550 Goat Anti-rat IgM	Yates et al., 1996
Arabinoxylan	LM11	Rat IgM	DyLight 550 Goat Anti-rat IgM	McCartney et al., 2005
Pectin	LM19	Rat IgM	DyLight 550 Goat Anti-rat IgM	Verhertbruggen et al., 2009

Table 2-3. Measurements of the sizes of the meristem and elongation zones and average number of layers of cortical cells in the meristem zone. The size of the meristem zone was determined by the distance between the root tip and the first most outer cortical cell that doubled in cell length. The size of the elongation zone was determined by the distance from the end of the meristem zone to the first epidermal cell that formed a root hair. The number of cortical cell layers was measured by counting the number of cell files of the cortical cells in the meristem zone. SD represents standard deviations. Sample size N=5.

Line	Size of meristem zone (μm)		Size of elongation zone (μm)		Number of cortical cell layers
	Average	SD	Average	SD	Average
Golden Promise	1100.6	132.9	912.8	59.5	5-6
WI4330	1009.6	221.5	911.9	62.8	5-6
AKA909	1176.8	95.8	948.0	79.9	5-6
AKA237	1132.3	122.7	745.5	83.8	5-6
OUM125	998.7	88.6	548.9	76.4	5-6

References

- Aditya J, Lewis J, Shirley N, Tan H-T, Henderson M, Fincher G, Burton R, Mather D, Tucker M** (2015) The dynamics of cereal cyst nematode infection differ between susceptible and resistant barley cultivars and lead to changes in (1,3;1,4)- β -glucan levels and HvCslF gene transcript abundance. *New Phytologist* **207**: 135-147
- Albersheim P, Darvill A, Roberts K, Sederoff R, Staehelin A** (2010) *Plant cell walls*. Garland Science
- Atmodjo MA, Hao Z, Mohnen D** (2013) Evolving views of pectin biosynthesis. *Annual Review of Plant Biology* **64**: 747-779
- Bacic A, Stone B** (1981) Isolation and ultrastructure of aleurone cell walls from wheat and barley. *Functional Plant Biology* **8**: 453-474
- Baluška F, Liners F, Hlavačka A, Schlicht M, Van Cutsem P, McCurdy DW, Menzel D** (2005) Cell wall pectins and xyloglucans are internalized into dividing root cells and accumulate within cell plates during cytokinesis. *Protoplasma* **225**: 141-155
- Bamforth C** (1982) Barley β -glucans: their role in malting and brewing. *Brewers Dig* **57**: 22-27
- Barclay GF, Peterson CA, Tyree MT** (1982) Transport of fluorescein in trichomes of *Lycopersicon esculentum*. *Canadian Journal of Botany* **60**: 397-402
- Bates TR, Lynch JP** (2000) The efficiency of *Arabidopsis thaliana* (Brassicaceae) root hairs in phosphorus acquisition. *American Journal of Botany* **87**: 964-970
- Bernal A, Yoo C-M, Mutwil M, Jensen J, Hou G, Blaukopf C, Sørensen I, Blancaflor E, Scheller H, Willats W** (2008) Functional analysis of the cellulose synthase-like genes CSLD1, CSLD2, and CSLD4 in tip-growing *Arabidopsis* cells. *Plant Physiology* **148**: 1238-1253
- Buckeridge MS, Rayon C, Urbanowicz B, Tiné MAS, Carpita NC** (2004) Mixed linkage (1-3),(1-4)- β -D-glucans of grasses. *Cereal Chemistry* **81**: 115-127
- Burton RA, Collins HM, Kibble NAJ, Smith JA, Shirley NJ, Jobling SA, Henderson M, Singh RR, Pettolino F, Wilson SM, Bird AR, Topping DL, Bacic A, Fincher GB** (2011) Over-expression of specific HvCslF cellulose synthase-like genes in transgenic barley increases the levels of cell wall (1,3;1,4)- β -D-glucans and alters their fine structure. *Plant Biotechnology Journal* **9**: 117-135
- Burton RA, Fincher GB** (2009) (1,3;1,4)- β -D-glucans in cell walls of the Poaceae, lower plants, and fungi: a tale of two linkages. *Molecular Plant* **2**: 873-882
- Burton RA, Jobling SA, Harvey AJ, Shirley NJ, Mather DE, Bacic A, Fincher GB** (2008) The genetics and transcriptional profiles of the cellulose synthase-like HvCslF gene family in barley. *Plant Physiology* **146**: 1821-1833
- Burton RA, Shirley NJ, King BJ, Harvey AJ, Fincher GB** (2004) The Cesa gene family of barley. Quantitative analysis of transcripts reveals two groups of co-expressed genes. *Plant Physiology* **134**: 224-236
- Burton RA, Wilson SM, Hrmova M, Harvey AJ, Shirley NJ, Medhurst A, Stone BA, Newbigin EJ, Bacic A, Fincher GB** (2006) Cellulose synthase-like CslF genes mediate the synthesis of cell wall (1, 3; 1, 4)- β -D-glucans. *Science* **311**: 1940-1942
- Carpita NC, Defernez M, Findlay K, Wells B, Shoue DA, Catchpole G, Wilson RH, McCann MC** (2001) Cell wall architecture of the elongating maize coleoptile. *Plant Physiology* **127**: 551-565
- Carpita NC, Gibeaut DM** (1993) Structural models of primary cell walls in flowering plants: consistency of molecular structure with the physical properties of the walls during growth. *The Plant Journal* **3**: 1-30
- Carpita NC, Shea EM** (1988) Chromatography-mass spectrometry (GC-MS) of partially. *In* *Analysis of Carbohydrates by GLCMS*, p 157

- Chen XY, Kim JY** (2009) Callose synthesis in higher plants. *Plant Signaling & Behavior* **4**: 489-492
- Ciucanu I, Kerek F** (1984) A simple and rapid method for the permethylation of carbohydrates. *Carbohydrate Research* **131**: 209-217
- Cosgrove D** (1997) Assembly and enlargement of the primary cell wall in plants. *Annual Review of Cell Developmental Biology* **13**: 171-201
- Daum G, Medzihradsky A, Suzaki T, Lohmann JU** (2014) A mechanistic framework for noncell autonomous stem cell induction in Arabidopsis. *Proceedings of the National Academy of Sciences of the United States of America* **111**: 14619-14624
- Dhugga KS, Barreiro R, Whitten B, Stecca K, Hazebroek J, Randhawa GS, Dolan M, Kinney AJ, Tomes D, Nichols S** (2004) Guar seed β -mannan synthase is a member of the cellulose synthase super gene family. *Science* **303**: 363-366
- Ding L, Zhu JK** (1997) A role for arabinogalactan-proteins in root epidermal cell expansion. *Planta* **203**: 289-294
- Doblin MS, De Melis L, Newbigin E, Bacic A, Read SM** (2001) Pollen tubes of *Nicotiana glauca* express two genes from different β -glucan synthase families. *Plant Physiology* **125**: 2040-2052
- Doblin MS, Pettolino FA, Wilson SM, Campbell R, Burton RA, Fincher GB, Newbigin E, Bacic A** (2009) A barley cellulose synthase-like CslH gene mediates (1, 3; 1, 4)- β -D-glucan synthesis in transgenic Arabidopsis. *Proceedings of the National Academy of Sciences of the United States of America* **106**: 5996-6001
- Douchkov D, Lueck S, Hensel G, Kumlehn J, Rajaraman J, Johrde A, Doblin MS, Beahan CT, Kopischke M, Fuchs R, Lipka V, Niks RE, Bulone V, Chowdhury J, Little A, Burton RA, Bacic A, Fincher GB, Schweizer P** (2016) The barley (*Hordeum vulgare*) cellulose synthase-like D2 gene (*HvCslD2*) mediates penetration resistance to host-adapted and nonhost isolates of the powdery mildew fungus. *New Phytologist* **212**: 421-433
- Drakakaki G** (2015) Polysaccharide deposition during cytokinesis: challenges and future perspectives. *Plant Science* **236**: 177-184
- Fincher G** (1975) Morphology and chemical composition of barley endosperm cell walls. *Journal of the Institute of Brewing* **81**: 116-122
- Fincher G** (1986) Cell walls and their components in cereal grain technology. *Advances in Cereal Science Technology* **8**: 207-295
- Gibeaut DM, Carpita NC** (1991) Tracing cell wall biogenesis in intact cells and plants: selective turnover and alteration of soluble and cell wall polysaccharides in grasses. *Plant Physiology* **97**: 551-561
- Gibeaut DM, Pauly M, Bacic A, Fincher GB** (2005) Changes in cell wall polysaccharides in developing barley (*Hordeum vulgare*) coleoptiles. *Planta* **221**: 729-738
- González-Calle V, Barrero-Sicilia C, Carbonero P, Iglesias-Fernández R** (2015) Mannans and endo- β -mannanases (MAN) in *Brachypodium distachyon*: expression profiling and possible role of the BdMAN genes during coleorhiza-limited seed germination. *Journal of Experimental Botany* **66**: 3753-3764
- Goubet F, Barton CJ, Mortimer JC, Yu X, Zhang Z, Miles GP, Richens J, Liepman AH, Seffen K, Dupree P** (2009) Cell wall glucomannan in Arabidopsis is synthesised by CSLA glycosyltransferases, and influences the progression of embryogenesis. *The Plant Journal* **60**: 527-538
- He C, Zhang J, Liu X, Zeng S, Wu K, Yu Z, Wang X, Da Silva JAT, Lin Z, Duan J** (2015) Identification of genes involved in biosynthesis of mannan polysaccharides in *Dendrobium officinale* by RNA-seq analysis. *Plant Molecular Biology* **88**: 219-231
- Höfte H, Peaucelle A, Braybrook S** (2012) Cell wall mechanics and growth control in plants: the role of pectins revisited. *Frontiers in Plant Science* **3**: 121-126
- Houston K, Tucker MR, Chowdhury J, Shirley N, Little A** (2016) The plant cell wall: a

complex and dynamic structure as revealed by the responses of genes under stress conditions. *Frontiers in Plant Science* **7**: 984-1001

Kim CM, Park S, Je BI, Park S, Park S, Piao H-L, Eun M, Dolan L, Han C-d (2007) OsCSLD1, a Cellulose Synthase-Like D1 gene, is required for root hair morphogenesis in rice. *Plant Physiology* **143**: 1220-1230

Kim JB, Olek AT, Carpita NC (2000) Cell wall and membrane-associated exo- β -D-glucanases from developing maize seedlings. *Plant Physiology* **123**: 471-486

Kirschner GK, Stahl Y, Von Korff M, Simon R (2017) Unique and conserved features of the barley root meristem. *Frontiers in Plant Science* **8**: 1240-1240

Knipfer T, Fricke W (2010) Water uptake by seminal and adventitious roots in relation to whole-plant water flow in barley (*Hordeum vulgare* L.). *Journal of Experimental Botany* **62**: 717-733

Kučerová D, Kollárová K, Vatehová Z, Lišková D (2016) Interaction of galactoglucomannan oligosaccharides with auxin involves changes in flavonoid accumulation. *Plant Physiology and Biochemistry* **98**: 155-161

Li M, Xiong G, Li R, Cui J, Tang D, Zhang B, Pauly M, Cheng Z, Zhou Y (2009) Rice cellulose synthase-like D4 is essential for normal cell-wall biosynthesis and plant growth. *The Plant Journal* **60**: 1055-1069

Li R, Xiong G, Zhang B, Zhou Y (2010) Rice plants response to the disruption of OsCSLD4 gene. *Plant Signaling & Behavior* **5**: 136-139

Little A, Lahnstein J, Jeffery DW, Khor SF, Schwerdt JG, Shirley NJ, Hooi M, Xing X, Burton RA, Bulone V (2019) A novel (1, 4)- β -linked glucoxylan is synthesized by members of the Cellulose Synthase-Like F gene family in land plants. *ACS Central Science* **5**: 73-84

Little A, Schwerdt JG, Shirley NJ, Khor SF, Neumann K, O'Donovan LA, Lahnstein J, Collins HM, Henderson M, Fincher GB, Burton RA (2018) Revised phylogeny of the Cellulose Synthase Genes Superfamily: insights into cell wall evolution. *Plant Physiology* **177**: 1124-1141

Marzec M, Muszynska A, Melzer M, Sas-Nowosielska H, Kurczynska EU (2014) Increased symplasmic permeability in barley root epidermal cells correlates with defects in root hair development. *Plant Biology* **16**: 476-484

Marzec M, Szarejko I, Melzer M (2014) Arabinogalactan proteins are involved in root hair development in barley. *Journal of Experimental Botany* **66**: 1245-1257

McCartney L, Marcus SE, Knox JP (2005) Monoclonal antibodies to plant cell wall xylans and arabinoxylans. *Journal of Histochemistry and Cytochemistry* **53**: 543-546

Meier H, Reid JSG (1982) Reserve polysaccharides other than starch in higher plants. *In* FA Loewus, W Tanner, eds, *Plant Carbohydrates I: Intracellular Carbohydrates*. Springer Berlin Heidelberg, Berlin, Heidelberg, pp 418-471

Miart F, Desprez T, Biot E, Morin H, Belcram K, Höfte H, Gonneau M, Vernhettes S (2014) Spatio-temporal analysis of cellulose synthesis during cell plate formation in *Arabidopsis*. *The Plant Journal* **77**: 71-84

Milewska-Hendel A, Witek W, Rypień A, Zubko M, Baranski R, Stróż D, Kurczyńska EU (2019) The development of a hairless phenotype in barley roots treated with gold nanoparticles is accompanied by changes in the symplasmic communication. *Scientific Reports* **9**: 4724-4258

Mohnen D (2008) Pectin structure and biosynthesis. *Current Opinion in Plant Biology* **11**: 266-277

Northcote D, Davey R, Lay J (1989) Use of antisera to localize callose, xylan and arabinogalactan in the cell-plate, primary and secondary walls of plant cells. *Planta* **178**: 353-366

Pettolino FA, Hoogenraad NJ, Ferguson C, Bacic A, Johnson E, Stone BA (2001) A (1-4)- β -mannan-specific monoclonal antibody and its use in the immunocytochemical

- location of galactomannans. *Planta* **214**: 235-242
- Piršelová B, Matušíková I** (2013) Callose: the plant cell wall polysaccharide with multiple biological functions. *Acta Physiologiae Plantarum* **35**: 635-644
- Richmond TA, Somerville CR** (2001) Integrative approaches to determining Csl function. *In* Plant cell walls. Springer, pp 131-143
- Šamaj J, Braun M, Baluška F, Ensikat H-J, Tsumuraya Y, Volkmann D** (1999) Specific localization of arabinogalactan-protein epitopes at the surface of maize root hairs. *Plant Cell Physiology* **40**: 874-883
- Scheller HV, Ulvskov P** (2010) Hemicelluloses. *Annual Review of Plant Biology* **61**
- Schiefelbein JW, Benfey PN** (1991) The development of plant roots: new approaches to underground problems. *The Plant Cell* **3**: 1147
- Schreiber M, Wright F, MacKenzie K, Hedley PE, Schwerdt JG, Little A, Burton RA, Fincher GB, Marshall D, Waugh R, Halpin C** (2014) The barley genome sequence assembly reveals three additional members of the CslF (1,3;1,4)- β -glucan synthase gene family. *Plos One* **9**: e90888
- Schwerdt JG** (2017) The evolutionary history and dynamics of the cellulose synthase superfamily. University of Adelaide
- Schwerdt JG, MacKenzie K, Wright F, Oehme D, Wagner JM, Harvey AJ, Shirley NJ, Burton RA, Schreiber M, Halpin C, Zimmer J, Marshall DF, Waugh R, Fincher GB** (2015) Evolutionary dynamics of the Cellulose Synthase gene superfamily in grasses. *Plant Physiology* **168**: 968-983
- Shevell DE, Leu W-M, Gillmor CS, Xia G, Feldmann KA, Chua N-H** (1994) EMB30 is essential for normal cell division, cell expansion, and cell adhesion in *Arabidopsis* and encodes a protein that has similarity to Sec7. *Cell* **77**: 1051-1062
- Somssich M, Khan GA, Persson S** (2016) Cell wall heterogeneity in root development of *Arabidopsis*. *Frontiers in Plant Science* **7**: 1242-1252
- Stahl Y, Grabowski S, Bleckmann A, Kühnemuth R, Weidtkamp-Peters S, Pinto KG, Kirschner GK, Schmid JB, Wink RH, Hülsewede A** (2013) Moderation of *Arabidopsis* root stemness by CLAVATA1 and ARABIDOPSIS CRINKLY4 receptor kinase complexes. *Current Biology* **23**: 362-371
- Suzuki K, Kitamura S, Kato Y, Itoh T** (2000) Highly substituted glucuronoarabinoxylans (hsGAXs) and low-branched xylans show a distinct localization pattern in the tissues of *Zea mays* L. *Plant Cell Physiology* **41**: 948-959
- Taketa S, Yuo T, Tonooka T, Tsumuraya Y, Inagaki Y, Haruyama N, Larroque O, Jobling SA** (2011) Functional characterization of barley betaglucanless mutants demonstrates a unique role for CslF6 in (1, 3; 1, 4)- β -D-glucan biosynthesis. *Journal of Experimental Botany* **63**: 381-392
- Tonooka T, Aoki E, Yoshioka T, Taketa S** (2009) A novel mutant gene for (1-3, 1-4)- β -D-glucanless grain on barley (*Hordeum vulgare* L.) chromosome 7H. *Breeding Science* **59**: 47-54
- Trethewey JA, Campbell LM, Harris PJ** (2005) (1-3),(1-4)- β -D-glucans in the cell walls of the Poales (sensu lato): an immunogold labeling study using a monoclonal antibody. *American Journal of Botany* **92**: 1660-1674
- Trethewey JA, Harris P** (2002) Location of (1-3)-and (1-3),(1-4)- β -D-glucans in vegetative cell walls of barley (*Hordeum vulgare*) using immunogold labelling. *New Phytologist* **154**: 347-358
- Tucker MR, Lou H, Aubert MK, Wilkinson LG, Little A, Houston K, Pinto SC, Shirley NJ** (2018) Exploring the role of cell wall-related genes and polysaccharides during plant development. *Plants* **7**: 42-58
- Ursache R, Andersen TG, Marhavý P, Geldner N** (2018) A protocol for combining fluorescent proteins with histological stains for diverse cell wall components. *The Plant Journal* **93**: 399-412

- van den Berg C, Willemsen V, Hendriks G, Weisbeek P, Scheres B** (1997) Short-range control of cell differentiation in the Arabidopsis root meristem. *Nature* **390**: 287-289
- Vandesompele J, De Preter K, Pattyn F, Poppe B, Van Roy N, De Paepe A, Speleman F** (2002) Accurate normalization of real-time quantitative RT-PCR data by geometric averaging of multiple internal control genes. *Genome Biology* **3**: research0034. 0031
- Verhertbruggen Y, Marcus SE, Haeger A, Ordaz-Ortiz JJ, Knox JP** (2009) An extended set of monoclonal antibodies to pectic homogalacturonan. *Carbohydrate Research* **344**: 1858-1862
- Verhertbruggen Y, Yin L, Oikawa A, Scheller HV, behavior** (2011) Mannan synthase activity in the CslD family. *Plant Signaling* **6**: 1620-1623
- Wilkie KCB** (1979) The hemicelluloses of grasses and cereals. *In* *Advances in Carbohydrate Chemistry and Biochemistry*, Vol 36. Elsevier, pp 215-264
- Wilson SM, Burton RA, Doblin MS, Stone BA, Newbigin EJ, Fincher GB, Bacic A** (2006) Temporal and spatial appearance of wall polysaccharides during cellularization of barley (*Hordeum vulgare*) endosperm. *Planta* **224**: 655-667
- Wolf S, Deom CM, Beachy R, Lucas WJ** (1991) Plasmodesmatal function is probed using transgenic tobacco plants that express a virus movement protein. *The Plant Cell* **3**: 593-604
- Yates EA, Valdor J-F, Haslam SM, Morris HR, Dell A, Mackie W, Knox JP** (1996) Characterization of carbohydrate structural features recognized by anti-arabinogalactan-protein monoclonal antibodies. *Glycobiology* **6**: 131-139
- Yin L, Verhertbruggen Y, Oikawa A, Manisseri C, Knierim B, Prak L, Jensen JK, Knox JP, Auer M, Willats WG** (2011) The cooperative activities of CSLD2, CSLD3, and CSLD5 are required for normal Arabidopsis development. *Molecular Plant* **4**: 1024-1037
- Yu Q, Hlavacka A, Matoh T, Volkmann D, Menzel D, Goldbach HE, Baluška F** (2002) Short-term boron deprivation inhibits endocytosis of cell wall pectins in meristematic cells of maize and wheat root apices. *Plant Physiology* **130**: 415-421

Chapter 3

Cellulose synthase-like F (CslF) genes control barley root growth and differentiation by mediating cell wall polysaccharide synthesis



Statement of Authorship

Title of Paper	Cellulose synthase-like F (CslF) genes control barley root growth and differentiation by mediating cell wall polysaccharide synthesis
Publication Status	<input type="checkbox"/> Published <input type="checkbox"/> Accepted for Publication <input type="checkbox"/> Submitted for Publication <input checked="" type="checkbox"/> Unpublished and Unsubmitted work written in manuscript style
Publication Details	Cellulose synthase-like F (CslF) genes control barley root growth and differentiation by mediating cell wall polysaccharide synthesis Haoyu Lou, Neil Shirley, Jelle Lahnstein, Rachel Burton, Riccardo Fusi, Xiujuan Yang, Chao Ma, Leah Band, Malcolm Bennett, Matthew Tucker, Vincent Bulone

Principal Author

Name of Principal Author (Candidate)	Haoyu Lou		
Contribution to the Paper	Performed experiments and analysed data. Wrote the manuscript.		
Overall percentage (%)	70%		
Certification:	This paper reports on original research I conducted during the period of my Higher Degree by Research candidature and is not subject to any obligations or contractual agreements with a third party that would constrain its inclusion in this thesis. I am the primary author of this paper.		
Signature		Date	24/02/2020

Co-Author Contributions

By signing the Statement of Authorship, each author certifies that:

the candidate's stated contribution to the publication is accurate (as detailed above);

permission is granted for the candidate to include the publication in the thesis; and

the sum of all co-author contributions is equal to 100% less the candidate's stated contribution.

Name of Co-Author	Vincent Bulone		
Contribution to the Paper	Principle supervisor. Conceived the project and designed experiments. Assisted with writing of the manuscript. I hereby certify that the statement of authorship is accurate.		
Signature		Date	24/02/2020

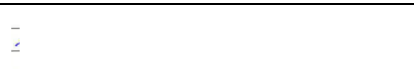
Name of Co-Author	Matthew Tucker
-------------------	----------------

Chapter 3 – *Cellulose synthase-like F (CslF)* genes control barley root growth and differentiation by mediating cell wall polysaccharide synthesis

Contribution to the Paper	Co-supervisor. Conceived the project and designed experiments. Assisted with writing of the manuscript. I hereby certify that the statement of authorship is accurate.		
Signature		Date	24/02/2020

Name of Co-Author	Malcolm Bennett		
Contribution to the Paper	Co-supervisor at University of Nottingham. Conceived the project and designed experiments. Assisted with writing of the manuscript. I hereby certify that the statement of authorship is accurate.		
Signature		Date	24/2/20

Name of Co-Author	Leah Band		
Contribution to the Paper	Co-supervisor at University of Nottingham. Conceived the project and designed experiments. Assisted with writing of the manuscript. I hereby certify that the statement of authorship is accurate.		
Signature		Date	25/02/2020

Name of Co-Author	Neil Shirley		
Contribution to the Paper	Assisted with experiment and data analysis. I hereby certify that the statement of authorship is accurate.		
Signature		Date	25/2/2020

Name of Co-Author	Jelle Lahnstein		
Contribution to the Paper	Assisted with experiment and data analysis and editing of the manuscript. I hereby certify that the statement of authorship is accurate.		

Chapter 3 – *Cellulose synthase-like F (CslF)* genes control barley root growth and differentiation by mediating cell wall polysaccharide synthesis

Signature		Date	25/2/2020
-----------	--	------	-----------

Name of Co-Author	Rachel Burton		
Contribution to the Paper	Provide transgenic material for analysis I hereby certify that the statement of authorship is accurate.		
Signature		Date	24/02/2020

Name of Co-Author	Xiujuan Yang		
Contribution to the Paper	Assisted with experiment and data analysis. I hereby certify that the statement of authorship is accurate.		
Signature		Date	24/02/2020

Name of Co-Author	Chao Ma		
Contribution to the Paper	Assisted with experiment and data analysis. I hereby certify that the statement of authorship is accurate.		
Signature		Date	24/02/2020

Name of Co-Author	Riccardo Fusi		
Contribution to the Paper	Assisted with experiment and data analysis. I hereby certify that the statement of authorship is accurate.		
Signature		Date	27/02/2020

Abstract

Plant cell walls are composed of polymers that confer distinct chemical and mechanical properties. Enzymes involved in the formation of cell walls are encoded by large gene families and represent attractive targets to modify cell wall composition for novel applications in agriculture and food processing. However, we currently lack information regarding the functions of many putative cell wall-related genes. The barley *CslF* gene family includes 9 members, which are related to the *CesA* genes involved in cellulose biosynthesis and the *CsID* genes that influence root hair development in Arabidopsis. Characterization of the barley *CslF* genes has focused mainly on the grain, and only *HvCslF6* has been shown to play a significant role *in planta*, contributing to the synthesis of (1,3;1,4)- β -glucan. Tissue-specific qPCR studies revealed that *HvCslF3* and *HvCslF9* accumulate in the barley root tip, suggesting a potential role during root development. In order to further understand the roles of *HvCslF3* and *HvCslF9*, genetic, molecular, microscopic and computational mathematical approaches were used. qPCR and RNA *in situ* hybridization revealed that *HvCslF3* and *HvCslF9* accumulate in the elongation and young differentiation regions of the root, and levels are notably higher than *HvCslF6*, which was the most highly expressed *CslF* gene in other studied tissues. In *HvCslF3* and *HvCslF9* RNAi knock-down lines, roots exhibited slower growth rates due to the reduced elongation length and decreased numbers of cortical cell layers. Shorter seminal and lateral roots, and less root hairs observed in agar environments, resulting in significant reduction of the overall root system and surface area. Immunolocalization of major cell wall polysaccharides revealed the absence of (1,3;1,4)- β -glucan in *HvCslF9-RNAi* root tips, suggesting a role of *HvCslF9* in (1,3;1,4)- β -glucan synthesis in the newly formed primary cell walls of the meristem and elongation zones. In contrast, *HvCslF3-RNAi* lines showed normal (1,3;1,4)- β -glucan accumulation, but a reduction in (1,4)- β -linked glucoxytan levels, consistent with recent studies of *HvCslF3* in *Nicotiana benthamiana*. CRISPR/Cas9 knockout lines have also been generated

Chapter 3 – *Cellulose synthase-like F (CslF)* genes control barley root growth and differentiation by mediating cell wall polysaccharide synthesis

to probe the developmental functions of these genes at a cellular level. Our study provides insight into the role of *CslF* genes in the regulation of cell wall polysaccharide biosynthesis in barley root tips and their key role in root development.

Introduction

Barley was one of the first cereal crops domesticated for agricultural uses and the cultivation history can be traced back over 10,000 years (Newman and Newman, 2006; Ullrich, 2010). Nowadays, barley is the fourth most important crop worldwide, and its products are utilised in diverse applications, including traditional uses for malting and brewing, whilst there is increasing interest in using barley for healthy food related products (Ullrich, 2010). Barley also plays a significant role in many research fields as an experimental organism for plant genetics, physiology, agronomy, nutrition, pathology and entomology (Ullrich, 2010). Barley is a self-pollinated, diploid monocot species with seven pairs of chromosomes, and its genome has been sequenced (The International Barley Genome Sequencing et al., 2012; Mascher et al., 2017). This provides an excellent fundamental basis to support studies aimed at revealing the genetic basis for barley growth and development.

Many studies have focused on barley reproductive development over the past decades because of the direct effects on grain quality and yield. Less attention has been dedicated to understanding the development of vegetative organs including roots, despite their importance during plant growth. Barley develops a fibrous root system composed of distinct root types that form at different developmental stages. Primary and seminal root primordia are formed during embryogenesis, and unlike other cereals such as rice or maize, it is difficult to distinguish the two types of roots in barley (Luxová, 1986; Kirschner et al., 2017). The post-embryonic roots, i.e. the nodal roots, are shoot-borne and constitute the majority of the root system in the subsequent life of the barley plant (Orman-Ligeza et al., 2013; Kirschner et al., 2017). The roots provide mechanical strength to anchor the plant in soil, and absorb water and minerals to support plant growth by transporting these nutrients to the other parts of the plant (Imani et al., 2011). The roots can be divided into meristematic, elongation and maturation zones, representing all cellular developmental stages along the root longitudinal axis (Ivanov and

Dubrovsky, 2013). Although the pathways have not been comprehensively characterised in barley, evidence from research in *Arabidopsis* suggests that the development of different root regions is dependent upon multiple hormone signals, including auxin, gibberellic acid, cytokinin, and brassinosteroids (Kirschner et al., 2017).

Barley root tissues are organized in a centripetal symmetric pattern. The radial patterning is established in the root meristem at an early stage of root development. The root apical meristem (RAM) gives rise to different cell types and root tissues. The RAM contains a group of quiescent centre (QC) cells that maintain their identity and those of the surrounding initial cells, while allowing daughter cells (no longer in direct contact) to undergo division and differentiation to establish the radial pattern (Somssich et al., 2016). The central stele contains a metaxylem and eight small xylem vessels, while the surrounding cell layers include pericycle, endodermis, cortex and epidermis (Kirschner et al., 2017). Chimungu et al. (2014) reported that the patterning of root tissues is associated with drought resistance at a functional level. Once cells transit to the elongation zone, cell division ceases and rapid longitudinal expansion occurs. The cell expansion process is regulated by various hormones, mediated by a plethora of downstream genes including cell wall synthesis and modification enzymes (Petricka et al., 2012). In the maturation zone, cells cease elongating, fully differentiating and gaining specialised functions.

The cell wall plays an important role during plant development. Cell walls surround the cells to support the flexibility and stability of cell structures. They also function against pathogen defence, and act as carbohydrate sinks to meet the growth requirements of the plant (Tucker et al., 2018). The synthesis and composition of cell walls are complex, and the heterogeneity of *Arabidopsis* cell walls of different root tissues has been reported previously (Somssich et al., 2016). Consistent with this observation, variation on polysaccharide composition in different cell types of barley roots highlights the heterogeneous nature of cell

walls (Chapter 2).

Cellulosic and non-cellulosic polysaccharides, phenolic acids and proteins form the cell wall matrix (Fincher, 2009). Cell wall polysaccharide synthesis and modification are the result of the action of glycosyltransferases (GTs), glycoside hydrolases (GHs), methyltransferases and acetyltransferases (Lombard et al., 2014; Tucker et al., 2018). One large group of glycosyltransferases is represented by the *Cellulose synthase (CesA)* and *Cellulose synthase-like (Csl)* families. Studies have shown their roles in the synthesis of various cell wall polysaccharides, including cellulose (*CesA*) (Doblin et al., 2002), (1,3;1,4)- β -glucan (*CslF*, *CslH*, *CslJ*) (Burton et al., 2006; Doblin et al., 2009; Taketa et al., 2011; Cseh et al., 2013), mannan (*CslA*, *CslD*) (Goubet et al., 2009; Verhertbruggen et al., 2011; Yin et al., 2011), callose (*CslD*) (Douchkov et al., 2016), (1,4)- β -linked glucoxytan (*CslF*) (Little et al., 2019), and xyloglucan (*CslC*) (Cocuron et al., 2007). Recent studies on *Csl* genes demonstrated their importance during root development; for instance, *cslD2/3/5* mutants in *Arabidopsis* develop small plants with disrupted root hair development (Yin et al., 2011), while similar phenotypes were also described in the rice *cslD1* and *cslD4* mutants (Kim et al., 2007; Li et al., 2009).

Burton et al. (2008) analysed expression profiles of seven *HvCslF* genes in barley and noted the high abundance of *HvCslF6* in most barley tissues. Expression of *HvCslF3* and *HvCslF9*, specifically in rapidly growing organs, was also reported (Burton et al., 2008), which suggests a potential role in meristem development. However, whether these genes are essential to root growth remains unknown. Of the nine *CslF* genes in the barley genome, only *HvCslF6* has been studied in detail, in terms of its role during the synthesis and regulation of (1,3;1,4)- β -glucan, one of the major hemicellulose found in barley primary cell walls (Burton et al., 2006; Taketa et al., 2011; Schwerdt et al., 2015). Heterologous studies have highlighted a potential role of *HvCslF3* and *HvCslF9* in the synthesis of (1,4)- β -linked glucoxytan and (1,3;1,4)- β -glucan, respectively (Cseh et al., 2013; Little et al., 2019), although this has not been confirmed

in planta. In this study, we used transgenic barley plants downregulated in *HvCslF3* and *HvCslF9* expression to probe their roles in root development. A range of methods including morphological analysis, phenotypic assays, immunohistochemistry, and compositional analysis, were used to demonstrate the importance of these genes in root elongation, root tissue patterning, and cell wall polysaccharides synthesis.

Materials and methods

Plant material preparation

The RNAi lines were developed by Prof. Rachel Burton (University of Adelaide) by expressing 35S promoter driven hairpin sequence in a Gateway destination vector. Seeds of the barley cultivar Golden Promise and homozygous transgenic lines (#27, #29, #30, #33, #34, #36) were harvested from glasshouse grown plants and used in the present experiments. Prior to sowing, all seeds were surface sterilized in 20% (v/v) sodium hypochlorite solution for 10 min, then rinsed with MilliQ water five times before pre-germination overnight. Root material from germinated seeds was harvested according to the requirements of the different experiments.

RNA extraction and cDNA synthesis

Plate germinated seeds were kept in the dark for 5 days. Whole root tip (1 cm) and dissected root tips (0-1 mm, 1-2 mm, 3-5 mm, and 5-10 mm from the tips) were harvested using a razor blade, collected in tubes pre-chilled in liquid nitrogen, and stored at -80°C before processing. The dissected regions represent meristem, elongation, young maturation and old maturation zones of root tips. The Spectrum Plant Total RNA Kit (Sigma-Aldrich) was used to extract total RNA according to the protocol provided by the manufacturer. DNA residues were removed using the TURBO DNA-free kit (Ambion). The SuperscriptIII Reverse Transcriptase kit (Invitrogen) was used to synthesize cDNA following the manufacturer's instructions, except

that during the final extension step, only 0.25 μ l of enzyme was added. Once synthesized, the cDNA samples were tested with the *HvGAPDH* (HORVU6Hr1G054520) control gene primers to ensure the quality of reverse transcription.

Quantitative polymerase chain reaction (qPCR)

The primers used in the present study are listed in Table 3-1. Primers were designed using Primer3 aiming to include the end of the coding sequences to the 3'-untranslated region (3'UTR) of each gene. qPCR was performed following Burton et al. (2004). The raw transcript abundance data were normalized against normalization factors calculated according to the transcript levels of housekeeping genes, namely *HvGAPDH* (HORVU6Hr1G054520), *HvTubulin* (HORVU1Hr1G081280), *HvHSP70* (HORVU5Hr1G113180), and *HvCyclophilin* (HORVU6Hr1G012570) (Vandesompele et al., 2002). The data shown are from representatives of three replicate experiments. The fold changes of transcript abundance were expressed in Log values with respect to the reference genes.

mRNA *in situ* hybridization

Fresh Golden Promise root tips (2 cm) at 5 days post germination (dpg) were harvested and fixed in Formalin-Acetic acid-Alcohol (FAA) (50%v/v 100% ethanol, 5%v/v glacial acetic acid, 25%v/v 16% paraformaldehyde (electron microscopy grade), 20%v/v diethyl pyrocarbonate (DEPC)-H₂O, 0.1%v/v Tween 20). Root tips with FAA were placed on ice for 2 h including 15 min of vacuum infiltration, followed by two 10 min washes in 70% ethanol/DEPC-H₂O, and then stored at 4°C overnight. The samples were dehydrated and cleared with a series of ethanol and Histochoice washes before being embedded in molten paraffin wax. The embedded samples were stored at 4°C under RNase free conditions before sectioning. The paraffin wax blocks with the root samples were sectioned at 7 μ m thickness using a Leica microtome and mounted onto poly-L-lysine coated slides prior to *in situ* hybridization.

Digoxigenin-labeled antisense and sense probes were synthesized according to Yang et al. (2018). The probes specific to *HvCslF3* and *HvCslF9* were amplified from Golden Promise root cDNA, using primers fused with the T7 promoter sequence at the 5' end to allow *in vitro* transcription. The probes were designed to recognize the end of the coding sequence and 3' untranslated region (UTR) of each gene (Figure 3-S1). The barley histone H4 gene was used as a positive control. The *in situ* hybridization and detection were performed using the InsituPro VSi robot (Intavis) with protocol described by Zeng et al. (2017).

Root growth rate measurement

Surface sterilized and pre-germinated seeds (Golden Promise, #27, #29, #30, #33, #34, and #36) were placed onto 1% agar plates (pH5.8) with the embryo side down for growth. Plates were kept vertically in a growth chamber (16/8 hours, 23°C, day/night) to allow the roots to grow downwards. The growth of roots was traced daily for seven days, and all data were collected at the approximate same time every day. Growth rates were defined by the increment of the root total length per seedling per day. The data shown are the average of measurements on 12 seedlings.

Root hair quantification

Root tips of 7 dpg seedlings grown on agar plates were photographed using a Zeiss Stemi SV 6 microscope to determine the root hair number on the surface of the root tips, and the photos were processed with the Zeiss Zen software. Only the seminal roots growing flat on the agar surface were selected for the measurements. The determination of the number of root hairs was performed using Fiji ImageJ. The measurement were made on the surface of approximately 40 mm root tips, on section of 5 mm. The root hair numbers were calculated from the average of 10 seminal root tips per barley line.

Root clearing with Hoyer's solution

Barley seeds were surface sterilized and germinated on a sealed Petri dish for five days at room temperature in the dark. Fresh seminal root tips were collected and fixed in freshly prepared FAA as described above. The dehydration and clearing protocols were performed as per Wilkinson and Tucker (2017). The cleared specimens were photographed using a Zeiss Axio Imager M2 microscope and an AxioCam MR R3 camera under bright field. The data were processed with the Zeiss ZEN imaging software.

Analysis of root tip morphology by microscopy

Barley seeds were placed on 1% agar (pH 5.8) plates and grown in a growth chamber under controlled conditions (24 hours light, 21°C). Seminal root tips of 5 dpg seedlings were collected to study the cellular structure and tissue arrangement in the root tips.

To visualize the longitudinal structure of the root tips, 2 cm of the root tips were fixed in freshly prepared 4% paraformaldehyde in PBS (w/v, pH 6.9) for 2 h at room temperature under vacuum infiltration. The fixed tissues were washed with PBS twice before clearing with aClearSee solution. The protocol for root tissue clearing and staining was adapted from Ursache et al. (2018) with the following modifications: root samples were cleared for at least one week before staining, and the ClearSee solution was changed every two days; roots were stained with Direct Yellow 96 (Sigma, CAS-No: 61725-08-4) in the ClearSee solution (0.1% w/v; excitation 488 nm, emission 519 nm) for two hours under vacuum infiltration. Cleared and stained specimens were stored in ClearSee solution at room temperature before further analysis. The root longitudinal images were taken using the Leica SP8 confocal microscope. The centre of the root tip was captured by z-stacks to follow the root cell files from the meristem to the maturation zones. Images were processed and stitched using Fiji ImageJ (Schindelin et al., 2012) and Adobe Photoshop. The data shown represent the average of 10 root tip specimens per barley

line.

For the root transverse imaging, 1.5 cm of fresh seminal root tips were collected and immediately embedded into 3.5% agarose. The solidified agarose blocks were mounted onto a metal specimen holder and sectioned transversely at 100 μm using a vibratome. A staining solution of 0.1% Calcofluor White (excitation 405 nm, emission 425-275 nm) was used to stain the cell walls. The cross sections were photographed with a Leica SP5 inverted confocal microscope. The data were processed using Fiji ImageJ (Schindelin et al., 2012) to adjust the brightness. The pictures shown are representatives of 10 root tips per barley line.

Immunolocalisation of major cell wall polysaccharides in barley root tips

Barley seeds were germinated for 5 days in the dark, and 5 mm of fresh root tips were collected for fixation and embedding. Specimens were fixed in TEM fixative in PBS (0.25% glutaraldehyde, 4% paraformaldehyde, 4% sucrose) overnight with at least one-hour vacuum infiltration. The fixed root tips were rinsed in PBS twice for 8 h. Root tips were embedded in 4% agarose gel to the desired angle and orientation, and the agarose gels were shaped to cuboid using a razor blade. The following steps for dehydration and LM White Resin embedding were carried out according to Burton et al. (2011). Longitudinal sections at 1 μm were sectioned using a Leica Microtome EM UC6 with either a glass or diamond knife. The sections were mounted onto glass slides and dried on a hot plate at 60°C for at least 1 h. The antibodies specific to (1,3;1,4)- β -glucan, callose, arabinogalactan protein (AGP), mannan, arabinoxylan and pectin were used for immunolabelling, and the detailed antibody list is recorded in Table 3-2. The immunolabelling was performed as described in Burton et al. (2011). Images were taken and processed by an Axio Imager M2 microscope using an AxioCam MR R3 camera and Zeiss ZEN imaging software.

Enzymatic hydrolysis, oligosaccharide fractionation and (1,4)- β -linked glucoxytan

quantification

Surface sterilized barley seeds were soaked in water overnight before being placed into germination pouches (Phytotec). Water was supplied as required and 1 cm of root tips was harvested at day 5 using a razor blade. Fresh root materials were transferred into liquid nitrogen pre-chilled tubes and freeze-dried overnight. Dried root materials were then grounded with a Retsch Mill tissue grinder and kept at room temperature in a dry environment. The alcohol insoluble residues (AIR) of each sample were extracted according to Little et al. (2019), except that the materials were resuspended and washed in a sequence of 1 ml of 70% ethanol, 100% ethanol, and 100% acetone, and dried under vacuum (SpeedVac). Five mg of AIR samples was hydrolysed with cellulase (endo-glucanase, *Trichoderma longibrachiatum* (E-CELTR), Megazyme). The AIR samples were mixed with 20 μ l 100% ethanol before adding the hydrolysis buffer (0.7% (v/v) E-CELTR and 2% (v/v) 1M sodium acetate in water). The mixtures were kept at 40°C for 18 h, rotated gently on a slow rotation shaker. The hydrolysed samples were centrifuged for 10 min at 10,000g and the supernatants were fractionated on graphitized carbon SPE cartridges (1 ml/50 mg, Bond Elute, Agilent Technologies). The cartridges were pre-treated with 1 ml 100% acetonitrile and 1 ml water. One ml of supernatant was loaded onto the cartridges, which are washed in water. Elution was performed with 8% acetonitrile followed by 55% acetonitrile to extract the remaining oligosaccharides. The oligosaccharide fractions were dried on a rotary evaporator and re-dissolved in 50 μ l water. A Dionex ICS-5000 (Thermo Fisher Scientific) with a CarboPac PA200 (3 \times 250 mm) column with guard (3 \times 50mm) was used to analyze the fractions (Little et al., 2019) with modifications on solvents (A, 0.1 M sodium hydroxide; B, 0.1 M sodium hydroxide, 1 M sodium acetate; C, water; D, 20 mM sodium hydroxide, 100 mM sodium acetate) and gradients (Figure 3-8), in order to optimise the separation of Glcp-(1,4)- β -Xylp from xylobiose, and Xylp-(1,4)- β -Glcp from cellobiose, as well as separation from larger oligosaccharides that were eluted later in the

chromatogram. Samples were injected using the Pushpartial_1s mode with a 10 µl partial loop, limited sample injection mode was used. Results show the average of three reproducible replicates.

Results

***HvCslF3* and *HvCslF9* are expressed in different zones of barley root tips**

High levels of *HvCslF3* and *HvCslF9* expression were previously reported in young roots by Burton et al. (2008). In the present study, gene expression analysis was performed on RNA collected from finely dissected Golden Promise root tips (0-1 mm, 1-2 mm, 3-5 mm, and 5-10 mm sections) representing the meristem (zone 1), elongation (zone 2), young maturation (zone 3), and old maturation (zone 4) zones. Transcript levels of *HvCslF3*, *HvCslF6* and *HvCslF9* were determined by qPCR. *HvCslF6* was included in the experiment as an internal control as it was reported to maintain high transcript levels in different barley tissues (Burton et al., 2008). Consistent with previous studies, *HvCslF6* transcripts were abundant in the mature root. However, surprisingly low levels of expression were detected in the meristem and elongation zones, where the cells remain incompletely differentiated (Figure 3-1B). In contrast with *HvCslF6*, the transcript levels of *HvCslF3* and *HvCslF9* were more abundant in the younger parts of the root. *HvCslF3* was barely expressed in the meristem zone but the transcript level of this gene increased dramatically and peaked in the elongation zone. As cells enter maturation and start to differentiate, the transcripts reduced to very low levels as detected in zone 4 (Figure 3-1B). *HvCslF9* had a similar expression pattern to *HvCslF3*, the only difference being that *HvCslF9* transcripts were relatively more abundant in zone 1 (Figure 3-1B). Importantly, in the meristem and elongation zones, the expression levels of *HvCslF3* and *HvCslF9* were significantly higher than that of *HvCslF6*, which suggested a potential role in the cells that undergo rapid division and expansion.

To confirm the qPCR results and further investigate the location of gene expression, RNA *in situ* hybridisation was performed. Figure 3-1C, D revealed that expression of *HvCslF3* is elevated in epidermis and cortex cells in the elongation zone. Less intensive staining was found in the central stele and meristem, with no staining in the root cap and mature cells surrounding the stele. These results were consistent with the qPCR analysis. *HvCslF9* expression was restricted to the root tip but showed a broader expression pattern compared to *HvCslF3* (Figure 3-1E, F). The staining was uniformly detected in all cell types except for the lateral root caps and mature columella cells, and the intensity of the staining was evenly distributed in the meristem and elongation zones. The expression pattern of *HvCslF3* and *HvCslF9* reveals important spatial information regarding where these genes might function during the growth of the barley root.

***HvCslF3* and *HvCslF9* are down-regulated in the root tips of the 35S:RNAi lines**

To study the role of *HvCslF3* and *HvCslF9* in barley, RNA interference silencing (*RNAi*) was used to generate transgenic plants with reduced *HvCslF3* and *HvCslF9* gene expression. The two *RNAi* plasmids were designed to independently target *HvCslF3* and *HvCslF9*, and the sequence fragments were amplified from Golden Promise and driven by the constitutive 35S promoter. Seeds from confirmed homozygous T3 plants and the wild-type control were used in the present study, including three *HvCslF3-RNAi* lines (#27, #29, #30), three *HvCslF9-RNAi* lines (#33, #34, #36), and the wild-type Golden Promise. Gene expression levels in the first cm of the root tips were determined by qPCR. Figure 3-2A shows the fold changes in transcript abundance of the genes of interest in comparison with Golden Promise. Down regulation of the target genes was confirmed in all transgenic lines, although the level of down regulation varied. For *HvCslF3-RNAi*, line #27 showed the most severe effect, retaining 30% of wild-type *HvCslF3* expression. The *HvCslF3* transcripts reduction in #29 (60%) and #30 (70%) was less significant compared to wild-type levels. Confirmed down regulation of *HvCslF9* was observed

in *HvCslF9-RNAi* lines #33, #34, and #36 with slight variations.

Some variation in the transcript levels of other *Csl* genes was also detected in the transgenic roots (Figure 3-2B, S3-2). For example, *HvCslF9* showed some down-regulation in *HvCslF3-RNAi* lines #27 and #30, although line #29 was unchanged. By contrast, *HvCslF3* expression levels were either unchanged or slightly up-regulated in the *HvCslF9-RNAi* lines. The expression level of three *HvCslD* and one *HvCslH* genes were determined due to their potential in root development and cell wall biosynthesis (Figure S3-1). The expression of *HvCslD1* was higher towards the maturation zone, and the levels of transcripts were not affected in the *HvCslF3-RNAi* and *HvCslF9-RNAi* lines. *HvCslD2* showed highest expression in the young maturation zone, and it expressed at higher level in lines #27, #29, #30, #33. In contrast, *HvCslD4* was highly expressed in the meristem, and expression decreased rapidly towards the maturation zone. Higher transcripts level of *HvCslD4* was detected in the *HvCslF3-RNAi* lines, but not the *HvCslF9-RNAi* lines. *HvCslH1* only expressed in the mature root. The levels of expression were higher in the transgenic lines. Given the RNAi constructs were designed to be highly specific, these results suggest some potential co-expression or feedback regulation between the *CslF* genes in barley roots.

***HvCslF3* and *HvCslF9* down-regulation leads to changes in seedling growth**

To examine the effects of reduced *HvCslF3* and *HvCslF9* gene expression on barley development, transgenic and wild-type seeds were germinated on 1% agar plates to perform root growth rate measurements (Figure 3-3). Total root length was recorded daily for seven days (Figure 3-3C), and the density of root hairs was quantified at approximately 4 cm from the root tip (Figure 3-3D).

Root growth was assessed over time. At day 7, the transgenic lines exhibited generally smaller seedlings with a reduced root system (Figure 3-3A). After germination, root growth

increased rapidly until 3 dpg when most of the lines reached the highest root elongation rate. From 3 dpg onwards root growth rate stabilised with minor fluctuations (Figure 3-3C). Interestingly, the daily root growth of transgenic RNAi lines was significantly slower compared to Golden Promise, resulting in smaller plants. At 3 dpg, the average root growth rate of the *HvCslF3-RNAi* and *HvCslF9-RNAi* plants was only 84 mm/day and 116 mm/day, respectively, whereas the growth rate of Golden Promise was 165 mm/day. The reduced growth rates in the transgenic lines were maintained during the entire time course, with the daily elongation eventually stabilising at 125 mm/day (Golden Promise), 90 mm/day (*HvCslF3-RNAi*) and 105 mm/day (*HvCslF9-RNAi*).

Notably, defects in development were not limited to seminal roots. Indeed, the number of root hairs on the root tips was also decreased. Figure 3-3D shows the root hair density was relatively stable within each line, except for the first 5 mm of the root tip where the root meristem and elongation zone are located. However, significant differences in root hair number were observed between the wild type and transgenic barleys, with 481 ± 30 root hairs on Golden Promise, and 285 ± 16 and 310 ± 23 root hairs on the *HvCslF3-RNAi* and *HvCslF9-RNAi* roots, respectively. Moreover, the root hairs of the transgenic lines were particularly sensitive to a treatment with chloride hydrate-based clearing solutions. Figure 3-3B shows cleared root samples treated with Hoyer's solution. Compared to the Golden Promise control, damage and/or removal of root hairs from the root surfaces of the transgenic barleys was more important, especially for line #27 and #36, where the root hairs were almost completely removed. In summary, this study on seedlings root morphology revealed the relationship between reduced *HvCslF3* or *HvCslF9* gene expression and shorter seminal roots and reduced root hair development, which is likely to have a negative impact on overall plant growth. Also, the loss of *HvCslF3* or *HvCslF9* gene expression affected the strength and stability of root hairs, indicating these genes may be involved in the synthesis of cell wall components that contribute

to mechanical strength.

***HvCslF3* and *HvCslF9* RNAi lines show a shorter meristem and elongation zone**

To understand the basis of the observed defects in root development, root tips were cleared with a ClearSee solution to examine the cellular organisation. The anatomy of the root tips was similar to that previously described by Kirschner et al. (2017). However, differences in the length of the meristem and elongation zones were observed between the lines. To compare the size of the meristem and elongation zones, we identified the end of the meristem zone and the beginning of the elongation zone based on the criterion that the first cortex cell adjacent to the epidermis doubles in length; whilst the end of elongation zone was marked where the first root hair emerges. Figure 3-4A highlights the variable meristem and elongation zone length from different lines. The length of the meristem and elongation zones for each line was measured as shown in Figure 3-4B. In *HvCslF9-RNAi* lines #33, #34, and #36, the average meristem sizes showed a significant reduction, from 1070 μm in Golden Promise to 567 μm , 540 μm , and 529 μm in the lines #33, 34 and 36, respectively. The Golden Promise meristem size is comparable with that previously described in 4-day-old Morex roots (1000 μm) (Kirschner et al., 2017). On the other hand, the meristem size of the *HvCslF3-RNAi* plants was more variable, ranging between 589 and 1027 μm . However, the size of the elongation zone of all transgenic lines showed a significant reduction (Golden Promise: 924 μm , #27: 324 μm , #29: 335 μm , #30: 358 μm , #33: 325 μm , #34: 364 μm , #36: 360 μm). The reduced length of the elongation zone corresponded to decreased level of *HvCslF3* gene expression. The consequence of the elongation (and meristem) zone defect is likely to be a shorter root and slower root growth, consistent with root measurements (see above).

***HvCslF3* and *HvCslF9* RNAi lines developed thinner roots**

Transverse sections were prepared using the agar-grown root materials to observe root

anatomy, including the number of cells in each layer. Figure 3-5 presents representative root sections for each line at approximately 1 cm from the root tip. A notable trend of thinner roots was found in the transgenic barley plants. Interestingly, the size of the central stele of all samples was comparable to wildtype at approximately 130-150 μm , suggesting that the decrease in root diameter was likely due to a reduced area of outer tissues. We hypothesised that this might be due to smaller cells or a reduced number of cell layers. Compared with Golden Promise, which usually contains an average of 5 to 6 cortical cell layers, only 3 to 4 layers of cortical cells were detected in transgenic lines with no obvious change identified in cell size. Furthermore, because the roots were thinner, the numbers of epidermal cells of *HvCslF3-RNAi* plants (80-90) and *HvCslF9-RNAi* (70-90) plants were reduced compared to Golden Promise (>100). Hence, the lower root hair density might be indirectly due to the decreased number of epidermis cells surrounding the reduced number of cortical layers.

The deposition and distribution of major cell wall polysaccharides are not affected

HvCslF3 and *HvCslF9* have previously been implicated in the biosynthesis of (1,4)- β -linked glucoxytan and (1,3;1,4)- β -glucan, respectively (Burton et al., 2008; Cseh et al., 2013; Little et al., 2019). However, most of these studies focussed on aerial organs including grains and leaves. To understand the impact of reduced *HvCslF3* and *HvCslF9* expression on polysaccharide composition in barley root tips, the deposition of major cell wall polysaccharides including (1,3;1,4)- β -glucan, callose, AGP, mannan, arabinoxytan and pectin was analysed using immunolabelling. Figure 3-6 and 3-7 indicated there was no obvious difference in cell wall polysaccharide deposition and distribution in the *HvCslF3* and *HvCslF9* plant cell walls, except for (1,3;1,4)- β -glucan. In Golden Promise and *HvCslF3-RNAi* samples, (1,3;1,4)- β -glucan was found in all cell types above the root cap, and the intensity of the labelling increased as cells leave the meristem zone. (1,3;1,4)- β -Glucan labelling in the root cap was restricted to the lateral root cap and young columella cells. However, in cell walls of

HvCslF9-RNAi root tips, (1,3;1,4)- β -glucan was barely detectable. This was particularly obvious in the meristem and elongation zones where *HvCslF9* is highly expressed (Figure 3-1E, F). This indicates an endogenous role for *HvCslF9* gene in regulating the synthesis of (1,3;1,4)- β -glucan in newly formed immature primary cell walls in roots. Interestingly, the labelling of (1,3;1,4)- β -glucan was recovered in the mature root cells, which correlates with the location of *HvCslF6* gene expression.

Another well-known polysaccharide, arabinoxylan, was not detectable in the cell wall of root tip tissues, which is consistent with our previous finding (Chapter 2). Callose showed a change in deposition during root development. In the meristem, callose was detected in cell plates of most cells but callose labelling was considerably less intense in the cells surrounding the stem cell niche and cells undergoing rapid cell division. In more mature cells, the callose signal was detected as bright punctate dots in the cell walls demarking plasmodesmata. AGP was found in cell walls of the central stele and outermost layer of the root cap, while pectin was restricted to cortex cells. Mannan showed a distinct localisation compared to other polysaccharides since fluorescent labelling was found in the cytoplasm, rather than at the cell walls. This was particularly obvious in the meristem and elongation zones. Similar labelling was identified when cells had entered a maturation phase, although the enlarging vacuole appeared to push the fluorescent signal towards the cell periphery, and the signal occasionally detected in the cell walls.

Down regulation of *HvCslF3* reduced (1,4)- β -linked glucoxytan accumulation

The role of *HvCslF3* in the synthesis of (1,4)- β -linked glucoxytan in tobacco leaves was recently described by Little et al. (2019). Root samples from different genotypes were hydrolysed with the cellulase E-CELTR from *Trichoderma longibrachiatum* and oligosaccharide products were quantified by HPLC (Dionex) to determine (1,4)- β -linked

glucoxytan concentration. Figure 3-8A shows the products from E-CELTR treatment, which are identified as xyl-(1,4)- β -glc, xylobiose, glc-(1,4)- β -xyl, and cellobiose according to their retention times. Of these, xyl-(1,4)- β -glc and glc-(1,4)- β -xyl are the disaccharide products from hydrolysed (1,4)- β -linked glucoxytan. In the Golden Promise root tip, 1290 ng/mg of (1,4)- β -linked glucoxytan was detected, which was more than 10 times higher than previously detected in barley root tip tissues (Little et al., 2019). This indicates a high concentration of (1,4)- β -linked glucoxytan in the first cm of the barley root tip, which is mainly composed of young cells and represents a smaller region than that collected in Little et al. (2019). Furthermore, the concentration of (1,4)- β -linked glucoxytan in the root tips of all three *HvCslF3-RNAi* and *HvCslF9-RNAi* lines decreased significantly, showing concentrations of 782, 1021, and 1004 ng/mg and 842, 933, and 1013 ng/mg in lines #27, #29, #30 and #33, #34, #36, respectively. However, no correlation between the level of gene downregulation and the (1,4)- β -linked glucoxytan reduction was observed.

Discussion

GT2 cell wall related genes are key regulators of root cell elongation

The *HvCslF3* and *HvCslF9* genes belong to a family of putative GT2 that includes *HvCslF6*, the major determinant of barley (1,3;1,4)- β -glucan biosynthesis. Of the nine *CslF* genes in the barley genome, transcript profiling of seven members was studied in different tissues and organs (Burton et al., 2008; Schwerdt et al., 2015). Burton et al. (2008) investigated the organ-specific and temporal expression of *CslFs* by qPCR and found that *HvCslF6* was the most abundant gene in all studied tissues. Here we finely dissected barley root tips into sections representing different developmental zones and used qPCR to demonstrate abundant expression of *HvCslF3* and *HvCslF9* in root meristem and elongation zones. The cells in these zones undergo rapid division and longitudinal expansion, during which cell wall assembly and

modification are exceptionally important. mRNA *in situ* hybridization revealed the two genes have distinct yet partially overlapping tissue-specific expression patterns. The expression of *HvCslF3* in elongating cortical and epidermal cells is of interest, since it suggested an important role for this gene in the regulation of cell expansion in outer root tissues, potentially via modification of cell wall composition.

Previous studies in different species have identified expression of genes in the root elongation zone that includes cell wall loosening enzymes and polysaccharide synthases (Yang et al., 2011; Markakis et al., 2012). A soybean expansin gene *GmEXPI* involved in cell wall loosening is specifically expressed in the elongating epidermal and underlying cell layers, and induces cell elongation in soybean secondary root initials and transgenic tobacco roots (Lee et al., 2003). A similar correlation between *OsEXPI* and cell elongation was also reported in rice (Yang et al., 2006). In another study, Bassani et al. (2004) successfully identified six genes involved in cell wall metabolism to be up-regulated in the maize root elongation zone using suppression subtractive hybridization. *CslF* members also participate in regulating root elongation, for instance, the *OsCslF2* is expressed in the rice root tips, and it is the corresponding to *HvCslF4* and *HvCslF11* in barley. Increased *OsCslF2* expression was reported in elongating rice root tips under water stress, and the regulation of *OsCslF2* correlated with the modification of cell wall polysaccharide content (Yang et al., 2006). The abundant and specific expression of *HvCslF3* and *HvCslF9* in the root meristematic and elongation zones of barley is consistent with a role in early root development, and this was subsequently confirmed through the analysis of transgenic RNAi lines.

Root length and surface area are one of the most important features of root architecture that relate to nutrient uptake and stress responses (Yao et al., 2002). The elongation of roots is largely dependent on hormone regulation (Petricka et al., 2012), although studies in *Arabidopsis* have demonstrated a key role for cell wall related genes. For example, *radially swollen 1 (rsw1)*

mutants alter cellulose synthase complexes resulting in short roots (Arioli et al., 1998), *stunted plant-1 (stp-1)* and *constitutive response-1 (ctr-1)* modify pectin accumulation and show disturbed root cell elongation (McCartney et al., 2003), class III peroxidases, *prx33* and *prx34*, encode cell wall associated peroxidases that regulate cell elongation (Passardi et al., 2006), and the *cslD2/3/5* mutants with altered mannan synthase activity have altered root hair development and root morphology (Yin et al., 2011). Such a relationship between cell wall remodelling and early root development remains under investigation for monocot crops. Root hairs contribute to the total root surface area to improve contact between roots and the surrounding soil environment, and play an important role in water and nutrient uptake to support plant development (Pallardy, 2008). In cereals, cell wall related genes such as *CsIDI* (Kim et al., 2007), *EXPI7* (Yu et al., 2011) and *XXTI* (Wang et al., 2014), impact root hair initiation and elongation, but their influence on primary and seminal root development was not reported. Even though the total number of root hairs was decreased in the *HvCslF3* and *HvCslF9* RNAi plants, the formation of root hairs *per se* did not seem to be affected. Indeed, based on the root morphology analysis, the reduction was more likely caused by a reduced root diameter rather than a root hair initiation defect.

Previous investigations of the molecular genetic basis for short root mutants in rice and maize did not specify whether the genes contribute to cell wall polysaccharide synthesis (Yao et al., 2002; Hochholdinger et al., 2004). However, a common feature of these cereal mutants is defective cortical cell elongation. Similar defects in root cell elongation were observed in the *HvCslF3-RNAi* and *HvCslF9-RNAi* plants. Considering the specificity of *HvCslF3* expression in the elongating cortical and epidermal cells and the conservation of the *CslF* family in cereal species, it is possible that altered gene expression leads to the short mutant phenotypes previously reported in other cereals.

***HvCslF3* and *HvCslF9* affect root radial patterning**

The meristematic and elongation zones contribute to root growth in distinct ways. The root meristem contains the stem cell niche which comprises QC and initial cells, and determines the amount of cell proliferation (Petricka et al., 2012). Kirschner et al. (2017) reported there are approximately 30 QC cells in the barley stem cell niche and described the structure of the meristem in the Morex cultivar. These observations are consistent with our own characterisation of the root cellular organisation in the Golden Promise cultivar. The *HvCslF3-RNAi* and Golden Promise roots exhibited a similar meristem size and cell arrangement, indicating that tissue patterning and early stages of cell division were not affected. However, in the maturation zone, the number of cortex cell layers showed variation. While Morex produced 4-5 cortical cell layers (Kirschner et al. (2017)), Golden Promise produced 5-6 layers of cortical cells. By comparison, cross sections of *HvCslF3-RNAi* and *HvCslF9-RNAi* roots exhibited only 3-4 layers of cortical cells. These findings highlight the importance of *HvCslF3* and *HvCslF9* in determining numbers of root cortical cell layers.

Root radial patterning is established during embryogenesis and maintained in the root meristem by the stem cell niche (Benková and Hejácíko, 2008). Two genes (*SHORTROOT* and *SCARECROW*) from the *GRAS* gene family control radial patterning in Arabidopsis, maize, and rice (Lim et al., 2000; Hochholdinger and Zimmermann, 2008). The regulation of these genes is essentially important for the determination of endodermis and cortex cell fate (Cui et al., 2007). A multi-layered cortex is one of the morphological characteristics that distinguishes cereal species from the model dicot Arabidopsis. Natural variation in the number of cortex cell layers was described in maize and rice (Coudert et al., 2010; Burton et al., 2013; Chimungu et al., 2014). It is reported to be genetically controlled (Chimungu et al., 2014) and also influenced by asymmetric periclinal divisions in the root meristem, reflecting meristem radial patterning (Lux et al., 2004; Coudert et al., 2010). However, the specific molecular and physiological basis remains unclear (Chimungu et al., 2014). Our results suggest that cell wall related genes may

contribute to the determination of cell files in root meristem, especially in the regulation of periclinal cell division during the early stage of root development. How this is achieved remains unclear but may relate to feedback from the wall due to polysaccharide deposition and changes in binding of key receptors (Tucker et al., 2018). Alternatively, modifications of plasmodesmata formation or aperture could impact cell-cell movement of regulators such as mobile transcription factors like SHORTROOT that control radial patterning of cortical cells layers in monocot and eudicot plant roots (Gallagher et al., 2004; Cui et al., 2007).

The number of cortical cells in a barley root may be of agricultural significance, since studies have shown a correlation between cortical cell file number and drought tolerance in maize. Maize plants containing less cortical cell layers retain lower metabolic costs to improve the adaptation to water stress (Chimungu et al., 2014). In addition, the reduced cortical cell layers associate with low respiration rate, which increases carbon source to improve the plant performance especially under drought (Jaramillo et al., 2013; Chimungu et al., 2014). However, whether *HvCslF3-RNAi* and *HvCslF9-RNAi* plants can resist water stress and outperform wild-type controls under drought conditions remains unknown. Such an assessment will require additional studies in climate-controlled growth chambers, field experiments and/or computational modelling to fill the knowledge gap.

Another critical alteration in the root cortex during plant development is the formation of cortical aerenchyma or senescence. In both cases, cortical cells undergo programmed cell death to create air spaces (Evans, 2004). This occurs in many plant species including barley and improves aeration, thus benefiting root respiration (Yamauchi et al., 2013; Schneider et al., 2017). *Respiratory burst oxidase homolog* and *metallothionein* regulate the formation of aerenchyma in rice and maize (Steffens and Sauter, 2009; Yamauchi et al., 2011), while genes encoding cell wall polysaccharide hydrolases function in the later stage of programmed cell death to accomplish aerenchyma maturation (Yamauchi et al., 2013). One common feature

shared by aerenchyma formation and cortical cell layer variation is the effects on root respiration costs (Schneider et al., 2017). Chimungu et al. (2014) highlighted the possible correlation between the two traits and their significance for plants to adapt to stress during development. Therefore, another question arises as to whether less cortical cell layers in *HvCslF3* and *HvCslF9* RNAi plants affect aerenchyma formation in mature root.

The short root phenotype in barley RNAi lines is caused by abnormal root elongation

Notable differences were identified in the elongation zone of wild-type and transgenic barley lines. After rapid cell division, cells enter the elongation zone and initiate longitudinal cell expansion. Although hormones play a critical part of this process, alterations in cell shape and morphology are also important since they allow the transition of cells into the elongation phase. One essential feature that regulates cell expansion is turgor pressure, which was described as water uptake via the root epidermis and the enlargement of the vacuole (Petricka et al., 2012; Guerriero et al., 2014). A γ -tonoplast intrinsic protein accumulates in the cells that initiate elongation (Olbrich et al., 2007), and plant cells with defects in vacuole development fail to elongate (Schumacher et al., 1999). Our data highlighted a reduction in the number of root hairs in the RNAi lines, which may result in the limitation of water uptake. However, no difference in vacuole size was detected.

Another important event that occurs during cell elongation is the remodelling of cell walls. Many cell wall biosynthetic and modifying related genes have been identified in elongating tissues, including peroxidase (*PER64*), AGP synthases, xyloglucan hydrolases, and pectin synthases and hydrolases (Hématy and Höfte, 2006; Guerriero et al., 2014). The *cellulose synthase interacting 1* mutant, which alters CesA transportation along microtubules, shows defects during root cell elongation, suggesting an important role for cellulose in this process (Bringmann et al., 2012). In addition, the termination of cell elongation is usually marked by

the upregulation of genes involved in secondary cell wall synthesis (Hall and Ellis, 2013). High expression of *HvCslF3*, *HvCslF6*, *HvCslF7* and *HvCslF9* was previously reported in rapidly growing barley tissues, including coleoptiles and roots, which suggested a role of the *CslF* genes in modifying the flexibility and stiffness of extending cell walls (Burton et al., 2008). From the perspective of a single cell in *Arabidopsis*, the unidirectional expansion of elongating root cells is controlled by multiple pathways, including the horizontal orientated cortical microtubules (*bot1*, *fra2*, *mor1*, *ton2*) (Bichet et al., 2001; Burk et al., 2001; Whittington et al., 2001; Camilleri et al., 2002), the directional assembly of cell wall polysaccharides (*rsw1-3*, *procuste*) (Fagard et al., 2000; Petricka et al., 2012), and the COBRA proteins that affect cell elongation by defining the longitudinal side of growth (Schindelman et al., 2001). The barley RNAi plants examined in this study showed a shorter elongation (and meristem) zone, which directly affects the process of cell expansion and results in cells entering maturation earlier than wild type. Why this occurs at a biochemical level remains unclear, since few differences were seen in the RNAi lines in terms of cell wall polysaccharide distribution. It also remains unclear whether this phenotype is directly related to the alterations in cortical cell number discussed above. One possibility is that the *HvCslF3* and *HvCslF9* genes are involved in modifying the flexibility and stiffness of cell walls in multiple zones of the root. Whether this relates to the synthesis of specific polysaccharides that directly promote elongation, impact cell-cell movement of key regulators like SHORTROOT or through inhibition of cell wall biosynthetic activities that block elongation requires further investigation.

***HvCslF3* and *HvCslF9* are involved in the synthesis of different cell wall polysaccharides**

Studies have only recently begun to report the multi-functional and cross-functional nature of *Csl* families in the synthesis of different cell wall polysaccharides. For example, genes from both the *CslA* and *CslD* families affect mannan synthesis, contributing to cell wall synthesis and cell expansion (Dhugga et al., 2004; Cosgrove, 2005; Goubet et al., 2009;

Verherbruggen et al., 2011). In addition, Douchkov et al. (2016) reported a potential role of *HvCsID2* in callose modification during defence against fungal pathogen attack. Similarly, the synthesis of (1,3;1,4)- β -glucan can be independently controlled by *CsIF* and *CsIH* genes (Burton et al., 2006; Doblin et al., 2009). Within the *CsIF* family, Burton et al. (2011) and Taketa et al. (2011) revealed the significant role of *HvCsIF6* in mediating the biosynthesis (1,3;1,4)- β -glucan in the grain, and a potential temporally-restricted role of *HvCsIF9* in the same process (Burton et al., 2008; Cseh et al., 2013). A recent report challenged this role of *HvCsIF9*, since CRISPR/Cas9 *csif9-2* knockouts showed no difference in the location or accumulation of (1,3;1,4)- β -glucan in the barley grain (Garcia et al., personal communication). In terms of vegetative tissues, a weak or absence of accumulation of (1,3;1,4)- β -glucan was highlighted using immunolabelling in the meristem and elongation regions of *HvCsIF9-RNAi* root tips, supporting a role for *HvCsIF9* in (1,3;1,4)- β -glucan biosynthesis. A possible explanation for this discrepancy is that *HvCsIF6* expression, which is known to be the main determinant of (1,3;1,4)- β -glucan synthesis, remained high in the grains from the barley *csif9-2* knockout. Therefore, in the presence of *HvCsIF6*, it may be difficult to distinguish any alteration of (1,3;1,4)- β -glucan content in the grain. The decrease in (1,3;1,4)- β -glucan in *HvCsIF9-RNAi* root tips may be more obvious since *HvCsIF6* is not abundant in these tissues.

The predominate expression of *HvCsIF6* in mature roots may reflect the importance of this gene in cell maturation, which involves secondary cell wall development. In contrast, the correlation between the absence of (1,3;1,4)- β -glucan and decreased *HvCsIF9* expression may indicate a role for *HvCsIF9* and (1,3;1,4)- β -glucan in newly formed primary cell walls, similar to the role of different *CesA* genes during cellulose synthesis in different tissues and wall types (Richmond and Somerville, 2000; Taylor et al., 2003; Hématy and Höfte, 2006), *HvCsIF6* and *HvCsIF9* may represent another example of different *CsIF* genes being involved in the synthesis of the same polysaccharide, (1,3;1,4)- β -glucan, but in distinct primary and secondary wall types.

To further confirm the role of *HvCslF9* in (1,3;1,4)- β -glucan synthesis in root tips, additional quantitative experiments and genetic tools, such as the *cslf9* CRISPR lines, are required.

Even though the primary function of *CslF* proteins has overwhelmingly been linked to the regulation of (1,3;1,4)- β -glucan synthesis, growing evidence suggests that the *CslF* family may play far more diverse roles. Distinct from the *HvCslF9* lines, the immunolabelling of *HvCslF3-RNAi* barley root tips did not show any significant difference in terms of presence and distribution of the major cell wall polysaccharides. This is consistent with the results of Little et al. (2019), who introduced *HvCslF3* into tobacco leaves via *Agrobacterium* infiltration and failed to detect any (1,3;1,4)- β -glucan derived oligosaccharide products. The same study reported the potential role of *HvCslF3* and *HvCslF10* in the synthesis of (1,4)- β -linked glucoxytan upon heterologous expression in tobacco leaves (Little et al., 2019), and the presence of constituent oligosaccharides (xyl-(1,4)- β -glc and glc-(1,4)- β -xyl) in barley root tips. In this study, we measured the concentration of both oligosaccharides in 1 cm root tips of Golden Promise and the *HvCslF3-RNAi* and *HvCslF9-RNAi* plants using a method adapted and modified from Little et al. (2019). Compared to the previous report, (1,4)- β -linked glucoxytan showed an even higher concentration in the first cm of the wild-type barley root, and this was significantly decreased in the *HvCslF3-RNAi* plants. Surprisingly, a reduced (1,4)- β -linked glucoxytan was also observed in *HvCslF9-RNAi* roots, suggesting *HvCslF9* gene may contribute indirectly to (1,4)- β -linked glucoxytan biosynthesis. Taken together, the heterologous expression data provided by Little et al (2019) and the endogenous assays reported here provide compelling support for a direct role of *HvCslF3* in (1,4)- β -linked glucoxytan biosynthesis.

Glucoxytan was previously identified in the cell wall of a green alga and based on solubility and Glc/Xyl ratio, it was divided into four fractions (Ray and Lahaye, 1995). The (1,4)- β -linked glucoxytan synthesised by *HvCslF3* and *HvCslF10* in tobacco leaves is predicted

to contain a high Glc/Xyl ratio based on the high molecular weight observed. This makes (1,4)- β -linked glucoxylan difficult to extract, and suggests a potential ability to form intermolecular alignments with other cell wall polysaccharides (Little et al., 2019). Here we identified xyl-(1,4)- β -glc and glc-(1,4)- β -xyl from native barley root material with the cellulase E-CELTR, and the fraction was successfully extracted with 8% acetonitrile. Despite this, further analyses are needed to determine the Glc/Xyl ratio and physicochemical properties of the isolated polysaccharide.

In conclusion, we used transgenic approaches to generate *HvCslF3* and *HvCslF9* down regulated lines and demonstrated the negative effects of reduced gene expression on root development. The transgenic plants exhibited smaller root elongation zones, and consequently led to slower root development and reduced root surface area in barley seedlings. Genes from the *Csl* families play important roles in different biological activities, and this study helps to understand some of the complexities. *HvCslF3* and *HvCslF9* are potentially important in the synthesis of (1,4)- β -linked glucoxylan and (1,3;1,4)- β -glucan in barley root tips, respectively. However, the regulatory machinery influencing the expression of these genes, the potential interaction of their products, and the consequences for root cell elongation require further investigations. To better understand the importance of these *Csl* genes in root development, we are currently assessing knock-out mutants for *HvCslF3* and *HvCslF9* using a CRISPR/Cas9 approach.

Figures

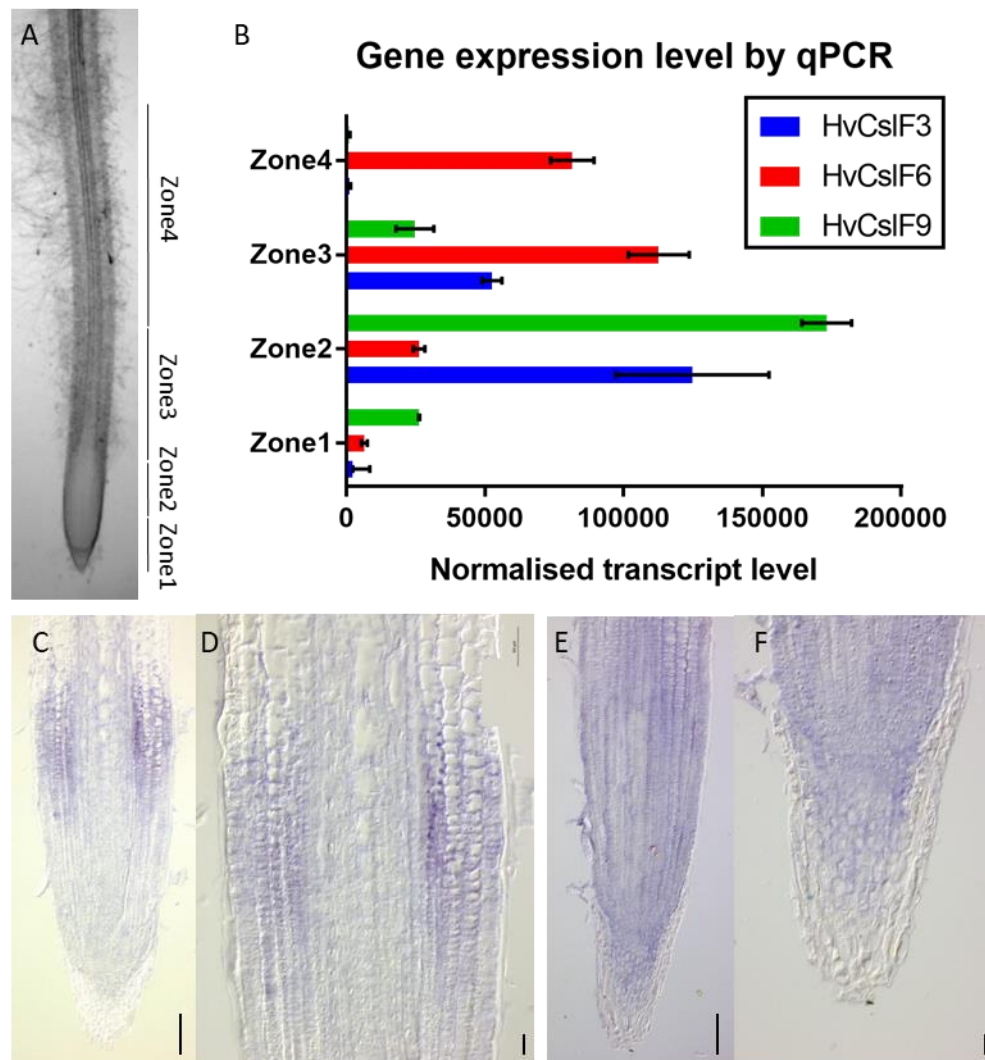


Figure 3-1. Gene expression analysis of Golden Promise root tips. A, schematic diagram of the regions used for root tip dissection: zone 1, 2, 3, and 4 represent the root meristematic, elongation, young maturation, and old maturation zones, respectively. B, qPCR results showing the normalized transcript abundance of *HvCsIF3*, *HvCsIF9*, and *HvCsIF6* in different zones of the root. *HvCsIF9* expresses higher than *HvCsIF3* and *HvCsIF9* in zone 1. The highest expression of *HvCsIF3* and *HvCsIF9* was found in zone 2, and the transcript levels for this gene were of more than 3-fold higher than for *HvCsIF6*. *HvCsIF6* expression continued to increase in zone 3, while expression of *HvCsIF3* and *HvCsIF9* started to decrease. In zone 4, transcript of *HvCsIF3* and *HvCsIF9* are barely detectable, while the expression of *HvCsIF6* remained high

Chapter 3 – *Cellulose synthase-like F (CslF)* genes control barley root growth and differentiation by mediating cell wall polysaccharide synthesis

in mature root cells. Error bars indicate standard errors. C-F, mRNA *in situ* hybridization on longitudinal root sections. C (10X) and D (20X) represent the specific expression of *HvCslF3* in the epidermis and cortex of the root elongation zone. E (10X) and F (20X) revealed the broader expression of *HvCslF9* in all cell types of the root tip, except for the root cap cells. Scale bar = 100 μm .

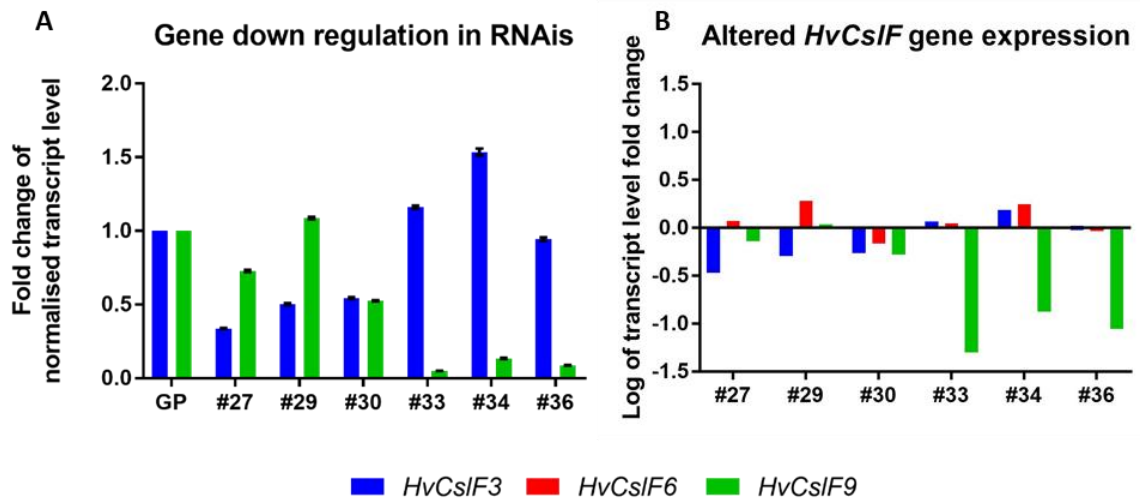


Figure 3-2. Gene expression analysis by qPCR of root tips from Golden Promise, *HvCslF3-RNAi*, and *HvCslF9-RNAi* lines. A, fold change of normalised transcript abundance of transgenic barley lines compared to Golden Promise. Down regulation of *HvCslF3* and *HvCslF9* expression was confirmed in the *HvCslF3-RNAi* (#27, #29, #30) and *HvCslF9-RNAi* (#33, #34, and #36) lines, respectively. The level of down regulation was significant with variability between transgenic lines ($P < 0.0001$). B, Log-fold changes of *HvCslF3*, *HvCslF6*, and *HvCslF9* in different transgenic lines, representing the up and down regulation of specific gene in different transgenic lines. The transcript data were normalised with at least three housekeeping genes. Error bars represent SE.

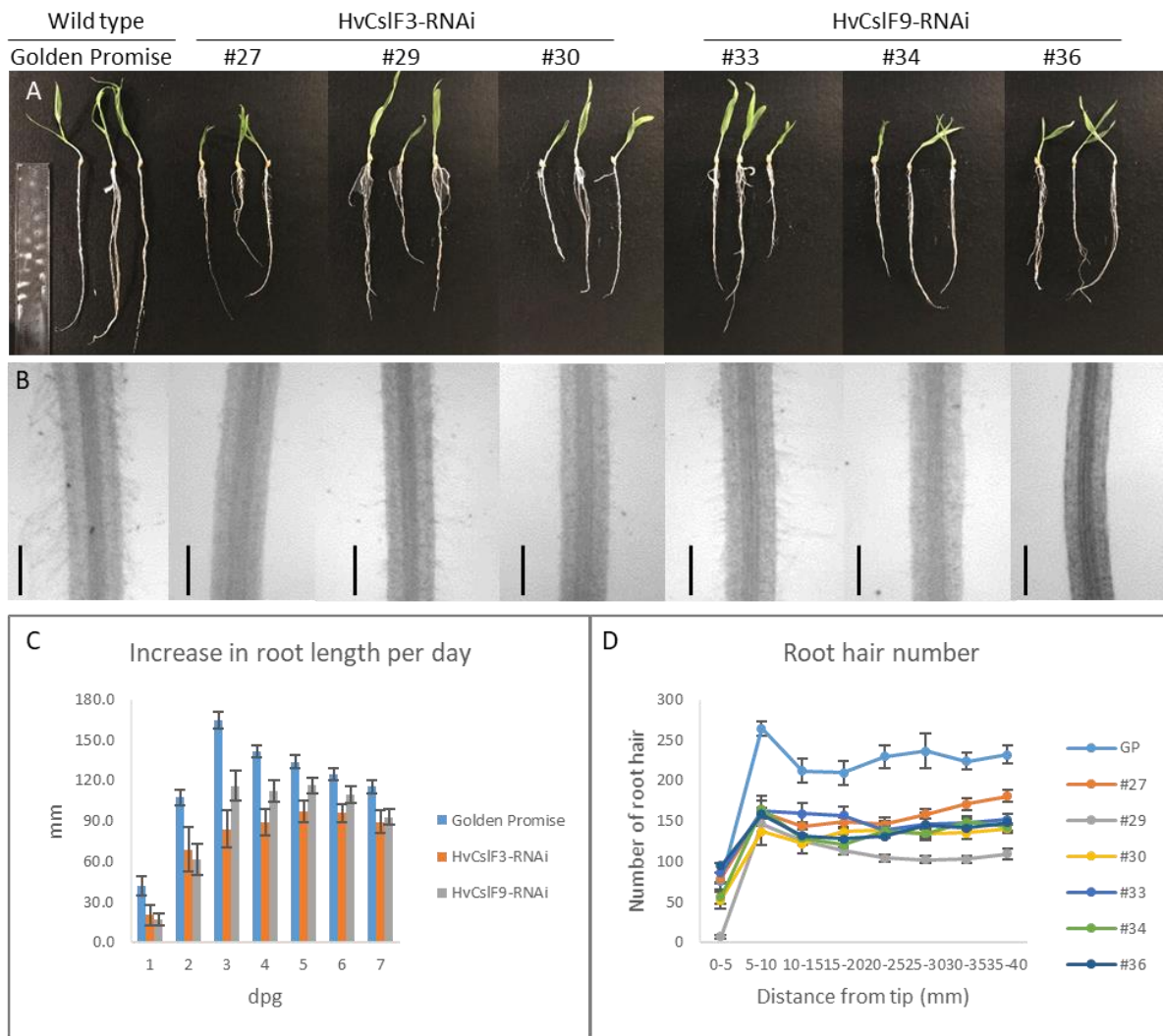


Figure 3-3. Variation in root morphology and development between Golden Promise and transgenic barley lines. A, 7 dpg seedlings of wild-type (Golden Promise), *HvCslF3-RNAi* (#27, #29, #30), and *HvCslF9-RNAi* (#33, #34, #36) lines. Seedlings were pre-germinated before being placed onto agar plates. The plates were positioned vertically in a growth chamber (16/8 hours, 23°C, day/night) for seven days. Reduced root growth was observed in the *RNAi* barley seedlings. B, light microscopy pictures of root tips in Hoyer's solution. Roots were collected from 5 dpg seedlings germinated in the dark. Golden Promise retained dense and long root hairs. Removed or broken root hairs were found in the transgenic barleys indicating more vulnerable root hairs and cell wall structure. Scale bar = 500 μ m. C, the total root length of the seedlings was measured every day for seven days. The histogram shows the average length of

elongated roots per day for the wild-type and transgenic barleys. The growth increased from 1 to 3 dpg, and after 4 dpg, the daily elongation stabilised. Transgenic barleys exhibited slower root growth compared with Golden Promise at all time points. Data were collected from roots of 12 seedlings per genotype. Error bars indicate standard errors. D, number of root hairs on the surface of the root tips. The root hairs were analysed every 5 mm from fresh root tips of seedlings at 7 dpg. All transgenic barleys showed decreased root hair numbers in each measured root section. Data represent the average of ten primary/seminal roots collected from different seedlings. Error bars indicate standard errors.

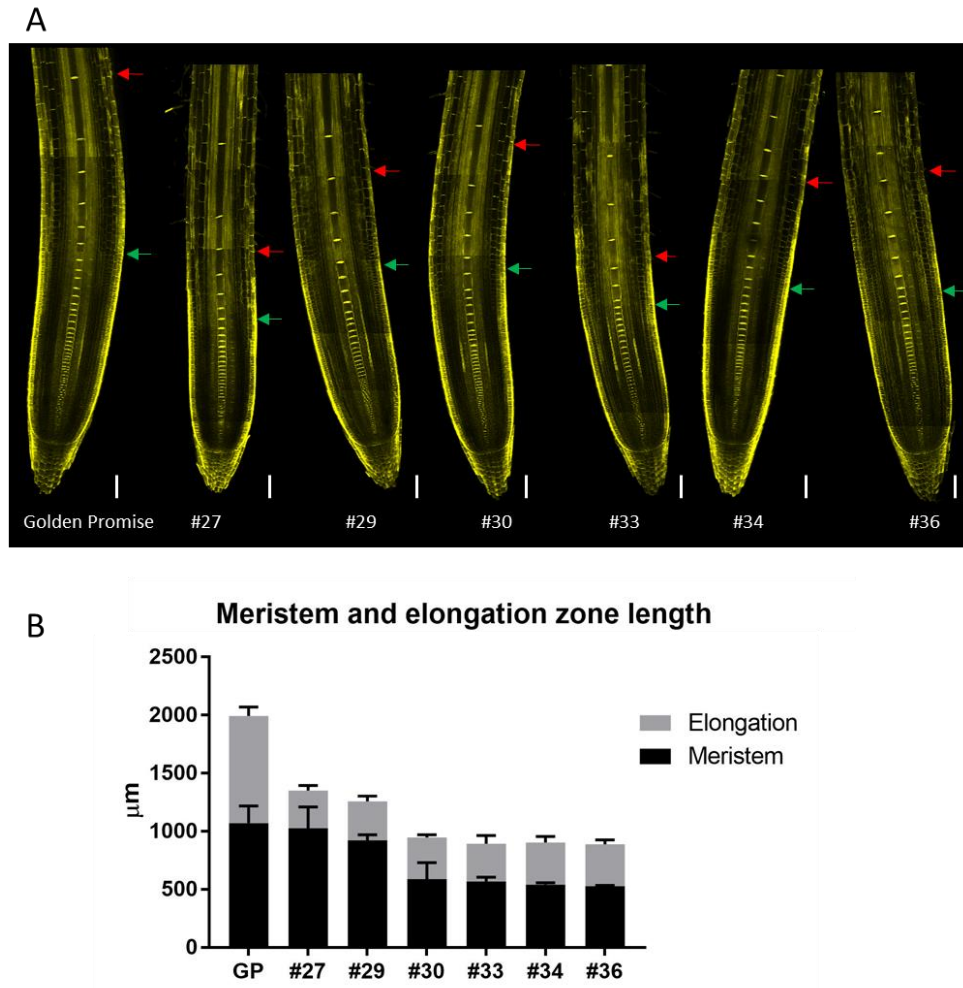


Figure 3-4. ClearSee and Direct Yellow 96 reveal differences in root development. A, 5 dpg root tips were fixed and cleared, stained, and visualized using a Leica SP8 confocal microscope. Green arrows indicate the first cortical cell that doubles in length to mark the end of the meristematic zone and the beginning of the elongation zone. Red arrows indicate the first root hair to mark the end of the elongation zone and the beginning of the maturation zone. A significant reduction of the size of the elongation zone was found in the transgenic barley lines ($P < 0.0001$). Fluorescent signals were detected at 488/519 nm (excitation/emission). Z-stacks at the centre of the roots were taken at five positions with overlaps. Pictures were stitched using Adobe Illustrator. Photos shown are representative of the images of 10 individual specimens. Scale bar = 100 μm . B, Measured average size of meristem and elongation zones of each genotype. $N=10$.

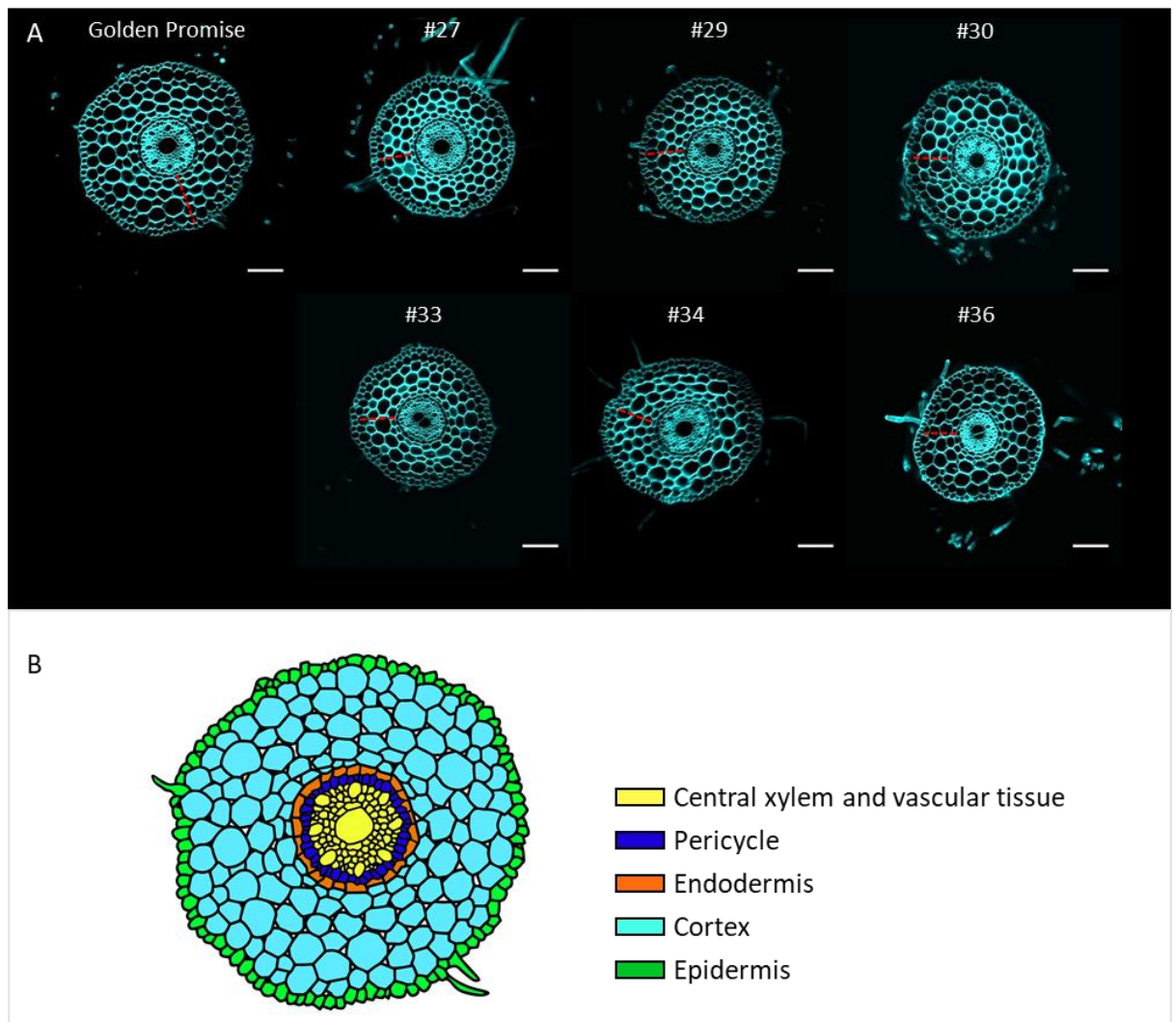


Figure 3-5. Transverse sections of wild type (**Golden Promise**), *HvCslF3-RNAi* (**#27, #29, #30**), and *HvCslF9-RNAi* (**#33, #34, #36**) lines. A, Golden Promise showed 5-6 layers of cortical cells, whereas the transgenic barleys showed approximately 3-4 cell layers (marked with red dash lines). Sections of 100 μm thickness were taken at 1 to 1.5 cm from the root tip and stained with Calcofluor White. Photos were taken using a Leica SP5 confocal microscope with an excitation wavelength of 405 nm and an emission wavelength of 425-475 nm. Pictures were stitched using Adobe Illustrator. Photos shown the representative of the images of 10 individual specimens. Scale bar = 100 μm . B, the schematic diagram of the radial patterning of different root cell types in maturation zone.

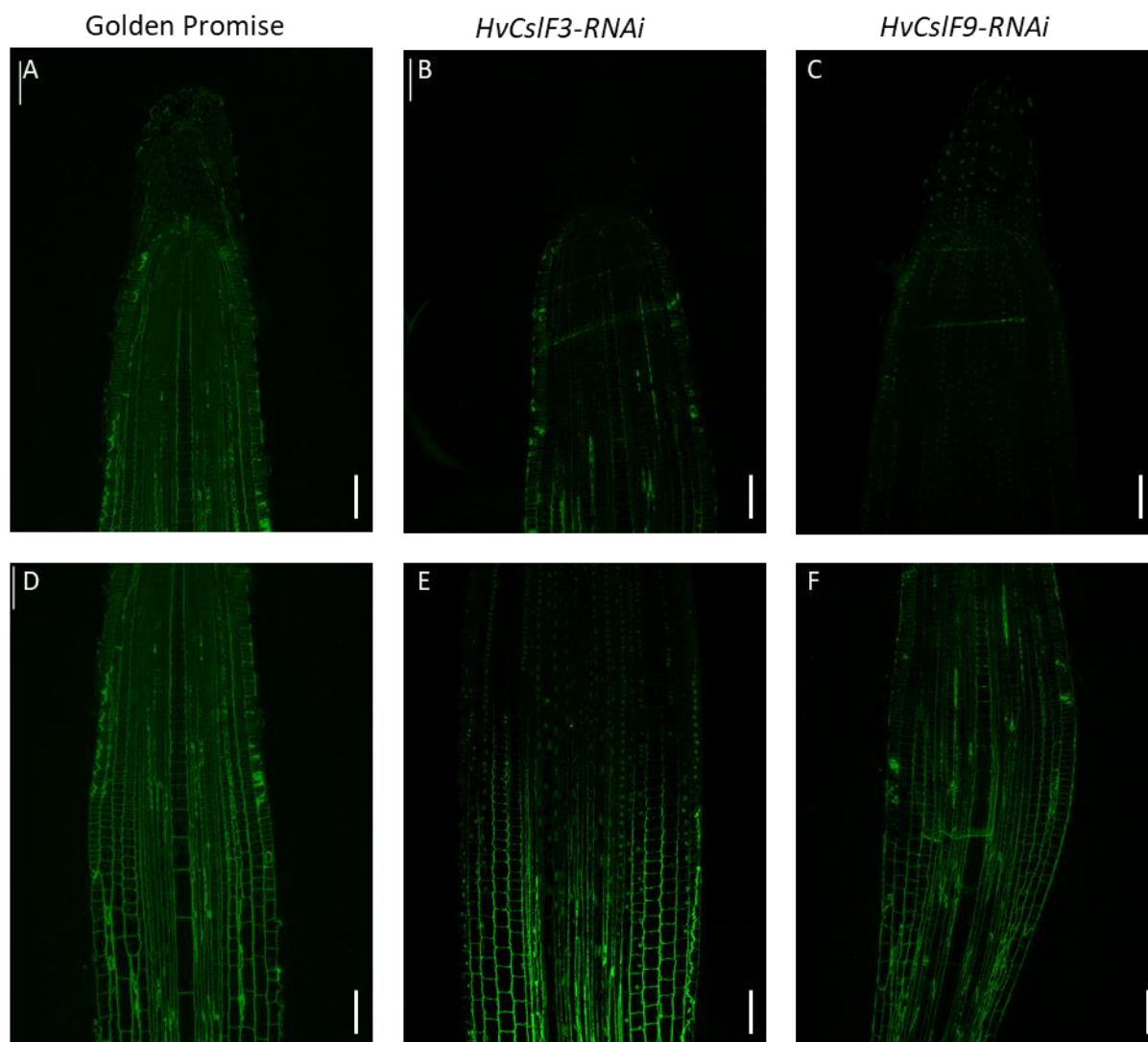


Figure 3-6. Immunolabelling of (1,3;1,4)- β -glucan in the root tips of Golden Promise, *HvCsIF3-RNAi*, and *HvCsIF9-RNAi* lines. A-C, root tips contain meristem and elongation zones. A and B, weak labelling was observed in all cell types except for mature columella cells, indicating less (1,3;1,4)- β -glucan content in the cell walls of newly formed cell. C, no signal was detected in the cell walls of *HvCsIF9-RNAi* root tips, suggesting an absence of (1,3;1,4)- β -glucan in the specimens. Nuclear fluorescence signal indicating low level of detectable labelling. Successful detection of other cell wall polysaccharides indicating the specimens were undamaged. D-F, elongation and young maturation root zones. In the Golden Promise and *HvCsIF3-RNAi* samples, strong fluorescent signals are detected in all tissues, with more intensive labelling appearing as cells develop and enter the maturation zone (D, E).

Fluorescence is not detected in the young root cells of *HvCslF9-RNAi* lines, but the signal recovered to normal level in mature roots (F). The detection of other cell wall polysaccharides in the same regions as C and F showed positive results (Figure 3-7). Scale bar = 100 μm .

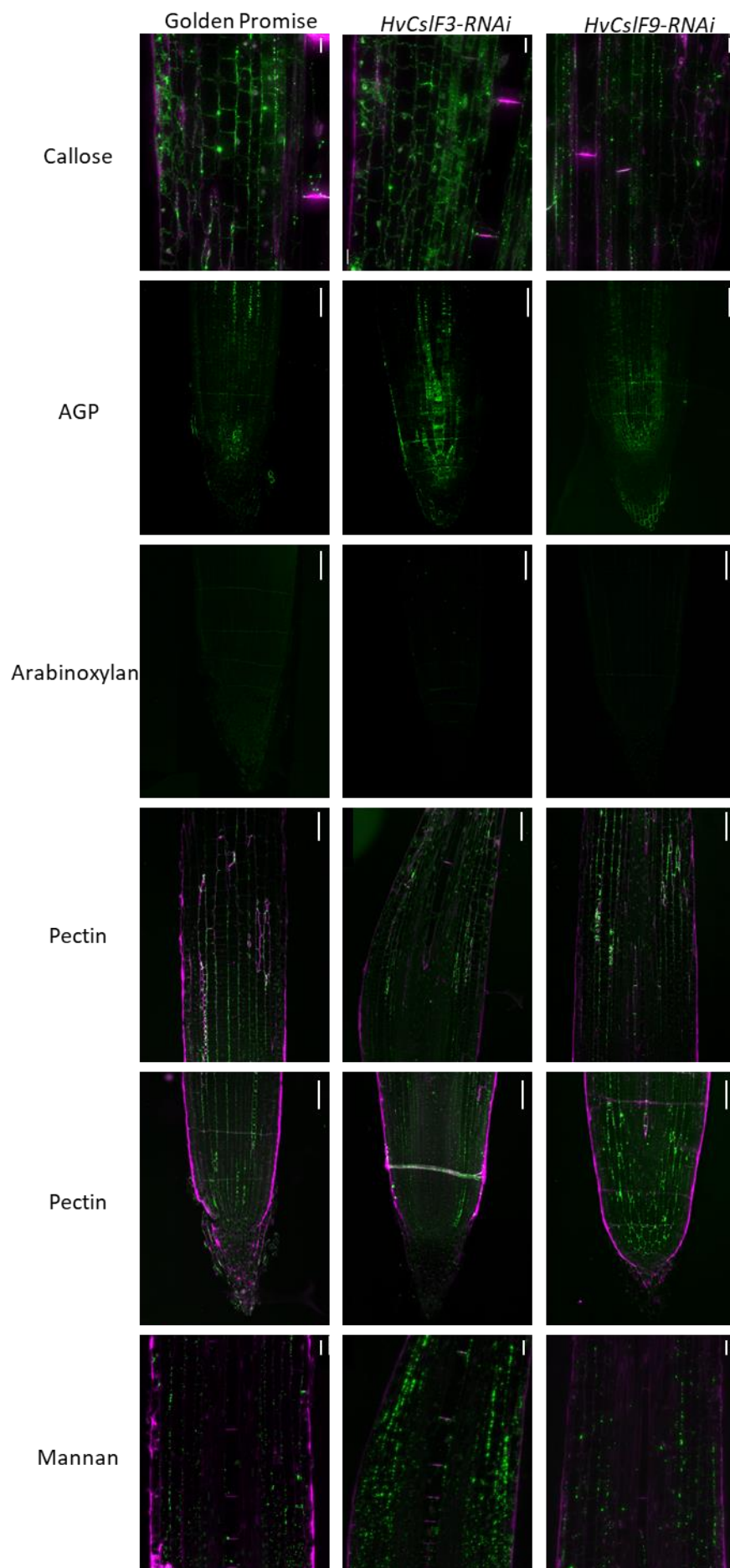


Figure 3-7. Immunolabelling of major cell wall polysaccharides in the root tips of Golden Promise, *HvCslF3-RNAi*, and *HvCslF9-RNAi* lines. Antibodies specific to callose, AGP (arabinogalactan proteins), arabinoxylan, pectin, and mannan were used to detect the presence of distinct cell wall polysaccharides in the longitudinal sectioned root tips. Green fluorescence indicates the targeted epitopes, violet signals are Calcofluor White stained cell walls. No significant difference was observed in polysaccharide presence and distribution between Golden Promise and the transgenic samples. Callose was found as dots in the cell walls, potentially indicating the location of plasmodesmata. AGPs were evenly distributed in the cell walls of the central stele and two outer most layers of columella cells. Arabinoxylan was not detected in any cell type. LM19 labelled unesterified homogalacturonan in the cortex area with strong signals detected in the junctions of cortical cells. Different from other major cell wall polysaccharides, mannan was not located in the cell wall, but in the cytoplasm, especially in the young root cells. As cells develop, mannan labelling moves towards the cell wall. Scale bar = 100 μm .

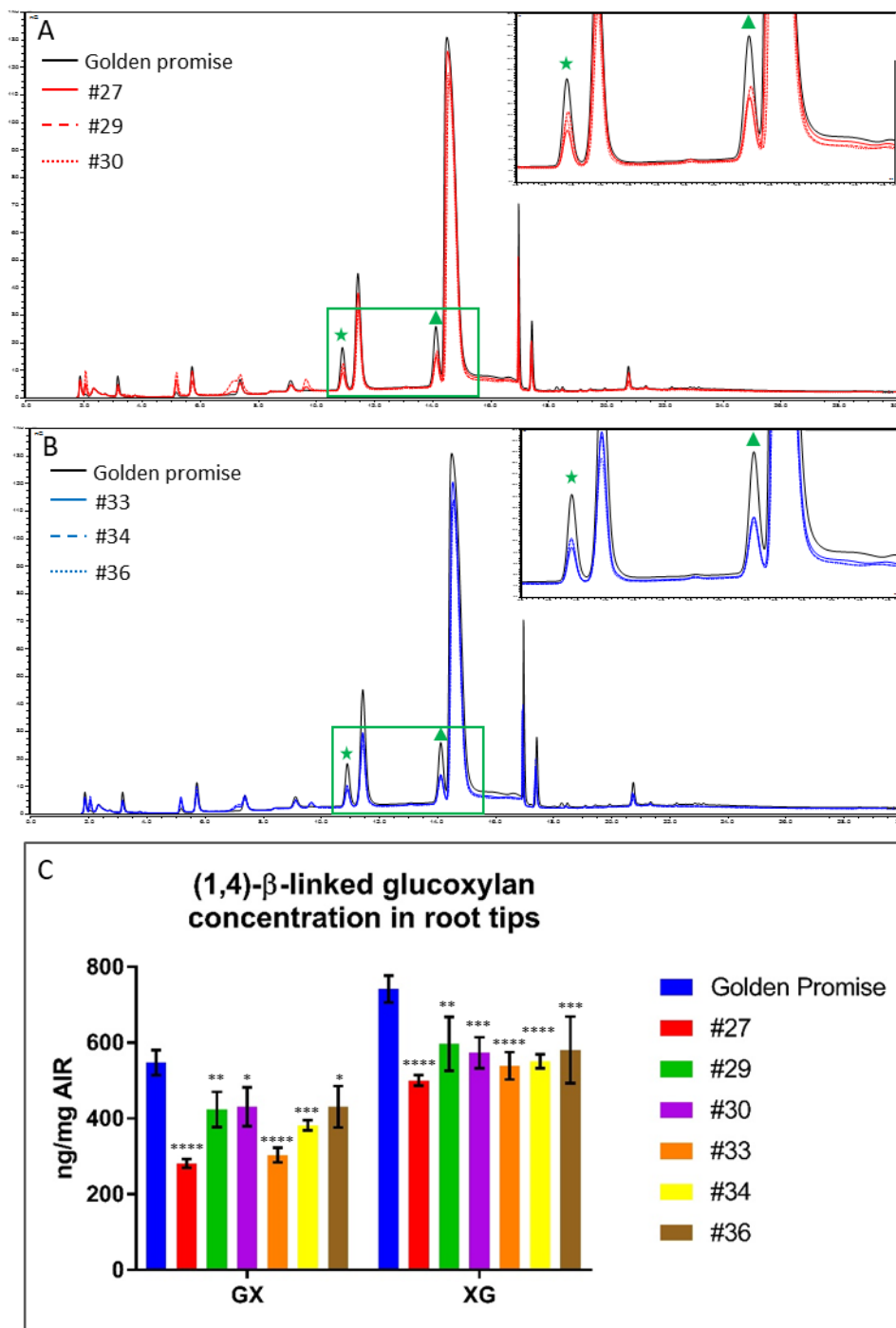


Figure 3-8. Quantification of (1,4)-β-linked glucoxytan in the root tips of Golden Promise, *HvCslF3-RNAi* and *HvCslF9-RNAi* plants. AIR root tissues were treated with the cellulase E-CELTR, and the hydrolysed clarified solutions were fractionated with 8% acetonitrile, and analysed using a Dionex ICS-5000 (Thermo Fisher Scientific) HPLC fitted with a CarboPac PA200 (3×250 mm) column. A and B, chromatogram of the hydrolysates. In the green box, peaks corresponding to glc-(1,4)-β-xyl (★), xylobiose, xyl-(1,4)-β-glc (▲), and cellobiose are

indicated (from left to right). The sum of glc-(1,4)- β -xyl and xyl-(1,4)- β -glc represent the products released from the E-CELTR hydrolysed (1,4)- β -linked glucoxytan. The transgenic samples (*HvCslF3-RNAi*: red; *HvCslF9-RNAi*: blue) showed smaller peak areas of xyl-(1,4)- β -glc and glc-(1,4)- β -xyl than Golden Promise (black), indicating lower concentrations of (1,4)- β -linked glucoxytan in root tips of *HvCslF3-RNAi* and *HvCslF9-RNAi* plants. B, average concentration of glc-(1,4)- β -xyl (GX) and xyl-(1,4)- β -glc (XG) in root tips. Significant decreases in the concentration of both oligosaccharides was observed, while the level of reduction varies between genotypes. Error bars represent standard errors. Significance was tested with 2way ANOVA and indicated as * (P<0.1), ** (P<0.01), *** (P<0.001), **** (P<0.0001).

A

Time	Flow (ml/min)	%A	%B	%C	%D
0		Run			
0	0.5	10	0	90	0
2	0.5	10	0	90	0
15	0.5	8.4	0	83.6	8
35	0.5	0	0	50	50
36	0.5	0	0	0	100
36.5	0.5	10	0	90	0
57.5		Stop Run			

B

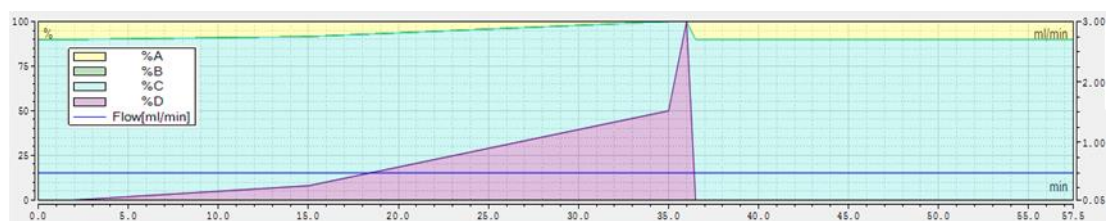


Figure 3-8. Solvent gradients used for (1,4)- β -linked glucoxytan quantification. A, composition of injected solvents over time. Solvent A: 0.1 M sodium hydroxide. Solvent B, 0.1 M sodium hydroxide, 1 M sodium acetate. Solvent C, water. Solvent D, 20 mM sodium hydroxide, 100 mM sodium acetate. Consistent flow at 0.5 ml/min of solvent was used throughout the analysis. Number percentage indicate the amount of each solvent. B, the gradient of each solvent over time. The gradient was optimized for better separating different oligosaccharides.

Tables

Table 3-1. List of primers used in the present study.

Primer name	Sequence
HvCsIF3_F	CTTGTTGCCGGTTGCCTTTACA
HvCsIF3_R	TCAATTGGCTAAAATGGAAGAAAATA
HvCsIF6_F	TGGGCATTACCTTCGTCAT
HvCsIF6_R	TGTCCGGCAAACCTCATCAA
HvCsIF9_F	CTGCCACCGCGTCCGTGTA
HvCsIF9_R	AGGTTTTGCAGCATTACTTGA
HvCsID1_F	CCGTCCCAGAACTCGCAGAT
HvCsID1_R	CATGACCCACCCACCGTTT
HvCsID2_F	GCCGCACAATTTASCAGCACAA
HvCsID2_R	GCCTGCTAGGGAACCAATA
HvCsID4_F	CGCTGCTCTGGGTCTATATCA
HvCsID4_R	CTGCTTAGGAATCCACCATCA
HvCsIH1_F	TGCTGTGGCTGGATGGTGTT
HvCsIH1_R	GCTTTATTATTGAGAGAGATTGGGAGA
GAPDH_F	GTGAGGCTGGTCTGATTACG
GAPDH_R	TGGTGCAGCTAGCATTGAGAC
HSP70_F	CGACCAGGGCAACCGCACCCAC
HSP70_R	ACGGTGTGATGGGGTTCATG
α -Tubulin_F	AGTGTCTGTCCACCCACTC
α -Tubulin_R	AGCATGAAGTGGATCCTTGG
Cyclophilin_F	CCTGTCGTGTCGTCGGTCTAAA
Cyclophilin_R	ACGCAGATCCAGCAGCCTAAAG
Hyg_F	GCCGTGGTTGGCTGTATG
Hyg_R	GGGGCGTCGGTTTCCACTAT
ISH_F3_AS_F	AATGTTGGTGAATCGGTGT
ISH_F3_AS_R	TAATACGACTCACTATAGGGCTCCAGCTTACTACAGAACCT
ISH_F3_S_F	TAATACGACTCACTATAGGGAATGTTGGTGAATCGGTGT
ISH_F3_S_R	CTCCAGCTTACTACAGAACCT
ISH_F9_AS_F	GGTGGTCATGGCCGTGAA
ISH_F9_AS_R	TAATACGACTCACTATAGGGGCTTTTACAGGTTTTGCAGCA
ISH_F9_S_F	TAATACGACTCACTATAGGGGGTGGTTCATGGCCGTGAA
ISH_F9_S_R	GCTTTTACAGGTTTTGCAGCA
BiFC_F3_F	AAAAAGATCTATGGCGTCGGCGGCCGGTGC
BiFC_F3_R	AAAAGGTACCCTAAAATGGAAGAAAATAAAGAAG
BiFC_F9_F	AAAAAGATCTTG TAAAACGACGGCCAGT
BiFC_F9_R	AAAAGGTACCCAGGAAACAGCTATGAC

Table 3-2. List of antibodies used for immunolabelling.

Epitope	Primary antibody	Type	Secondary antibody	Reference
(1,3;1,4)- β -glucan	BG1	Mouse IgG	Alexa Fluor 488 Goat Anti-rat IgG	Meikle et al., 1994
Callose	(1,3)- β -glucan	Mouse IgG	Alexa Fluor 488 Goat Anti-rat IgG	Delmer et al., 1993
Mannan	Anti-mannan	Mouse IgG	Alexa Fluor 488 Goat Anti-rat IgG	Pettolino et al., 2001
AGP	LM2	Rat IgM	DyLight 550 Goat Anti-rat IgM	Yates et al., 1996
Arabinoxylan	LM11	Rat IgM	DyLight 550 Goat Anti-rat IgM	McCartney et al., 2005
Pectin	LM19	Rat IgM	DyLight 550 Goat Anti-rat IgM	Verhertbruggen et al., 2009

Supplementary materials

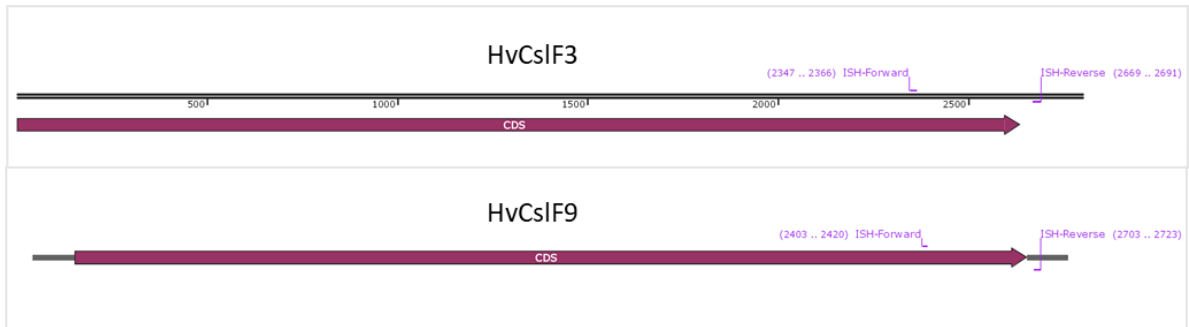


Figure 3-S1. Schematic diagrams of probe design for RNA-ISH. Probes are designed to contain the end of coding sequence and partial 3' UTR to improve the specificity.

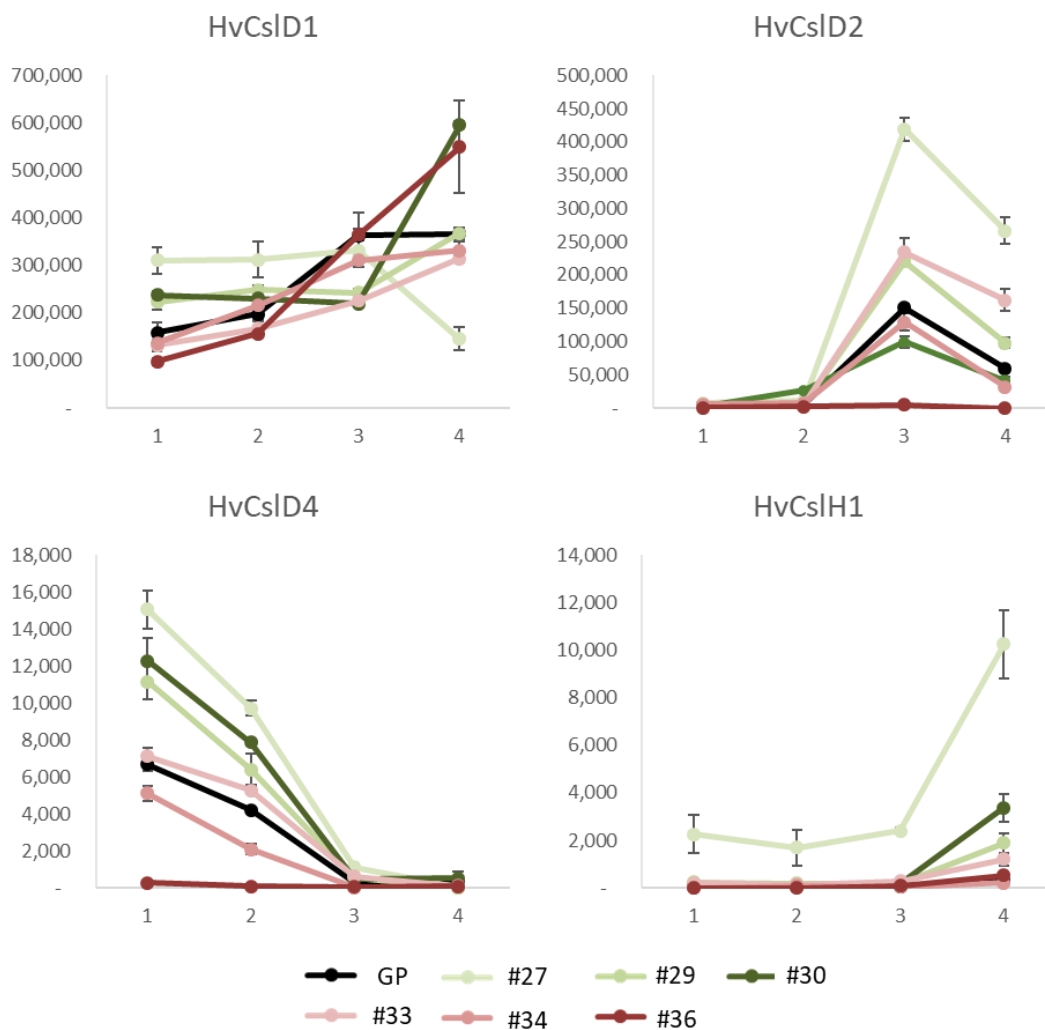


Figure 3-S2. Gene expression analysis by qPCR of different regions of root tips from Golden Promise, *HvCsIF3-RNAi* (#27, #29, #30), and *HvCsIF9-RNAi* (#33, #34, #36) lines. X axis represent the dissected root tips: 1, meristematic zone; 2, elongation zone; 3, young maturation zone; 4, old maturation zone. *HvCsID1* expressed higher towards maturation with no change observed in the *HvCsIF3-RNAi* and *HvCsIF9-RNAi* lines. *HvCsID2* was high expressed in the young maturation zone, and it expressed at higher level in lines #27, #29, #30, #33. *HvCsID4* showed highest expression in the meristem, and the expression decreased rapidly towards maturation zone. *HvCsIF3-RNAi* lines showed higher transcripts level of *HvCsID4*, whereas the *HvCsIF9-RNAi* lines were not affected. *HvCsIH1* only expressed in the mature root. The levels of expression were higher in the transgenic lines.

Reference

- Arioli T, Peng L, Betzner AS, Burn J, Wittke W, Herth W, Camilleri C, Höfte H, Plazinski J, Birch R** (1998) Molecular analysis of cellulose biosynthesis in Arabidopsis. *Science* **279**: 717-720
- Bassani M, Neumann PM, Gepstein S** (2004) Differential expression profiles of growth-related genes in the elongation zone of maize primary roots. *Plant Molecular Biology* **56**: 367-380
- Benková E, Hejátko J** (2008) Hormone interactions at the root apical meristem. *Plant Molecular Biology* **69**: 383-396
- Bichet A, Desnos T, Turner S, Grandjean O, Höfte H** (2001) BOTERO1 is required for normal orientation of cortical microtubules and anisotropic cell expansion in Arabidopsis. *The Plant Journal* **25**: 137-148
- Bringmann M, Li E, Sampathkumar A, Kocabek T, Hauser M-T, Persson S** (2012) POM-POM2/cellulose synthase interacting1 is essential for the functional association of cellulose synthase and microtubules in Arabidopsis. *The Plant Cell* **24**: 163-177
- Burk DH, Liu B, Zhong R, Morrison WH, Ye Z-H** (2001) A Katanin-like protein regulates normal cell wall biosynthesis and cell elongation. *The Plant Cell* **13**: 807-827
- Burton AL, Brown KM, Lynch JP** (2013) Phenotypic diversity of root anatomical and architectural traits in Zea species. *Crop Science* **53**: 1042-1055
- Burton RA, Collins HM, Kibble NAJ, Smith JA, Shirley NJ, Jobling SA, Henderson M, Singh RR, Pettolino F, Wilson SM, Bird AR, Topping DL, Bacic A, Fincher GB** (2011) Over-expression of specific HvCslF cellulose synthase-like genes in transgenic barley increases the levels of cell wall (1,3;1,4)- β -D-glucans and alters their fine structure. *Plant Biotechnology Journal* **9**: 117-135
- Burton RA, Jobling SA, Harvey AJ, Shirley NJ, Mather DE, Bacic A, Fincher GB** (2008) The genetics and transcriptional profiles of the cellulose synthase-like HvCslF gene family in barley. *Plant Physiology* **146**: 1821-1833
- Burton RA, Shirley NJ, King BJ, Harvey AJ, Fincher GB** (2004) The CesA gene family of barley. Quantitative analysis of transcripts reveals two groups of co-expressed genes. *Plant Physiology* **134**: 224-236
- Burton RA, Wilson SM, Hrmova M, Harvey AJ, Shirley NJ, Medhurst A, Stone BA, Newbigin EJ, Bacic A, Fincher GB** (2006) Cellulose synthase-like CslF genes mediate the synthesis of cell wall (1, 3; 1, 4)- β -D-glucans. *Science* **311**: 1940-1942
- Camilleri C, Azimzadeh J, Pastuglia M, Bellini C, Grandjean O, Bouchez D** (2002) The Arabidopsis TONNEAU2 gene encodes a putative novel protein phosphatase 2A regulatory subunit essential for the control of the cortical cytoskeleton. *The Plant Cell* **14**: 833-845
- Chimungu JG, Brown KM, Lynch JP** (2014) Reduced root cortical cell file number improves drought tolerance in maize. *Plant Physiology* **166**: 1943-1955
- Cocuron J-C, Lerouxel O, Drakakaki G, Alonso AP, Liepman AH, Keegstra K, Raikhel N, Wilkerson CG** (2007) A gene from the cellulose synthase-like C family encodes a β -1, 4 glucan synthase. *Proceedings of the National Academy of Sciences of the United States of America* **104**: 8550-8555
- Cosgrove DJ** (2005) Growth of the plant cell wall. *Nature Reviews Molecular Cell Biology* **6**: 850
- Coudert Y, Périn C, Courtois B, Khong NG, Gantet P** (2010) Genetic control of root development in rice, the model cereal. *Trends in Plant Science* **15**: 219-226
- Cseh A, Soós V, Rakszegi M, Türkösi E, Balázs E, Molnár-Láng M** (2013) Expression of HvCslF9 and HvCslF6 barley genes in the genetic background of wheat and their

- influence on the wheat β -glucan content. *Annals of Applied Biology* **163**: 142-150
- Cui H, Levesque MP, Vernoux T, Jung JW, Paquette AJ, Gallagher KL, Wang JY, Blilou I, Scheres B, Benfey PN** (2007) An evolutionarily conserved mechanism delimiting SHR movement defines a single layer of endodermis in plants. *Science* **316**: 421-425
- Dhugga KS, Barreiro R, Whitten B, Stecca K, Hazebroek J, Randhawa GS, Dolan M, Kinney AJ, Tomes D, Nichols S** (2004) Guar seed β -mannan synthase is a member of the cellulose synthase super gene family. *Science* **303**: 363-366
- Doblin MS, Kurek I, Jacob-Wilk D, Delmer DP** (2002) Cellulose biosynthesis in plants: from genes to rosettes. *Plant Cell Physiology* **43**: 1407-1420
- Doblin MS, Pettolino FA, Wilson SM, Campbell R, Burton RA, Fincher GB, Newbigin E, Bacic A** (2009) A barley cellulose synthase-like CslH gene mediates (1, 3; 1, 4)- β -D-glucan synthesis in transgenic Arabidopsis. *Proceedings of the National Academy of Sciences of the United States of America* **106**: 5996-6001
- Douchkov D, Lueck S, Hensel G, Kumlehn J, Rajaraman J, Johrde A, Doblin MS, Beahan CT, Kopischke M, Fuchs R, Lipka V, Niks RE, Bulone V, Chowdhury J, Little A, Burton RA, Bacic A, Fincher GB, Schweizer P** (2016) The barley (*Hordeum vulgare*) cellulose synthase-like D2 gene (*HvCslD2*) mediates penetration resistance to host-adapted and nonhost isolates of the powdery mildew fungus. *New Phytologist* **212**: 421-433
- Evans DE** (2004) Aerenchyma formation. *New Phytologist* **161**: 35-49
- Fagard M, Desnos T, Desprez T, Goubet F, Refregier G, Mouille G, McCann M, Rayon C, Vernhettes S, Höfte H** (2000) PROCUSTE1 encodes a cellulose synthase required for normal cell elongation specifically in roots and dark-grown hypocotyls of Arabidopsis. *The Plant Cell* **12**: 2409-2423
- Fincher GB** (2009) Revolutionary times in our understanding of cell wall biosynthesis and remodeling in the grasses. *Plant Physiology* **149**: 27-37
- Gallagher KL, Paquette AJ, Nakajima K, Benfey PN** (2004) Mechanisms regulating SHORT-ROOT intercellular movement. *Current Biology* **14**: 1847-1851
- Goubet F, Barton CJ, Mortimer JC, Yu X, Zhang Z, Miles GP, Richens J, Liepman AH, Seffen K, Dupree P** (2009) Cell wall glucomannan in Arabidopsis is synthesised by CSLA glycosyltransferases, and influences the progression of embryogenesis. *The Plant Journal* **60**: 527-538
- Guerriero G, Hausman J-F, Cai G** (2014) No stress! Relax! Mechanisms governing growth and shape in plant cells. *International Journal of Molecular Sciences* **15**: 5094-5114
- Hall H, Ellis B** (2013) Transcriptional programming during cell wall maturation in the expanding Arabidopsis stem. *BMC Plant Biology* **13**: 14-30
- Hématy K, Höfte H** (2006) Cellulose and cell elongation. *In* *The Expanding Cell*. Springer, pp 33-56
- Hochholdinger F, Park WJ, Sauer M, Woll K** (2004) From weeds to crops: genetic analysis of root development in cereals. *Trends in Plant Science* **9**: 42-48
- Hochholdinger F, Zimmermann R** (2008) Conserved and diverse mechanisms in root development. *Current Opinion in Plant Biology* **11**: 70-74
- Imani J, Li L, Schäfer P, Kogel KH** (2011) STARTS—A stable root transformation system for rapid functional analyses of proteins of the monocot model plant barley. *The Plant Journal* **67**: 726-735
- Ivanov VB, Dubrovsky JG** (2013) Longitudinal zonation pattern in plant roots: conflicts and solutions. *Trends in Plant Science* **18**: 237-243
- Jaramillo RE, Nord EA, Chimungu JG, Brown KM, Lynch JP** (2013) Root cortical burden influences drought tolerance in maize. *Annals of Botany* **112**: 429-437
- Kim CM, Park S, Je BI, Park S, Park S, Piao H-L, Eun M, Dolan L, Han C-d** (2007) OsCSLD1, a Cellulose Synthase-Like D1 gene, is required for root hair morphogenesis

- in rice. *Plant Physiology* **143**: 1220-1230
- Kirschner GK, Stahl Y, Von Korff M, Simon R** (2017) Unique and conserved features of the barley root meristem. *Frontiers in Plant Science* **8**: 1240-1240
- Lee D-K, Ahn JH, Song S-K, Do Choi Y, Lee JS** (2003) Expression of an expansin gene is correlated with root elongation in soybean. *Plant Physiology* **131**: 985-997
- Li M, Xiong G, Li R, Cui J, Tang D, Zhang B, Pauly M, Cheng Z, Zhou Y** (2009) Rice cellulose synthase-like D4 is essential for normal cell-wall biosynthesis and plant growth. *The Plant Journal* **60**: 1055-1069
- Lim J, Helariutta Y, Specht CD, Jung J, Sims L, Bruce WB, Diehn S, Benfey PN** (2000) Molecular analysis of the SCARECROW gene in maize reveals a common basis for radial patterning in diverse meristems. *The Plant Cell* **12**: 1307-1318
- Little A, Lahnstein J, Jeffery DW, Khor SF, Schwerdt JG, Shirley NJ, Hooi M, Xing X, Burton RA, Bulone V** (2019) A novel (1, 4)- β -linked glucoxytan is synthesized by members of the Cellulose Synthase-Like F gene family in land plants. *ACS Central Science* **5**: 73-84
- Lombard V, Ramulu HG, Drula E, Coutinho PM, Henrissat B** (2014) The carbohydrate-active enzymes database (CAZy) in 2013. *Nucleic Acids Research* **42**: D490-D495
- Lux A, Luxová M, Abe J, Morita S** (2004) Root cortex: structural and functional variability and responses to environmental stress. *Root Research* **13**: 117-131
- Luxová M** (1986) The seminal root primordia in barley and the participation of their non-meristematic cells in root construction. *Biologia Plantarum* **28**: 161
- Markakis MN, De Cnodder T, Lewandowski M, Simon D, Boron A, Balcerowicz D, Doubbo T, Taconnat L, Renou J-P, Höfte H, Verbelen J-P, Vissenberg K** (2012) Identification of genes involved in the ACC-mediated control of root cell elongation in *Arabidopsis thaliana*. *BMC Plant Biology* **12**: 208
- Mascher M, Gundlach H, Himmelbach A, Beier S, Twardziok SO, Wicker T, Radchuk V, Dockter C, Hedley PE, Russell J, Bayer M, Ramsay L, Liu H, Haberer G, Zhang X-Q, Zhang Q, Barrero RA, Li L, Taudien S, Groth M, Felder M, Hastie A, Šimková H, Staňková H, Vrána J, Chan S, Muñoz-Amatriaín M, Ounit R, Wanamaker S, Bolser D, Colmsee C, Schmutzer T, Aliyeva-Schnorr L, Grasso S, Tanskanen J, Chailyan A, Sampath D, Heavens D, Clissold L, Cao S, Chapman B, Dai F, Han Y, Li H, Li X, Lin C, McCooke JK, Tan C, Wang P, Wang S, Yin S, Zhou G, Poland JA, Bellgard MI, Borisjuk L, Houben A, Doležel J, Ayling S, Lonardi S, Kersey P, Langridge P, Muehlbauer GJ, Clark MD, Caccamo M, Schulman AH, Mayer KFX, Platzer M, Close TJ, Scholz U, Hansson M, Zhang G, Braumann I, Spannagl M, Li C, Waugh R, Stein N** (2017) A chromosome conformation capture ordered sequence of the barley genome. *Nature* **544**: 427-433
- Mayer KFX, Waugh R, Langridge P, Close TJ, Wise RP, Graner A, Matsumoto T, Sato K, Schulman A, Muehlbauer GJ, Stein N, Ariyadasa R, Schulte D, Poursarebani N, Zhou R, Steuernagel B, Mascher M, Scholz U, Shi B, Langridge P, Madishetty K, Svensson JT, Bhat P, Moscou M, Resnik J, Close TJ, Muehlbauer GJ, Hedley P, Liu H, Morris J, Waugh R, Frenkel Z, Korol A, Bergès H, Graner A, Stein N, Steuernagel B, Scholz U, Taudien S, Felder M, Groth M, Platzer M, Stein N, Steuernagel B, Scholz U, Himmelbach A, Taudien S, Felder M, Platzer M, Lonardi S, Duma D, Alpert M, Cordero F, Beccuti M, Ciardo G, Ma Y, Wanamaker S, Close TJ, Stein N, Cattonaro F, Vendramin V, Scalabrin S, Radovic S, Wing R, Schulte D, Steuernagel B, Morgante M, Stein N, Waugh R, Nussbaumer T, Gundlach H, Martis M, Ariyadasa R, Poursarebani N, Steuernagel B, Scholz U, Wise RP, Poland J, Stein N, Mayer KFX, Spannagl M, Pfeifer M, Gundlach H, Mayer KFX, Gundlach H, Moisy C, Tanskanen J, Scalabrin S, Zuccolo A, Vendramin V, Morgante M, Mayer KFX, Schulman A, Pfeifer M, Spannagl M, Hedley P, Morris**

- J, Russell J, Druka A, Marshall D, Bayer M, Swarbreck D, Sampath D, Ayling S, Febrer M, Caccamo M, Matsumoto T, Tanaka T, Sato K, Wise RP, Close TJ, Wannamaker S, Muehlbauer GJ, Stein N, Mayer KFX, Waugh R, Steuernagel B, Schmutzer T, Mascher M, Scholz U, Taudien S, Platzer M, Sato K, Marshall D, Bayer M, Waugh R, Stein N, Mayer KFX, Waugh R, Brown JWS, Schulman A, Langridge P, Platzer M, Fincher GB, Muehlbauer GJ, Sato K, Close TJ, Wise RP, Stein N, The International Barley Genome Sequencing C** (2012) A physical, genetic and functional sequence assembly of the barley genome. *Nature* **491**: 711-716
- McCartney L, Steele-King CG, Jordan E, Knox JP** (2003) Cell wall pectic (1-4)- β -D-galactan marks the acceleration of cell elongation in the Arabidopsis seedling root meristem. *The Plant Journal* **33**: 447-454
- Newman C, Newman R** (2006) A brief history of barley foods. *Cereal Foods World* **51**: 4-7
- Olbrich A, Hillmer S, Hinz G, Oliviusson P, Robinson DG** (2007) Newly formed vacuoles in root meristems of barley and pea seedlings have characteristics of both protein storage and lytic vacuoles. *Plant Physiology* **145**: 1383-1394
- Orman-Ligeza B, Parizot B, Gantet PP, Beeckman T, Bennett MJ, Draye X** (2013) Post-embryonic root organogenesis in cereals: branching out from model plants. *Trends in Plant Science* **18**: 459-467
- Pallardy SG** (2008) CHAPTER 2 - The woody plant body. *In* SG Pallardy, ed, *Physiology of Woody Plants* (Third Edition). Academic Press, San Diego, pp 9-38
- Passardi F, Tognolli M, De Meyer M, Penel C, Dunand C** (2006) Two cell wall associated peroxidases from Arabidopsis influence root elongation. *Planta* **223**: 965-974
- Petriccka JJ, Winter CM, Benfey PN** (2012) Control of Arabidopsis root development. *Annual Review of Plant Biology* **63**: 563-590
- Ray B, Lahaye M** (1995) Cell-wall polysaccharides from the marine green alga *Ulva* "rigida" (Ulvales, Chlorophyta). Extraction and chemical composition. *Carbohydrate Research* **274**: 251-261
- Richmond TA, Somerville CR** (2000) The cellulose synthase superfamily. *Plant Physiology* **124**: 495-498
- Schindelin J, Arganda-Carreras I, Frise E, Kaynig V, Longair M, Pietzsch T, Preibisch S, Rueden C, Saalfeld S, Schmid B, Tinevez J-Y, White DJ, Hartenstein V, Eliceiri K, Tomancak P, Cardona A** (2012) Fiji: an open-source platform for biological-image analysis. *Nature Methods* **9**: 676-682
- Schindelman G, Morikami A, Jung J, Baskin TI, Carpita NC, Derbyshire P, McCann MC, Benfey PN** (2001) COBRA encodes a putative GPI-anchored protein, which is polarly localized and necessary for oriented cell expansion in Arabidopsis. *Genes Development* **15**: 1115-1127
- Schneider HM, Postma JA, Wojciechowski T, Kuppe C, Lynch JP** (2017) Root cortical senescence improves growth under suboptimal availability of N, P, and K. *Plant Physiology* **174**: 2333-2347
- Schneider HM, Wojciechowski T, Postma JA, Brown KM, Lücke A, Zeisler V, Schreiber L, Lynch JP** (2017) Root cortical senescence decreases root respiration, nutrient content and radial water and nutrient transport in barley. *Plant, Cell Environment* **40**: 1392-1408
- Schumacher K, Vafeados D, McCarthy M, Sze H, Wilkins T, Chory J** (1999) The Arabidopsis *det3* mutant reveals a central role for the vacuolar H⁺-ATPase in plant growth and development. *Genes Development* **13**: 3259-3270
- Schwerdt JG, MacKenzie K, Wright F, Oehme D, Wagner JM, Harvey AJ, Shirley NJ, Burton RA, Schreiber M, Halpin C, Zimmer J, Marshall DF, Waugh R, Fincher GB** (2015) Evolutionary dynamics of the Cellulose Synthase gene superfamily in grasses. *Plant Physiology* **168**: 968-983

- Somssich M, Khan GA, Persson S** (2016) Cell wall heterogeneity in root development of *Arabidopsis*. *Frontiers in Plant Science* **7**: 1242-1252
- Steffens B, Sauter M** (2009) Epidermal cell death in rice is confined to cells with a distinct molecular identity and is mediated by ethylene and H₂O₂ through an autoamplified signal pathway. *The Plant Cell* **21**: 184-196
- Taketa S, Yuo T, Tonooka T, Tsumuraya Y, Inagaki Y, Haruyama N, Larroque O, Jobling SA** (2011) Functional characterization of barley betaglucanless mutants demonstrates a unique role for CslF6 in (1, 3; 1, 4)- β -D-glucan biosynthesis. *Journal of Experimental Botany* **63**: 381-392
- Taylor NG, Howells RM, Huttly AK, Vickers K, Turner SR** (2003) Interactions among three distinct CesA proteins essential for cellulose synthesis. *Proceedings of the National Academy of Sciences of the United States of America* **100**: 1450-1455
- Tucker MR, Lou H, Aubert MK, Wilkinson LG, Little A, Houston K, Pinto SC, Shirley NJ** (2018) Exploring the role of cell wall-related genes and polysaccharides during plant development. *Plants* **7**: 42-58
- Ullrich SE** (2010) *Barley: Production, improvement, and uses*, Vol 12. John Wiley & Sons
- Ursache R, Andersen TG, Marhavý P, Geldner N** (2018) A protocol for combining fluorescent proteins with histological stains for diverse cell wall components. *The Plant Journal* **93**: 399-412
- Vandesompele J, De Preter K, Pattyn F, Poppe B, Van Roy N, De Paepe A, Speleman F** (2002) Accurate normalization of real-time quantitative RT-PCR data by geometric averaging of multiple internal control genes. *Genome Biology* **3**: research0034. 0031
- Verherbruggen Y, Yin L, Oikawa A, Scheller HV, behavior** (2011) Mannan synthase activity in the CslD family. *Plant Signaling* **6**: 1620-1623
- Wang C, Li S, Ng S, Zhang B, Zhou Y, Whelan J, Wu P, Shou H** (2014) Mutation in xyloglucan 6-xylosyltransferase results in abnormal root hair development in *Oryza sativa*. *Journal of Experimental Botany* **65**: 4149-4157
- Whittington AT, Vugrek O, Wei KJ, Hasenbein NG, Sugimoto K, Rashbrooke MC, Wasteney GO** (2001) MOR1 is essential for organizing cortical microtubules in plants. *Nature* **411**: 610-613
- Wilkinson LG, Tucker MR** (2017) An optimised clearing protocol for the quantitative assessment of sub-epidermal ovule tissues within whole cereal pistils. *Plant Methods* **13**: 67-76
- Yamauchi T, Rajhi I, Nakazono M** (2011) Lysigenous aerenchyma formation in maize root is confined to cortical cells by regulation of genes related to generation and scavenging of reactive oxygen species. *Plant Signaling Behavior* **6**: 759-761
- Yamauchi T, Shimamura S, Nakazono M, Mochizuki T** (2013) Aerenchyma formation in crop species: a review. *Field Crops Research* **152**: 8-16
- Yang JL, Zhu XF, Peng YX, Zheng C, Li GX, Liu Y, Shi YZ, Zheng SJ** (2011) Cell wall hemicellulose contributes significantly to aluminum adsorption and root growth in *Arabidopsis*. *Plant Physiology* **155**: 1885-1892
- Yang L, Wang CC, Guo WD, Li XB, Lu M, Yu CL** (2006) Differential expression of cell wall related genes in the elongation zone of rice roots under water deficit. *Russian Journal of Plant Physiology* **53**: 390-395
- Yang X, Li G, Tian Y, Song Y, Liang W, Zhang D** (2018) A rice glutamyl-tRNA synthetase modulates early anther cell division and patterning. *Plant Physiology* **177**: 728-744
- Yao S-G, Taketa S, Ichii M** (2002) A novel short-root gene that affects specifically early root development in rice (*Oryza sativa* L.). *Plant Science* **163**: 207-215
- Yin L, Verherbruggen Y, Oikawa A, Manisseri C, Knierim B, Prak L, Jensen JK, Knox JP, Auer M, Willats WG** (2011) The cooperative activities of CSLD2, CSLD3, and CSLD5 are required for normal *Arabidopsis* development. *Molecular Plant* **4**: 1024-

1037

Yu Z, Kang B, He X, Lv S, Bai Y, Ding W, Chen M, Cho HT, Wu P (2011) Root hair-specific expansins modulate root hair elongation in rice. *The Plant Journal* **66**: 725-734

Zeng J, Dong Z, Wu H, Tian Z, Zhao Z (2017) Redox regulation of plant stem cell fate. *The EMBO Journal* **36**: 2844-2855

Chapter 4

***HvCsIF3* affects root epidermal cell proliferation and root hair elongation**



Statement of Authorship

Title of Paper	HvCslF3 Affects Root Epidermal Cell Proliferation and Root Hair Elongation
Publication Status	<input type="checkbox"/> Published <input type="checkbox"/> Accepted for Publication <input type="checkbox"/> Submitted for Publication <input checked="" type="checkbox"/> Unpublished and Unsubmitted work written in manuscript style
Publication Details	HvCslF3 Affects Root Epidermal Cell Proliferation and Root Hair Elongation Haoyu Lou, Julian Schwerdt, Jelle Lahnstein, Leah Band, Malcolm Bennett, Matthew Tucker, Vincent Bulone

Principal Author

Name of Principal Author (Candidate)	Haoyu Lou		
Contribution to the Paper	Performed experiments and analysed data. Wrote the manuscript.		
Overall percentage (%)	70%		
Certification:	This paper reports on original research I conducted during the period of my Higher Degree by Research candidature and is not subject to any obligations or contractual agreements with a third party that would constrain its inclusion in this thesis. I am the primary author of this paper.		
Signature		Date	24/02/2020

Co-Author Contributions

By signing the Statement of Authorship, each author certifies that:

the candidate's stated contribution to the publication is accurate (as detailed above);

permission is granted for the candidate to include the publication in the thesis; and

the sum of all co-author contributions is equal to 100% less the candidate's stated contribution.

Name of Co-Author	Vincent Bulone		
Contribution to the Paper	Principle supervisor. Conceived the project and designed experiments. Assisted with writing of the manuscript. I hereby certify that the statement of authorship is accurate.		
Signature		Date	24/02/2020

Name of Co-Author	Matthew Tucker		
-------------------	----------------	--	--

Chapter 4 – *HvCs1F3* affects root epidermal cell proliferation and root hair elongation

Contribution to the Paper	Co-supervisor. Conceived the project and designed experiments. Assisted with writing of the manuscript. I hereby certify that the statement of authorship is accurate.		
Signature		Date	24/02/2020

Name of Co-Author	Malcolm Bennett		
Contribution to the Paper	Co-supervisor at University of Nottingham. Conceived the project and designed experiments. Assisted with writing of the manuscript. I hereby certify that the statement of authorship is accurate.		
Signature		Date	24/2/20

Name of Co-Author	Leah Band		
Contribution to the Paper	Co-supervisor at University of Nottingham. Conceived the project and designed experiments. Assisted with writing of the manuscript. I hereby certify that the statement of authorship is accurate.		
Signature		Date	25/02/2020

Name of Co-Author	Jelle Lahnstein		
Contribution to the Paper	Assisted with experiment and data analysis and editing of the manuscript. I hereby certify that the statement of authorship is accurate.		
Signature		Date	25/2/2020

Name of Co-Author	Julian Schwerdt		
Contribution to the Paper	Assisted with experiment and data analysis and editing of the manuscript. I hereby certify that the statement of authorship is accurate.		
Signature		Date	26/02/2020

Abstract

Cellulose synthase-like (Csl) gene families play important roles in cell wall polysaccharide biosynthesis in many plant species. To date, at least ten different families have been identified. Phylogenetic studies have highlighted the close relationship between the *CsID* and *CesA* gene families during evolution. *CsID* genes are known to participate in pollen tube development, root hair emergence and root hair elongation, and some studies have suggested *AtCsID2/3/5* and *AtCsID1/4* are involved in mannan and cellulose biosynthesis, respectively. Despite this, the functional characterization of individual *CsID* genes has yet to be performed. The *CsIF* family branch out from the *CsID* family as a major family specific to the Poaceae. It is hypothesized the *CsIF* family may maintain ancestral functions similar to *CsID* genes during evolution. Barley *CsIF* genes are responsible for the synthesis of cell wall polysaccharides (1,3;1,4)- β -glucan (*HvCsIF6*) and (1,4)- β -linked glucoxytan (*HvCsIF3* and *HvCsIF10*). Of these, *HvCsIF3* appears to function in normal root tip and root hair development in barley seedlings. However, functional characterization of *HvCsIF3* is challenging due to the presence of multiple barley *CsIF* genes, a lack of mutant resources and the complexity of barley root structure. The Arabidopsis genome lacks the *CsIF* family and therefore provides an ideal heterologous system to study the role of *HvCsIF3* during root development. By expressing *HvCsIF3* in wild type (Col-0) and root hair deficient mutants (*csld3* and *csld5*) in Arabidopsis, I demonstrated the ability of *HvCsIF3* to complement the *csld5* mutant phenotype. *HvCsIF3* also positively affected root hair elongation in different Arabidopsis genotypes and led to alterations in epidermal cell fate determination. Despite the importance of *HvCsIF3* in the regulation of root hair growth, no (1,4)- β -linked glucoxytan was detected in complemented Arabidopsis *csld5* plants, conflicting with previous experiments using tobacco leaf transient expression. My results reveal functional redundancy between the *CsID* and *CsIF* gene families and support a role for *HvCsIF3* during root hair development.

Introduction

Roots are essential underground organs that anchor the plant to its substrate and absorb water and nutrients from the surrounding environment to support growth. The development of the whole plant is largely dependent on a functional root system. Monocot cereals such as barley develop a fibrous root system, whereas tap root systems are commonly found in dicot species including *Arabidopsis*. The complexity of the root tissue arrangement and the difficulty of accessing underground material presents challenges for root developmental studies (Petricka et al., 2012). Despite this, the root provides an exceptional *in vitro* system to study cell division, growth and differentiation. The root longitudinal axis can be divided into three distinct developmental stages termed root apical meristem, elongation and maturation zones. A stem cell niche made up of quiescent centre (QC) cells surrounded by initial cells located just above the root cap. The size of the QC and number of initial cells varies between species. For example, *Arabidopsis* roots have 2-4 QC cells, while the number of QC cells in cereal crops varies between 30 to 1200 cells (Hochholdinger and Zimmermann, 2008; Petricka et al., 2012; Kirschner et al., 2017). The QC maintains the undifferentiated status of initial cells. When initial cells divide, the QC produces short range signals to adjacent daughter cells to maintain stem cell identity, while the other daughter cell escapes from the stem cell niche and starts to differentiate to form specific tissues (van den Berg et al., 1997; Petricka et al., 2012). Cells in the meristem zone undergo rapid division before entering the elongation zone, where cell division stops, and longitudinal expansion functions to lengthen the root. Genes involved in cell wall synthesis and remodelling are important in this process as they regulate the stiffness and flexibility of cell walls during elongation. At maturation, cell elongation ceases, secondary cell walls forms, and different cell types finalize differentiation to form fully functional tissues. The maturation zone is demarked by the formation of root hairs (Shibata and Sugimoto, 2019).

Over the last few decades, intense efforts have been dedicated to the understanding of

the development and regulation of Arabidopsis roots because of their simple cellular organization (Petricka et al., 2012). Arabidopsis roots are composed of concentric layers of epidermis, cortex, endodermis, pericycle and central stele tissues which is established during embryogenesis (Dolan et al., 1993). The cortex and endodermis are each comprised of eight cells, while epidermal cell number exhibits more variability (Dolan et al., 1993). A single layered cortex is one of the features found in Arabidopsis roots. The cortex is significant for the determination of the position-dependent root hair cell fate. Arabidopsis root hair forming cells, or trichoblasts, are organized in cell files and follow a position-dependent pattern, where only the eight epidermal cells in direct contact with two cortex cells form root hairs (Dolan et al., 1993; Salazar-Henao et al., 2016). In contrast to Arabidopsis, the formation of root hair in monocots follow either an asymmetric cell division dependent pattern (e.g. Brachypodium) or random patterns (e.g. in barley and rice) (Pemberton et al., 2001; Salazar-Henao et al., 2016). The process of root hair development provides an excellent model for cellular morphogenesis studies, especially in investigations focused on cell shape and tip growth processes. The transcriptional and hormonal control of Arabidopsis root hair development is well characterized compared to other plant species.

Recent findings from various species have indicated the importance of *CsID* genes at different stages of root hair development. The *CsID* genes belong to the *CesA/Csl* superfamily, whose members are proven to participate in the synthesis and regulation of various cell wall polysaccharides including cellulose (*CesA*), mannan (*CslA*), xyloglucan (*CslC*), (1,3;1,4)- β -glucan (*CslF6*, *CslHI*) and (1,4)- β -linked glucoxytan (*CslF3/10*) (Doblin et al., 2002; Burton et al., 2006; Cocuron et al., 2007; Doblin et al., 2009; Goubet et al., 2009; Little et al., 2019). The cooperative activities of *AtCsID2*, *AtCsID3*, and *AtCsID5* were demonstrated using loss of function *cslD2/3/5* double and triple mutants that exhibited significant defects in plant development, with the most severe effects found during root hair development (Yin et al., 2011). Similar phenotypes were also observed in rice *cslD1* and *cslD4* mutants, the apparent

Chapter 4 – *HvCsIF3* affects root epidermal cell proliferation and root hair elongation

orthologues to *AtCslD3* and *AtCslD5*, respectively. *OsCslD1* is specifically expressed in the root hair forming cells and knockout of *OsCslD1* resulted in aborted root hairs (Kim et al., 2007). In contrast, *OsCslD4* expression is detected in a range of different rice tissues, with high levels detected in growing regions including root tips (Li et al., 2009). Alterations in cell wall polysaccharide composition were also reported in rice *cslD4* mutant plants, which showed reduced xylan and cellulose content and an increased amount of homogalacturonans (Li et al., 2009). More recently, the poplar *PtrCslD5* gene has been shown to be the functional ortholog of *AtCslD3*, as the Arabidopsis *cslD3* mutant was successfully complemented with *PtrCslD5* (Peng et al., 2019). However, any association between *CsID* genes and root hair development has not been reported in barley. One *CsID* member in barley, i.e. *HvCslD2*, functions in pathogen defence through alterations in callose deposition and cell wall composition (Douchkov et al., 2016). Unlike the high expression of *CsID* genes in tip growing tissues of other species, *HvCslD2* showed increased transcript levels in leaves under powdery mildew attack, indicating a different role of *CsID* genes in barley (Douchkov et al., 2016). In addition to *CsID* genes, the related *CsIF* family is of interest as it is largely limited to Poaceae species with distinct functions in the synthesis of (1,3;1,4)- β -glucan (*CsIF6*) and (1,4)- β -linked glucoxytan (*HvCsIF3*, *HvCsIF10*) in cell walls (Burton et al., 2006; Little et al., 2019). A close relationship between the *CsID* and *CsIF* gene families has been described from an evolutionary point of view, whereby *CsIF* genes appear to have evolved from *CsIDs* (Schwerdt et al., 2015; Schwerdt, 2017). One possibility is that *CsIF* and *CsID* genes may share some ancestral functions through evolution. In the present study, we aimed to explore the function of *HvCsIF3* during root development by employing *HvCsIF3* in complementation experiments of Arabidopsis *cslD3* and *cslD5* mutants. Successful phenotypic recovery of *cslD5* complemented with *HvCsIF3* was demonstrated. Expression of *HvCsIF3* in Arabidopsis not only enhanced root hair growth and elongation, but also altered the fate of epidermal cells from non-hair cells to hair-forming cells. However, no significant (1,4)- β -linked glucoxytan accumulated in

transgenic *Arabidopsis* expressing *HvCslF3*, contrasting the report of Little et al. (2019), who reported the accumulation of (1,4)- β -linked glucoxyylan after transient expression of *HvCslF3* in tobacco leaves.

Materials and methods

Plant growth conditions

Soil grown *Arabidopsis* were stratified at 4°C for 48 h and moved into growth chambers (16/8 h day/night under 23°C) for further development. For root hair analysis, seeds were surface-sterilized with 70% (v/v) ethanol containing Triton X-100 (0.01% v/v) for 2 m, followed by a treatment with 5% (v/v) sodium hypochlorite for 8 m. Seeds were washed with sterile distilled water 4 times before being sowed on growth medium (1% agar, 2.22g/L Murashige and Skoog basal salts, pH 5.8). Plates were sealed with micropore tape and stratified at 4°C for 48 h before being moved into a growth chamber (24 h day light, 21°C). Plates were kept vertically to allow root development.

Gene phylogenetic analysis

cDNA sequences of *CslD* and *CslF* members of *Arabidopsis* (*Arabidopsis thaliana*), tomato (*Solanaceae lycopersicum*), barley (*Hordeum vulgare*) and rice (*Oryza sativa Japonica*) were obtained from the Ensembl databases (<https://doi.org/10.1093/nar/gky1113>). Candidate sequences were translated and aligned with the MUSCLE (Edgar, 2004) plugin for Geneious 8.1.9 (<https://www.geneious.com>) using default parameters. An unrooted phylogenetic tree was constructed with the RAxML (7.2.8) (Stamatakis, 2006) plugin for Geneious using the WAG+G substitution model. Node support was assessed using 500 rapid bootstrap replicates.

Construct design

The GreenGate cloning system was used for design of the constructs (Lampropoulos et

al., 2013). The *HvCsIF3* (HORVU2Hr1G042350) sequence was amplified from the cDNA of the wild-type barley cultivar Golden Promise. *AtCsID3* (At3g03050) and *AtCsID5* (At1g02730) sequences were obtained from Arabidopsis wild type cultivar Col-0 genomic DNA and cDNA, respectively. The *BsaI* recognition sites were mutated silently by PCR (*HvCsIF3*: ⁶²¹G → A; *AtCsID3*: ⁸³¹A → G; *AtCsID5*: ²⁵³²A → G) and the resulting amplified coding sequences were cloned into the GGC000 module. The *Ubiquitin10* and *Cobra-like9* promoters were amplified from Col-0 genomic DNA and cloned into the GGA000 module. They served as over-expression and root hair cell specific expression modules, respectively. The assembly of the destination vectors were based on the pGGZ003 module backbone, and the detailed list of the modules used for the construction of the destination vectors is shown in Table 4-1. At least 150 ng plasmid was used for each module. The GreenGate reaction for ligation was adapted from Lampropoulos et al. (2013). The ligated plasmids were transformed by electroporation into *E. coli* strain DH5-alpha cells. The primers used for the construct design are listed in Table 4-2.

Agrobacterium-mediated plant transformation

The destination vectors were transformed into *Agrobacterium tumefaciens* strain GV310. Transformation of Arabidopsis was performed by the floral dip method, essentially as described in Clough and Bent (1998), except for the immersion of the inflorescence in *Agrobacterium* suspension for 1 m, and by omitting the low light/dark treatment after dipping. Each construct was dipped in three Arabidopsis background genotypes (Col-0, *csld3* (SALK_112105C), and *csld5* (SALK_002118C)). The above SALK lines were obtained from the Nottingham Arabidopsis stock centre (NASC).

Plant selection

The harvested T0 seeds were subsequently surface sterilized in 70% (v/v) ethanol and 5% (v/v) sodium hypochlorite, then washed with sterile distilled water before sowing. The

selection medium consisted of 2.2 g/L MS medium containing 1% agar at pH 5.8, containing 40 µg/ml hygromycin B for selection. Seeds were stratified at 4°C for 48 h before being transferred into a growth chamber for 6 h incubation at 21°C to stimulate germination. The plates were wrapped in aluminum foil and kept at 21°C for 3 days for the selection of elongated hypocotyls. Confirmed transgenic seedlings were transferred onto growth medium without hygromycin B and grown for at least 3 weeks before being transferred into soil. Three independent homozygous events for each transformation were selected and used for the root phenotyping experiments.

Root morphology

Wild-type and transgenic *Arabidopsis* seeds were sterilised as described above and plated on *Arabidopsis* growth medium. Seeds were stratified at 4°C for 48 h and kept in controlled condition chambers for seven days prior to analysis. A Stemi SV 6 microscope was used to photograph the root tips. To quantify the number of root hairs and measure the root hair length, the photographs were processed using the Fiji ImageJ (Schindelin et al., 2012) and Zen software. Data represent the average of at least three independent transgenic events with five replications each. All data obtained for root hair number and length were subjected to analysis of significance using One-way ANOVA multiple comparisons (GraphPad Prism V7.03) with *Col-0*, *cslD3* or *cslD5* as the main factors.

Root hair morphology

One cm of root tip was collected from the materials used for the root morphology experiments and embedded in 1% agarose in microfiber glass tubes. The position of the root samples in the microfiber glass tubes was adjusted using a sterilised needle. The microfiber glass tubes were inserted vertically into the sample imaging chamber of the light-sheet fluorescence microscope (Zeiss Z1). The setup of the microscope chamber was described by

von Wangenheim et al. (2017) with following modifications. The solvent exchange unit was disabled, and the imaging chamber was filled with distilled water instead of Arabidopsis growth medium. Once the sample position was verified through the camera, the agarose gel containing the root sample was pushed out using the piston inside the microfiber glass tube, with the excess agarose gel remaining inside the tube to hold the sample position in the imaging chamber. Z-stack images of whole roots were captured under 10X magnification and UV light using the Zen software. 3D reconstruction of whole roots was performed using the Arivis Vision4D software. The photographs in Figure 4-4 and 4-5 represent the result of at least five replications from each individual transgenic event and control plants.

Biomolecular fluorescence complementation (BiFC)

The complete coding sequences of *HvCsIF3*, *AtCsID3*, and *AtCsID5* were amplified from cDNAs of Golden Promise and Col-0 roots, respectively. The amplified sequences were cloned individually into the pSAT1-nEYFP and pSAT1-cEYFP vectors, and the sequences of the cloning were verified via sequencing. To visualize the subcellular localization of protein-protein interaction, gold particles (1 μm , Bio-Rad) coated with 10 μg of plasmid DNA (5 μg for each) were transformed into onion epidermal cells using a PDS-1000/He particle delivery system (Bio-Rad) as per Yang et al. (2018). The water saturated onion pieces (2 \times 2 cm) were incubated in high osmosis medium (D-sorbitol 3.65% w/v, D-mannitol 3.65% w/v, MS basal media 0.44% w/v, phytigel 0.18% w/v, pH5.8) prior to biolistics. All combinations used for the protein-protein interaction experiments are listed in Table 4-3. After bombardment, the dishes were sealed with parafilm and stored in the dark for 16-18 h at 28°C for fluorescent signal development. After incubation, the epidermal layers of the onion tissues were peeled off and mounted onto glass slides in glycerol (50%, v/v) for visualization. YFP signal (excitation 514 nm, emission 525-546 nm) was captured using a Nikon A1R Laser Scanning Confocal microscopy fitted with a DS-Ri1 CCD camera.

Enzymatic hydrolysis, oligosaccharide fractionation and (1,4)- β -linked glucoxytan quantification

Surface sterilized *Arabidopsis* seeds (Col-0 and *HvCsIF3* overexpression transgenic *Arabidopsis*) were plated on *Arabidopsis* growth medium and stratified at 4°C for 48 hours. The plates were placed vertically in a growth chamber, and the seedlings were harvested after 4 weeks of growth. Plant materials were transferred into liquid nitrogen pre-chilled tubes and freeze-dried overnight. The dried materials were ground using a Retsch Mill tissue grinder and kept at room temperature under dry conditions. AIR (alcohol insoluble residue) samples were prepared from powdered samples according to Little et al. (2019), except that the materials were resuspended and washed in a sequence of 1 ml of 70% ethanol, 100% ethanol, and 100% acetone, and dried on a rotary evaporator. Five mg of AIR samples were hydrolysed with endo-glucanase (*Trichoderma longibrachiatum* (E-CELTR), Megazyme). The AIR samples were mixed with 20 μ l 100% ethanol before the addition of the 980 μ l digestion buffer (0.7% (v/v) E-CELTR and 2% (v/v) 1M sodium acetate in water). The hydrolysis was performed for 18 h at 40°C under slow rotation. The hydrolysed samples were centrifuged for 10 m at 10,000g and the supernatants were fractionated on graphitized carbon solid phase extraction cartridges (1 ml/50 mg, Bond Elute, Agilent Technologies). The cartridges were pre-treated with 1 ml 100% acetonitrile and 1 ml water. One ml of supernatant was loaded onto the pre-treated cartridges, and then fractionated firstly with 8% acetonitrile after a water wash, then 55% acetonitrile to elute all remaining components. The oligosaccharide fractions were dried using a rotation evaporator and re-dissolved in 50 μ l water each. A Dionex ICS-5000 (Thermo Fisher Scientific) HPLC fitted with a CarboPac PA200 (3 \times 250 mm) column with guard (3 \times 50mm) was used to analyse the fractions. Operation of the instrument was adapted from Little et al. (2019) with the following modifications: solvent A, 0.1 M sodium hydroxide; solvent B, 0.1 M sodium hydroxide, 1 M sodium acetate; solvent C, water; solvent D, 20 mM sodium hydroxide, 100 mM sodium acetate; gradients (See Chapter 3 method), in order to optimize the separation of

GlcP-(1,4)- β -XylP from xylobiose, XylP-(1,4)- β -GlcP from cellobiose, and the larger oligosaccharides eluted later in the fractions. Samples were injected using the Pushpartial_1s mode with 10 μ l partial-loop, limited sample injection. Results are presented as the average of three replications.

Results

Phylogenetic study of the *CsID* and *CsIF* gene families

CsID and *CsIF* genes represent two close related families in the *CesA/CsI* superfamily. It has been shown previously that the *CsIF* and *CsID* gene families are sister clades although their evolutionary history remains to be fully resolved (Hazen et al., 2002; Little et al., 2018). We obtained cDNA sequences of genes from both families of four species (*Arabidopsis thaliana*), tomato (*Solanaceae lycopersicum*), barley (*Hordeum vulgare*) and rice (*Oryza sativa Japonica*). Concordant with the literature, *CsIF* and *CsID* genes are separated into two major clades, with *CsIF* resolved as monocot specific (Figure 4-1). *HvCsIF9* is nested in Clade I that contains *HvCsIF8*. Overexpression of *HvCsIF8* in barley lead to increased (1,3;1,4)- β -glucan content (Burton et al., 2011). The *HvCsIF3* and *OsCsIF3* belong to the same subclade and are close related to the *HvCsIF10* in Clade II, of which, *HvCsIF3* and *HvCsIF10* have shown play an important role in the biosynthesis of (1,4)- β -linked glucoxytan (Little et al., 2019). Furthermore, Clade III, the sister clade of Clade II, contains *HvCsIF4*, which also showed increased (1,3;1,4)- β -glucan accumulation in overexpression barleys (Burton et al., 2011). Clade IV is the earliest branching clade in the *CsIF* family which includes *OsCsIF6* and *HvCsIF6* that are important genes regulating (1,3;1,4)- β -glucan biosynthesis (Taketa et al., 2011; Vega-Sánchez et al., 2012). In the *CsID* family, *AtCsID5* is nested with *OsCsID4* and *HvCsID4* in Clade V. *AtCsID5* and *OsCsID4* are known to be essential to the cell wall biosynthesis for root hair elongation and emergence in *Arabidopsis* and rice, respectively (Li et al., 2009; Yin et al., 2011). Clade V is also the second earliest branching lineages. The gene pair *AtCsID2* and

AtCsID3 belong to Clade VI, and these genes are well characterized of their role in root hair development during the early stages (Yin et al., 2011). From the same clade, *OsCsID1* is expressed only in root hair cells and essential for rice root hair growth (Kim et al., 2007). The *OsCsID1* homologues, *HvCsID2* is highly expressed in the barley root tips, and the level of expression increases along the root vertical axis from the meristem to mature root (Chapter2). This suggests a potential role for *HvCsID1* in root growth. Clade VII includes *AtCsID1* and *AtCsID4*, that are important in tip growing tissues including pollen tube growth. The function of other members in Clade VII and Clade VIII are yet to be identified.

Expression of *HvCsIF3* promotes root hair development in Arabidopsis

The Arabidopsis genome lacks *CsIF* genes and therefore provides an ideal heterologous expression model to study the role of *HvCsIF3* during plant development. *HvCsIF3* was transformed into wild type Arabidopsis with either a *Ubiquitin10* or a *CobraL9* promoter, for either overexpression or tissue specific expression in root hair cells, respectively. Homozygous T3 generation seeds were germinated on growth medium and root morphology was examined. Figure 4-2 presents the enhanced root hair development observed in the transgenic plants expressing *HvCsIF3* and *AtCsID5*. The average length of mature root hairs in the Col-0|pUbq10::HvCsIF3 and Col-0|pCobL9::HvCsIF3 lines ranged from 0.41-0.56 mm and 0.40-0.53 mm, respectively. The lengths are significantly longer than those observed in the Col-0 plants (0.22mm) (Figure 4-3A). This suggests a potential role of *HvCsIF3* in root hair elongation. In addition to the effects on root hair length, the root hair density also increased in these transformed plants (Figure 4-3B). The average root hair number per millimeter of root surface was increased by 1.6 and 1.5 fold in the Col-0|pUbq10::HvCsIF3 and Col-0|pCobL9::HvCsIF3 transgenic plants, respectively (Figure 4-3B). However, the mechanisms responsible for the increased root hair number remains to be determined.

***HvCsIF3* rescues the *Atcsld5* mutant phenotype but not the *Atcsld3* mutant phenotype**

Defective root hair initiation and elongation in *csld3* and *csld5* was previously described by Yin et al. (2011). Consistent with this observation, defective root hair development was observed in mutant roots grown at our facility, as shown in Figure 4-2 B,C. Considering the close phylogenetic relationship between the *CsIF* and *CsID* families, and the enhanced root hair development of Col-0 plants expressing *HvCsIF3*, we expressed *HvCsIF3* in both *csld3* and *csld5* mutant backgrounds to examine the possibility of functional complementation. As expected, the aborted root hair phenotype in *csld3* was successfully recovered in transgenic plants expressing *AtCsID3* under both *Ubiquitin10* and *CobraL9* promoters (Figure 4-2 B3, B4). However, the *csld3* defect in root hair development was not rescued in either the *csld3|pUbq10::HvCsIF3* nor *csld3|pCobL9::HvCsIF3* transgenic plants. Interestingly, even though the majority of root hairs were aborted in *csld3* plants, successful root hair initiation was observed occasionally, especially in the more mature parts of the roots. In *csld3* plants expressing *HvCsIF3*, the number of root hair cells increased, from an average of 24 cells in *csld3* to 32 cells in *csld3|pUbq10::HvCsIF3* and 38 cells in *csld3|pCobL9::HvCsIF3* transgenic plants, whereas the root hair density of the lines complemented with *AtCsID3* remained comparable to the wild-type (Figure 4-3 B2). No significant difference on other aspects of seedling development was observed between the *csld3* and the complemented plants.

The mutant phenotype of *csld3* is epistatic to *csld5*, where the latter mutant is able to initiate root hair formation but subsequent elongation was disrupted, suggesting the two genes act in the same pathway (Yin et al., 2011). Figure 4-2 C illustrates the short root hair phenotype of the *csld5* mutant which is in agreement with previous observations (Yin et al., 2011). Remarkably, transgenic *csld5* plants expressing *HvCsIF3* restored root hair lengths of 0.37 mm and 0.35 mm when driven by *Ubiquitin10* and *CobraL9* promoters, respectively. These average lengths of root hairs were similar to those observed in the plants complemented with *AtCsID5* (Figure 4-3 C1). This result highlights a potentially conserved (or redundant) cross-species function of the *HvCsIF3* and *AtCsID5* genes during root hair elongation. Also, similar to the

Col-0 plants that express *HvCsIF3*, the complemented *csld5* plants exhibited an increasing number of root hairs (1.4-1.9 fold) compared with Col-0 and *csld5* plants (Figure 4-3 C2). Therefore, expression of *HvCsIF3* in Arabidopsis not only contributes to root hair elongation but is also accompanied by a gain of function phenotype characterised by an increased number of root hairs.

Abnormal trichoblast cell fate in Arabidopsis roots expressing *HvCsIF3*

Differences in the patterning of root hair and non-hair cells are found between species. Arabidopsis root hairs are positioned between the junction of two adjacent cortical cells and are organized in cell files with interspersed non-hair cells (Salazar-Henao et al., 2016). In contrast, barley root hairs display a random or irregular pattern, similar to other cereal crops to allow a plastic response to the surrounding growth environment (Hochholdinger et al., 2004; Dolan, 2017). To investigate the reason behind the increased root hair number in Arabidopsis plants expressing *HvCsIF3*, we examined the root epidermis from freshly harvested mature roots with LightSheet microscopy. Figure 4-4 shows the position of the root hairs on the root surface. In Col-0, *csld3*, *csld5*, and the *AtCsID3/5* complemented plants, trichoblasts and atrichoblasts were arranged in a position-dependent pattern. However, in the Arabidopsis plants expressing *HvCsIF3*, the arrangement of the root hair cells was disrupted, with the root hairs frequently emerging from adjacent epidermal cells (Figure 4-4 A1, A2, B1, B2, C1, C2). The transverse view of the reconstructed root sections indicated no change in cellular organization in the cortical cell. However, epidermal cells in contact with only one cortical cell were able to form root hairs (Figure 4-5 B, C). Such observations suggest an effect of *HvCsIF3* on epidermal cell fate determination in Arabidopsis. Whether the influence is due to direct regulation from individual epidermal cells or an indirect control by adjacent cellular communication remains unclear. Despite the lack of full understanding of the underlying mechanism, altered root hair cell proliferation appears to explain the increased root hair numbers in this line (see Figure 4-

2, 4-3).

CsID and CslF proteins form heterodimers when co-expressed in onion cells

Despite the importance of the *AtCsID3* and *AtCsID5* genes in root hair initiation and development, the relationship between the products of these genes is currently unclear. Hence, we cloned coding sequences of *AtCsID3* and *AtCsID5* into pSAT1-nEYFP and pSAT1-cEYFP vectors and used onion epidermal cells to determine whether the proteins form a complex with each other and with CslF proteins. Table 4-3 summarizes the results obtained by bimolecular fluorescence complementation (BiFC). Negative bombardment controls showed no signal in the YFP channel. In contrast, multiple experiments observed pSAT1-*AtCsID3*-nEYFP and pSAT1-*AtCsID5*-cEYFP can interact, with bright YFP signals detected at the periphery of transformed cells (Figure 4-6A). Notably, the signals were more concentrated on one side of the cell. Similar polarised fluorescence was observed from the combination of pSAT1-*HvCslF3*-nEYFP and pSAT1-*HvCslF9*-cEYFP. To confirm the possible functional redundancy between the *AtCsID5* and *HvCslF3* proteins, pSAT1-*AtCsID3*-nEYFP and pSAT1-*HvCslF3*-nEYFP was bombarded into onion epidermal cells. Once again, reproducible interactions were identified, albeit less intense than previous combinations. Figure 4-6B shows a weak fluorescent signal found at the cell periphery and spotty signals inside the cells, although the precise subcellular location of the signal is yet to be determined. In addition to the heterodimers, *HvCslF3* and *AtCsID5* proteins were able to self-interact and form homodimers. Figure 4-6C and D highlight a patchy YFP signal at the cell periphery. This confirmed the similarity in protein self-interaction of the two proteins. Based on the results of complementation experiments on root hair development and on protein-protein interactions, we proposed a model of the regulation of root hair development in the presence of *HvCslF3* expression, in combination with previous findings summarized by Hwang et al. (2016) and Salazar-Henao et al. (2016) (Figure 4-7).

Over-expressing *HvCslF3* has no effect on (1,4)- β -linked glucoxytan accumulation

In the previous chapter we demonstrated that the downregulation of *HvCslF3* in barley resulted in reduced (1,4)- β -linked glucoxytan accumulation in root tips. Here we selected three independent homozygous events of Col-0 expressing pUbq10::*HvCslF3* and collected the young seedlings to analyse their cell wall composition. The endo-glucanase *Trichoderma longibrachiatum* (E-CELTR) was used to hydrolyse the plant materials to release (1,4)- β -linked glucoxytan and a Dionex ICS-5000 (Thermo Fisher Scientific) was used to detect specific oligosaccharides. In the Col-0 plants, (1,4)- β -linked glucoxytan was barely detectable (Figure 4-8A). Out of the two essential oligosaccharides, only glc-(1,4)- β -xyl showed a very weak signal on the spectrometer, whereas the other oligosaccharide xyl-(1,4)- β -glc was undetectable. This suggests that no (1,4)- β -linked glucoxytan is found in the cell walls of wild type *Arabidopsis* seedlings. Curiously, no differences in the abundance of either oligosaccharide was induced by overexpression of *HvCslF3* (Figure 4-8A). This contrasts with the findings of Little et al. (2019) who suggested a direct connection between the *HvCslF3* gene and the biosynthesis of (1,4)- β -linked glucoxytan in transformed tobacco leaves. Interestingly, differences in the composition of the hydrolyzed materials were identified in different fractions (Figure 4-8B). However, the identity of the oligosaccharides still needs to be determined.

Discussion

A close evolutionary relationship between the *CsID* and *CsIF* genes

The *CsID* and *CsIF* genes belong to the glycosyltransferase (GT) 2 cellulose synthase superfamily and they are the closest related subfamilies that are most homologous to the *CesA* genes during evolution (Richmond and Somerville, 2000; Schwerdt, 2017). This relationship has previously been discussed, whereby the *CsIF* subfamily is reported to be the sister clade to the *CsID* genes (Schwerdt et al., 2015). More recently, Little et al. (2018) analysed the gene

sequences from 46 species and presented phylogenetic evidence to indicate that the *CsIF* clade may have evolved from the *CsID* subfamily. In the present study, we analysed the coding sequences of *CsID* and *CsIF* genes from dicot species, Arabidopsis and tomato, and monocot species, barley and rice, and further confirmed the close relationship between *AtCsID3/AtCsID5* and *CsIF* genes.

Despite similar tissue and stage-specific expression profiles (Burton et al., 2008), the developmental role of most *CsIF* genes is unclear. Studies in barley, wheat and rice (Burton et al., 2006; Nemeth et al., 2010; Taketa et al., 2011) suggest that *HvCsIF6* is the most important family member, as mutations or RNAi down regulation leads to stunted growth and alterations in grain filling. In contrast, the developmental importance of the *CsID* genes in regulating tip growth in pollen tube and root hair development has been described in a wide range of species, including Arabidopsis (Yin et al., 2011), rice (Li et al., 2009), and poplar (Peng et al., 2019). The Arabidopsis root hair defective lines, *csld2/3/5*, have been well characterized and Yin et al. (2011) highlighted the importance of *AtCsID3* in root hair initialization, while the *AtCsID2* and *AtCsID5* genes function in later stage of root hair elongation. In other species, including rice and poplar, a root hair-less phenotype was identified when the functional orthologue of *AtCsID3* was mutated (*OsCsID1* and *PtrCsID5*). In rice, *OsCsID1* specifically expresses in the root hair forming epidermal cells, indicating a conserved mechanism of root hair morphogenesis across species (Kim et al., 2007; Peng et al., 2019).

The phylogenetic relationship, and the similar tendency to be expressed in roots, provided an impetus to assess the function of *HvCsIF3* in Arabidopsis plants carrying mutations in *AtCsID3/AtCsID5* genes, which are affected in root hair development as previously described by Yin et al. (2011). This revealed potential functional redundancy between the *HvCsIF3* and *AtCsID5* genes in regulating the elongation of root hairs after emergence, and a gain of function phenotype caused by *HvCsIF3* in the cell fate determination of Arabidopsis root epidermal cells.

How the “rescue” of *cslD5* is achieved biochemically remains unclear. One possibility is that *HvCslF3* and *AtCslD5* proteins contribute to the synthesis of the same polysaccharide; alternatively, *HvCslF3* may synthesise a different polysaccharide that is functionally redundant with one synthesised by *AtCslD3*. Somewhat remarkably, the precise biochemical roles of individual *CsID* genes in the barley and Arabidopsis genomes, are yet to be assigned. Yin et al. (2011) demonstrated increased mannan synthase activity in Arabidopsis root hairs when *AtCslD2* and *AtCslD3* are simultaneously over-expressed, whereas studies in barley and rice suggested a potential role of these *CsID* genes in the synthesis of other cell wall polysaccharides, including callose (*HvCslD2*) (Douchkov et al., 2016), arabinoxylan, cellulose and homogalacturonan (*OsCslD4*) (Li et al., 2009). However, no endogenous difference in primary cell wall composition has been reported in species showing reduced *CsID* expression (Doblin et al., 2001; Burton et al., 2005; Galway, 2006; Yin et al., 2011).

***Csl* genes affect the regulation of Arabidopsis root hair development**

The development of root hairs requires multiple gene networks in response to hormonal and environmental signals. Shibata and Sugimoto (2019) reviewed the regulatory network of Arabidopsis root hair development, focusing mainly on transcription factors and environmental responses. For simplicity, root hair development can be divided into two main phases: (1) specification/initiation and (2) growth/elongation. The determination of root hair cell fate is negatively regulated by the R2R3-type MYB transcription factor *GLABLA2* (*GL2*), the expression of which is increased through interaction with a WER-GL3-TTG1 protein complex (*WERWOLF-GLABLA3-TRANSPARENT TESTA GLABLA1*) and functions in the maintenance of non-hair cell properties (Galway et al., 1994; Masucci et al., 1996; Lee and Schiefelbein, 1999; Bernhardt et al., 2003). On the other hand, a positive influence on root hair cell specification is contributed by a R3-type MYB transcription factor, *CAPRICE* (*CPC*), and its homologs, *TRIPTYCON* (*TRY*) and *ENHANCER OF TRY AND CPC 1* (*ETC1*). These

transcription factors are induced by the WER-GL3-TTG1 complex in the non-hair cells and transported to the neighbouring cells to initiate the formation of root hair by inducing the bHLH transcription factor *ROOT HAIR DEFECTIVE 6 (RHD6)* (Masucci and Schiefelbein, 1994; Wada et al., 1997; Salazar-Henao et al., 2016). To date, the proposed cell fate determination model (phase 1) is mainly focused on hormone and transcription factor regulation, whereas cell wall remodelling is thought to be more important in the later stages of root hair development (phase 2), involving polysaccharide rearrangement and elongation (Shibata and Sugimoto, 2019). The data from this study suggest that cell wall genes may influence both of these phases.

Altered epidermis cell identity induced by *Csl* expression (phase 1)

Perhaps even more interesting than the cell elongation phenotype were the distinct roles revealed for *HvCslF3* and *AtCslD5* in epidermal cell fate determination. Compared with root hair cells, the non-hair cells exhibit early vacuole development and longer cell length (Masucci et al., 1996; Shibata and Sugimoto, 2019). The morphology of non-hair cells in *cslD5* complementation lines expressing *AtCslD5* remained unaffected. However, distance between root hairs was notably reduced. This suggests a negative effect on the length of root hair forming cells induced by overexpression *AtCslD5*; thus, the root hair density increased without disturbing epidermal cell fate determination. In contrast, the increased root hair number in *HvCslF3* overexpression plants (Col-0 and *cslD5*) was most likely a consequence of disrupted root epidermal cell fate determination, as evidenced by the disordered root hair patterns shown in Figure 4-4, 4-5. Lee and Schiefelbein (1999) first described the specific expression of *WER* gene in non-hair cells. This gene maintains normal epidermal cell status by forming an active complex with GL2. The corresponding mutant shows cell fate alteration on the root epidermal cells from non-hair cells to root hair forming cells. Such mutant phenotype was highly similar with what we observed on the *HvCslF3* overexpression plants. This suggests that *HvCslF3* potentially affects the expression of *WER* or disrupts the downstream protein complex and leads

to a switch in cell fate from non-hair cells to root hair identity. However, to verify this, more efforts need to be contributed on gene regulation network. Interestingly, both (global) *Ubiquitin10* and (epidermal) *CobraL9* driven *HvCslF3* expression resulted in similar epidermal cell fate disorders. This suggests the effects brought about by *HvCslF3* can be both direct (from the non-hair cells) and indirect (transported into non-hair cells from the surrounding cells) regulation.

Contrasting positionally-determined Arabidopsis root hair patterning, barley root hairs emerge from random epidermal cells, similar to most cereal crops. The determination of root hair cells in cereal crops such as barley and rice is dependent on the size of daughter cells dividing from the single epidermis cell (Dolan, 2017). The daughter cell with high expansion rate becomes a longer cell that retains epidermal cell fate, while the relatively slower expanding cell differentiates to a root hair cell (Marzec et al., 2013; Dolan, 2017). Studies have shown the asymmetric cell development is the consequence of the difference in the timing of cell elongation. Marzec et al. (2013) highlighted cell walls of root hair cells are more compact and auto-fluorescent than non-hair cells, indicating a potentially different cell wall composition in the two cell types. Even though no research to date has identified the direct regulation between cell wall related genes and root hair fate determination, it is possible that *HvCslF3* is part of a cell-wall dependent pathway that influences this. By expressing *HvCslF3* in Arabidopsis resulted in the gain of function in the determination of epidermal cell fates.

***ClsF* and *CsID* genes contribute to root hair elongation (phase 2)**

By transforming *HvCslF3* into Arabidopsis, a conserved function for *AtCslD5* in root hair elongation was revealed. *HvCslF3* was able to recover the mutant phenotype of *cslD5*, and in addition, promoted root hair elongation in wild type Arabidopsis by nearly 2-fold. Moreover, expression of *AtCslD5* in the *cslD5* mutant rescued root growth and led to increased elongation, similar to the effect of *HvCslF3*.

Root hair growth is regulated by a number of pathways. For example, developmental and environmental cues induce root hair differentiation, followed by a group of *ROOT HAIR SPECIFIC (RHS)* genes that are proposed to be directly regulated by the *ROOT HAIR SPECIFIC TRANSCRIPTION FACTOR (RHF)* to determine the balance of root hair length (Hwang et al., 2016). *RHS* genes come from multiple families, including genes regulating cell wall loosening, ion transport, receptor-like kinases, and calcium signalling. The *RHS* genes can be divided into two groups, positive regulators and negative regulators (Hwang et al., 2016). For example, *RHS10* genes in Arabidopsis, rice and poplar maintain the proper length of root hairs by negative feedback. Mutants of *AtRHS10* developed root hairs that were 50% longer than wild-type, while its overexpression inhibited root hair growth (Hwang et al., 2016). While there is no evidence to date that the *Csl* genes belong to the *RHS* group in Arabidopsis, studies on rice and poplar indicate *OsCslD1* (Kim et al., 2007) and *PtrCslD2* (Peng et al., 2019) are specifically expressed in the root hairs.

In addition to the *RHS* genes, the *ROOT HAILRESS SIX LIKE (RSL)* genes also affect the elongation of root hairs. *AtRSL4* is a key *RSL* class II gene that positively affects root hair elongation by enhancing the expression of genes involved in cell wall synthesis and modification, endomembrane transportation, and cell signalling. *AtRSL4* is upregulated by *RHD6* in root hair forming cells at a later developmental stage (Yi et al., 2010; Dolan, 2017), while the wheat homologue *TaRSL4* also controls root hair elongation (Han et al., 2016). Shpigel et al. (1998) proposed root hair elongation is simulated by the weakened primary cell wall and turgor pressure, and inhibition of crystallization of glucan chains to microfibrils to increase root hair length. *OsEXPI7* specifically expresses in root hairs and catalyses the breakage of cell wall polysaccharide hydrogen bonds to regulate cell wall remodelling (ZhiMing et al., 2011). In addition, *OsXXT1* catalyses the trans-glycosylation of xylose to cellulose chains and the corresponding loss-of-function mutants result in short root hairs (Wang et al., 2014).

There are a number of possible explanations for the appearance of longer root hairs in *Arabidopsis HvCslF3* overexpression and complemented *HvCslF3/AtCslD3/AtCslD5 cslD5* lines. First, *AtCslD3/5* and *HvCslF3* may function as RHS-enhancers or by inhibiting the RHS-inhibitors (Figure 4-7). This might relate to indirect feedback from the cell wall on these factors, and/or to synthesis of specific cell wall polysaccharides that stimulate pathways promoting cell elongation. Along similar lines, *HvCslF3* and *AtCslD3/5* may alter the expression of *AtRSL4* in the root hair forming cells to enhance root hair elongation (Figure 4-7), or may act as endogenous downstream targets of the *RSL4* pathway in *Arabidopsis* and barley. Alternatively (but not mutually exclusive), the *UBQ* and *COBL9* promoters may have uncoupled the cell elongation pathway from endogenous negative *RHS* regulators, leading to prolonged function of *HvCslD3/5* and *HvCslF3* in promoting cell growth. Although it was not attempted in this study, future research might focus on the molecular pathways impacted by *HvCslF3* overexpression in *Arabidopsis*.

The synthesis of (1,4)- β -linked glucoxytan is not controlled by *HvCslF3* solely

(1,4)- β -Linked glucoxytan is one of the non-cellulosic polysaccharides found in the cell walls of green seaweed *Ulva rigida* (Ray and Lahaye, 1995; Little et al., 2019). It consists of an insoluble linear chain rich in glucose and xylose, and Little et al. (2019) successfully demonstrated the accumulation of (1,4)- β -linked glucoxytan in 35S promoter driven transient overexpression of *HvCslF3* and *HvCslF10* in tobacco leaves. The presence of (1,4)- β -linked glucoxytan in barley was also confirmed in different tissues, with exceptionally high level detected in barley coleoptiles (Little et al., 2019). Our previous finding also confirmed high (1,4)- β -linked glucoxytan content in the first 1 cm of barley root tips, and the location corresponded with the region where *HvCslF3* transcript is abundant (Chapter 3). In contrast to the results of Little et al., (2019) in tobacco leaves, Col-0 plants revealed very small amounts of glc-(1,4)- β -xyl, indicating the likely absence (or insufficient extraction) of (1,4)- β -linked

glucoxytan, and this was not altered by *HvCslF3* overexpression. This may indicate that *Arabidopsis* lacks a substrate or interacting partner for *HvCslF3* that is required for (1,4)- β -linked glucoxytan biosynthesis. Alternatively, the (1,4)- β -linked glucoxytan showed a different structure that was not successfully extracted or was resistant to enzyme digestion. The synthesis of a polysaccharide is a complex process, and often involves the regulation of multiple enzymes. A well-studied example is the cellulose synthase complex, which requires multiple *CesA* members (Hill et al., 2014). For example, in *Arabidopsis*, *AtCesA1/3/6* and *AtCesA4/7/8* are required for cellulose synthesis in primary and secondary cell walls, respectively (Taylor et al., 2003; Persson et al., 2007). In addition, there are other *CesA* members with partially redundant functions and participating in more tissue-specific processes (Gardiner et al., 2003; Hill et al., 2014). Although the cellulose synthase complex is critical for cellulose biosynthesis, a single *CesA* protein can catalyse the formation of glucan chains in bacteria (Morgan et al., 2013). Moreover, genes outside of the *CesA* family also function in cellulose synthesis, including *KORI* and *CsICs* (Dwivany et al., 2009; Vain et al., 2014). Therefore, it is possible that (1,4)- β -linked glucoxytan synthesis requires more complicated machinery in different heterologous expression system. The *CsIF* family is known to be associated with (1,3;1,4)- β -glucan synthesis and the control of grain quality in barley. However, whether the undetectable (1,4)- β -linked glucoxytan in *Arabidopsis* is due to the complete absence of the polysaccharide, or low level for detection, or insufficient extraction due to the complexity of *Arabidopsis* cell walls, remains under investigation. To solve this problem, improved biochemical and immunohistological approaches and are required.

In conclusion, we investigated the role of *HvCslF3* in root development in a heterologous expression system, *Arabidopsis*, and in different genetic backgrounds. *HvCslF3* was able to complement the *csld5* mutant phenotype and convert epidermal cells with non-hair cell fate to root hair forming cells. Our results indicate a possible conserved function between members of the *CsIF* and *CsID* families in root hair elongation, and a potentially new function

of the *CsIF3* gene (or the polysaccharide it produces) in root patterning. Given that most of the research on root hair development focuses mainly on hormone and transcriptional factor controls, our findings highlight the potential importance of cell wall related genes in the regulation and emergence of root hairs. The contrasting observations of (1,4)- β -linked glucoxytan synthesis in a different heterologous expression system also suggest the mechanism behind the biosynthesis of this polysaccharide may be more complicated than predicted. Many well-known cell wall polysaccharides, including cellulose and pectin, require multiple genes to cooperate in the biosynthesis and accumulation of these carbohydrate structures. Therefore, it is possible that (1,4)- β -linked glucoxytan biosynthesis needs other elements, which requires further investigation.

Figures

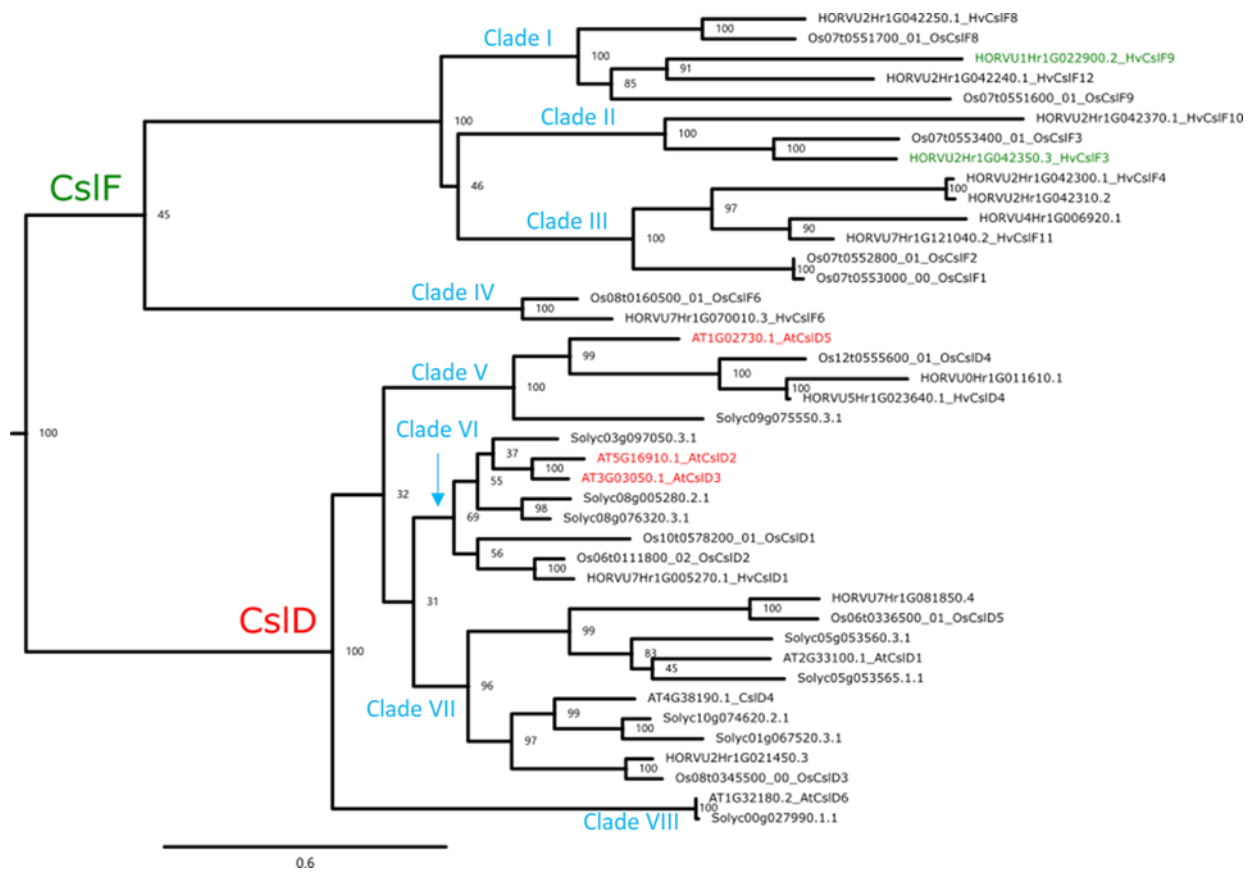


Figure 4-1. The phylogenetic tree for the *CsIF* and *CsID* gene families. cDNA sequences of *Arabidopsis* (*Arabidopsis thaliana*), tomato (*Solanaceae lycopersicum*), barley (*Hordeum vulgare*) and rice (*Oryza sativa Japonica*) were obtained for phylogenetic tree construction. An unrooted phylogenetic tree constructed with RAxML(7.2.8) using the WAG+G substitution model. Node support was assessed using 500 rapid bootstrap replicates. The tree shows two distinct clades, *CsID* and *CsIF*.

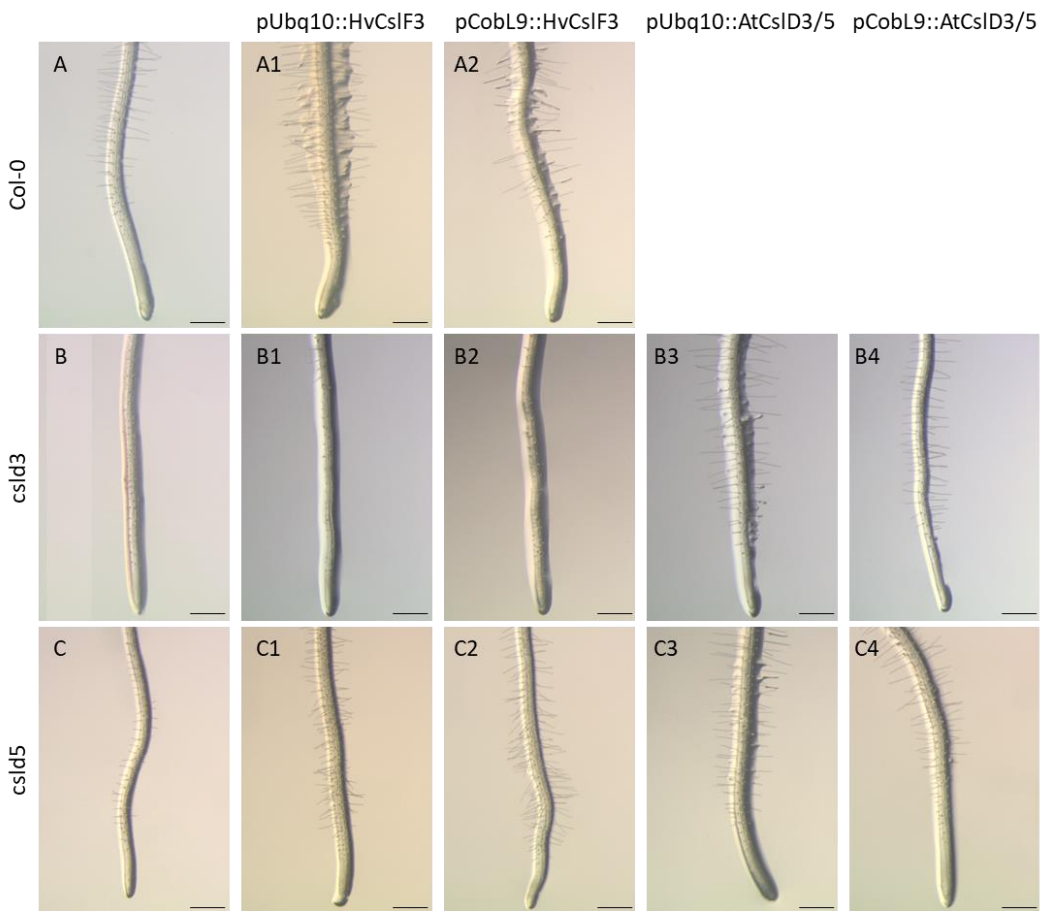


Figure 4-2. Complementation experiments with *HvCslF3*, *AtCslD3*, *AtCslD5* driven by *Ubiquitin 10* and *CobraL9* promoters. All roots photographed from 7-day old seedlings grown vertically on 1/2 MS medium under controlled conditions in a growth chamber. A, Col-0 wild type Arabidopsis root tips. A1-A2, Col-0 expressing *HvCslF3* driven by *Ubiquitin10* promoter and *CobraL9* promoter, respectively, and showing enhanced root hair growth. B, *csld3* mutant (SALK_112105C) showing aborted or abnormal root hair growth. B1-B2, *HvCslF3* expression in *csld3* mutants, the mutant phenotype was not restored (*Ubiquitin10* and *CobraL9* driven expressing, respectively). B3-B4, *AtCslD3* complemented *csld3* mutants with recovered root hair phenotype. C, *csld5* (SALK_002118C) mutant showing short and disrupted root hairs. C1-C2, *HvCslF3* complemented *csld5* mutants with restored root hair development (*Ubiquitin10* and *CobraL9* driven expressing, respectively). C3-C4, *AtCslD5* complemented *csld5* mutant with recovered root hair phenotype. Scale bar = 0.5mm.

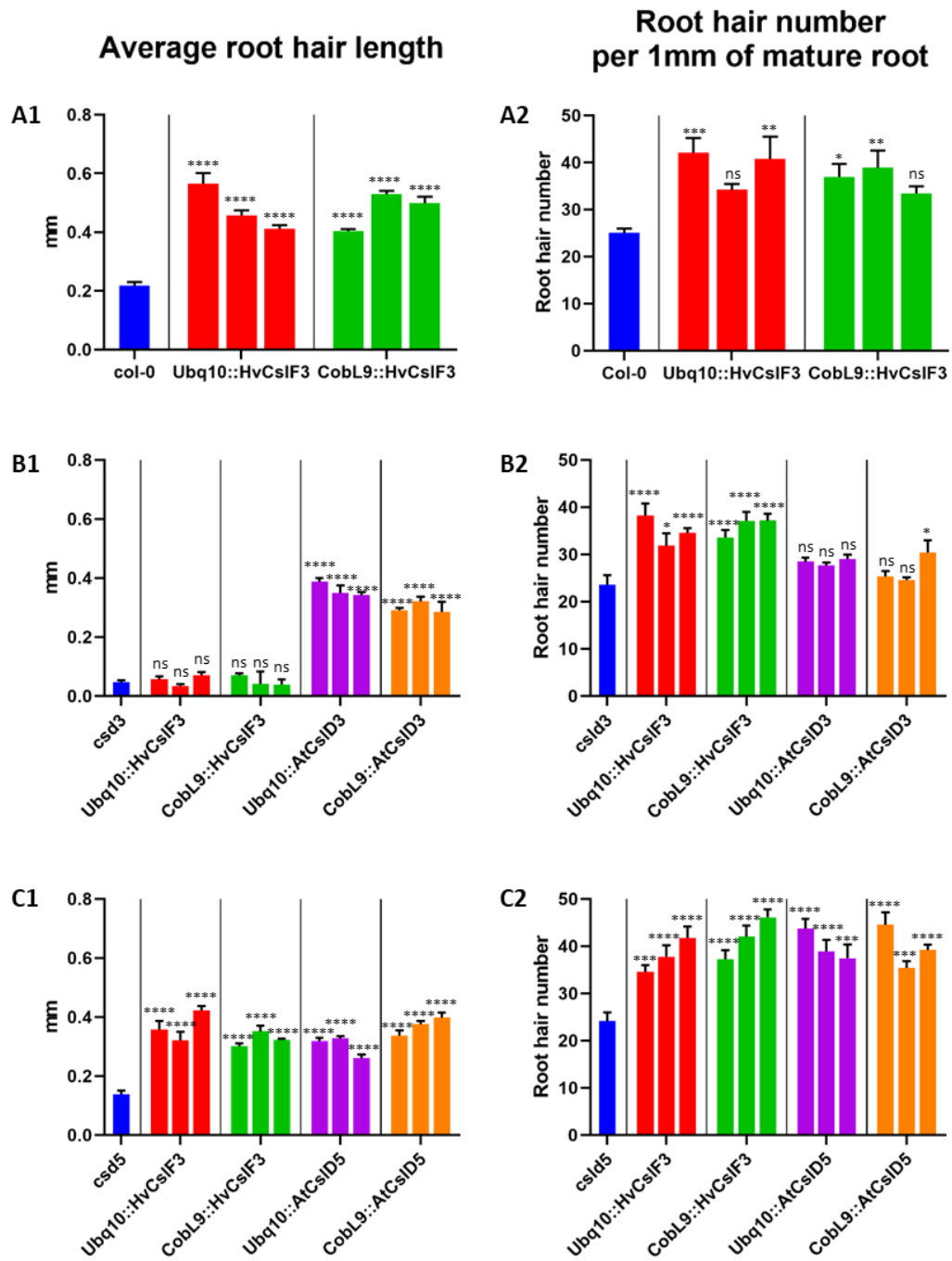


Figure 4-3. Quantification of root hair length and density in complementation lines. Average root hair length and average root hair density were measured from the 7-day old Arabidopsis seedlings grown vertically on 1/2 MS media under controlled conditions. Left panels represent the average root hair length. Each column represents the average value of individual genotype or transgenic event. Three individual transgenic events per complementation experiment were included in this study. A1-A2, Col-0 (Blue) and *HvCsIF3*

expressed in a Col-0 background driven by *Ubiquitin10* (Red) and *CobraL9* (Green) promoter. B1-B2, *cslD3* mutant (SALK_112105C) phenotype (Blue) and the complementation with *HvCslF3* (Red- *Ubiquitin10* promoter; Green- *CobraL9* promoter) and *AtCslD3* (Purple- *Ubiquitin10* promoter; Orange- *CobraL9* promoter). C1-C2, *cslD5* mutant (SALK_002118C) phenotype (Blue) and the complementation with *HvCslF3* (Red- *Ubiquitin10* promoter; Green- *CobraL9* promoter) and *AtCslD5* (Purple- *Ubiquitin10* promoter; Orange- *CobraL9* promoter). Error bars represent standard errors. All data were analysed for significance using One-way ANOVA multiple comparison with the control plants (Col-0, *cslD3* or *cslD5*) as the main factor. Level of significance are labelled on each column in the bar graphs. ns- not significant. *- P<0.1. **- P<0.01. ***- P<0.001. ****- P<0.0001.

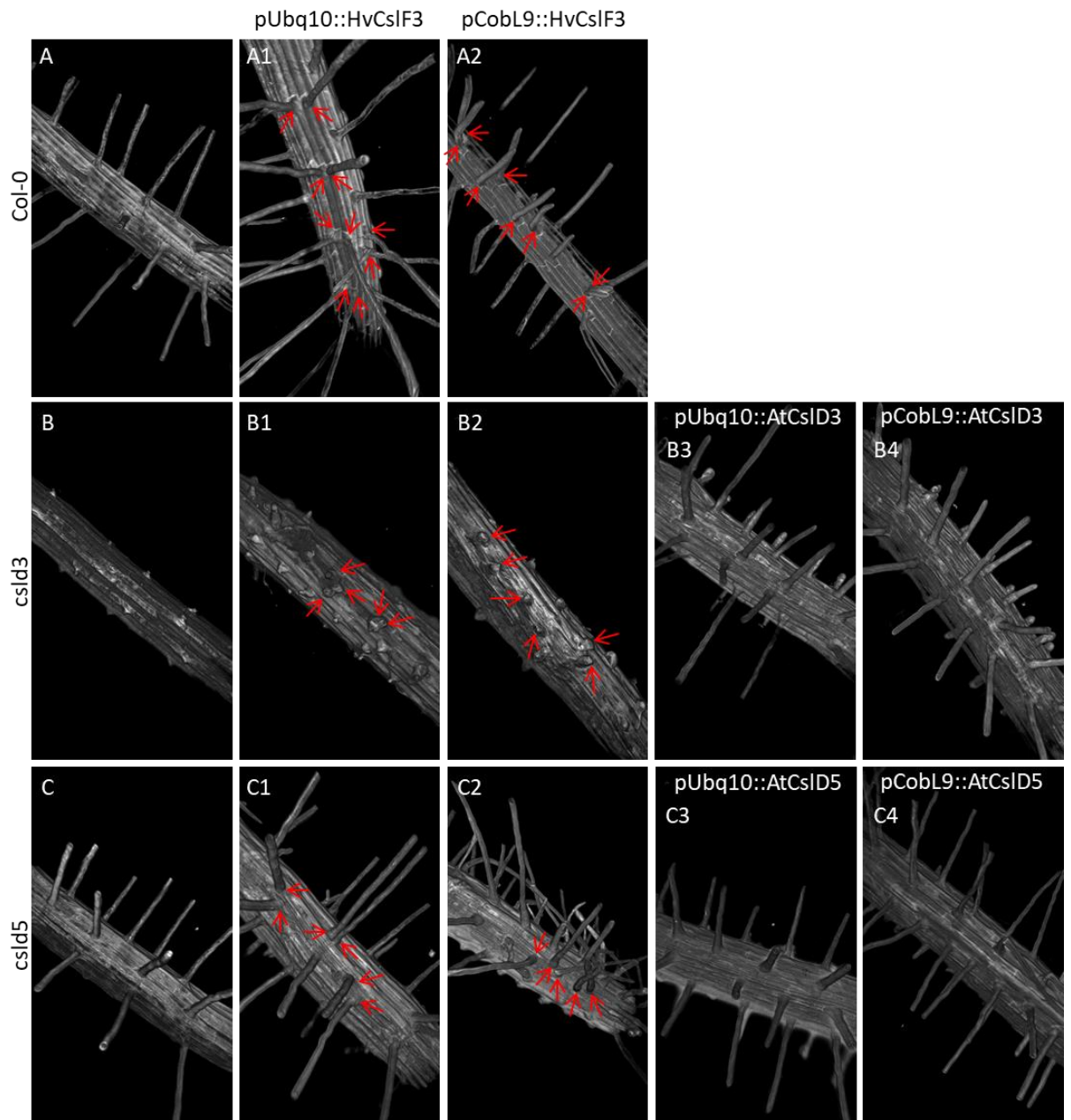


Figure 4-4. 3D reconstructed view of root surfaces using Lightsheet microscopy. Red arrows indicate the abnormal and altered root hair formation in the *HvCsIF3* complemented Arabidopsis. A, Col-0 wild type. A1-A2, Col-0 expressing *HvCsIF3* driven by *Ubiquitin10* promoter and *CobraL9* promoter, respectively. B, *csld3* mutant (SALK_112105C) showing aborted root hair growth. B1-B2, *HvCsIF3* complemented *csld3* mutants, the mutant phenotype was not restored (*Ubiquitin10* and *CobraL9* driven expressing, respectively), however root hairs emerged from abnormal epidermal cells. B3-B4, *AtCsID3* complemented *csld3* mutants with recovered root hairs. C, *csld5* (SALK_002118C) mutant. C1-C2, *HvCsIF3* complemented

csl5 mutants with restored root hair development (*Ubiquitin10* and *CobraL9* driven expressing, respectively) and abnormal root hair positions. C3-C4, *AtCSID5* complemented *csl5* mutant with recovered root hair development.

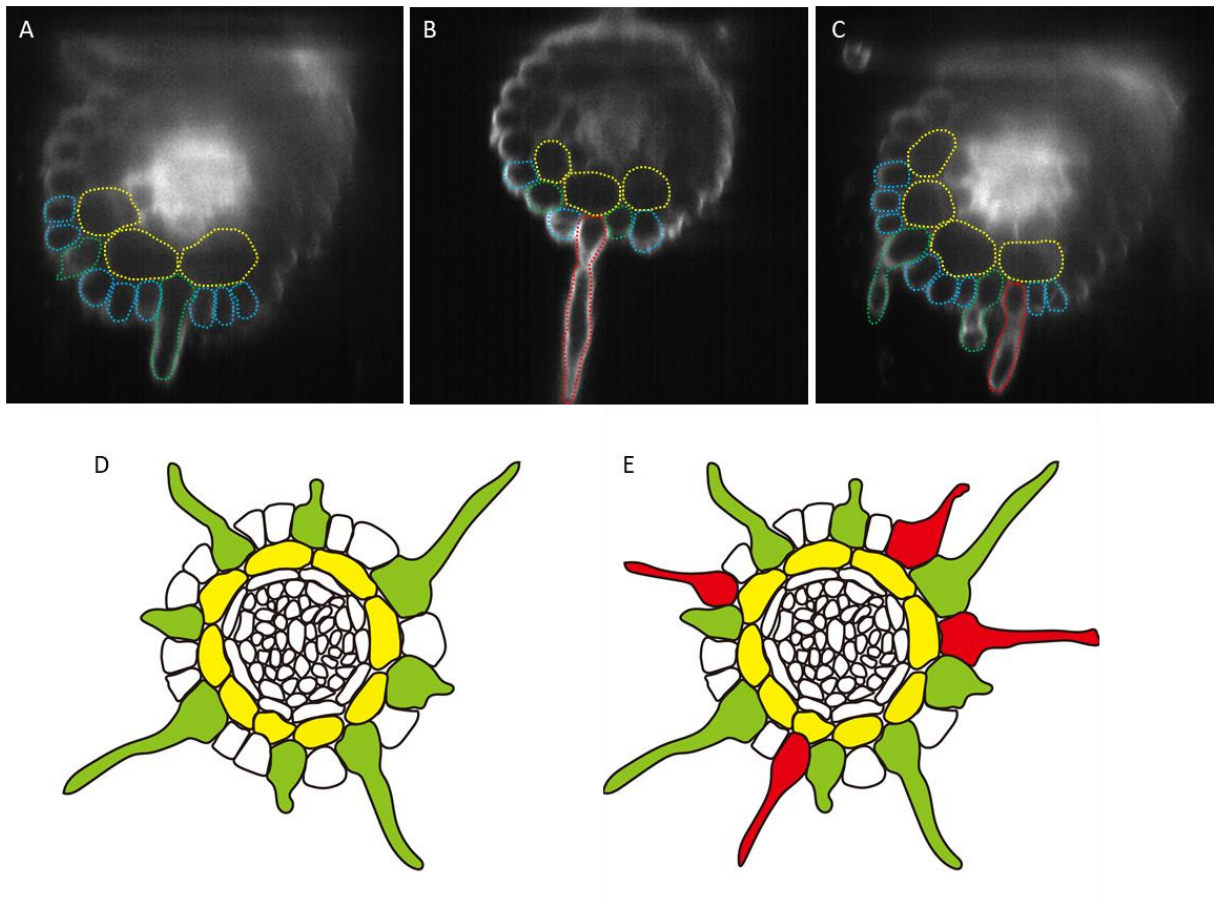


Figure 4-5. Transverse view of 3D reconstructed roots by Lightsheet microscopy. A, Col-0 showing normal root hair emerge from the epidermal cell in direct contact with two cortex cells. B, Col-0 expressing *HvCslF3* driven by *Ubiquitin10* promoter. C, Col-0 expressing *HvCslF3* driven by *CobraL9* promoter. Yellow dashed lines outline cortex cells. Blue dashed lines indicate epidermis cells with non-hair fate, or the atrichoblasts. Green dashed lines represent epidermal cells with root hair fate, or the tritoblasts. Red dashed lines outline the abnormal root hair formation in *Arabidopsis* expressing *HvCslF3*, where the abnormal root hair emerged from the epidermal cell only in contact with one cortex cell. D and E, the schematic diagram showing the root hair organization of normal plant (D) and *Arabidopsis* expressing *HvCslF3* gene (E). Yellow indicates cortical cells, green indicated normal tritoblasts, red indicates abnormal root hair formation.

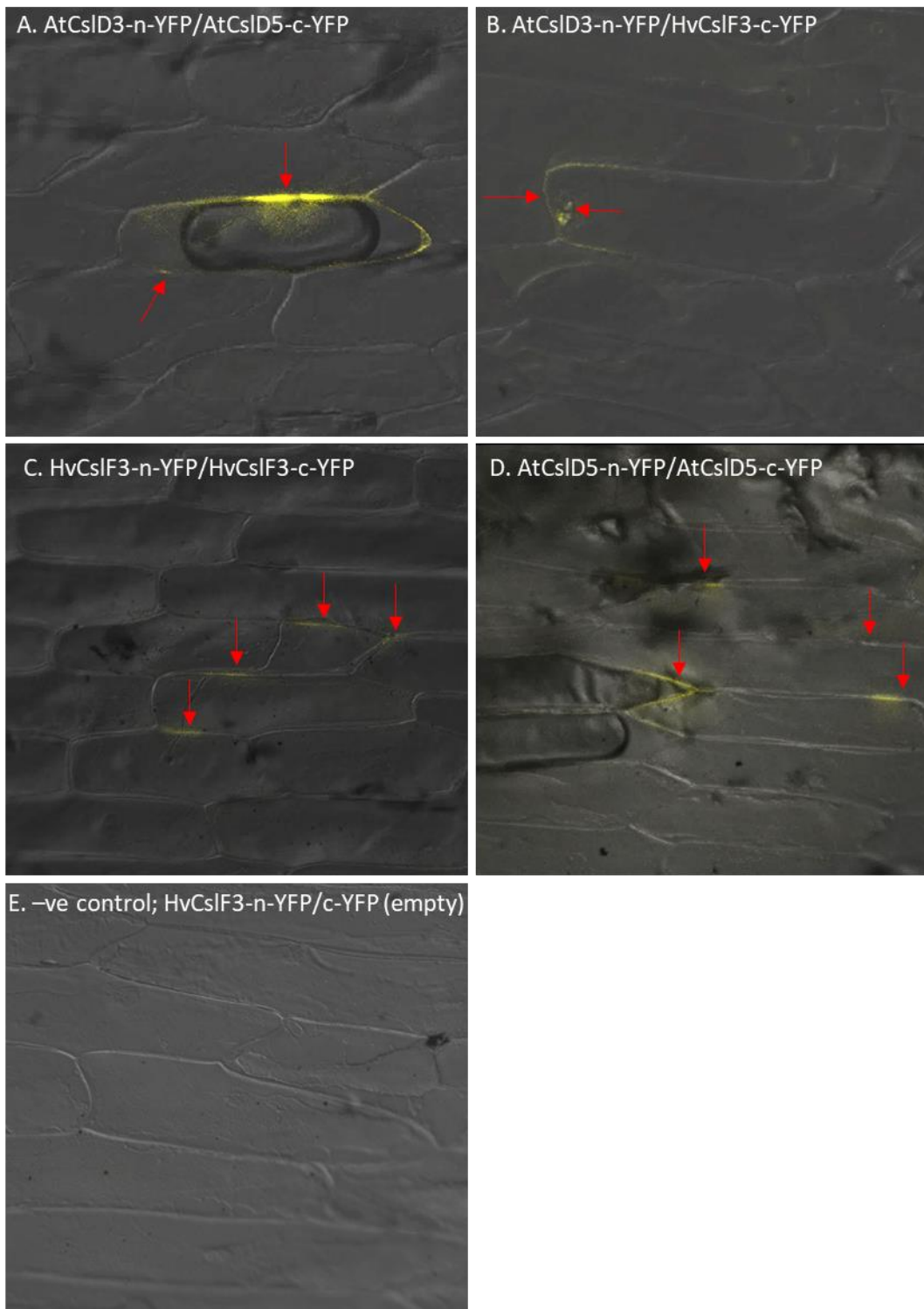


Figure 4-6. BiFC experiments of protein-protein interactions among *HvCslF3*, *AtCslD3*, and *AtCslD5* proteins. Complete coding sequences of three genes were cloned into pSAT1-nEYFP and pSAT1-cEYFP vectors and paired for transiently expressed in onion epidermal cells according to Table 4-3. Red arrows pointing site of interactions. A, *AtCslD3*-n-YFP and *AtCslD5*-c-YFP co-expression showed strong YFP signal on the edge of cells B, *AtCslD3*-n-YFP and *HvCslF3*-c-YFP co-expression showed strong YFP signal on the edge of cells C, *HvCslF3*-n-YFP and *HvCslF3*-c-YFP co-expression showed strong YFP signal on the edge of cells D, *AtCslD5*-n-YFP and *AtCslD5*-c-YFP co-expression showed strong YFP signal on the edge of cells E, -ve control; *HvCslF3*-n-YFP/c-YFP (empty) co-expression showed no YFP signal.

YFP and *HvCslF3*-c-YFP showed weak YFP signal with the same pattern as the *AtCslD3*-*AtCslD5* dimers. C. *HvCslF3* formed a homodimer on the cell wall with patchy patterns. D, *AtCslD5* also formed a homodimer on the cell walls with the same pattern as the *HvCslF3*. *AtCslD3* proteins did not interact with each other, no YFP signal detected in the combination of *AtCslD3*-n-YFP and *AtCslD3*-c-YFP co-expression (data not shown).

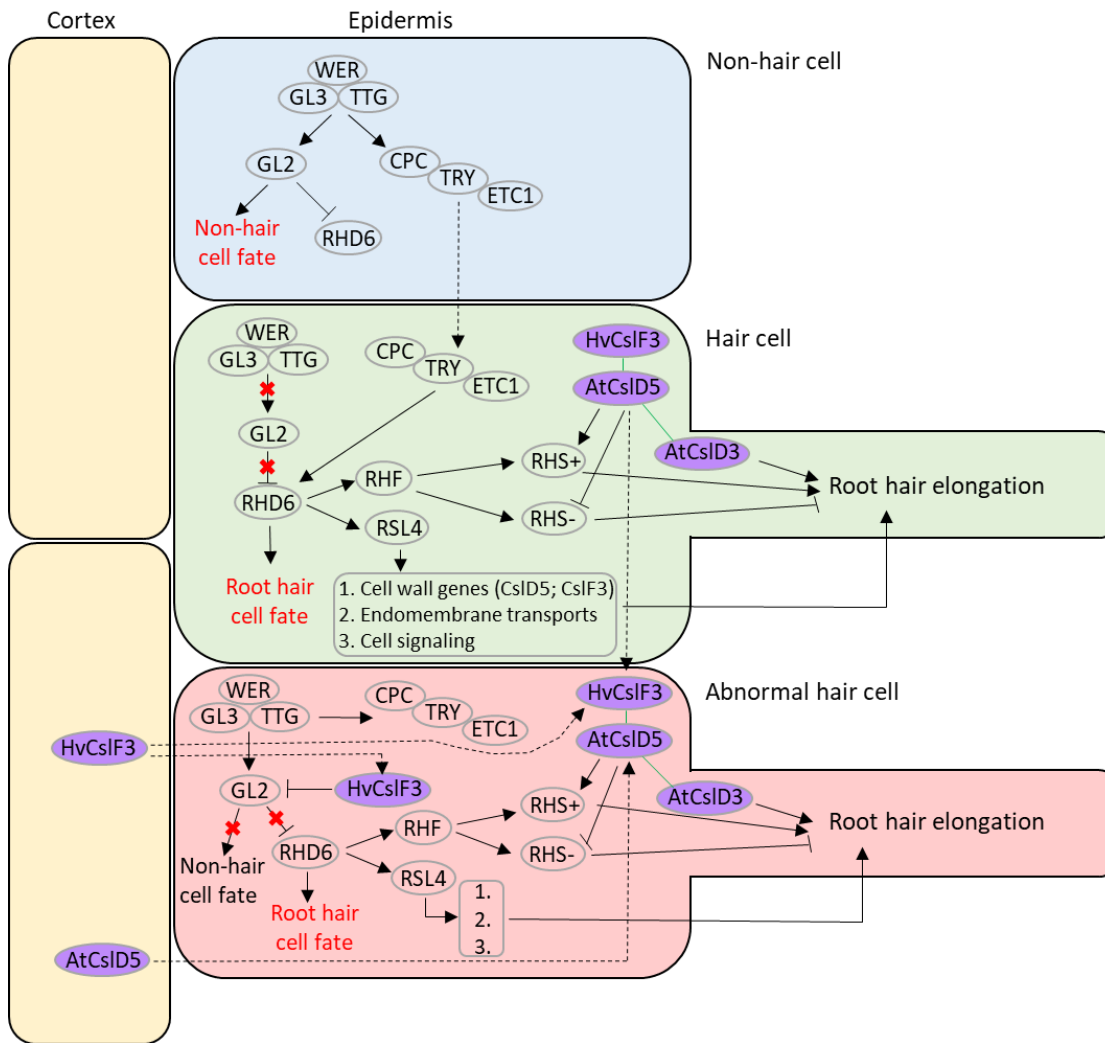


Figure 4-7. Proposed model of *CsID/F* genes interfere with root hair cell fate determination and elongation pathways. Transcriptional activation and up-regulation are indicated by arrows. Transcriptional repression and inhibition are shown by blunted lines. Dashed lines with arrows indicate protein movement. Green lines indicate protein-protein interaction. Yellow boxes represent cortical cells. Epidermis cells with three different fates are colour coded: non-hair cell/atrichoblast (blue), root hair cell/trichoblast (green), non-hair cell converted to hair forming cell due to the expression of *HvCsIF3* (red). Purple circles highlighted the roles of *AtCsID3*, *AtCsID5* and *HvCsIF3* in the model. The gene regulatory networks for position dependent root hair cell specification and balanced root hair elongation were adapted from previous studies (Yi et al., 2010; Hwang et al., 2016; Salazar-Henao et al., 2016).

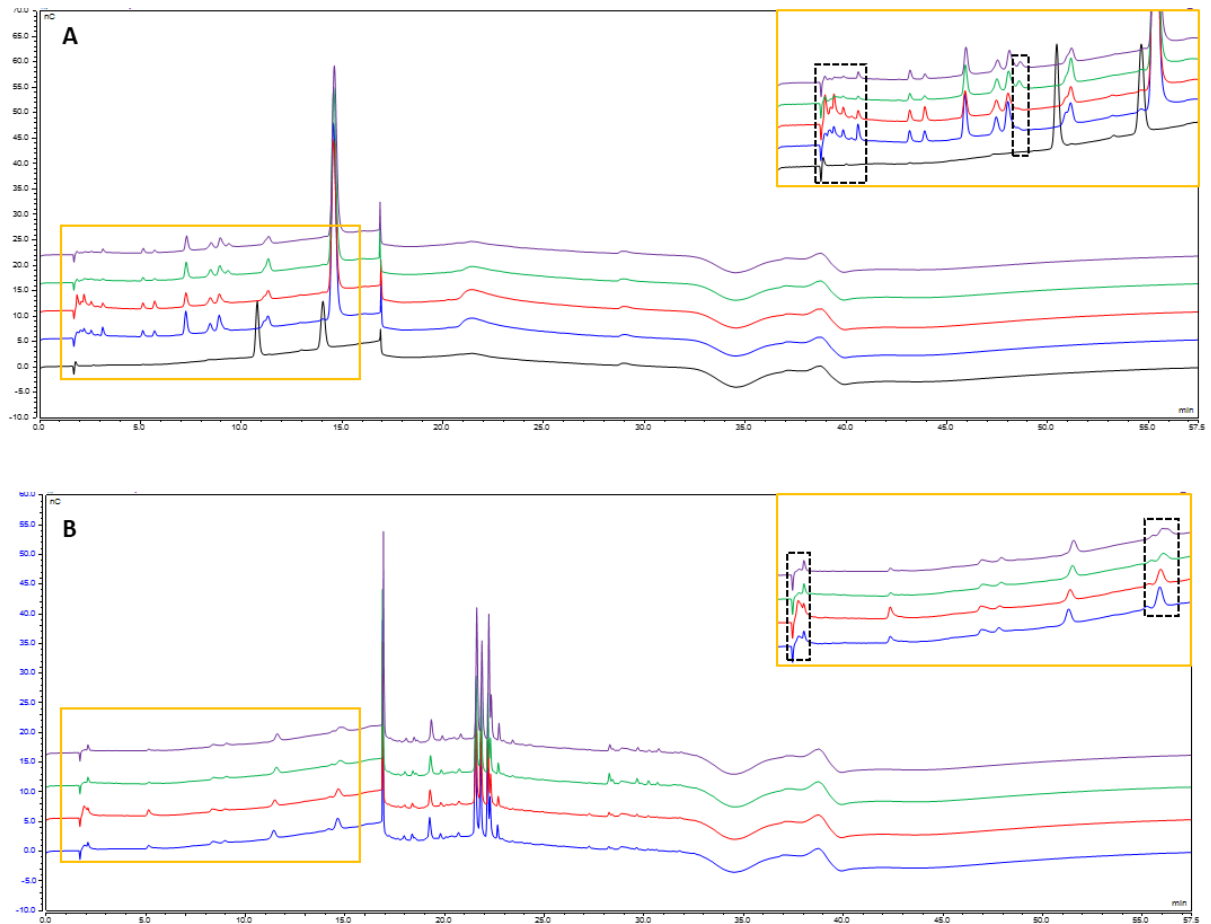


Figure 4-8. Quantitative Dionex analysis of oligosaccharides in the clarified solutions of E-CELTR hydrolysed *Arabidopsis* seedlings samples, including Col-0 (blue) and three individual events of *Ubiquitin10* promoter driving *HvCslF3* expression in Col-0 background (rep1, red; rep2, green; rep3, purple). Orange boxes represent a magnified view of regions of interests. Black dashed boxes highlight the unidentified difference in peaks between Col-0 and transgenic lines. A, the 8% acetonitrile fractions. The standards (black) indicate the peaks for Glcp-(1,4)- β -Xylp and Xylp-(1,4)- β -Glcp, which are combined to represented (1,4)- β -linked glucoxylan. No (1,4)- β -linked glucoxylan is detected in the *Arabidopsis* cell walls of any genotypes. B, the 55% acetonitrile fractions. X-axis, time; y-axis, abundance.

Tables

Table 4-1. Assembly of GreenGate destination vectors for the Arabidopsis complementation experiments. The A,B,C,D,E,F modules represent the vectors contain promoter, N-tag, coding sequence, C-tag, terminator, and resistance. A and C modules were built base on the empty modules (pGGA000 and pGGC000) to include the designed promoter and coding sequences. The B and D modules contain default random sequences with no desired functions. The D module also contains a stop codon. pGGE001 contains the RBCS terminator sequence from pea. pGGF005 contains hygromycin B resistance sequence for plant selection. The six modules were assembled on the backbone of pGGZ003 vector, which contains the plant resistance at LB.

Construct name	A-module	B-module	C-module	D-module	E-module	F-module
pUbq10::HvCsIF3	pGGAUbq10	pGGB003	pGGCHvCsIF3	pGGD002	pGGE001	pGGF005
pCobL9::HvCsIF3	pGGACobL9	pGGB003	pGGCHvCsIF3	pGGD002	pGGE001	pGGF005
pUbq10::AtCslD3	pGGAUbq10	pGGB003	pGGCAtCslD3	pGGD002	pGGE001	pGGF005
pCobL9::AtCslD3	pGGACobL9	pGGB003	pGGCAtCslD3	pGGD002	pGGE001	pGGF005
pUbq10::AtCslD5	pGGAUbq10	pGGB003	pGGCAtCslD5	pGGD002	pGGE001	pGGF005
pCobL9::AtCslD5	pGGACobL9	pGGB003	pGGCAtCslD5	pGGD002	pGGE001	pGGF005

Table 4-2. List of primers used in this study.

Primer name	Sequence
Hyg_F	GCCGTGGTTGGCTTGTATG
Hyg_R	GGGGCGTCGGTTTCCACTAT
BiFC_F3_F	AAAAAGATCTATGGCGTCGGCGGCCGGTGC
BiFC_F3_R	AAAAGGTACCCTAAAATGGAAGAAAATAAGAAG
BiFC_F9_F	AAAAAGATCTTGAAAACGACGGCCAGT
BiFC_F9_R	AAAAGGTACCCAGGAAACAGCTATGAC
BiFC_D3_F	AAAAGGTACCATGGCGTCTAATAATCATTTTCATG
BiFC_D3_R	AAAAGGGCCCTCATGGGAAAGTGAAAGATCCTCC
BiFC_D5_F	AAAAGAGCTCAAATGGTGAAATCAGCAGCTTCTC
BiFC_D5_R	AAAAGGTACCTCAAGGGAATTGAAACTGCATATAG
GG_F3_P1	ACCAGGTCTCGGGCTATGGCGTCGGCGGCCGGTGC
GG_F3_P2	TTTGGTCTCAGTTTCAACTAAGGCCTCGTATTGAATCAATGC
GG_F3_P3	TTTGGTCTCAAACCGCAAAGTTTGCTACTTTGTG
GG_F3_P4	AACAGGTCTCTCTGAGGCTAAAATGGAAGAAAATAAGAAG
GG_D3_P1	ACCAGGTCTCGGGCTATGGCGTCTAATAATCATTTTCATG
GG_D3_P2	AACAGGTCTCTGCCTCCACGGTCTGCTCATCAGATCC
GG_D3_P3	ACCAGGTCTCGAGGCCACTTACTCGGAAACTGCAG
GG_D3_P4	AACAGGTCTCTCTGATCATGGGAAAGTGAAAGATCCTCC
GG_D5_P1	ACCAGGTCTCGGGCTATGGTGAAATCAGCAGCTTCTC
GG_D5_P2	AACAGGTCTCTGCCTCCTCAGCGATATCTTGACTTTTC
GG_D5_P3	ACCAGGTCTCGAGGCCAAAAGCCATGATGAAGAAAGACG
GG_D5_P4	AACAGGTCTCTCTGATCAAGGGAATTGAAACTGCATATAG
GG_UBQ10_F	AACAGGTCTCGACCTATGCATATGAGTCTAGCTCAAC
GG_UBQ10_R	ACCAGGTCTCGTGTCTGTTAATCAGAAAATACTCAG

Table 4-3. A summary of the combinations and results of the BiFC experiment for the conformation of protein-protein interactions.

N-YFP	C-YFP	Type	YFP signal	Notes
OsARC	OsERS1	+ve, Heterodimer	√	Positive control, signals shown in cytoplasm
Empty	HvCsIF3	-ve	X	Negative control.
HvCsIF3	Empty	-ve	X	Negative control.
AtCsID5	AtCsID3	Heterodimer	√	Cell wall, polarised.
HvCsIF3	AtCsID3	Heterodimer, Barley with Arabidopsis	√	Cell wall, polarised.
HvCsIF3	AtCsID5	Heterodimer, Barley with Arabidopsis	X	No signal
HvCsIF3	HvCsIF3	Homodimer	√	Cell wall, patchy, weak
AtCsID3	AtCsID3	Homodimer	X	No signal
AtCsID5	AtCsID5	Homodimer	√	Cell wall, patchy, weak

Supplementary materials

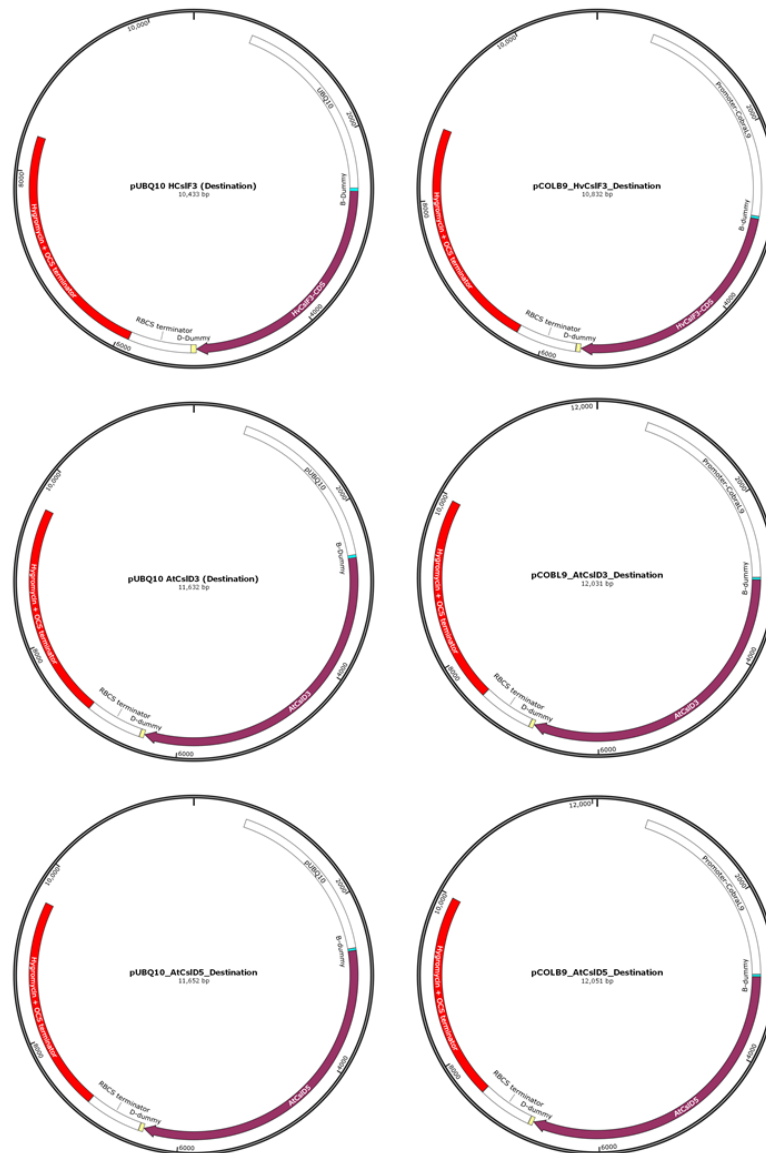


Figure 4-S1. Map of the destination vectors used for Arabidopsis transformation. UBQ10 and CobraL9 represent the *Ubiquitin10* and *CobraL9* promoter sequences, A-module. B-Dummy contains random sequence, B-module. Purple annotations shown the CDS of each gene (*HvCslF3*, *AtCslD3*, and *AtCslD5*), C-module. D-Dummy is the D-module with random sequence. RBCS terminator is E-module containing the ribulose-1,5-bisphosphate carboxylase (RBCS) terminator sequence. F-module contains the hygromycin resistance sequence. The reassembly of the destination vectors were based on the GGZ003 backbones.

Reference

- Bernhardt C, Lee MM, Gonzalez A, Zhang F, Lloyd A, Schiefelbein J** (2003) The bHLH genes *GLABRA3* (*GL3*) and *ENHANCER OF GLABRA3* (*EGL3*) specify epidermal cell fate in the Arabidopsis root. *Development* **130**: 6431-6439
- Burton RA, Collins HM, Kibble NAJ, Smith JA, Shirley NJ, Jobling SA, Henderson M, Singh RR, Pettolino F, Wilson SM, Bird AR, Topping DL, Bacic A, Fincher GB** (2011) Over-expression of specific *HvCslF* cellulose synthase-like genes in transgenic barley increases the levels of cell wall (1,3;1,4)- β -D-glucans and alters their fine structure. *Plant Biotechnology Journal* **9**: 117-135
- Burton RA, Farrokhi N, Bacic A, Fincher GB** (2005) Plant cell wall polysaccharide biosynthesis: real progress in the identification of participating genes. *Planta* **221**: 309-312
- Burton RA, Jobling SA, Harvey AJ, Shirley NJ, Mather DE, Bacic A, Fincher GB** (2008) The genetics and transcriptional profiles of the cellulose synthase-like *HvCslF* gene family in barley. *Plant Physiology* **146**: 1821-1833
- Burton RA, Wilson SM, Hrmova M, Harvey AJ, Shirley NJ, Medhurst A, Stone BA, Newbigin EJ, Bacic A, Fincher GB** (2006) Cellulose synthase-like *CslF* genes mediate the synthesis of cell wall (1, 3; 1, 4)- β -D-glucans. *Science* **311**: 1940-1942
- Clough SJ, Bent AF** (1998) Floral dip: a simplified method for *Agrobacterium*-mediated transformation of *Arabidopsis thaliana*. *The Plant Journal* **16**: 735-743
- Cocuron J-C, Lerouxel O, Drakakaki G, Alonso AP, Liepman AH, Keegstra K, Raikhel N, Wilkerson CG** (2007) A gene from the cellulose synthase-like C family encodes a β -1, 4 glucan synthase. *Proceedings of the National Academy of Sciences of the United States of America* **104**: 8550-8555
- Doblin MS, De Melis L, Newbigin E, Bacic A, Read SM** (2001) Pollen tubes of *Nicotiana glauca* express two genes from different β -glucan synthase families. *Plant Physiology* **125**: 2040-2052
- Doblin MS, Kurek I, Jacob-Wilk D, Delmer DP** (2002) Cellulose biosynthesis in plants: from genes to rosettes. *Plant Cell Physiology* **43**: 1407-1420
- Doblin MS, Pettolino FA, Wilson SM, Campbell R, Burton RA, Fincher GB, Newbigin E, Bacic A** (2009) A barley cellulose synthase-like *CslH* gene mediates (1, 3; 1, 4)- β -D-glucan synthesis in transgenic Arabidopsis. *Proceedings of the National Academy of Sciences of the United States of America* **106**: 5996-6001
- Dolan L** (2017) Root hair development in grasses and cereals (Poaceae). *Current Opinion in Genetics Development* **45**: 76-81
- Dolan L, Janmaat K, Willemsen V, Linstead P, Poethig S, Roberts K, Scheres B** (1993) Cellular organisation of the *Arabidopsis thaliana* root. *Development* **119**: 71-84
- Douchkov D, Lueck S, Hensel G, Kumlehn J, Rajaraman J, Johrde A, Doblin MS, Beahan CT, Kopischke M, Fuchs R, Lipka V, Niks RE, Bulone V, Chowdhury J, Little A, Burton RA, Bacic A, Fincher GB, Schweizer P** (2016) The barley (*Hordeum vulgare*) cellulose synthase-like D2 gene (*HvCslD2*) mediates penetration resistance to host-adapted and nonhost isolates of the powdery mildew fungus. *New Phytologist* **212**: 421-433
- Dwivany FM, Yulia D, Burton RA, Shirley NJ, Wilson SM, Fincher GB, Bacic A, Newbigin E, Doblin MS** (2009) The Cellulose-synthase like C (*CslC*) family of barley includes members that are integral membrane proteins targeted to the plasma membrane. *Molecular Plant* **2**: 1025-1039
- Edgar RC** (2004) MUSCLE: multiple sequence alignment with high accuracy and high throughput. *Nucleic Acids Research* **32**: 1792-1797
- Galway ME** (2006) Root hair cell walls: filling in the framework. *Canadian Journal of Botany*

84: 613-621

- Galway ME, Masucci JD, Lloyd AM, Walbot V, Davis RW, Schiefelbein JW** (1994) The TTG gene is required to specify epidermal cell fate and cell patterning in the Arabidopsis root. *Developmental Biology* **166**: 740-754
- Gardiner JC, Taylor NG, Turner SR** (2003) Control of cellulose synthase complex localization in developing xylem. *The Plant Cell* **15**: 1740-1748
- Goubet F, Barton CJ, Mortimer JC, Yu X, Zhang Z, Miles GP, Richens J, Liepman AH, Seffen K, Dupree P** (2009) Cell wall glucomannan in Arabidopsis is synthesised by CSLA glycosyltransferases, and influences the progression of embryogenesis. *The Plant Journal* **60**: 527-538
- Han Y, Xin M, Huang K, Xu Y, Liu Z, Hu Z, Yao Y, Peng H, Ni Z, Sun Q** (2016) Altered expression of Ta RSL 4 gene by genome interplay shapes root hair length in allopolyploid wheat. *New Phytologist* **209**: 721-732
- Hazen SP, Scott-Craig JS, Walton JD** (2002) Cellulose synthase-like genes of rice. *Plant Physiology* **128**: 336-340
- Hill JL, Hammudi MB, Tien M** (2014) The Arabidopsis cellulose synthase complex: a proposed hexamer of CESA trimers in an equimolar stoichiometry. *The Plant Cell* **26**: 4834-4842
- Hochholdinger F, Park WJ, Sauer M, Woll K** (2004) From weeds to crops: genetic analysis of root development in cereals. *Trends in Plant Science* **9**: 42-48
- Hochholdinger F, Zimmermann R** (2008) Conserved and diverse mechanisms in root development. *Current Opinion in Plant Biology* **11**: 70-74
- Hwang Y, Lee H, Lee Y-S, Cho H-T** (2016) Cell wall-associated ROOT HAIR SPECIFIC 10, a proline-rich receptor-like kinase, is a negative modulator of Arabidopsis root hair growth. *Journal of Experimental Botany* **67**: 2007-2022
- Kim CM, Park S, Je BI, Park S, Park S, Piao H-L, Eun M, Dolan L, Han C-d** (2007) OsCSLD1, a Cellulose Synthase-Like D1 gene, is required for root hair morphogenesis in rice. *Plant Physiology* **143**: 1220-1230
- Kirschner GK, Stahl Y, Von Korff M, Simon R** (2017) Unique and conserved features of the barley root meristem. *Frontiers in Plant Science* **8**: 1240-1240
- Lampropoulos A, Sutikovic Z, Wenzl C, Maegele I, Lohmann JU, Forner J** (2013) GreenGate - A novel, versatile, and efficient cloning system for plant transgenesis. *Plos One* **8**: e83043
- Lee MM, Schiefelbein J** (1999) WEREWOLF, a MYB-related protein in Arabidopsis, is a position-dependent regulator of epidermal cell patterning. *Cell* **99**: 473-483
- Li M, Xiong G, Li R, Cui J, Tang D, Zhang B, Pauly M, Cheng Z, Zhou Y** (2009) Rice cellulose synthase-like D4 is essential for normal cell-wall biosynthesis and plant growth. *The Plant Journal* **60**: 1055-1069
- Little A, Lahnstein J, Jeffery DW, Khor SF, Schwerdt JG, Shirley NJ, Hooi M, Xing X, Burton RA, Bulone V** (2019) A novel (1, 4)- β -linked glucoxytan is synthesized by members of the Cellulose Synthase-Like F gene family in land plants. *ACS Central Science* **5**: 73-84
- Little A, Schwerdt JG, Shirley NJ, Khor SF, Neumann K, O'Donovan LA, Lahnstein J, Collins HM, Henderson M, Fincher GB, Burton RA** (2018) Revised phylogeny of the Cellulose Synthase GenesSuperfamily: insights into cell wall evolution. *Plant Physiology* **177**: 1124-1141
- Marzec M, Melzer M, Szarejko I** (2013) Asymmetric growth of root epidermal cells is related to the differentiation of root hair cells in *Hordeum vulgare* (L.). *Journal of Experimental Botany* **64**: 5145-5155
- Masucci JD, Rerie WG, Foreman DR, Zhang M, Galway ME, Marks MD, Schiefelbein JW** (1996) The homeobox gene GLABRA2 is required for position-dependent cell differentiation in the root epidermis of Arabidopsis thaliana. *Development* **122**: 1253-

1260

- Masucci JD, Schiefelbein JW** (1994) The *rh6* mutation of *Arabidopsis thaliana* alters root-hair initiation through an auxin-and ethylene-associated process. *Plant Physiology* **106**: 1335-1346
- Morgan JL, Strumillo J, Zimmer J** (2013) Crystallographic snapshot of cellulose synthesis and membrane translocation. *Nature* **493**: 181-186
- Nemeth C, Freeman J, Jones HD, Sparks C, Pellny TK, Wilkinson MD, Dunwell J, Andersson AAM, Aman P, Guillon F, Saulnier L, Mitchell RAC, Shewry PR** (2010) Down-regulation of the *CslF6* gene results in decreased (1,3;1,4)- β -D-glucan in endosperm of wheat. *Plant Physiology* **152**: 1209-1218
- Pemberton LM, Tsai S-L, Lovell PH, Harris PJ** (2001) Epidermal patterning in seedling roots of eudicotyledons. *Annals of Botany* **87**: 649-654
- Peng X, Pang H, Abbas M, Yan X, Dai X, Li Y, Li Q** (2019) Characterization of Cellulose synthase-like D (CSLD) family revealed the involvement of *PtrCslD5* in root hair formation in *Populus trichocarpa*. *Scientific Reports* **9**: 1452-1460
- Persson S, Paredez A, Carroll A, Palsdottir H, Doblin M, Poindexter P, Khitrov N, Auer M, Somerville CR** (2007) Genetic evidence for three unique components in primary cell-wall cellulose synthase complexes in *Arabidopsis*. *Proceedings of the National Academy of Sciences of the United States of America* **104**: 15566-15571
- Petricka JJ, Winter CM, Benfey PN** (2012) Control of *Arabidopsis* root development. *Annual Review of Plant Biology* **63**: 563-590
- Ray B, Lahaye M** (1995) Cell-wall polysaccharides from the marine green alga *Ulva "rigida"*(Ulvales, Chlorophyta). Extraction and chemical composition. *Carbohydrate Research* **274**: 251-261
- Richmond TA, Somerville CR** (2000) The cellulose synthase superfamily. *Plant Physiology* **124**: 495-498
- Salazar-Henao JE, Vélez-Bermúdez IC, Schmidt W** (2016) The regulation and plasticity of root hair patterning and morphogenesis. *Development* **143**: 1848-1858
- Schindelin J, Arganda-Carreras I, Frise E, Kaynig V, Longair M, Pietzsch T, Preibisch S, Rueden C, Saalfeld S, Schmid B, Tinevez J-Y, White DJ, Hartenstein V, Eliceiri K, Tomancak P, Cardona A** (2012) Fiji: an open-source platform for biological-image analysis. *Nature Methods* **9**: 676-682
- Schwerdt JG** (2017) The evolutionary history and dynamics of the cellulose synthase superfamily. University of Adelaide
- Schwerdt JG, MacKenzie K, Wright F, Oehme D, Wagner JM, Harvey AJ, Shirley NJ, Burton RA, Schreiber M, Halpin C, Zimmer J, Marshall DF, Waugh R, Fincher GB** (2015) Evolutionary dynamics of the Cellulose Synthase gene superfamily in grasses. *Plant Physiology* **168**: 968-983
- Shibata M, Sugimoto K** (2019) A gene regulatory network for root hair development. *Journal of Plant Research* **132**: 301-309
- Shpigel E, Roiz L, Goren R, Shoseyov O** (1998) Bacterial cellulose-binding domain modulates in vitro elongation of different plant cells. *Plant Physiology* **117**: 1185-1194
- Stamatakis A** (2006) RAxML-VI-HPC: maximum likelihood-based phylogenetic analyses with thousands of taxa and mixed models. *Bioinformatics* **22**: 2688-2690
- Taketa S, Yuo T, Tonooka T, Tsumuraya Y, Inagaki Y, Haruyama N, Larroque O, Jobling SA** (2011) Functional characterization of barley betaglucanless mutants demonstrates a unique role for *CslF6* in (1, 3; 1, 4)- β -D-glucan biosynthesis. *Journal of Experimental Botany* **63**: 381-392
- Taylor NG, Howells RM, Huttly AK, Vickers K, Turner SR** (2003) Interactions among three distinct *CesA* proteins essential for cellulose synthesis. *Proceedings of the National Academy of Sciences of the United States of America* **100**: 1450-1455
- Vain T, Crowell EF, Timpano H, Biot E, Desprez T, Mansoori N, Trindade LM, Pagant S,**

- Robert S, Höfte H** (2014) The cellulase KORRIGAN is part of the cellulose synthase complex. *Plant Physiology* **165**: 1521-1532
- van den Berg C, Willemsen V, Hendriks G, Weisbeek P, Scheres B** (1997) Short-range control of cell differentiation in the Arabidopsis root meristem. *Nature* **390**: 287-289
- Vega-Sánchez ME, Verhertbruggen Y, Christensen U, Chen X, Sharma V, Varanasi P, Jobling SA, Talbot M, White RG, Joo M, Singh S, Auer M, Scheller HV, Ronald PC** (2012) Loss of Cellulose synthase-like F6 function affects mixed-linkage glucan deposition, cell wall mechanical properties, and defense responses in vegetative tissues of rice. *Plant Physiology* **159**: 56-69
- von Wangenheim D, Hauschild R, Friml J** (2017) Light sheet fluorescence microscopy of plant roots growing on the surface of a gel. *JoVE (Journal of Visualized Experiments)* **119**: e55044
- Wada T, Tachibana T, Shimura Y, Okada K** (1997) Epidermal cell differentiation in Arabidopsis determined by a Myb homolog, CPC. *Science* **277**: 1113-1116
- Wang C, Li S, Ng S, Zhang B, Zhou Y, Whelan J, Wu P, Shou H** (2014) Mutation in xyloglucan 6-xylosyltransferase results in abnormal root hair development in *Oryza sativa*. *Journal of Experimental Botany* **65**: 4149-4157
- Yang X, Li G, Tian Y, Song Y, Liang W, Zhang D** (2018) A rice glutamyl-tRNA synthetase modulates early anther cell division and patterning. *Plant Physiology* **177**: 728-744
- Yi K, Menand B, Bell E, Dolan L** (2010) A basic helix-loop-helix transcription factor controls cell growth and size in root hairs. *Nature Genetics* **42**: 264-267
- Yin L, Verhertbruggen Y, Oikawa A, Manisseri C, Knierim B, Prak L, Jensen JK, Knox JP, Auer M, Willats WG** (2011) The cooperative activities of CSLD2, CSLD3, and CSLD5 are required for normal Arabidopsis development. *Molecular Plant* **4**: 1024-1037
- ZhiMing Y, Bo K, XiaoWei H, ShaoLei L, YouHuang B, WoNa D, Ming C, Hyung-Taeg C, Ping W** (2011) Root hair-specific expansins modulate root hair elongation in rice. *The Plant Journal* **66**: 725-734

Chapter 5

Knock-down of *HvCslF3* and *HvCslF9* gene expressions in barley is predicted to increase plant tolerance to low nutrient stresses over the vegetative stage



Statement of Authorship

Title of Paper	Knock-down of HvCsIF3 and HvCsIF9 gene expressions in barley is predicted to increase plant tolerance to low nutrient stresses over the vegetative stage
Publication Status	<input type="checkbox"/> Published <input type="checkbox"/> Accepted for Publication <input type="checkbox"/> Submitted for Publication <input checked="" type="checkbox"/> Unpublished and Unsubmitted work written in manuscript style
Publication Details	HvCsIF3 Affects Root Epidermal Cell Proliferation and Root Hair Elongation Haoyu Lou, Ishan Ajmera, Leah Band, Malcolm Bennett, Matthew Tucker, Vincent Bulone

Principal Author

Name of Principal Author (Candidate)	Haoyu Lou		
Contribution to the Paper	Performed experiments and analysed data. Wrote the manuscript.		
Overall percentage (%)	70%		
Certification:	This paper reports on original research I conducted during the period of my Higher Degree by Research candidature and is not subject to any obligations or contractual agreements with a third party that would constrain its inclusion in this thesis. I am the primary author of this paper.		
Signature		Date	24/02/2020

Co-Author Contributions

By signing the Statement of Authorship, each author certifies that:

- i. the candidate's stated contribution to the publication is accurate (as detailed above);
- ii. permission is granted for the candidate to include the publication in the thesis; and
- iii. the sum of all co-author contributions is equal to 100% less the candidate's stated contribution.

Name of Co-Author	Vincent Bulone		
Contribution to the Paper	Principle supervisor. Conceived the project and designed experiments. Assisted with writing of the manuscript. I hereby certify that the statement of authorship is accurate.		
Signature		Date	24/02/2020

Name of Co-Author	Matthew Tucker		
-------------------	----------------	--	--

Chapter 5 – Knock-down of *HvCs1F3* and *HvCs1F9* gene expressions in barley is predicted to increase plant tolerance to low nutrient stresses over the vegetative stage

Contribution to the Paper	Co-supervisor. Conceived the project and designed experiments. Assisted with writing of the manuscript. I hereby certify that the statement of authorship is accurate.		
Signature		Date	24/02/2020

Name of Co-Author	Malcolm Bennett		
Contribution to the Paper	Co-supervisor at University of Nottingham. Conceived the project and designed experiments. Assisted with writing of the manuscript. I hereby certify that the statement of authorship is accurate.		
Signature		Date	24/2/20

Name of Co-Author	Leah Band		
Contribution to the Paper	Co-supervisor at University of Nottingham. Conceived the project and designed experiments. Assisted with writing of the manuscript. I hereby certify that the statement of authorship is accurate.		
Signature		Date	25/02/2020

Name of Co-Author	Ishan Ajmera		
Contribution to the Paper	Assisted with experiment and data analysis and editing of the manuscript. I hereby certify that the statement of authorship is accurate.		
Signature		Date	24/02/2020

Abstract

The *Cellulose Synthase-Like F* (*CslF*) genes belong to the *CesA/Csl* superfamily and are important for the synthesis and assembly of cell wall components. The barley *HvCslF3* and *HvCslF9* genes are highly expressed in the root tips and their down-regulation results in reduced root growth in seedlings compared to the wild type cultivar, Golden Promise. Root traits such as root number, length, and branching density, are essential for the root-soil interaction that affects water and nutrient uptake. To investigate the impact of modified root growth on whole-plant phenotypes, Golden Promise, *HvCslF3-RNAi* and *HvCslF9-RNAi* plants were grown in a soil environment. Both constructs led to restricted shoot development over the vegetative stage. This includes shoot morpho-physiological parameters such as plant height, leaf and tiller number, weight, leaf area, transpiration rate and stomatal conductance. In addition, the root system of the transgenics was significantly smaller than that of Golden Promise, indicating a continuous negative effect of gene down regulation on root development. Using these phenotypic data, the development of the three genotypes was assessed *in silico* by combining different nitrogen, phosphorus, and potassium regimes by incorporating our measurements into a functional-structural root model - *OpenSimRoot* (OSR). The transgenic lines were predicted to have reduced ability for soil nutrient capture but greater tolerance to nutrient stresses. Although these models are yet to be tested in the field, they highlight the potential of using cell wall-related genes to affect root architecture, and their potential utility in low input agriculture.

Introduction

Roots are a critical underground plant organ that interacts with the surrounding soil environment to support plant growth. Roots take-up nutrients and water from soil, anchor plants to their substrates, participate in the synthesis of growth hormones, function in defence against pathogens, and also provide carbohydrate storage (Yao et al., 2002; Cook, 2006; Imani et al., 2011). Barley is a major cereal crop and belonging to the grass family. Its high value in the malting and brewing industries and healthy food production makes it an economically important crop in many countries (Tricase et al., 2018). Barley develops a fibrous root system that comprises embryonic primary and seminal roots, post-embryonic nodal roots, and lateral roots emerging from parent roots (Hochholdinger and Zimmermann, 2008). Root and shoot development mutually affect each other (Yao et al., 2002). Roots support shoot growth by supplying water and nutrient requirements. While the shoot supplies carbon and essential hormones to the roots (Osaki et al., 1997; Hochholdinger and Feix, 1998; Yao et al., 2002).

The architecture of a root system is controlled by multiple genetic regulators that interact with each other and the surrounding environments (Lynch, 2019). However, the genetic control of most root traits is poorly understood (Lynch, 2019). In our previous studies, we have shown the negative effects of down-regulating the cell wall-related *Cellulose synthase-like F* (*CslF*) genes (*HvCslF3* and *HvCslF9*) on barley root development (Chapter 3). The expression of *HvCslF3* occurs only in roots, and is essentially concentrated in the elongation zone of the root tips, while *HvCslF9* is expressed in the root tips and developing inflorescences and grains (Chapter 3) (The International Barley Genome Sequencing et al., 2012). The effects of down-regulation were exceptionally severe during root elongation and root hair development, which largely affect the overall root architecture such as root length and surface area. In previous studies, a slight negative effect was reported for the barley *CslF6* mutant throughout plant growth, although it remains unclear whether this relates to specific defects in root or shoot

growth (Tonooka et al., 2009). A study of the rice *short root* mutant (*srt5*) showed inhibition of root development at the seedling stage, but the phenotype was recovered after transferring the plants to soil pots (Yao et al., 2002). Whether the effects on root development triggered by *HvCsIF3* and *HvCsIF9* gene down-regulation are restricted to the seedling stage or can be extended to the later stages of plant development remains unknown.

In a natural soil environment, the plant root system expands to increase the surface area for root-soil interactions and adapts to the uneven distribution of water and nutrients in soil (Lynch, 1995, 2019). Morphological features of the root system determine its nutrient absorption efficiency (Wang et al., 2006). This includes root length, density and growth angle, which are known to positively influence nitrate uptake due to enriched nitrate in deep soil (Sullivan et al., 2000). Due to nutrient immobilization, a large proportion of phosphorus (P) can be found in the topsoil. Thus, P uptake is largely influenced by the volume of shallow roots, lateral root density and long root hairs (Ge et al., 2000; Lynch, 2019). Similar to P, potassium (K) is also bound to soil constituents and is relatively less mobile. Root phenotypes that benefit P capture also optimise K absorption (Römheld and Kirkby, 2010; Lynch, 2019). Furthermore, different root classes display distinct abilities to take up nutrients and water (Peng et al., 2012; Liu, 2018). For example, post-embryonic crown roots in maize show a higher rate of nitrate maximum influx, while the seminal roots have higher substrate affinity (York et al., 2016). Studies in barley revealed higher water uptake ability in nodal roots compared to seminal roots due to the greater hydraulic conductivity of the nodal root cortex (Knipfer et al., 2011).

Transpiration provides the driving force for the movement of water and nutrients absorbed from the soil to the aerial tissues, and regulates the sub-stomata cavity water evaporation to the atmosphere (Nilson and Assmann, 2007; Lambers et al., 2008). Transpiration is largely controlled by the opening and closing of stomata on the epidermis of the plant aerial parts. Studies have shown a positive relationship between transpiration rate with stomatal

Chapter 5 – Knock-down of *HvCsIF3* and *HvCsIF9* gene expressions in barley is predicted to increase plant tolerance to low nutrient stresses over the vegetative stage

conductance and root water uptake (Penman, 1950; Pitman, 1965; Bartens et al., 2009; Knipfer and Fricke, 2010). Based on these observations, it can be inferred that root systems with higher water capture ability are also likely to increase N uptake (Lynch, 2019).

To evaluate the effects of *HvCsIF3* and *HvCsIF9* genes on vegetative growth in barley, we compared the plant morpho-physiology of two transgenic lines (*HvCsIF3-RNAi* and *HvCsIF9-RNAi*) with the wild-type barley cultivar, Golden Promise, over a 50-day period in glasshouse conditions. Root phenotyping and genomic selection is quite challenging in the natural soil environment as shoot development and root-soil interactions are simultaneously dependent on both structural and functional regulations. The functional structural model, *OpenSimRoot* (OSR) (Postma et al., 2014; Postma et al., 2017) is a valuable tool to analyse the feedback between genetically controlled phenotypes and plant responses to different environmental conditions. Following this paradigm, we combined glasshouse phenotypic data with a climate and soil environment data from Roseworthy (South Australia, Australia) to parameterise and optimise the functional-structural root model – OSR/barley (Schneider et al., 2017). This was undertaken for the wild-type and transgenics, in order to assess their behaviour in response to different combinations of NPK stresses. Based on the models, the transgenics were predicted to have a less severe reduction in various physiological parameters compared to the wild-type under the combinations of NPK stresses. Theoretically, these observations highlight the possibility of breeding nutrient-efficient crops by manipulating the expression of cell wall-related genes to achieve different cell wall composition and root architecture.

Materials and methods

Glasshouse conditions

Barley seeds (Golden Promise, *HvCsIF3-RNAi*, and *HvCsIF9-RNAi*) were surface sterilized by immersion in a 20% (v/v) sodium hypochlorite solution for 10 min, washed with

sterile distilled water four times before being placed onto autoclaved filter paper overnight for pre-germination. Seedlings at the same development stage (30 per genotype) were selected and transferred into pre-soaked soil in a glasshouse (23/15°C, 16/8 h). Sandy and Kettering loam soils (1:1) were mixed with Osmacote slow release fertilizer and added to pots (20 x 20 cm) and columns (20 x 60 cm). Uniformly germinated seeds were sown at a consistent depth of 1.5 cm in soil to minimise variation. An automatic irrigation system was used to water the pots and columns for 15 min, once per day.

Morpho-physiological phenotyping

Golden Promise (wild-type), *HvCsIF3-RNAi* (line #27) and *HvCsIF9-RNAi* (line #33) were used in the phenotyping study. Six plants of each genotype were measured and sampled at 10-day intervals until day 50. At each time point, plant height, leaf number, tiller number, fresh weight (root/shoot) and dry weight (shoot) were recorded. The SPAD chlorophyll meter was used to measure chlorophyll concentration in the second youngest leaf on each tiller, and the averaged results were recorded to represent the level of chlorophyll for an individual plant. Plant photosynthesis was measured using Licor LI6400Xt fitted with a leaf chamber fluorometer. The measurements were taken at the same time in the morning for each time point to ensure the consistency of light absorbance, at three positions on leaf (tip, middle and base) and from three young leaves per plant. After harvesting shoot samples, LI-3100 area meter was used to measure the leaf area, and fresh weights were recorded. These samples were then oven dried (60°C) for at least 3 d to measure their dry weight. The dried shoot materials were further used for elemental phenotyping (see next section). Plant roots were separated from pots and columns and thoroughly washed. After air drying, root fresh weight was measured, and the intact root samples were preserved in 30% ethanol (v/v) at 4°C. Root number were recorded from the fresh roots. WinRhizo root analyser (Regent; STD4800) was used to measure the total root length, average diameter, and total volume.

Elemental phenotyping

The oven dried shoot materials and grains were used to quantitatively determine elemental content. The grain and tissue samples were acid hydrolysed using an Anton Paar Multiwave PRO Microwave reaction system. 0.2 g samples were hydrolysed in nitric acid for 30 min. Tomato 1573A (May et al., 2000) and wheat flour samples were used as certified reference materials for shoot and grain samples, respectively. The hydrolysed samples were analysed by ICP-MS (Thermo Fisher Scientific iCAPQ, Thermo Fisher Scientific) for multielement analysis following the protocol described by Thomas et al. (2016). To measure the C and N concentrations in the harvested plant materials, the dried samples were finely ground with TissueLyser II (QIAGEN). Approximately 5 mg of ground samples was weighed and wrapped in aluminium foil, and analysed on a micro CN analyser (Thermo Scientific Flash 2000 CHNS/O Analyzer) following the protocol described by Fiacco et al. (2018).

***OpenSimRoot* parameterisation**

To assess the root growth and performance of the barley genotypes *in silico*, the published *OpenSimRoot*/barley (OSR) was re-optimised and implemented (Lynch et al., 1997; Postma and Lynch, 2011; Dathe et al., 2016; Schneider et al., 2017). OSR is a functional-structural plant model that simulates root growth in three-dimensional virtual soils. More details about the *OpenSimRoot* model can be found in Postma et al. (2017) (<https://rootmodels.gitlab.io/>). The current available *OpenSimRoot* barley model is based on Julich (Germany) climate and soil parameters with plant parameters of barley cultivar Scarlett. To parameterise the soil environment in OSR/barley model, we obtained soil data from the Roseworthy field trials (South Australia, Australia) by accessing the APSoil database (Site name: Roseworthy No300; <https://apsimdev.apsim.info/ApsoilWeb/ApsoilKML.aspx>) (Dalglish et al., 2012). The parameters, including soil type, bulk density, altitude, latitude, organic matter, and nutrient

contents, were obtained and used in the OSR to simulate the Roseworthy soil environment. To parameterise the atmosphere model for Roseworthy in OSR, four years of weather data (2014-2017) from the Roseworthy weather station (BoM station ID 23122, Roseworthy ag college) were averaged and included in the model. This includes daily temperature, rainfall, sunshine duration, solar exposure, radiation, evaporation, wind speed, and relative humidity. To incorporate the plant parameters for Golden Promise, *HvCsIF3-RNAi* and *HvCsIF9-RNAi*, glasshouse-measured parameters (leaf area, tiller and root number, shoot and root fresh and dry weights), root parameters measured using WhiRhizo (root length, root classes, root diameters, lateral branching density) and elemental data (concentrations of N, P and K in seeds and dry leaves) were included. The transgenic plants develop thinner roots with fewer cortical cell layers, hence have lighter roots. Therefore, the root density (OSR plant parameter) of each genotype were parameterised accordingly. To demonstrate the accuracy of the predictions of the simulations, root length, leaf area, shoot and root dry weight were compared between the simulated data and glasshouse measured data.

***In-silico* factorial design experiment**

The parameterised OSR/barley for the three genotypes were simulated over the vegetative stage, i.e. 50 days post-germination (dpg) to assess their behaviour under different combinations of NPK stresses. Initially, the three genotypes were simulated under five soil nutrient availabilities to identify the optimal, moderate and deficient soil nutrient levels for plant growth (Figure S1). The determined soil NPK levels were used to simulate a full factorial design experiment. This included 3 genotypes, 3 replicates, 3 levels of N, 3 level of P, 3 levels of K (i.e. $3^5 = 243$ plants). Plant growth was simulated using field conditions with 2 m soil depth and 25 cm row spacing.

Statistical analysis

All data obtained in the morpho-physiological phenotyping and elemental phenotyping experiments were subjected to analysis of significance using Two-way ANOVA multiple comparisons (GraphPad Prism V7.03) with Golden Promise as the main factor. The results are presented in Table 5-S1.

Results

The downregulation of *HvCslF3* and *HvCslF9* negatively affects barley shoot development

In the previous chapter, we demonstrated the negative effects of downregulating *HvCslF3* and *HvCslF9* gene expression on barley seedling development, especially on root elongation. To further assess whether the impacts were only severe during the early development stages, the Golden Promise and transgenic lines were sowed into a soil environment to examine vegetative growth. The transgenic lines were smaller compared to the wild type throughout the vegetative stage (Figure 5-1). The height of the barley plants increased at a stable rate and reached 45-55 cm at 50 dpv, with minor variations across genotypes (Figure 5-2 A). However, significant differences were observed in leaf area, fresh and dry shoot weight (Figure 5-2 B, C, D). The differences were distinct after 30 dpv. After 40 dpv, the leaf area and shoot weight of Golden Promise plants increased rapidly compared to the transgenic plants. At 50 dpv, Golden Promise had an average of 12 tillers, whereas the transgenic plants had only 6 tillers. Consistent with the tiller number, the number of leaves was also halved in the transgenic plants (Figure 5-2 F).

At 50 dpv, the Golden Promise average leaf area reached 628 cm², which was 2.8 and 2.0 fold larger than for the *HvCslF3-RNAi* and *HvCslF9-RNAi* plants, respectively (Figure 5-2 B). Similar fold changes were observed for the shoot fresh and dry weights. Plant water content ranged between 89-92% with no significant variation between genotypes and developmental stages. No significant difference in chlorophyll content was detected between Golden Promise

and the transgenic plants (Figure 5-2 E).

The *HvCsIF3* and *HvCsIF9* knock-down plants developed smaller root systems

The *HvCsIF3-RNAi* and *HvCsIF9-RNAi* seedlings showed slower growth rate and reduced root elongation zones (Chapter 3). To investigate whether the restrictions on root development also occur in a soil environment and to understand the duration of defects, washed roots were characterized according to the weight, length, surface area and diameter. Figure 5-3 shows representative photographs of the 10, 20, 30, 40 and 50-day old root systems of the three genotypes grown in soil. Severe differences in the size of the root system were observed from 10 dpv, and the effects continued throughout plant development (Figure 5-3). *HvCsIF3-RNAi* and *HvCsIF9-RNAi* plants developed significantly smaller root systems compared with Golden Promise. One obvious root trait showing a difference was the number of roots. Until 20 dpv, seminal roots dominated the root system, and the average number of emergences of seminal roots was similar across all plants (i.e. Golden Promise: 7, *HvCsIF3-RNAi*: 5, *HvCsIF9-RNAi*: 6). After 20 dpv, nodal roots started to emerge from the base of shoots, and a large number of lateral roots had emerged on seminal roots. Nodal roots became more abundant from 30 dpv, and lateral roots started to evenly distribute along the entire root. The number of nodal roots was lower in transgenics. At 50 dpv, the average number of nodal roots were 16, 10, and 11 in Golden Promise, *HvCsIF3-RNAi* and *HvCsIF9-RNAi*, respectively. The number of nodal roots is positively related to the number of tillers (Schneider et al., 2017). Thus, reduced tiller numbers in the transgenic plants resulted in less emergence of nodal roots. The most severe variation on the size of the root systems was observed from the 40 dpv plants, and the variation continued in the later stage of plant development.

At 50 dpv, the root system of Golden promise consisted of an average of 23 roots, while the *HvCsIF3-RNAi* and *HvCsIF9-RNAi* lines only had 15 and 17 roots, respectively. Not only

were the number of roots decreased, but root length was also significantly reduced. The WinRhizo root scanner was used to determine the total root length, total root surface area and average root diameters. Figure 5-4 A presents the total root length throughout plant development. The total root length of Golden Promise plants was between 1.5 to 2.6 and 1.3 to 1.7 folds higher than the *HvCsIF3-RNAi* and *HvCsIF9-RNAi* plants, respectively. Consequently, the root fresh weight and total root surface area showed a similar level of variation (Figure 5-4 B, C). In addition, the different root classes were separately measured based on the root diameters, including seminal roots, nodal roots, lateral roots and fine lateral roots. Despite a reduced root system in the transgenic plants, the root classification based on the diameters revealed that the ratios of each root type compared to the entire root system were not altered for individual plants (Figure 5-4 D). This suggests that the reduction of root development in transgenic barley plants is due to a general limitation rather than to defects in a specific root type. Root classification also indicated that the lateral and fine lateral roots are the main root types that contributed to root length and surface area. At 10 dpv, roots at 0-0.1 mm (fine lateral root) and 0.1-0.2mm (lateral root) contributed nearly 40% of total root length. This ratio increased significantly to 78% and 80% at 20 dpv and 30 dpv, respectively. After peaking at 30 dpv, a slight decrease brought the ratio down to 65% at 40 and 50 dpv. Notably, fine lateral roots were the major root class at 20 and 30 dpv, whereas lateral roots were more abundant at 10, 40, and 50 dpv.

Decreased *CsIF* gene expression affects the plant transpiration rate

No significant variation was observed in photosynthetic rate among the different genotypes across different time points over the vegetative stage (Figure 5-5 A). This indicates that the changes in shoot morphology induced by *HvCsIF3* and *HvCsIF9* gene expression had no impact on plant photosynthesis. The photosynthetic rate decreased similarly in all three genotypes, with the highest photosynthetic rate observed at 10 dpv, followed by a gradual reduction throughout

plant development.

Notably, the transpiration rate showed variations between Golden Promise and the transgenic plants (Figure 5-5 B). The transpiration rates of the transgenic lines were relatively stable, in the range of 2.5-3.4 mmol H₂O m⁻²s⁻¹, while the rates in Golden Promise fluctuated from 2.9 to 4.2 mmol H₂O m⁻²s⁻¹. Consistent with these measurements, stomatal conductance in the transgenics was lower than in Golden Promise (Figure 5-5 C). However, the variations were less severe than for the transpiration rates. The decreased stomatal conductance reveals that leaves from the *HvCsIF3-RNAi* and *HvCsIF9-RNAi* plants may reduce their transpiration rates by altering the status of stomata in response to the changes in root architecture. Additional parameters including intercellular and ambient CO₂ concentration, relative humidity, were also measured and no significant differences were observed among the genotypes (data not shown).

Golden Promise, *HvCsIF3* and *HvCsIF9* knock-down plants have uniform ionic profiles

Despite the distinct morpho-physiology features, no significant variations were observed in the shoot ionic profiles of the three genotypes (Figure 5-6). Phosphorus concentration remained at a stable level (6-7 g/kg) until 30 dpg, followed by a reduction to 5.3-6 g/kg at 40 dpg and recovery to higher level at 50 dpg (8-9 g/kg). The potassium concentration followed a trend similar to that of phosphorus. The shoot potassium concentration increased from approximately 65-80 g/kg at the initial stages of development to 90-96 g/kg at 50 dpg (Figure 5-6 B). Furthermore, the concentrations of phosphorus and potassium were higher in stems than leaves (data no shown). At 50 dpg, the stems contained approximately 20% and 30% more phosphorus and potassium than the leaves, respectively. The nitrogen and carbon content represent the level of proteins and organics in the plants. The concentrations of both these elements were measured on 20 to 50 dpg samples, while 10 dpg plants were excluded due to the limited amount of available plant material. Nitrogen and carbon concentrations remained at

Chapter 5 – Knock-down of *HvCsIF3* and *HvCsIF9* gene expressions in barley is predicted to increase plant tolerance to low nutrient stresses over the vegetative stage

a stable level (4.9-5.9 % and 32-42 %, respectively) throughout the vegetative stage in all three genotypes (Figure 5-6 C, D). The profiles of Ca, Mg, Zn, Cu, Fe and S in the three genotypes were similar (Figure S5-2). In addition, the grain ionic profiles revealed no difference among the three genotypes. An average of 6452 mg/kg phosphorus and 11629 mg/kg potassium were detected in the mature barley grains. Carbon comprised approximate 42% of the total grain weight. However, the proportion of protein (N) showed variation between the three genotypes, with 13.7% found in Golden Promise and *HvCsIF3-RNAi* grains, but only 10.2% in the grains of *HvCsIF9-RNAi*.

***In silico* evaluation of the barley genotypes over optimal nutrient supply**

Simulated 50-day old root system architectures of the three genotypes are depicted in Figure 5-7A. The videos showing the simulated root development are available in supplementary material (Figure 5-V1, V2). Figures 5-7 B, C, D compare the simulated results with the actual observations, which includes total root length, leaf area, and shoot dry weight. The predicted data are in good agreement with the observed data, thus indicating the accuracy of the optimised OSR/barley. Under the Roseworthy environmental conditions with optimal soil nutrient supply, the uptake of N, P and K is predicted to vary among the transgenic and reference (Golden promise) genotypes (Figure 5-8). Until 30 dpv, *HvCsIF3-RNAi* and *HvCsIF9-RNAi* plants showed slightly less water and nutrient uptake than Golden Promise. These variations were higher during the later stages of vegetative growth. Over the entire simulation (50 d), the Golden Promise plants took up a total of 642 cm³ of water, which was 2.2 and 1.5-fold higher than *HvCsIF3-RNAi* and *HvCsIF9-RNAi* plants, respectively (Figure 5-8 A). This indicates that the transgenic plants had decreased ability to capture water compared to Golden Promise throughout vegetative development, which is consistent with the transpiration rate measured on the glasshouse grown plants. Among the nutrients, the strongest difference was predicted for N uptake (Figure 5-8 B). At 50 dpv, N uptake by Golden Promise plants was

7567 μmol , whereas *HvCsIF3-RNAi* and *HvCsIF9-RNAi* plants showed 5250 and 5649 μmol , respectively. The P uptake by Golden Promise at 50 dpg was 366 μmol , which was approximately 1.4-fold more than *HvCsIF3-RNAi* and *HvCsIF9-RNAi* plants at the same developmental stage (Figure 5-8 C). The least effect was observed on K uptake, which ranged from 1062-1215 μmol at 30 dpg and 3441-3946 μmol at 50 dpg (Figure 5-8 D).

***In silico* evaluation of the barley genotypes under different combinations of NPK supply**

In a factorial design fashion, all three genotypes were simulated in different combinations of high, medium and low NPK supply, to assess their behaviour under simultaneous stresses of more than one nutrient. Figure 5-9 and Table 5-1 summarise the leaf area (A), shoot dry weight (B), total root length (C), and root dry weight (D) at 50 dpg. Overall, the negative impact of nutrient stress was larger in the wild type barley than the transgenic genotypes. Out of the three nutrients, when under single nutrient stress, P stress resulted in the strongest negative effects on plant growth. Under the low P condition, the shoot dry weight of all the three genotypes was predicted to be very low and ceased to increase after 25 dpg. At 50 dpg, the shoot dry weight and leaf area was 0.1 g and 25 cm^2 under low P condition, which were equivalent to 18-22 dpg plants grown under optimal nutrient condition.

Under medium N stress, the leaf area and shoot dry weight of Golden Promise decreased by 44-46%, whereas *HvCsIF3-RNAi* plants were not affected, and *HvCsIF9-RNAi* plants showed an 11-12% reduction. Under the low N stress, significant reductions in leaf area and shoot dry weight were observed, with a 77%, 42%, and 62% reduction compare with high N in Golden Promise, *HvCsIF3-RNAi* and *HvCsIF9-RNAi*, respectively. Less severe reduction in the total root length and root dry weight was observed under low N stress. Similar trends were observed in K stress conditions. In addition, simulations predicted the daily root water uptake throughout the plant development (Figure 5-10). Plants grown under medium K and N

conditions showed no effect (*HvCsIF3-RNAi* and *HvCsIF9-RNAi*) or minor effect (Golden Promise) on root water uptake compare with optimal condition. The water uptake was predicted to be severely reduced only under low nutrient conditions (NPK).

In addition, the shoot dry weight was analysed on the basis of combinations of NPK stress. The shoot dry weight of the three genotypes under different combinations of soil NPK supply are presented in Table 5-2. The percentages of shoot dry weight relative to the optimal condition for individual genotypes are presented in Table 5-3. The highest shoot dry weight was observed in Golden Promise with optimal nutrient supply, with about 2.2 g at 50 dpv. The lowest shoot dry weight for all three genotypes was found under the low P stress, regardless of the availability of N and K. These plants showed generally less than 0.1 g of shoot dry weight, accounting for 4-5%, 12%, and 7-8% of the data under optimal nutrient condition for Golden Promise, *HvCsIF3-RNAi*, and *HvCsIF9-RNAi* plants, respectively. Plants grown under medium P stress (regardless of the N and K supplements) and optimal P condition with low N availability are predicted to have moderate shoot dry weight, ranging from 0.4 to 0.7 g at 50 dpv regardless of the genotypes. Under medium N and P conditions, medium K availability did not result in decreased shoot dry weight compared with the simulations under optimal K application (Golden Promise, 0.75 g; *HvCsIF3-RNAi*, 0.45 g; *HvCsIF9-RNAi*, 0.50 g). Only under low K availability, severe reductions in shoot dry weight were observed (Golden Promise, 0.55 g; *HvCsIF3-RNAi*, 0.40 g; *HvCsIF9-RNAi*, 0.41 g). For the transgenic plants under sufficient P availability, the shoot dry weight was not affected under medium N and K stresses. These data contrasted with Golden Promise, which showed 57% reduction in shoot dry weight under medium N and K conditions. These results suggest a higher sensitivity of Golden Promise to soil N and K contents. Under the optimal N but P stressed conditions, none of the different K concentrations tested had any effect on the shoot dry weight for the three genotypes. These results indicate that the transgenic plants respond to NPK stresses in a different way from Golden Promise.

Discussion

The *Csl* genes affect barley root and shoot growth over the vegetative development stage

In the present study, phenotypes of the reference barley cultivar Golden Promise and the RNAi knock-down lines of *HvCsIF3* and *HvCsIF9* were obtained in a soil environment for both shoots and roots over 10-day intervals across the vegetative stage (i.e. 50 dpv). Plants grown in soil generally develop a more extensive root system compared to hydroponics, due to the uneven water and nutrients distribution in soil environments that require roots to expand more to support plant development (Mian et al., 1993; Tavakkoli et al., 2010). The Golden Promise genotype used in this study reached a total seminal root length of 600-800 cm at 50 dpv, which is slightly longer than that reported in a previous hydroponic study by Liu (2018), who reported a total seminal root length of approximately 420 cm at 53 dpv. Furthermore, the total root length of soil grown plants increased at a slower rate during the initial stages (0-30 dpv) and became more rapid towards the end of vegetative development. This also contrasts with the observations from hydroponically grown plants, which showed greater elongation at early stages and relatively stable status from 39 dpv onwards (Liu, 2018). These differences confirm that it is important to consider the suitability of the growth media depending on the requirements of the study.

Importantly, the total root length of the soil-grown *HvCsIF3-RNAi* and *HvCsIF9-RNAi* plants was reduced compared to that of Golden Promise. This indicates the effects of *HvCsIF3* and *HvCsIF9* genes on root elongation are likely to be maintained past the seedling stage and throughout plant development. This is different from the previous report on restricted root development of rice *str5* mutant that was limited to seedling stage (Yao et al., 2002). Notably, the impacts on *HvCsIF3-RNAi* and *HvCsIF9-RNAi* on root development were not restricted to a certain root class. Although we observed less nodal roots in the transgenic plants, this is the

consequence of less tiller developed in the transgenic plants, thus, less emergence of nodal roots (Schneider et al., 2017). Even though no study has explored the expression of *HvCslF3* and *HvCslF9* in other root classes, except for seminal roots, our results indicate the potential of *HvCslF3* and *HvCslF9* to regulate the meristems of later emerged root classes, including nodal roots, lateral roots, and fine lateral roots. Our previous study (Chapter 3) revealed the specific expression of *HvCslF3* in the elongation zone of the root, while the expression of *HvCslF9* is more broadly detected in the meristem and elongation regions. Interestingly, the reduction in root system was more severe in the *HvCslF3-RNAi* plants, consistent with our previous measurement of root elongation rate in barley seedlings and suggesting that this member of the *CslF* family fulfils a particularly important role during root growth.

Compared to Golden Promise, the *HvCslF3-RNAi* and *HvCslF9-RNAi* plants produced significantly reduced plant weight, leaf area, leaf and tiller numbers. This is despite almost ubiquitous expression of the *CslF6* gene, which encodes the main determinant of (1,3;1,4)- β -glucan biosynthesis in barley (Burton et al., 2011; Taketa et al., 2011), wheat (Nemeth et al., 2010) and rice (Vega-Sánchez et al., 2012). Curiously, the barley *HvCslF6* mutant only develops slightly shorter shoots at maturity (Tonooka et al., 2009), and rice *OsCslF6* mutants exhibit decreased plant height, internode length and stem diameter (Vega-Sánchez et al., 2012). These defects were related directly to altered cell wall (1,3;1,4)- β -glucan accumulation in the shoot. Both *HvCslF3* (HORVU2Hr1G042350) and *HvCslF9* (HORVU1Hr1G022900) are known to be expressed in barley roots and developing embryo (Colmsee et al., 2015), while *HvCslF9* transcripts are also found in developing inflorescences and grain (Burton et al., 2011). However, neither of these genes are expressed in vegetative tissues. Therefore, despite the possibility of protein transportation within plants, phenotypes in the transgenic *HvCslF3-RNAi* and *HvCslF9-RNAi* plants are likely to be the consequence of the alterations in root growth.

The regulatory mechanisms of *HvCslF3* and *HvCslF9* function *in vivo* remain ambiguous.

Research suggests the involvement of *HvCslF3* in (1,4)- β -linked glucoxyylan accumulation via heterologous overexpression in tobacco leaves (Little et al., 2019) and knockdown of *HvCslF3* in root tips of *HvCslF3-RNAi* lines (Chapter 3). Interestingly, (1,4)- β -linked glucoxyylan was detected in other barley tissues that lack *HvCslF3* expression (Little et al., 2019). This suggests (1,4)- β -linked glucoxyylan biosynthesis is complex and possibly involves additional genes. Whether the *HvCslF3-RNAi* plants accumulate (1,4)- β -linked glucoxyylan in aerial organs requires further study. In contrast to *HvCslF3*, *CslF9* is hypothesized to participate in (1,3;1,4)- β -glucan biosynthesis in barley (Burton et al., 2008) and wheat grain (Cseh et al., 2013). However, no additional (1,3;1,4)- β -glucan accumulation was observed in barley plants overexpressing *HvCslF9*, which also appeared phenotypically normal (Burton et al., 2011). Our previous immunolabelling studies indicated a specific lack of (1,3;1,4)- β -glucan in root tips from *HvCslF9-RNAi* plants (Chapter 3). It is therefore possible that this localised function of *HvCslF9* in (1,3;1,4)- β -glucan biosynthesis explains the broader vegetative phenotypes observed in the *HvCslF9-RNAi* lines. The similarities between the *HvCslF3-RNAi* and *HvCslF9-RNAi* lines may also suggest that any cell wall that contributes to altered elongation in these specific tissues may lead to similar overall vegetative defects.

The *HvCslF3-RNAi* and *HvCslF9-RNAi* plants show a reduction in transpiration and water uptake under optimal nutrient supply

One of the major functions of roots is to absorb water and nutrients from soil and transport the elements to the shoot, supporting plant development. The transgenic plants exhibited a smaller root system and lower surface area as compared to Golden Promise. One of the potential consequences of smaller root size and root depth is the limitation on water uptake (Penman, 1950; Bartens et al., 2009). Numerous studies have shown the positive relationship between root water uptake, plant transpiration and stomatal conductance. Bartens et al. (2009) concluded that the root water uptake can be affected by plant size, rooting depth and transpiration rate.

Studies in barley specifically measured the water uptake in different root regions and highlighted the maximum water uptake ability in young roots (Sanderson, 1983). Root length is essential for water uptake. In barley, the main axis located 10 cm away from the root tip is responsible for 50% of the water uptake, and once taken into account the lateral roots, this percentage increase to 75% of total water uptake (Sanderson, 1983). Under optimal glasshouse conditions, root water uptake was significantly reduced in the transgenic plants compared to the Golden Promise, throughout vegetative growth. The decreased transpiration rate and stomatal conductance also reflected the relationship between the reduced root system and root water uptake. Plants reduce transpiration to minimize water loss (Nilson and Assmann, 2007), while transpiration is essential to provide the driving force for water and nutrient transportation from the roots to the shoots (Chapin et al., 1998). Consistent with this, we also detected decreased stomatal conductance in the *HvCsIF3-RNAi* ($0.21 \text{ mol H}_2\text{O m}^{-2}\text{s}^{-1}$) and *HvCsIF9-RNAi* ($0.24 \text{ mol H}_2\text{O m}^{-2}\text{s}^{-1}$) plants compared with Golden Promise ($0.27 \text{ mol H}_2\text{O m}^{-2}\text{s}^{-1}$). These observations are consistent with the work of Knipfer et al. (2011) who reported the stomatal conductance to be approximately $0.25 \text{ mol H}_2\text{O m}^{-2}\text{s}^{-1}$ in wild type barley. The opening and closure of the stomata is one of the major methods for plants to regulate transpiration rate (Nilson and Assmann, 2007). In contrast to these transpiration traits, *HvCsIF3-RNAi* and *HvCsIF9-RNAi* plants showed no significant difference in photosynthetic rates compare with Golden Promise. This observation is consistent with a previous study in barley that suggested that plants maintain photosynthesis at normal levels under water shortage, but reduce stomatal conductance and hence transpiration to benefit the metabolism for plant growth (Robredo et al., 2007).

The OSR simulations predicted the performance of barley plants from three genotypes under the same environmental conditions and indicated lower root water uptake by *HvCsIF3-RNAi* and *HvCsIF9-RNAi* plants compared with Golden Promise throughout the entire

simulated period. To summarise the plant-environment interactions, we propose a model of regulation between root and shoot development, root water uptake, and transpiration (Figure 5-11). Elongation and branching are the two important determinants for root development. *HvCslF3* and *HvCslF9* expression directly regulates root elongation and alters root architecture. Root growth influences shoot growth and root-soil interaction, which includes water uptake. The shoot growth and root water uptake positively affect each other to maintain water use efficiency. The plant transpiration rate is regulated by the plant water content and stomatal opening and closure, which in turn affect the root water uptake to balance water transportation. Nutrient transfer from root to shoot is largely dependent on the transpiration force and water uptake (Knipfer and Fricke, 2010). With the negative effects on both elements, the shoots are likely to receive less nutrients, which ultimately result in nutrient deficiencies, hence, explaining the reduction in shoot dry weight and leaf area observed in both the glasshouse grown plants and in the OSR simulated plants.

Altered root system in the transgenic barleys may benefit nutrient uptake

Nutrient uptake can be directly or indirectly affected by water capture ability. For example, increased transpiration favours sodium uptake and negatively affects K uptake (Pitman, 1965), while the subsoil foraging root phenotypes that benefit N uptake also improve water capture (Lynch, 2018). Ionomics profiling of the shoot samples showed similar C, N, P and K concentrations in all three genotypes. No symptoms indicative of any micro or macro nutrients deficiency were detected in the transgenic plants (Figure 5-6). This indicates that the transport of nutrients from the roots to the shoots is not compromised *per se*.

Manipulating root architecture is one of the breeding approaches used to select plants with optimised nutrient uptake ability. Shallow roots are beneficial for P and K absorption, whereas deep and steep roots favour N and water uptake (Lynch, 2019). In maize, a reduced crown root

Chapter 5 – Knock-down of *HvCsIF3* and *HvCsIF9* gene expressions in barley is predicted to increase plant tolerance to low nutrient stresses over the vegetative stage

number benefits the acquisition of N under low soil N supply (Saengwilai et al., 2014). Furthermore, lower cortical cell file number and larger cortical cell size were predicted to improved N uptake in maize (Yang, 2017). These root traits have also been observed in the *HvCsIF3-RNAi* and *HvCsIF9-RNAi* plants (Chapter 3). This indicates that the root system of the transgenic barley presented in this study comprises traits that are potentially beneficial for N capture. Based on the modelling, the transgenic lines were predicted to have greater tolerance to NPK limitations compared to Golden Promise. These observations indicate the potential of genetically manipulating the root systems by modifying cell wall related genes and enzymes toward developing plant varieties requiring less fertilisers. Other traits that are known to improve N efficiency include steep root angle, less lateral root branching, more root hairs, increased cortical cell size, and root cortical senescence (Zhan and Lynch, 2015; Dathe et al., 2016; Schneider et al., 2017; Lynch, 2019). The root systems of our transgenic plants exhibit alteration in root hairs and lateral root branching densities. However, other anatomical traits of the transgenic root systems remain to be investigated.

Unlike water and nitrate, P and K are less mobile in soil and their bioavailability is mostly contributed from the release of plant residues in the topsoil (Lynch and Brown, 2001; Römheld and Kirkby, 2010). Studies on maize (Jia et al., 2018; Sun et al., 2018), barley (Schneider et al., 2017), and common bean (Miguel et al., 2013) have suggested root phenotypes, including increased axial roots, shallower axial root angles, larger occurrences of lateral root branching, root cortical aerenchyma and senescence, and greater root hair production are the ideal traits for breeding P and K efficient plants (Lynch, 2019). Soil nutrients are absorbed laterally across the root segments through cell-to-cell or diffusion pathways; thus, root thickness acts as an important determinant for nutrient acquisition in plants. Longer and thinner roots were observed to be more efficient in N capture (Eghball and Maranville, 1993). Root thickness is defined by the aggregate of different phenes (units of plant phenotypes that interact to affect resource

acquisition) namely cortical cell size, cortical cell file number, and stele diameter (York et al., 2013; Lynch, 2019). In general, thinner roots could be a useful adaptation in response to nutrient stresses, while trading-off with carbon cost of root formation and maintenance and soil hardness. Interestingly, phenes leading to thinner roots were observed in our transgenic plants examined here (Chapter 3, changes on cortical cell file layers). The roots of *HvCslF3-RNAi* and *HvCslF9-RNAi* transgenic plants contain reduced cortical cell file numbers and altered cell wall composition (Chapter 3). Based on these observations, the root density (i.e. root weight per unit area of root) parameter in the model was lowered for the transgenic plants while optimising the model for root dry weight and total root length. In response to different combinations of soil NPK supply, the model predicted better performance of the transgenic plants under medium P stress in compare with high P conditions. These observations indicated the thinner roots developed in the transgenic plants improve P uptake under moderate nutrient stress conditions.

P capture from soil is also largely dependent on root hairs, whose development is genetically associated with P utilisation from soil (Jungk, 2001; Lynch, 2019). Roots with longer and denser root hairs are able to capture more P from the soil by increasing the root surface area (Wen and Schnable, 1994; Zhu et al., 2010; Miguel et al., 2015). Our previous findings have highlighted the important roles of the *HvCslF3* and *HvCslF9* genes in root hair development (Chapters 3 and 4). Heterologous expression of *HvCslF3* in *Arabidopsis* resulted in extra root hair formation and longer root hairs (Chapter 4). Roots of the *HvCslF3-RNAi* and *HvCslF9-RNAi* plants exhibited reduced root hairs (Chapter 3). However, the current OSR model has simplistic module for root hair parameterisation, which is not ideal to examine the root hair traits. To further prove the importance of root hair development in P capture *in silico*, further parameterisation of the model is needed. Despite the importance of root hairs, root traits that reduce the metabolic cost of soil exploration are also important for P uptake. *In silico* studies on maize and barley have demonstrated the cortical aerenchyma and senescence are

beneficial for plant growth under P stresses (Postma and Lynch, 2011; Schneider et al., 2017). However, further studies are required to explore these traits in our three genotypes.

The simulations also predicted larger effects on shoot growth of Golden Promise plants in response to nutrient stresses. Less severe influences on shoot development under limited nutrient availabilities were predicted for *HvCsIF3-RNAi* and *HvCsIF9-RNAi* plants with altered root architecture. The transgenic plants developed less tillers which in turn decreased the nutrient requirement from the roots. Under optimal nutrient conditions, Golden Promise plants can capture enough nutrients to support the development of tillers. However, under low nutrient supply, tiller formation gets traded-off for root growth, and results in restrictions on aerial organ growth, especially in the later development stages. To support this, the simulations also predicted the alterations in root dry weight (Table 5-S2, S3). Especially in the *HvCsIF3-RNAi* plants, which develop fewest tillers, the root dry weight of plant simulated under the least nutrients was 84% of the one under the optimal condition.

In field conditions, plant development is determined by the interaction and cooperation of many phenes. The simulation studies predicted that the changed root architecture caused by down-regulation of *HvCsIF3* and *HvCsIF9* results in plants that are more tolerant to suboptimal soil nutrient conditions. This is likely to be the potential trade-offs between the decreased root density, fewer root number, and deeper roots. In the current simulations, the transgenic plants develop thinner roots that lead to spare carbon resources. This results in the simulated transgenic plants investing additional carbon resources into root length that leading to deeper root systems (Figure 5-7 A). However, other potential trade-offs of *HvCsIF3* and *HvCsIF9* down-regulation are poorly understood. The reduced root volume may have other negative influences for the fitness of plant. This includes negative effects on the ability to anchor plants, reduced soil exploration, altered defense against pathogens, and altered tolerance to toxic ions under salinity conditions (Schneider et al., 2017; Schneider et al., 2017). These potential effects

together with xylem number and soil impedance were not considered in the present OSR models, hence it is difficult to predict the potential influences on the conclusions. However, studies on various crop species have concluded that the phenes save the metabolic cost of soil exploration are prioritized in plant breeding based on modelling and field studies (Lynch, 2019). The *in silico* results from the present study indicated that the phenotypic changes brought by down-regulation of *HvCslF3* and *HvCslF9* genes may be beneficial under nutrient deficient soils, including limited availability of N, P and K. Plant growth was simulated for 50 d to study the vegetative plant development. To further analyse the effects of *HvCslF3* and *HvCslF9* in later developmental stages, extending OSR to represent plant reproduction and grain properties are needed to simulate the full plant life cycle.

In conclusion, the lack of understanding about the genetic control of root phenotypes has limit the possibilities for genomic selection in plant breeding. In the present study, we have highlighted the importance of two cell wall-related genes, *HvCslF3* and *HvCslF9*, during root development, particularly over the plant's vegetative growth stage. By down-regulating these genes, plants exhibited restricted root system development, which in turn negatively affected shoot growth, water and nutrient uptake. Furthermore, we utilised *OpenSimRoot* and show the adaptability of the model to different soil-climate conditions and genotypes. By optimising the physiological parameters of the three genotypes, we successfully demonstrated that the utilisation of *OpenSimRoot* to predict mutant phenotypes is a valid approach. The quantitative simulations have highlighted the better performance and tolerance of transgenic plants than Golden Promise in response to different combinations of NPK stresses. These observations raise the possibility of breeding nutrient-efficient crops by manipulating the expression of cell wall-related genes and the composition of plant cell walls. Although studies of root phenotypes in the natural soil environment are still required, the *OpenSimRoot* modelling platform provides a valuable approach to analyse the feedback between genetically controlled phenotypes and

Chapter 5 – Knock-down of *HvCsIF3* and *HvCsIF9* gene expressions in barley is predicted to increase plant tolerance to low nutrient stresses over the vegetative stage

plant responses to the environment.

Figures

Golden promise *HvCsIF3*-RNAi *HvCsIF9*-RNAi

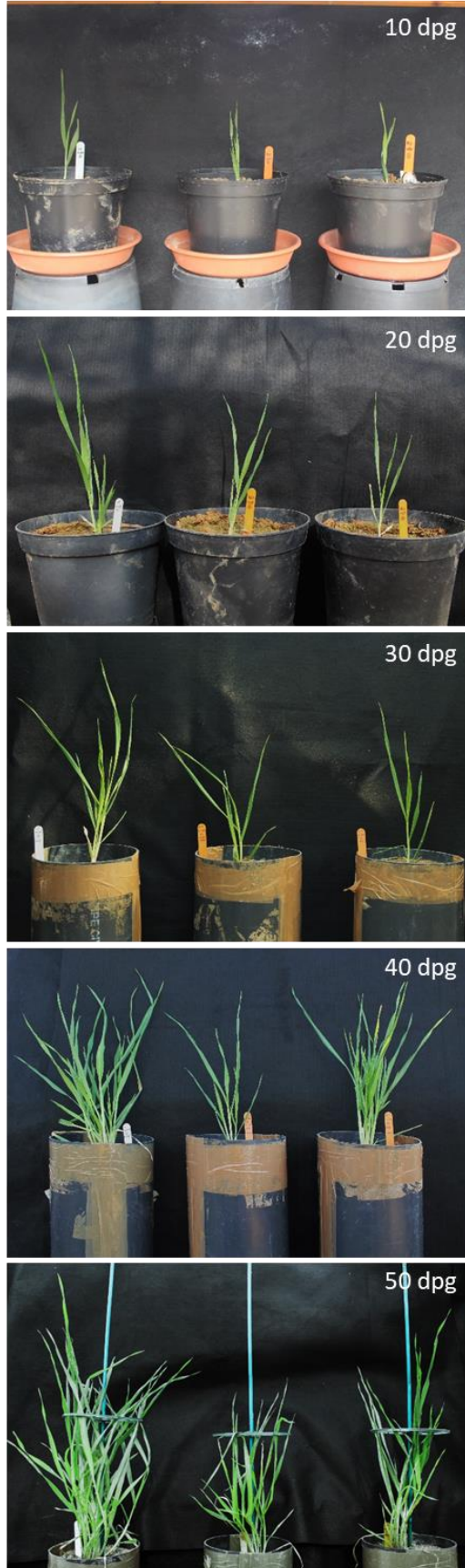


Figure 5-1. Shoot development of Golden Promise, *HvCsF3-RNAi*, and *HvCsIF9-RNAi* plants over vegetative growth (10, 20, 30, 40 and 50 dpg). Plants were pre-germinated before being trans-potted into sandy-loam soil supplemented with fertilizers. The shoot morphological and physiological traits were collected over each time point, including height, weight, tiller and leaf numbers, leaf area, chlorophyll content, photosynthetic rate, transpiration rate, and stomata conductance. The *HvCsIF3-RNAi* and *HvCsIF9-RNAi* plants exhibited shorter and smaller phenotype throughout the vegetative development. The photographs shown represent the average of at least six replicates.

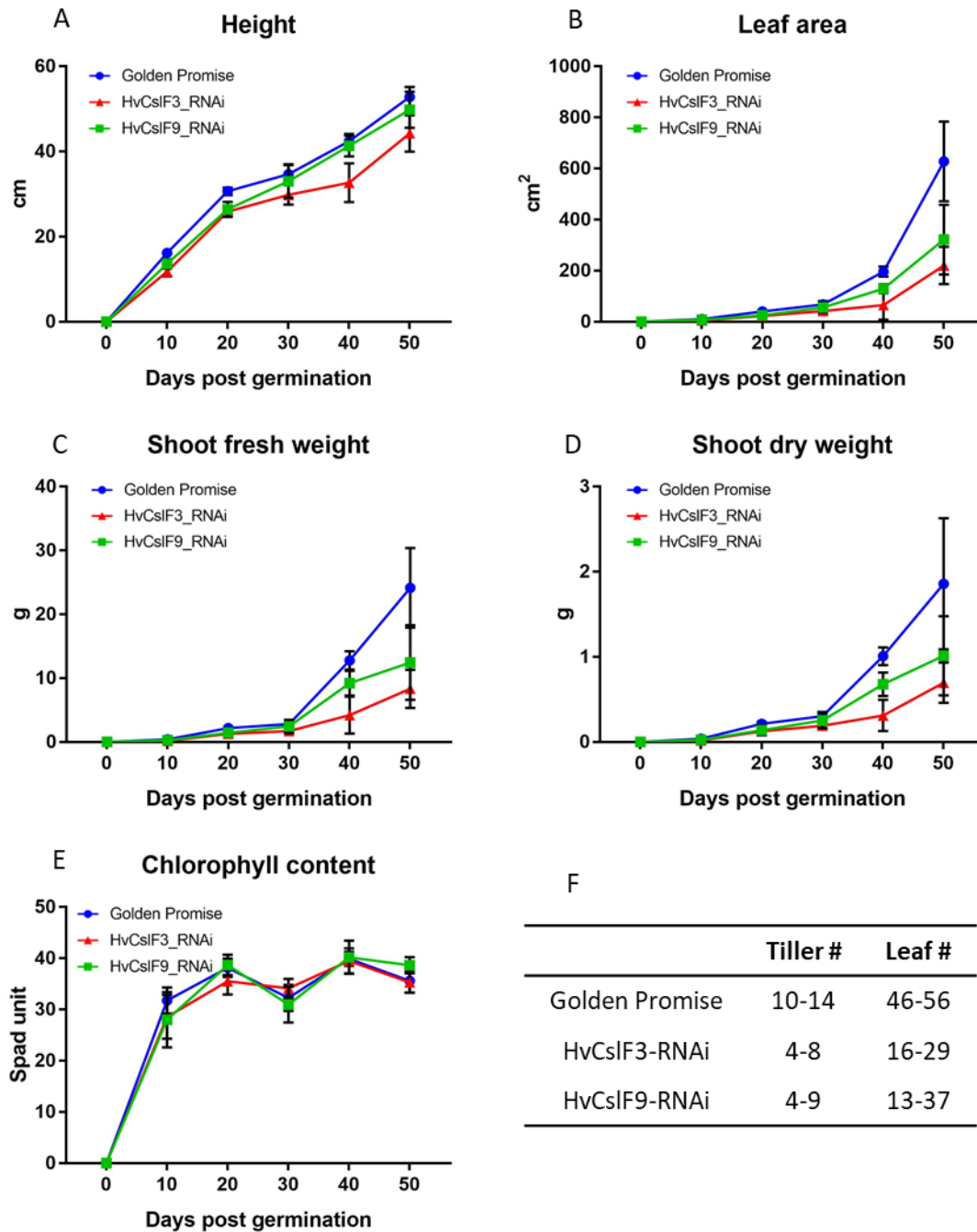


Figure 5-2. Quantitative analysis of barley shoot development during vegetative growth. A, height of the plants. *HvCslF3-RNAi* showed significant reduction compared with Golden Promise, especially in the later development stages. At 50 dpv, *HvCslF3-RNAi*: $P < 0.0001$, *HvCslF9-RNAi*: $P = 0.0623$. B, leaf area was measured using the LI-3100 area meter. The leaf area increased gradually during early development, and the rate increased rapidly from 30 dpv onwards. Golden Promise showed larger leaf area than both transgenic plants. At 50 dpv, *HvCslF3-RNAi*: $P < 0.0001$, *HvCslF9-RNAi*: $P < 0.0001$. C and D, fresh and dry weight of shoots.

Chapter 5 – Knock-down of *HvCsIF3* and *HvCsIF9* gene expressions in barley is predicted to increase plant tolerance to low nutrient stresses over the vegetative stage

The changes in shoot weight follow a similar trend as the leaf area. The water content was calculated from fresh and dry shoot weight; shoot water content is at approximately 89-92%. *HvCsIF3-RNAi* and *HvCsIF9-RNAi* plants exhibited 1/3 and 1/2 of Golden Promise fresh shoot weight at later development stage. At 50 dpg, *HvCsIF3-RNAi*: $P < 0.0001$, *HvCsIF9-RNAi*: $P < 0.0001$. E, the average chlorophyll content of leaves. Data are expressed in Spad units. At 50 dpg, *HvCsIF3-RNAi*: $P = 0.9738$, *HvCsIF9-RNAi*: $P = 0.0819$. F, quantified tiller and leaf number at 50 dpg. *HvCsIF3-RNAi* and *HvCsIF9-RNAi* comprise significant lower number of tillers and leaves. For tiller number, at 50 dpg, *HvCsIF3-RNAi*: $P < 0.0001$, *HvCsIF9-RNAi*: $P = 0.0025$. For leaf number, at 50 dpg, *HvCsIF3-RNAi*: $P < 0.0001$, *HvCsIF9-RNAi*: $P < 0.0001$. Error bars indicate standard deviation. See Table 5-S1 for full statistical analysis.

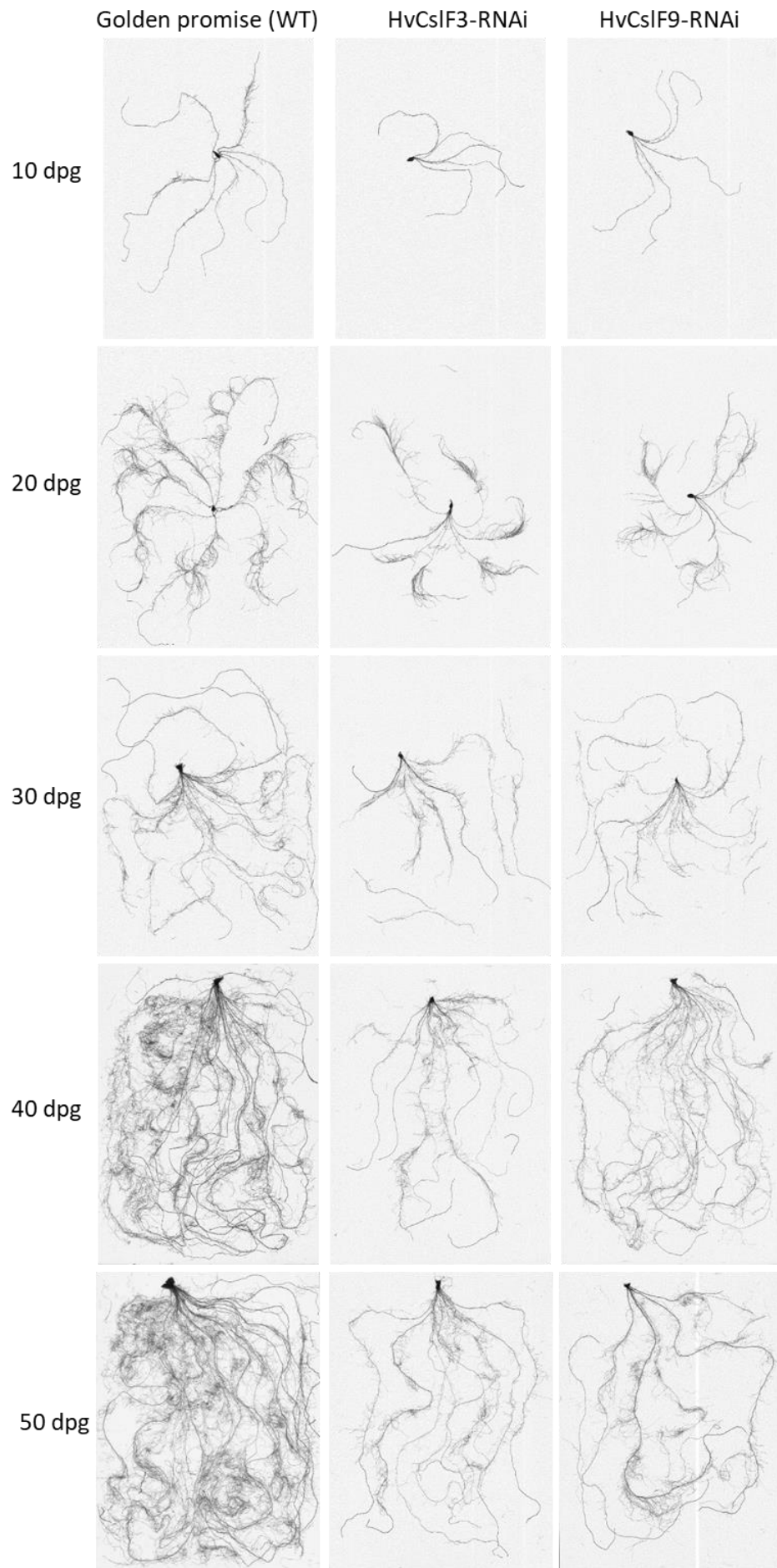


Figure 5-3. Root systems of Golden Promise, *HvCsIF3-RNAi*, and *HvCsIF9-RNAi* plants.

All root materials were extracted from the soil, preserved in 30% ethanol (v/v) before being imaged using WinRhizo root scanner. Golden Promise plants exhibited significant larger root systems compare with the *HvCsIF3-RNAi* and *HvCsIF9-RNAi* plants over all time points. Root number, length, surface area, branching density were measured based on the scanned root photographs. The photographs shown represent the average of at least six replicates.

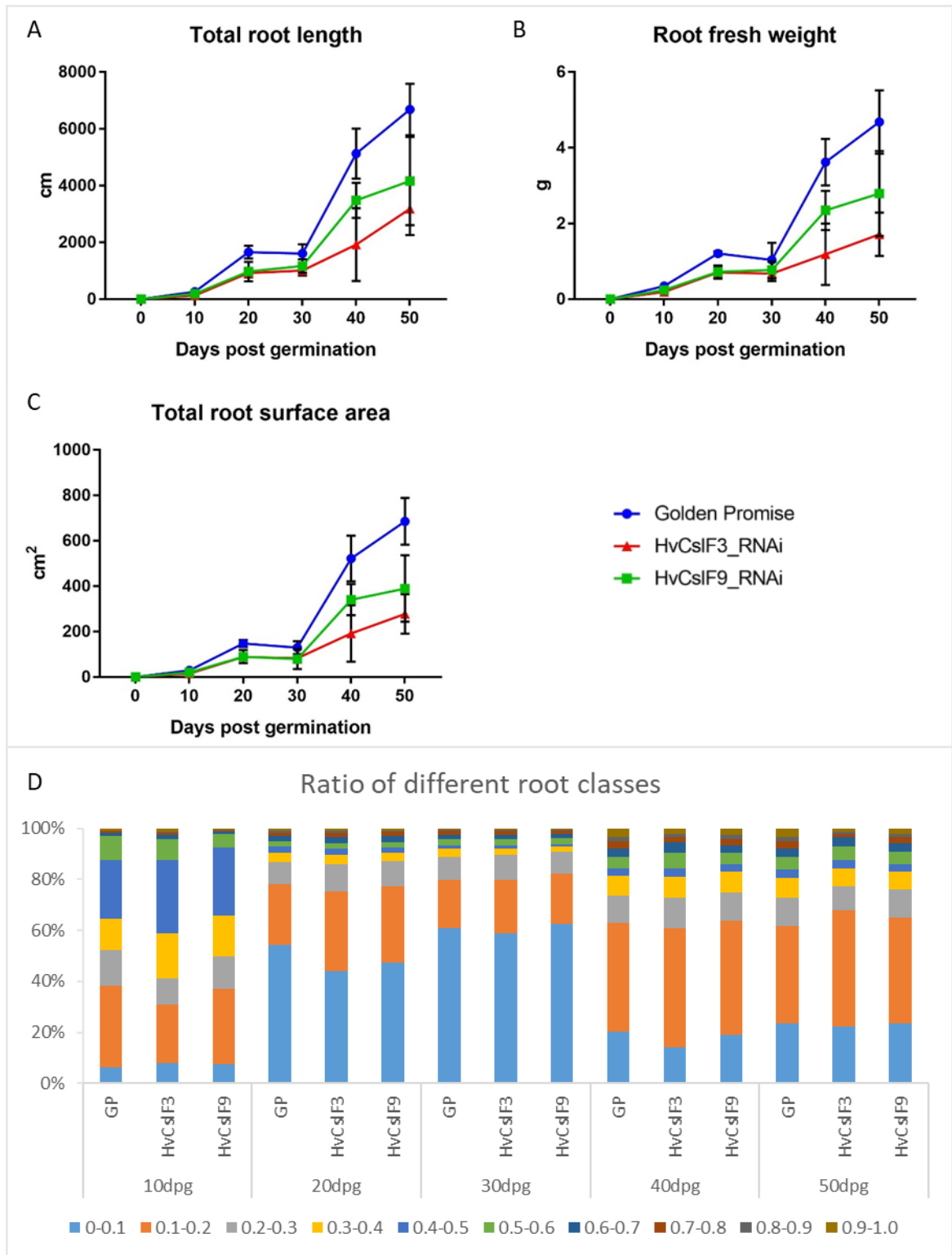


Figure 5-4. Quantitative analysis of barley root development during the vegetative growth.

A, the total root length. At 50 dp, *HvCslF3*-RNAi: $P < 0.0001$, *HvCslF9*-RNAi: $P < 0.0001$. B, the fresh root weight. At 50 dp, *HvCslF3*-RNAi: $P < 0.0001$, *HvCslF9*-RNAi: $P < 0.0001$. C, the total root surface area. At 50 dp, *HvCslF3*-RNAi: $P < 0.0001$, *HvCslF9*-RNAi: $P < 0.0001$. D, ratio of

Chapter 5 – Knock-down of *HvCsIF3* and *HvCsIF9* gene expressions in barley is predicted to increase plant tolerance to low nutrient stresses over the vegetative stage

different root classes based on root diameter. Golden Promise plants showed larger root systems than the *HvCsIF3-RNAi* and *HvCsIF9-RNAi* plants throughout the plant vegetative development. With reduced root systems, the ratio of different root classes was not affected. Roots of 0-0.1 mm diameter contributed to most of the total root length at 20 and 30 dpg. Roots of 0.1-0.2 mm diameter were the major root class at later stages of plant development. Error bars indicate standard deviation. See Table 5-S1 for full statistical analysis.

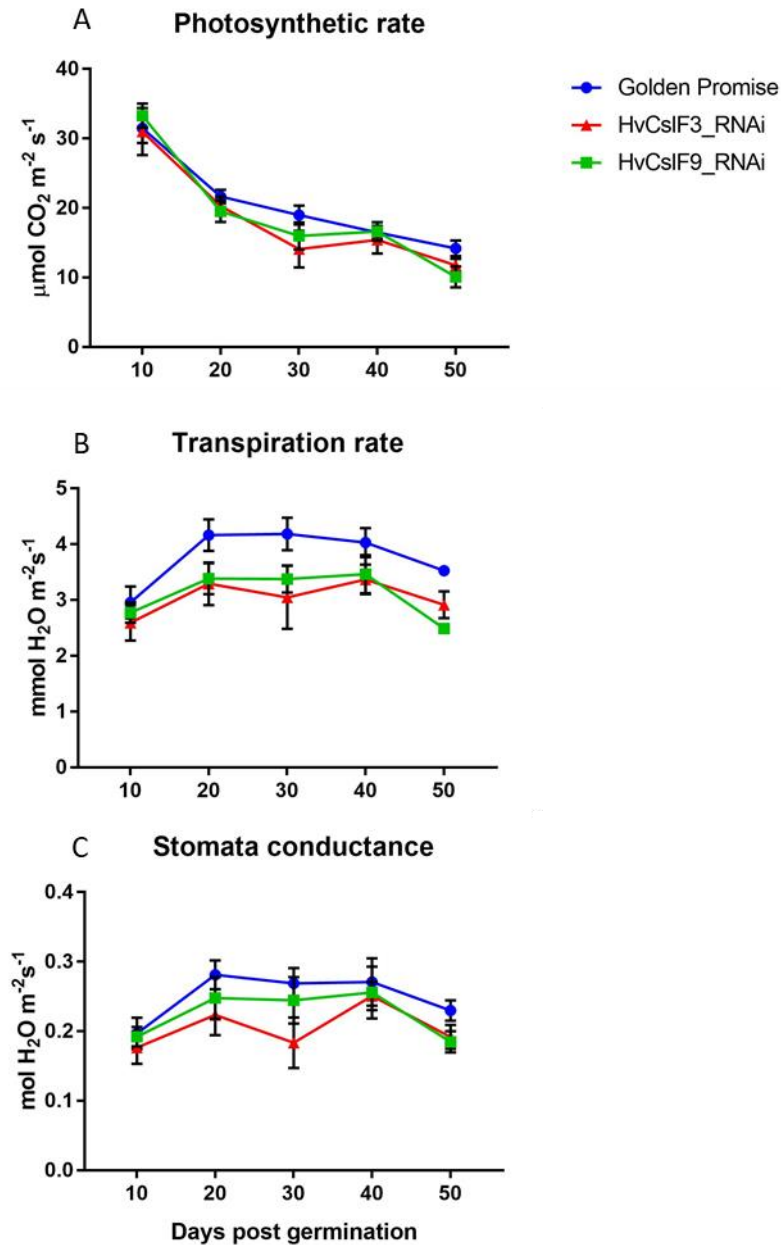


Figure 5-5. Photosynthetic rate (A), transpiration rate (B), and stomata conductance (C) of Golden Promise, *HvCsiF3*-RNAi and *HvCsiF9*-RNAi plants throughout vegetative growth. Data were obtained from young leaves using Licor LI6400Xt equipped with a leaf chamber fluorometer. A, the three genotypes showed similar photosynthetic rates throughout plant development, with a negative correlation as plants reach maturation. At 50 dpg, *HvCsiF3*-RNAi: P=0.0392, *HvCsiF9*-RNAi: P=0.0003. B, the transpiration rates were low at 10 dpg, and increased to a stable level from 20 dpg to 50 dpg. *HvCsiF3*-RNAi and *HvCsiF9*-RNAi plants

Chapter 5 – Knock-down of *HvCsIF3* and *HvCsIF9* gene expressions in barley is predicted to increase plant tolerance to low nutrient stresses over the vegetative stage

showed lower transpiration rates. At 50 dpv, *HvCsIF3-RNAi*: $P=0.0012$, *HvCsIF9-RNAi*: $P<0.0001$. Similar trends were observed in stomata conductance (C), except that the reduction in *HvCsIF3-RNAi* and *HvCsIF9-RNAi* plants was not as severe as for the transpiration rates. Error bars indicate standard deviations. At 50 dpv, *HvCsIF3-RNAi*: $P=0.0241$, *HvCsIF9-RNAi*: $P=0.0067$. See Table 5-S1 for full statistical analysis.

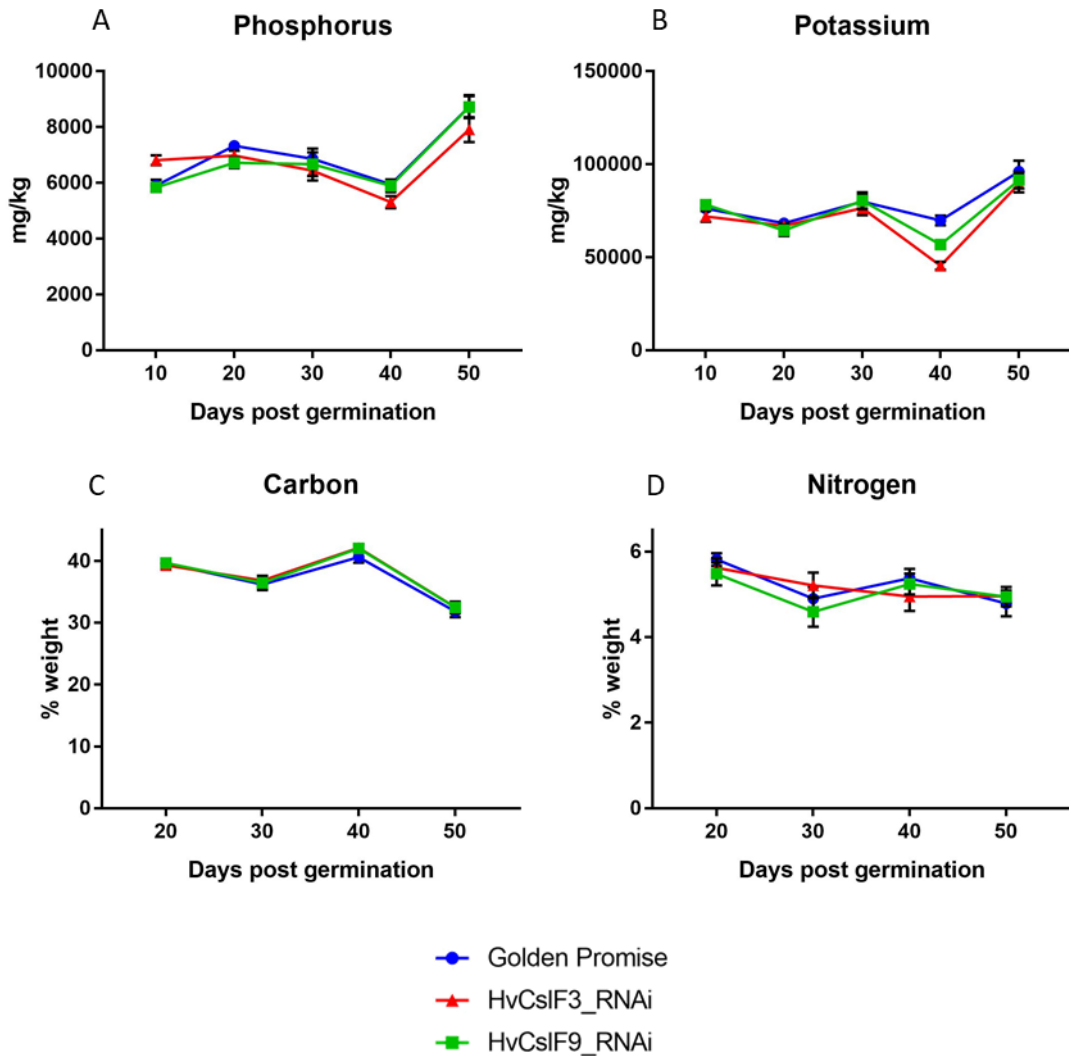


Figure 5-6. Quantification of Phosphorus (A), Potassium (B), Carbon (C), and Nitrogen (D) in dry leaves samples of Golden Promise, *HvCslF3*-RNAi, and *HvCslF9*-RNAi plants.

No significant difference was observed in the nutrient concentrations between the three genotypes, except for the P concentration of *HvCslF3*-RNAi, indicating the ability of nutrient uptake and transportation to aerial organs was not changed. Error bars indicate standard deviations. P, at 50 dpv, *HvCslF3*-RNAi: $P < 0.0001$, *HvCslF9*-RNAi: $P = 0.9972$. K, at 50 dpv, *HvCslF3*-RNAi: $P = 0.0022$, *HvCslF9*-RNAi: $P = 0.0344$. C, at 50 dpv, *HvCslF3*-RNAi: $P = 0.3943$, *HvCslF9*-RNAi: $P = 0.4566$. N, at 50 dpv, *HvCslF3*-RNAi: $P = 0.2407$, *HvCslF9*-RNAi: $P = 0.2787$. See Table 5-S1 for full statistical analysis.

Chapter 5 – Knock-down of *HvCslF3* and *HvCslF9* gene expressions in barley is predicted to increase plant tolerance to low nutrient stresses over the vegetative stage

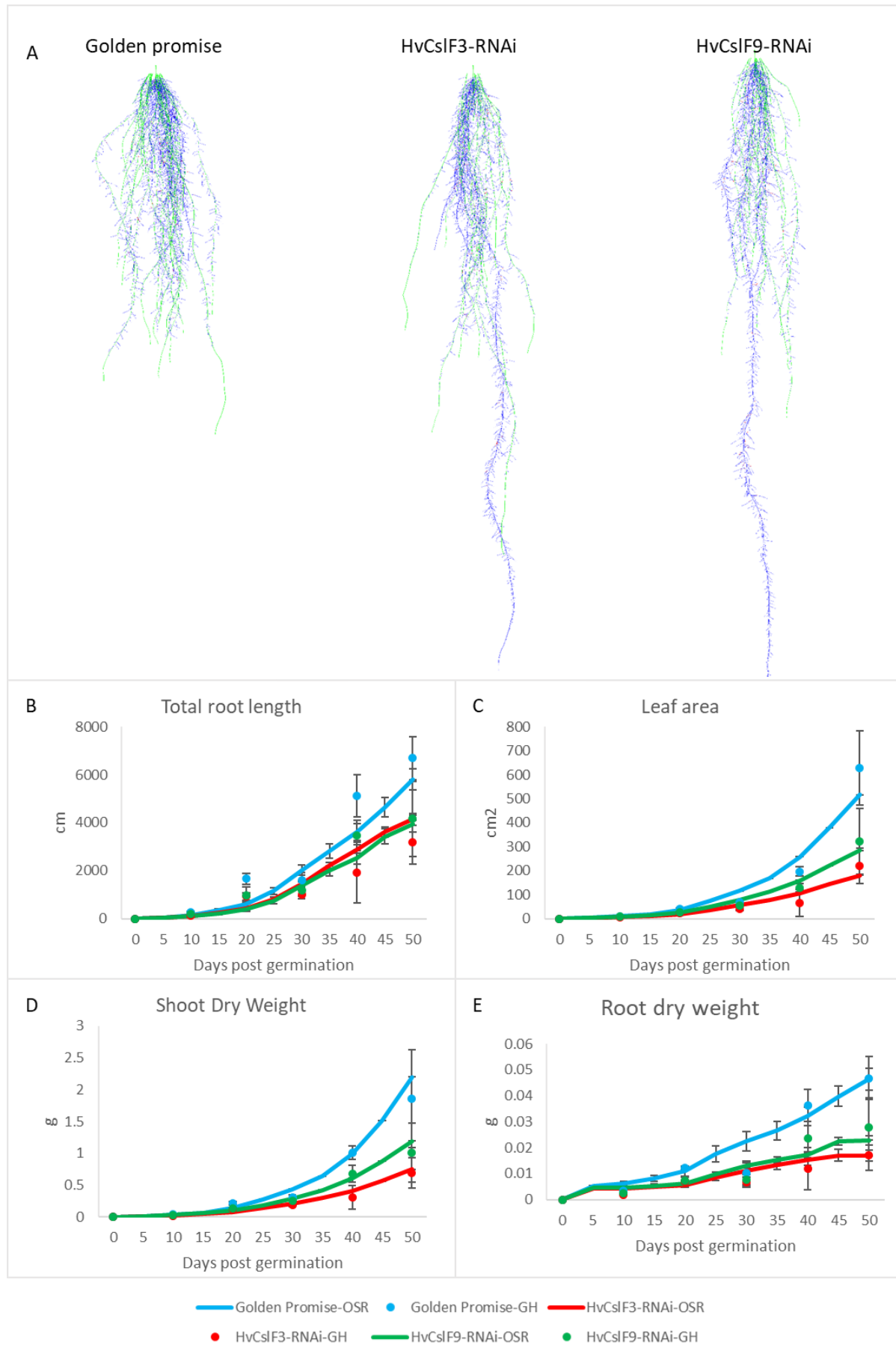


Figure 5-7. OSR simulated root development. Plant modules optimized for three genotypes (Golden Promise, *HvCsIF3-RNAi*, and *HvCsIF9-RNAi*) were simulated for 50 d under optimal soil nutrient availability. A, visualization of root development at 50 dpv. Golden Promise grew more roots than the other genotypes. B, C, D and E, comparison of total root length, leaf area, shoot dry weight and root dry weight between the *in silico* simulated plants (lines) and glasshouse grown plants (dots) throughout vegetative development. Overlaid data indicating the accuracy of OSR. Error bars indicate standard deviations in three (*in silico*) and six (glasshouse) replications.

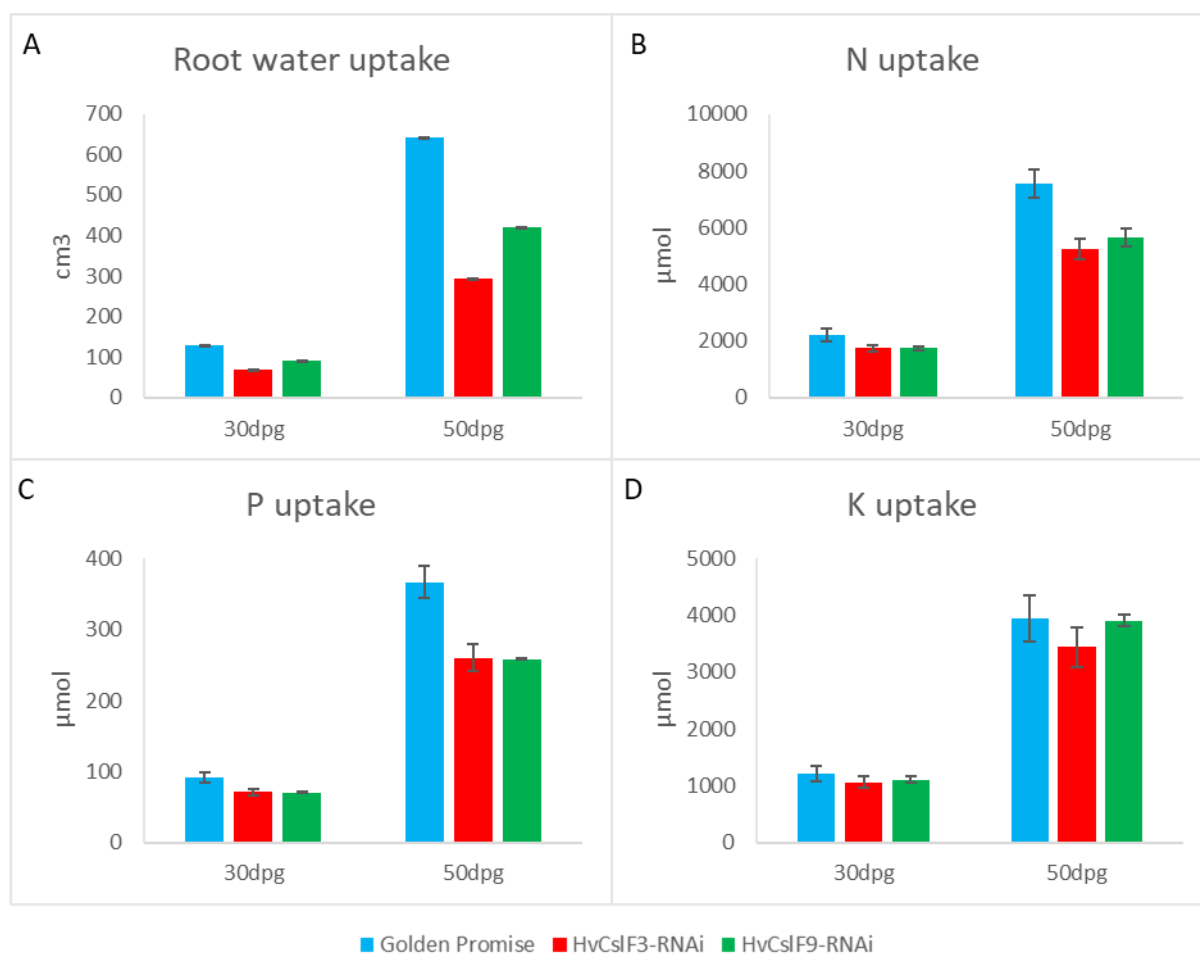


Figure 5-8. Variations in water and nutrients uptake between genotypes. Plant growth was simulated under optimal soil conditions. Minor variations were observed at 30 dpg. At 50 dpg, the root water uptake in the *HvCsIF3*-RNAi and *HvCsIF9*-RNAi plants was significantly lower than in Golden Promise (A). Similar trends were also found in N and P uptake, but with less marked differences (B and C). The three genotypes showed least variation in K uptake (D). Error bars indicate standard deviations of three repeat runs.

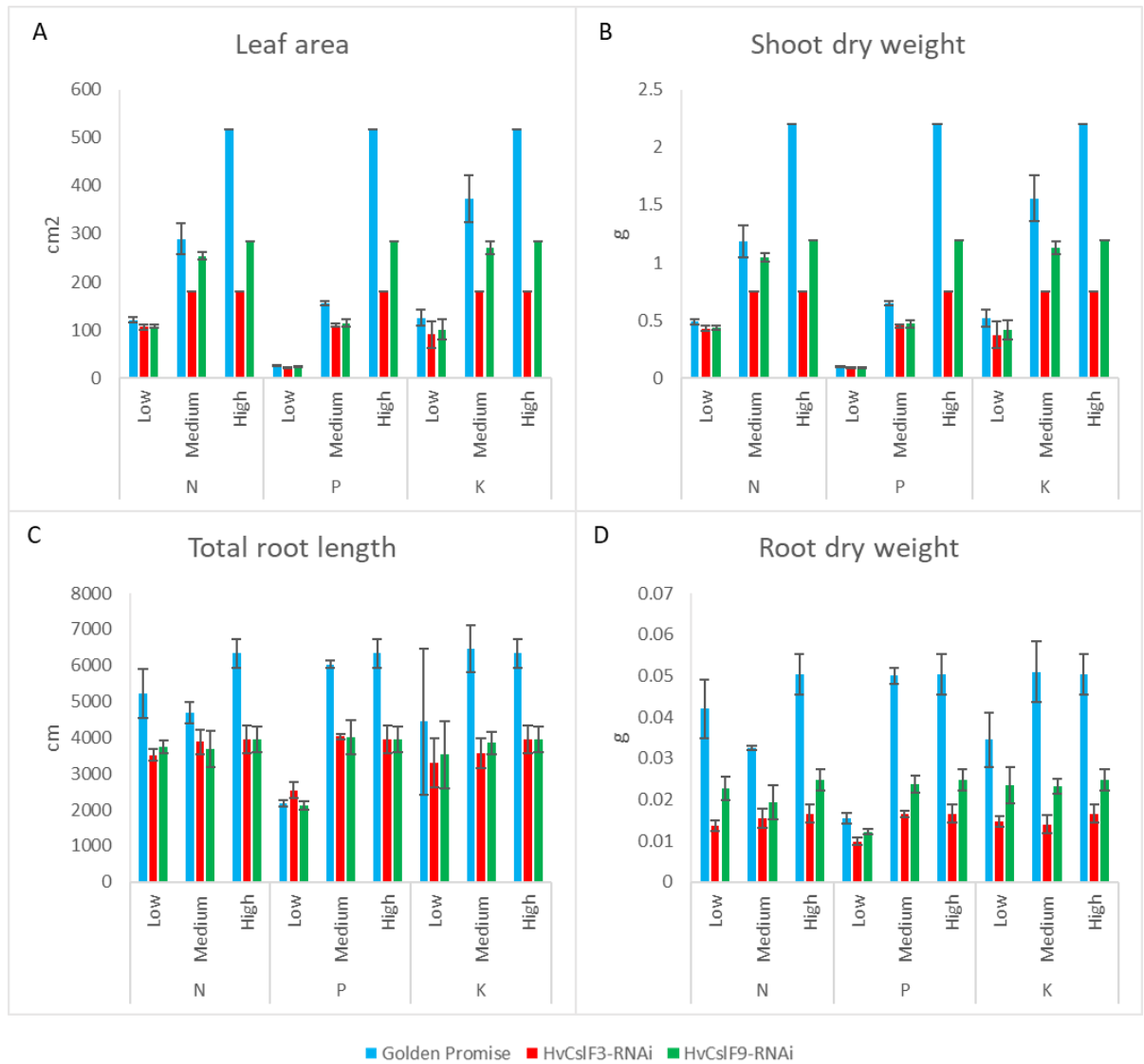


Figure 5-9. Effects of nutrient stresses on plant development. Low, medium and high represent 10%, 25%, and 100% of optimal nutrient availability in soil. The grouped bars show the differences of plant performance under each nutrient stress at 50 dpv. Greater restrictions on plant development were observed on the aerial tissues (A, leaf area; B, shoot dry weight) than underground tissues (C, total root length; D, root dry weight). Plants under low P availability had most severe reduced development. Error bars indicate standard deviations of three repeat runs.

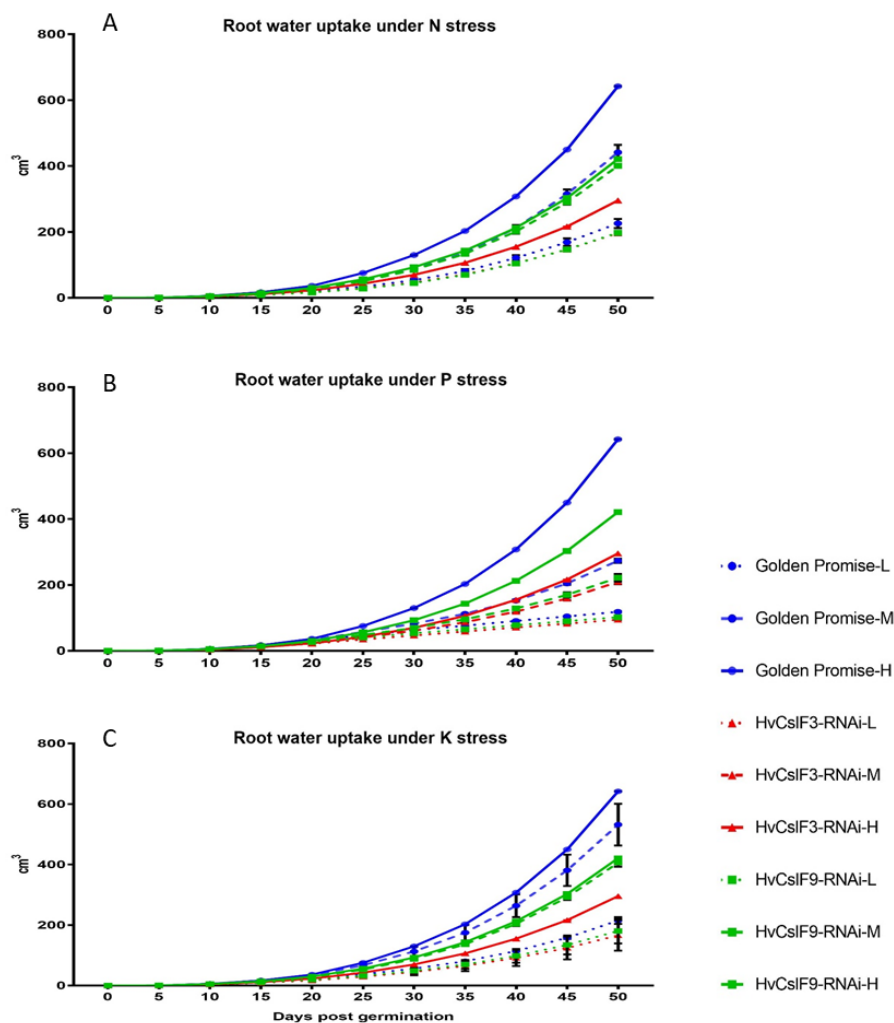


Figure 5-10. Effect on root water uptake of Golden Promise, *HvCsIF3-RNAi*, and *HvCsIF9-RNAi* plants under different NPK availabilities. The root water uptake increased more rapidly towards the later stages of plant development. L, low; M, medium; H, high. A, root water uptake under N stress. Under medium N stress, the root water uptake of Golden Promise decreased to a similar level as for *HvCsIF9-RNAi*, whereas little effects were found for the *HvCsIF3-RNAi* and *HvCsIF9-RNAi* plants. B, root water uptake under P stress. Great reductions were observed in the three genotypes under medium P stress. The reductions were more severe under low P treatment. C, root water uptake under K stress. The plants showed similar effects to the N stress conditions. Error bars indicate standard deviations of three repeat runs.

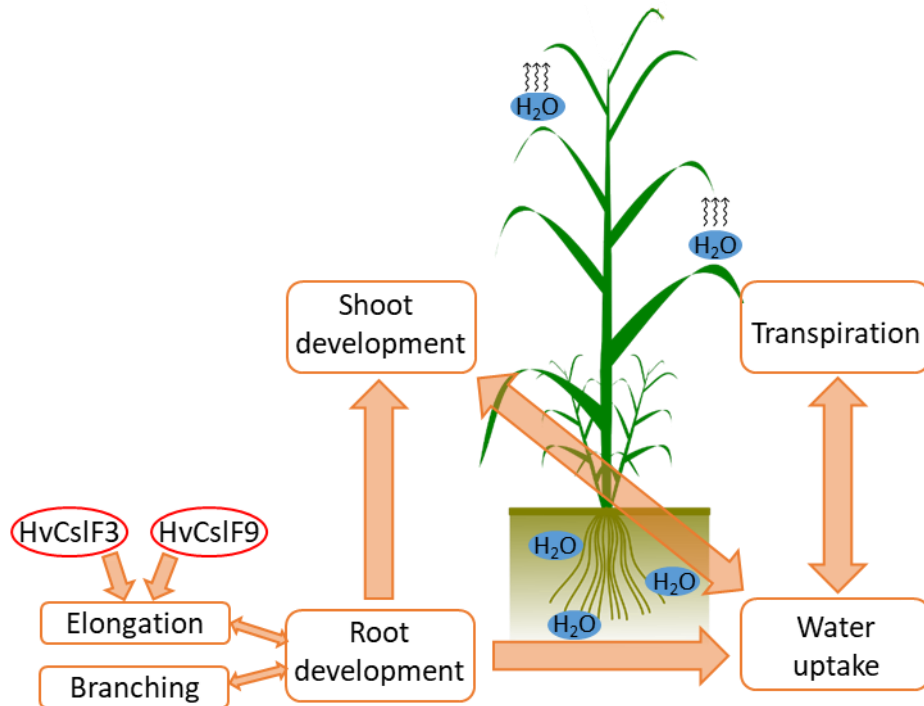


Figure 5-11. Schematic of the regulation and water transportation from soil to atmosphere through the plant. Arrows indicate positive effects. Elongation and branching are important determinants of root architecture. *HvCsIF3* and *HvCsIF9* gene expression affects root elongation. Root development positively affects shoot development and root water uptake. The efficiency and ability of root water uptake is dependent on root and shoot development and plant transpiration.

Tables

Table 5-1. Summary of effects of nutrient stress on plant development. Numbers represent the calculated percentage of reduction compared to the plants grown under optimal nutrient conditions. The colour code represents the level of reduction.


0%  100%		N		P		K	
		Low	Medium	Low	Medium	Low	Medium
Leaf area	Golden Promise	77%	44%	95%	70%	76%	28%
	HvCsIF3-RNAi	41%	0%	87%	39%	50%	0%
	HvCsIF9-RNAi	62%	11%	92%	60%	64%	5%
Shoot dry weight	Golden Promise	78%	46%	95%	70%	76%	29%
	HvCsIF3-RNAi	43%	0%	88%	40%	50%	0%
	HvCsIF9-RNAi	63%	12%	92%	60%	65%	5%
Total root length	Golden Promise	17%	26%	66%	5%	30%	-2%
	HvCsIF3-RNAi	11%	2%	36%	-2%	17%	10%
	HvCsIF9-RNAi	5%	7%	46%	-2%	11%	2%
Root dry weight	Golden Promise	17%	35%	69%	1%	32%	-1%
	HvCsIF3-RNAi	18%	7%	41%	0%	11%	15%
	HvCsIF9-RNAi	8%	22%	51%	4%	5%	6%

Table 5-2. OSR simulated shoot dry weight of Golden Promise, *HvCslF3*-RNAi and *HvCslF9*-RNAi under combinations of NKP stresses. L, low availability; M, medium availability; H, high availability. The size of the green bars within the cells reflects the value of the number shown in the cells. Cells with red outlines represent the shoot dry weight of individual genotypes under optimal NPK availability. Sample size N= 3.

	Golden Promise			<i>HvCslF3</i> -RNAi			<i>HvCslF9</i> -RNAi			
	L_N	M_N	H_N	L_N	M_N	H_N	L_N	M_N	H_N	
L_P	0.0984	0.1015	0.1003	0.0874	0.0890	0.0877	0.0884	0.0891	0.0915	L_K
	0.0986	0.1038	0.1058	0.0878	0.0904	0.0893	0.0889	0.0910	0.0928	M_K
	0.0987	0.1034	0.1063	0.0872	0.0899	0.0918	0.0877	0.0902	0.0927	H_K
M_P	0.4601	0.5587	0.5462	0.3780	0.4083	0.4196	0.4549	0.4139	0.4724	L_K
	0.5250	0.7414	0.6704	0.4582	0.4515	0.4418	0.4504	0.4932	0.5293	M_K
	0.5367	0.7545	0.6521	0.4420	0.4431	0.4530	0.4502	0.5162	0.4720	H_K
H_P	0.4737	0.4791	0.5199	0.3813	0.3832	0.3744	0.4253	0.4819	0.4204	L_K
	0.5088	1.2503	1.5566	0.4599	0.7498	0.7498	0.4316	1.1617	1.1329	M_K
	0.4885	1.1835	2.1994	0.4296	0.7498	0.7498	0.4363	1.0449	1.1909	H_K

Table 5-3. Change of shoot dry weights relative to the shoot dry weight of each genotype under optimal NPK conditions. Numbers represent the calculated percentage of reduction in shoot dry weight compared with the plants grown under optimal nutrient conditions. L, low availability; M, medium availability; H, high availability. The colour code represents the level of reduction. Cells with red outlines represent the shoot dry weight of individual genotypes under optimal NPK availability. Sample size N= 3.

	Golden Promise			HvCsIF3-RNAi			HvCsIF9-RNAi			
	L_N	M_N	H_N	L_N	M_N	H_N	L_N	M_N	H_N	
L_P	4%	5%	5%	12%	12%	12%	7%	7%	8%	L_K
	4%	5%	5%	12%	12%	12%	7%	8%	8%	M_K
	4%	5%	5%	12%	12%	12%	7%	8%	8%	H_K
M_P	21%	25%	25%	50%	54%	56%	38%	35%	40%	L_K
	24%	34%	30%	61%	60%	59%	38%	41%	44%	M_K
	24%	34%	30%	59%	59%	60%	38%	43%	40%	H_K
H_P	22%	22%	24%	51%	51%	50%	36%	40%	35%	L_K
	23%	57%	71%	61%	100%	100%	36%	98%	95%	M_K
	22%	54%	100%	57%	100%	100%	37%	88%	100%	H_K



Supplementary materials

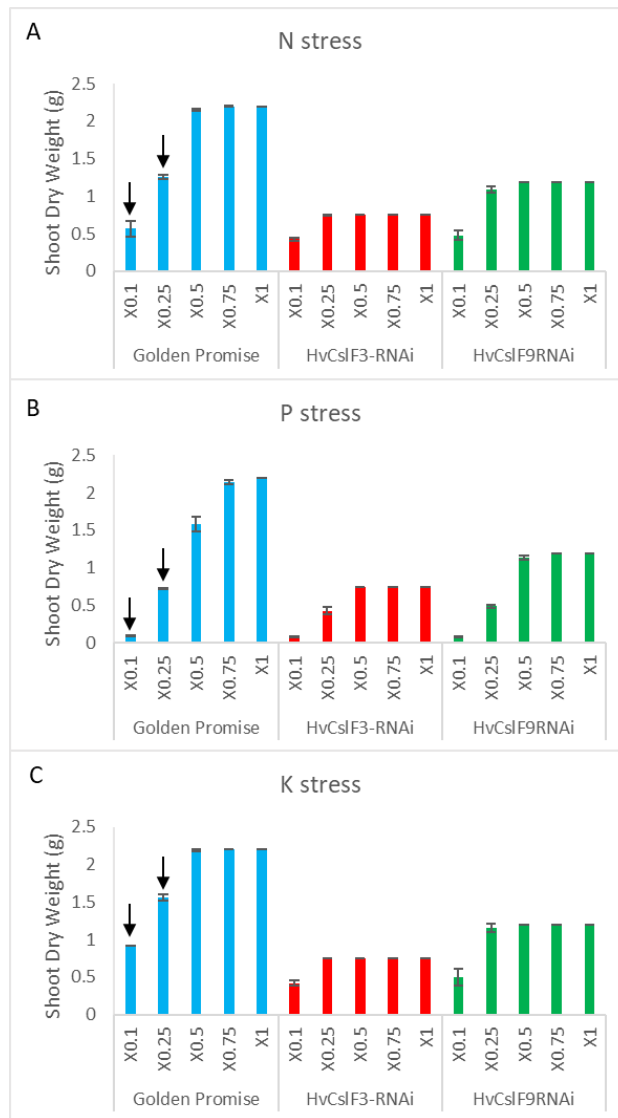


Figure 5-S1. OSR simulation predicted shoot dry weights of Golden Promise, *HvCslF3*-RNAi and *HvCslF9*-RNAi plants under single nutrient stress. Five nutrient levels were applied to simulate plant growth until 50 dpv. ×1 represents optimal nutrient availability in soil that does not cause stress throughout plant vegetative growth. ×0.75, 0.5, 0.25, 0.1 represent the soil nutrient content at 75%, 50%, 25%, and 10% of the optimal condition. Black arrows indicate the moderate or severe decreases observed. According to the levels of reduction, ×0.1, ×0.25, and ×1 were used as nutrient availabilities representing severe, moderate and optimal soil conditions in later studies.

Figure 5-V1. Video representing the Golden Promise root development over the entire simulation period (50 days). *OpenSimRoot* model was parameterised with Roseworthy (SA, Australia) climate and soil environments. Plant parameters were optimised using glasshouse measure data from barley cultivar Golden Promise. The development of Golden Promise root was simulated under optimal nutrient condition for 50 days. Different colours indicate different root classes. Video available on: <https://youtu.be/jMX7dXfYtGg>

Figure 5-V2. Video representing the interaction between Golden Promise root development and soil nitrate concentration over the entire simulation period (50 days). *OpenSimRoot* model was parameterised with Roseworthy (SA, Australia) climate and soil environments. Plant parameters were optimised using glasshouse measure data from barley cultivar Golden Promise. The development of Golden Promise root was simulated under optimal nutrient condition for 50 days. Different root colours indicate different root classes. The soil module is included to show the change of nitrate concentration in soil throughout the simulation period. Colour gradient represent the nitrate concentration (legend shown in video). Video available on: <https://youtu.be/1mFy808mic>

Table 5-S1. Statistical analysis of the significance of the data obtained from the phenotypic and ionomics experiments. Two-way ANOVA multiple comparisons were used to analyse the significance with Golden Promise as the main factor. ns- not significant. *- significant, P<0.1. **- significant, P<0.01. ***/****- significant, P<0.0001. nd- no data available. Photo, photosynthetic rate (umol CO₂ m⁻² s⁻¹); Cond, stomata conductance (mol H₂O m⁻² s⁻¹); Ci, intercellular CO₂ concentration (umol CO₂ mol⁻¹); Trmmol, transpiration rate (mmol H₂O m⁻² s⁻¹); VpdL, vapor pressure deficit based on Leaf temp (kPa); BLCond, total boundary layer conductance for the leaf (includes stomatal ratio) (mol m⁻² s⁻¹); VpdA, vapor pressure deficit based on Air temp (kPa); Ci/Ca, intercellular CO₂ / Ambient CO₂.

		10 dpg		20 dpg		30 dpg		40 dpg		50 dpg	
		Significant	P value	Significant	P value	Significant	P value	Significant	P value	Significant	P value
Height	HvCslF3-RNAi	**	0.0042	**	0.0018	**	0.0016	****	0.0001	****	0.0001
	HvCslF9-RNAi	ns	0.1225	**	0.0058	ns	0.3844	ns	0.6539	ns	0.0623
Leaf area	HvCslF3-RNAi	ns	0.983	ns	0.8074	ns	0.6053	***	0.0001	****	0.0001
	HvCslF9-RNAi	ns	0.9955	ns	0.8538	ns	0.903	ns	0.0646	****	0.0001
Shoot fresh weight	HvCslF3-RNAi	ns	0.9812	ns	0.7232	ns	0.6185	****	0.0001	****	0.0001
	HvCslF9-RNAi	ns	0.9931	ns	0.8002	ns	0.9495	*	0.0189	****	0.0001
Shoot dry weight	HvCslF3-RNAi	ns	0.985	ns	0.7255	ns	0.6017	****	0.0001	****	0.0001
	HvCslF9-RNAi	ns	0.994	ns	0.7943	ns	0.9051	*	0.0276	****	0.0001
Root fresh weight	HvCslF3-RNAi	ns	0.7926	ns	0.1198	ns	0.3102	****	0.0001	****	0.0001
	HvCslF9-RNAi	ns	0.8963	ns	0.1341	ns	0.5223	****	0.0001	****	0.0001
Tiller number	HvCslF3-RNAi	ns	0.382	ns	0.382	ns	0.6808	**	0.0019	****	0.0001
	HvCslF9-RNAi	ns	0.9054	ns	0.4364	ns	0.9454	*	0.0343	**	0.0025
Leaf number	HvCslF3-RNAi	ns	0.9972	ns	0.5181	ns	0.4786	****	0.0001	****	0.0001
	HvCslF9-RNAi	ns	0.9972	ns	0.4784	ns	0.7336	ns	0.3046	****	0.0001
Total root length	HvCslF3-RNAi	ns	0.9043	ns	0.0855	ns	0.1878	****	0.0001	****	0.0001
	HvCslF9-RNAi	ns	0.9681	ns	0.1171	ns	0.3814	****	0.0001	****	0.0001
Total root surface area	HvCslF3-RNAi	ns	0.9041	ns	0.2005	ns	0.3546	****	0.0001	****	0.0001
	HvCslF9-RNAi	ns	0.9582	ns	0.2097	ns	0.3069	****	0.0001	****	0.0001
Chlorophyll content	HvCslF3-RNAi	ns	0.0637	ns	0.1404	ns	0.3544	ns	0.9489	ns	0.9738
	HvCslF9-RNAi	*	0.0251	ns	0.906	ns	0.5892	ns	0.9675	ns	0.0819
Photos	HvCslF3-RNAi	ns	0.8535	ns	0.3183	****	0.0001	ns	0.468	*	0.0392
	HvCslF9-RNAi	ns	0.1505	ns	0.0745	**	0.0088	ns	0.991	***	0.0003
Trmmol	HvCslF3-RNAi	ns	0.063	****	0.0001	****	0.0001	***	0.0004	**	0.0012
	HvCslF9-RNAi	ns	0.4536	****	0.0001	****	0.0001	**	0.0027	****	0.0001
Cond	HvCslF3-RNAi	ns	0.3003	***	0.0005	****	0.0001	ns	0.3067	*	0.0241
	HvCslF9-RNAi	ns	0.9287	ns	0.0527	ns	0.1893	ns	0.498	**	0.0067
Ci	HvCslF3-RNAi	ns	0.9775	ns	0.8262	ns	0.9717	ns	0.9597	ns	0.9942
	HvCslF9-RNAi	ns	0.9902	ns	0.9993	ns	0.9634	ns	0.0608	ns	0.8652
VpdL	HvCslF3-RNAi	ns	0.6405	ns	0.7907	ns	0.0803	ns	0.6266	ns	0.989
	HvCslF9-RNAi	ns	0.2652	ns	0.9061	ns	0.985	ns	0.1517	ns	0.9496
BLCond	HvCslF3-RNAi	ns	0.9999	ns	0.4504	**	0.0081	**	0.0092	ns	0.2118
	HvCslF9-RNAi	ns	0.9999	ns	0.5615	ns	0.1708	ns	0.9309	ns	0.692
VpdA	HvCslF3-RNAi	ns	0.5777	ns	0.2427	ns	0.0791	ns	0.662	ns	0.9783
	HvCslF9-RNAi	ns	0.0835	ns	0.186	ns	0.9473	ns	0.1204	ns	0.645
Ci/Ca	HvCslF3-RNAi	ns	0.8052	ns	0.822	ns	0.9594	ns	0.9652	ns	0.9978
	HvCslF9-RNAi	ns	0.9156	ns	0.9997	ns	0.968	ns	0.0673	ns	0.9999
P	HvCslF3-RNAi	****	0.0001	ns	0.0704	*	0.0228	***	0.0005	****	0.0001
	HvCslF9-RNAi	ns	0.883	***	0.0009	ns	0.4033	ns	0.9242	ns	0.9972

Chapter 5 – Knock-down of *HvCslF3* and *HvCslF9* gene expressions in barley is predicted to increase plant tolerance to low nutrient stresses over the vegetative stage

K	HvCslF3-RNAi	ns	0.0566	ns	0.6887	ns	0.1328	****	0.0001	**	0.0022
	HvCslF9-RNAi	ns	0.4657	ns	0.0833	ns	0.9568	****	0.0001	*	0.0344
N	HvCslF3-RNAi	nd	nd	ns	0.3387	ns	0.0756	*	0.0111	ns	0.3943
	HvCslF9-RNAi	nd	nd	ns	0.0523	ns	0.0793	ns	0.5655	ns	0.4566
C	HvCslF3-RNAi	-	-	ns	0.6805	ns	0.2726	**	0.0026	ns	0.2407
	HvCslF9-RNAi	-	-	ns	0.9886	ns	0.8131	**	0.0043	ns	0.2787
Mg	HvCslF3-RNAi	ns	0.5875	ns	0.9952	ns	0.996	ns	0.7208	ns	0.998
	HvCslF9-RNAi	ns	0.9332	ns	0.9708	ns	0.9045	ns	0.9615	ns	0.8718
Ca	HvCslF3-RNAi	ns	0.2975	ns	0.5841	ns	0.3755	***	0.0007	ns	0.8849
	HvCslF9-RNAi	ns	0.9403	ns	0.9886	ns	0.933	****	0.0001	ns	0.7712
S	HvCslF3-RNAi	****	0.0001	**	0.0081	ns	0.9994	ns	0.1927	ns	0.3686
	HvCslF9-RNAi	*	0.0417	ns	0.1031	ns	0.907	ns	0.3905	ns	0.9786
Fe	HvCslF3-RNAi	ns	0.5166	ns	0.8984	ns	0.995	**	0.0066	ns	0.9865
	HvCslF9-RNAi	ns	0.9855	ns	0.9867	ns	0.9241	****	0.0001	ns	0.7374
Zn	HvCslF3-RNAi	*	0.0385	ns	0.1976	ns	0.842	ns	0.3989	*	0.0399
	HvCslF9-RNAi	ns	0.6777	ns	0.614	ns	0.9976	ns	0.9604	ns	0.9966
Cu	HvCslF3-RNAi	ns	0.0918	ns	0.6616	ns	0.9424	ns	0.2038	ns	0.9939
	HvCslF9-RNAi	ns	0.3616	ns	0.9999	ns	0.9662	ns	0.1951	ns	0.9925

Table 5-S2. OSR simulated root dry weight of Golden Promise, *HvCslF3-RNAi* and *HvCslF9-RNAi* under combinations of NKP stresses. L, low availability; M, medium availability; H, high availability. The size of the green bars within the cells reflects the value of the numbers in the cells. Cells with red outlines represent the shoot dry weight of individual genotypes under optimal NPK availability. Sample size N= 3.

	Golden Promise			HvCslF3-RNAi			HvCslF9-RNAi			
	L_N	M_N	H_N	L_N	M_N	H_N	L_N	M_N	H_N	
L_P	0.024	0.021	0.022	0.014	0.012	0.014	0.016	0.015	0.013	L_K
	0.023	0.018	0.016	0.013	0.011	0.013	0.016	0.014	0.012	M_K
	0.023	0.019	0.015	0.014	0.012	0.010	0.017	0.015	0.012	H_K
M_P	0.031	0.039	0.034	0.016	0.015	0.015	0.026	0.024	0.023	L_K
	0.047	0.052	0.049	0.016	0.017	0.017	0.023	0.023	0.028	M_K
	0.043	0.056	0.050	0.015	0.016	0.017	0.023	0.027	0.024	H_K
H_P	0.036	0.035	0.034	0.013	0.016	0.015	0.025	0.024	0.024	L_K
	0.046	0.037	0.051	0.014	0.015	0.014	0.020	0.025	0.023	M_K
	0.042	0.033	0.050	0.014	0.015	0.017	0.023	0.019	0.025	H_K

Table 5-S3. Change of root dry weights relative to the shoot dry weight of each genotype under optimal NPK conditions. Numbers represent the calculated percentage of reduction in shoot dry weight compared with the plants grown under optimal nutrient conditions. L, low availability; M, medium availability; H, high availability. The colour code represents the level of reduction. Cells with red outlines represent the shoot dry weight of individual genotypes under optimal NPK availability. Sample size N= 3.

	Golden Promise			HvCsIF3-RNAi			HvCsIF9-RNAi			
	L_N	M_N	H_N	L_N	M_N	H_N	L_N	M_N	H_N	
L_P	47%	41%	43%	84%	74%	83%	66%	62%	54%	L_K
	47%	36%	32%	80%	69%	76%	64%	57%	49%	M_K
	46%	37%	31%	86%	72%	59%	70%	59%	49%	H_K
M_P	61%	78%	67%	98%	92%	92%	107%	96%	93%	L_K
	93%	103%	97%	97%	100%	101%	92%	94%	112%	M_K
	86%	112%	99%	88%	94%	100%	93%	111%	96%	H_K
H_P	71%	68%	68%	81%	95%	89%	100%	95%	95%	L_K
	91%	73%	101%	84%	90%	85%	81%	103%	94%	M_K
	83%	65%	100%	82%	93%	100%	92%	78%	100%	H_K



References

- Bartens J, Day SD, Harris JR, Wynn TM, Dove JE** (2009) Transpiration and root development of urban trees in structural soil stormwater reservoirs. *Environmental Management* **44**: 646-657
- Burton RA, Collins HM, Kibble NAJ, Smith JA, Shirley NJ, Jobling SA, Henderson M, Singh RR, Pettolino F, Wilson SM, Bird AR, Topping DL, Bacic A, Fincher GB** (2011) Over-expression of specific *HvCslF* cellulose synthase-like genes in transgenic barley increases the levels of cell wall (1,3;1,4)- β -D-glucans and alters their fine structure. *Plant Biotechnology Journal* **9**: 117-135
- Burton RA, Jobling SA, Harvey AJ, Shirley NJ, Mather DE, Bacic A, Fincher GB** (2008) The genetics and transcriptional profiles of the cellulose synthase-like *HvCslF* gene family in barley. *Plant Physiology* **146**: 1821-1833
- Chapin FS, Lambers H, Pons T** (1998) Plant physiological ecology. *In*. Springer-Verlag Inc., New York
- Colmsee C, Beier S, Himmelbach A, Schmutzer T, Stein N, Scholz U, Mascher M** (2015) BARLEX – the Barley Draft Genome Explorer. *Molecular Plant* **8**: 964-966
- Cook RJ** (2006) Toward cropping systems that enhance productivity and sustainability. *Proceedings of the National Academy of Sciences of the United States of America* **103**: 18389-18394
- Cseh A, Soós V, Rakszegi M, Türkösi E, Balázs E, Molnár-Láng M** (2013) Expression of *HvCslF9* and *HvCslF6* barley genes in the genetic background of wheat and their influence on the wheat β -glucan content. *Annals of Applied Biology* **163**: 142-150
- Dalglish N, Cocks B, Horan H** (2012) APSoil-providing soils information to consultants, farmers and researchers. *In* 16th Australian Agronomy Conference, Armidale, NSW,
- Dathe A, Postma JA, Postma-Blaauw M, Lynch JP** (2016) Impact of axial root growth angles on nitrogen acquisition in maize depends on environmental conditions. *Annals of Botany* **118**: 401-414
- Fiacco DC, Lowe JA, Wiseman J, White GA** (2018) Evaluation of vegetable protein in canine diets: Assessment of performance and apparent ileal amino acid digestibility using a broiler model. *Journal of Animal Physiology and Animal Nutrition* **102**: e442-e448
- Ge Z, Rubio G, Lynch JP** (2000) The importance of root gravitropism for inter-root competition and phosphorus acquisition efficiency: results from a geometric simulation model. *Plant and Soil* **218**: 159-171
- Hochholdinger F, Feix G** (1998) Early post-embryonic root formation is specifically affected in the maize mutant *lrt1*. *The Plant Journal* **16**: 247-255
- Hochholdinger F, Zimmermann R** (2008) Conserved and diverse mechanisms in root development. *Current Opinion in Plant Biology* **11**: 70-74
- Imani J, Li L, Schäfer P, Kogel KH** (2011) STARTS—A stable root transformation system for rapid functional analyses of proteins of the monocot model plant barley. *The Plant Journal* **67**: 726-735
- Jia X, Liu P, Lynch JP** (2018) Greater lateral root branching density in maize improves phosphorus acquisition from low phosphorus soil. *Journal of Experimental Botany* **69**: 4961-4970
- Jungk A** (2001) Root hairs and the acquisition of plant nutrients from soil. *Journal of Plant Nutrition and Soil Science* **164**: 121-129
- Knipfer T, Besse M, Verdeil J-L, Fricke W** (2011) Aquaporin-facilitated water uptake in barley (*Hordeum vulgare* L.) roots. *Journal of Experimental Botany* **62**: 4115-4126
- Knipfer T, Fricke W** (2010) Water uptake by seminal and adventitious roots in relation to whole-plant water flow in barley (*Hordeum vulgare* L.). *Journal of Experimental Botany*

62: 717-733

- Lambers H, Chapin III FS, Pons TL** (2008) Plant physiological ecology. Springer Science & Business Media
- Little A, Lahnstein J, Jeffery DW, Khor SF, Schwerdt JG, Shirley NJ, Hooi M, Xing X, Burton RA, Bulone V** (2019) A novel (1, 4)- β -linked glucoxylan is synthesized by members of the Cellulose Synthase-Like F gene family in land plants. *ACS Central Science* **5**: 73-84
- Liu Z** (2018) Morphological, physiological and molecular characterization of root senescence in barley. University of Nairobi
- Lynch JP** (1995) Root architecture and plant productivity. *Plant Physiology* **109**: 7-13
- Lynch JP** (2018) Rightsizing root phenotypes for drought resistance. *Journal of Experimental Botany* **69**: 3279-3292
- Lynch JP** (2019) Root phenotypes for improved nutrient capture: an underexploited opportunity for global agriculture. *New Phytologist* **223**: 548-564
- Lynch JP, Brown KM** (2001) Topsoil foraging—an architectural adaptation of plants to low phosphorus availability. *Plant and Soil* **237**: 225-237
- Lynch JP, Nielsen KL, Davis RD, JablOKow AG** (1997) SimRoot: modelling and visualization of root systems. *Plant and Soil* **188**: 139-151
- May W, Parris R, Beck C, Fassett J, Greenberg R, Guenther F, Kramer G, Wise S, Gills T, Colbert J** (2000) Definitions of terms and modes used at NIST for value-assignment of reference materials for chemical measurements. NIST Special Publication **260**: 136
- Mayer KFX, Waugh R, Langridge P, Close TJ, Wise RP, Graner A, Matsumoto T, Sato K, Schulman A, Muehlbauer GJ, Stein N, Ariyadasa R, Schulte D, Poursarebani N, Zhou R, Steuernagel B, Mascher M, Scholz U, Shi B, Langridge P, Madishetty K, Svensson JT, Bhat P, Moscou M, Resnik J, Close TJ, Muehlbauer GJ, Hedley P, Liu H, Morris J, Waugh R, Frenkel Z, Korol A, Bergès H, Graner A, Stein N, Steuernagel B, Scholz U, Taudien S, Felder M, Groth M, Platzer M, Stein N, Steuernagel B, Scholz U, Himmelbach A, Taudien S, Felder M, Platzer M, Lonardi S, Duma D, Alpert M, Cordero F, Beccuti M, Ciardo G, Ma Y, Wanamaker S, Close TJ, Stein N, Cattonaro F, Vendramin V, Scalabrin S, Radovic S, Wing R, Schulte D, Steuernagel B, Morgante M, Stein N, Waugh R, Nussbaumer T, Gundlach H, Martis M, Ariyadasa R, Poursarebani N, Steuernagel B, Scholz U, Wise RP, Poland J, Stein N, Mayer KFX, Spannagl M, Pfeifer M, Gundlach H, Mayer KFX, Gundlach H, Moisy C, Tanskanen J, Scalabrin S, Zuccolo A, Vendramin V, Morgante M, Mayer KFX, Schulman A, Pfeifer M, Spannagl M, Hedley P, Morris J, Russell J, Druka A, Marshall D, Bayer M, Swarbreck D, Sampath D, Ayling S, Febrer M, Caccamo M, Matsumoto T, Tanaka T, Sato K, Wise RP, Close TJ, Wannamaker S, Muehlbauer GJ, Stein N, Mayer KFX, Waugh R, Steuernagel B, Schmutzer T, Mascher M, Scholz U, Taudien S, Platzer M, Sato K, Marshall D, Bayer M, Waugh R, Stein N, Mayer KFX, Waugh R, Brown JWS, Schulman A, Langridge P, Platzer M, Fincher GB, Muehlbauer GJ, Sato K, Close TJ, Wise RP, Stein N, **The International Barley Genome Sequencing C** (2012) A physical, genetic and functional sequence assembly of the barley genome. *Nature* **491**: 711-716**
- Mian M, Nafziger ED, Kolb FL, Teyker RH** (1993) Root growth of wheat genotypes in hydroponic culture and in the greenhouse under different soil moisture regimes. *Crop Science* **33**: 283-286
- Miguel M, Widrig A, Vieira R, Brown KM, Lynch JP** (2013) Basal root whorl number: a modulator of phosphorus acquisition in common bean (*Phaseolus vulgaris*). *Annals of Botany* **112**: 973-982
- Miguel MA, Postma JA, Lynch JP** (2015) Phene synergism between root hair length and basal root growth angle for phosphorus acquisition. *Plant Physiology* **167**: 1430-1439

- Nemeth C, Freeman J, Jones HD, Sparks C, Pellny TK, Wilkinson MD, Dunwell J, Andersson AAM, Aman P, Guillon F, Saulnier L, Mitchell RAC, Shewry PR** (2010) Down-regulation of the *CslF6* gene results in decreased (1,3;1,4)- β -D-glucan in endosperm of wheat. *Plant Physiology* **152**: 1209-1218
- Nilson SE, Assmann SM** (2007) The control of transpiration. Insights from Arabidopsis. *Plant physiology* **143**: 19-27
- Osaki M, Shinano T, Matsumoto M, Zheng T, Tadano T** (1997) A root-shoot interaction hypothesis for high productivity of field crops. *In* Plant nutrition for sustainable food production and environment. Springer, pp 669-674
- Peng Y, Yu P, Zhang Y, Sun G, Ning P, Li X, Li C** (2012) Temporal and spatial dynamics in root length density of field-grown maize and NPK in the soil profile. *Field Crops Research* **131**: 9-16
- Penman H** (1950) The dependence of transpiration on weather and soil conditions. *Journal of Soil Science* **1**: 74-89
- Pitman M** (1965) Transpiration and the selective uptake of potassium by barley seedlings (*Hordeum vulgare* cv. Bolivia). *Australian Journal of Biological Sciences* **18**: 987-998
- Postma JA, Kuppe C, Owen MR, Mellor N, Griffiths M, Bennett MJ, Lynch JP, Watt M** (2017) OpenSimRoot: widening the scope and application of root architectural models. *New Phytologist* **215**: 1274-1286
- Postma JA, Lynch JP** (2011) Theoretical evidence for the functional benefit of root cortical aerenchyma in soils with low phosphorus availability. *Annals of Botany* **107**: 829-841
- Postma JA, Schurr U, Fiorani F** (2014) Dynamic root growth and architecture responses to limiting nutrient availability: linking physiological models and experimentation. *Biotechnology Advances* **32**: 53-65
- Robredo A, Pérez-López U, de la Maza HS, González-Moro B, Lacuesta M, Mena-Petite A, Muñoz-Rueda A** (2007) Elevated CO₂ alleviates the impact of drought on barley improving water status by lowering stomatal conductance and delaying its effects on photosynthesis. *Environmental and Experimental Botany* **59**: 252-263
- Römheld V, Kirkby EA** (2010) Research on potassium in agriculture: needs and prospects. *Plant Soil* **335**: 155-180
- Saengwilai P, Tian X, Lynch JP** (2014) Low crown root number enhances nitrogen acquisition from low-nitrogen soils in maize. *Plant Physiology* **166**: 581-589
- Sanderson J** (1983) Water uptake by different regions of the barley root. Pathways of radial flow in relation to development of the endodermis. *Journal of Experimental Botany* **34**: 240-253
- Schneider HM, Postma JA, Wojciechowski T, Kuppe C, Lynch JP** (2017) Root cortical senescence improves growth under suboptimal availability of N, P, and K. *Plant Physiology* **174**: 2333-2347
- Schneider HM, Wojciechowski T, Postma JA, Brown KM, Lücke A, Zeisler V, Schreiber L, Lynch JP** (2017) Root cortical senescence decreases root respiration, nutrient content and radial water and nutrient transport in barley. *Plant, Cell Environment* **40**: 1392-1408
- Sullivan WM, Jiang Z, Hull RJ** (2000) Root morphology and its relationship with nitrate uptake in Kentucky bluegrass. *Crop Science* **40**: 765-772
- Sun B, Gao Y, Lynch JP** (2018) Large crown root number improves topsoil foraging and phosphorus acquisition. *Plant Physiology* **177**: 90-104
- Taketa S, Yuo T, Tonooka T, Tsumuraya Y, Inagaki Y, Haruyama N, Larroque O, Jobling SA** (2011) Functional characterization of barley betaglucanless mutants demonstrates a unique role for *CslF6* in (1, 3; 1, 4)- β -D-glucan biosynthesis. *Journal of Experimental Botany* **63**: 381-392
- Tavakkoli E, Rengasamy P, McDonald GK** (2010) The response of barley to salinity stress

- differs between hydroponic and soil systems. *Functional Plant Biology* **37**: 621-633
- Thomas CL, Alcock TD, Graham NS, Hayden R, Matterson S, Wilson L, Young SD, Dupuy LX, White PJ, Hammond JP, Danku JMC, Salt DE, Sweeney A, Bancroft I, Broadley MR** (2016) Root morphology and seed and leaf ionic traits in a *Brassica napus* L. diversity panel show wide phenotypic variation and are characteristic of crop habit. *BMC Plant Biology* **16**: 214
- Tonooka T, Aoki E, Yoshioka T, Taketa S** (2009) A novel mutant gene for (1-3, 1-4)- β -D-glucanless grain on barley (*Hordeum vulgare* L.) chromosome 7H. *Breeding Science* **59**: 47-54
- Tricase C, Amicarelli V, Lamonaca E, Rana RL** (2018) Economic analysis of the barley market and related uses. *In Grasses as Food and Feed*. IntechOpen
- Vega-Sánchez ME, Verherbruggen Y, Christensen U, Chen X, Sharma V, Varanasi P, Jobling SA, Talbot M, White RG, Joo M, Singh S, Auer M, Scheller HV, Ronald PC** (2012) Loss of Cellulose synthase-like F6 function affects mixed-linkage glucan deposition, cell wall mechanical properties, and defense responses in vegetative tissues of rice. *Plant Physiology* **159**: 56-69
- Wang H, Inukai Y, Yamauchi A** (2006) Root development and nutrient uptake. *Critical Reviews in Plant Sciences* **25**: 279-301
- Wen TJ, Schnable PS** (1994) Analyses of mutants of three genes that influence root hair development in *Zea mays* (Gramineae) suggest that root hairs are dispensable. *American Journal of Botany* **81**: 833-842
- Yang X** (2017) Enlarged cortical cells and reduced cortical cell file number improve maize growth under suboptimal nitrogen, phosphorus and potassium availability. Pennsylvania State University
- Yao S-G, Taketa S, Ichii M** (2002) A novel short-root gene that affects specifically early root development in rice (*Oryza sativa* L.). *Plant Science* **163**: 207-215
- York L, Nord E, Lynch J** (2013) Integration of root phenes for soil resource acquisition. *Frontiers in Plant Science* **4**: 355
- York LM, Silberbush M, Lynch JP** (2016) Spatiotemporal variation of nitrate uptake kinetics within the maize (*Zea mays* L.) root system is associated with greater nitrate uptake and interactions with architectural phenes. *Journal of Experimental Botany* **67**: 3763-3775
- Zhan A, Lynch JP** (2015) Reduced frequency of lateral root branching improves N capture from low-N soils in maize. *Journal of Experimental Botany* **66**: 2055-2065
- Zhu J, Zhang C, Lynch JP** (2010) The utility of phenotypic plasticity of root hair length for phosphorus acquisition. *Functional Plant Biology* **37**: 313-322

Chapter 6

Summary and Future Directions



Thesis Summary

Understanding the development and regulation of root growth is important for plant breeding to benefit agricultural practices, and to contribute new knowledge to fundamental science. The synthesis and assembly of cell walls is essential for root development and the complexity of cell wall composition influences the development and functions of cells in different tissues. Over the past few decades, intensive studies have been undertaken in model dicots to reveal the genetic basis for root growth and architecture, while studies in monocotyledonous plants have focused more on the development of nodal roots, lateral roots and root hairs rather than seminal roots. The current study adds to this body of knowledge, and provides new information regarding the potential function of the cell wall-related *CsIF* genes in root architecture determination and modification of cell elongation.

Currently, understanding of the gene expression and cell wall composition in the root tips arises largely from the model species *Arabidopsis*, while relatively little information is available for cereal crops, including barley, due to their complex cellular organisation. In Chapter 2, investigations of gene expression profiling, qualitative and quantitative analyses of cell wall composition provided insights in cell wall heterogeneity in barley root tips. The *CsI* genes showed distinct expression patterns in the different developmental zones along the root tips. High expression levels in the meristem zone (*HvCsID4*, *HvCsIF9*), elongation zone (*HvCsID4*, *HvCsIF3*, *HvCsIF9*), and maturation zone (*HvCsID1*, *HvCsIF6*) indicated the potential functions of these genes in the regulation of cellular activities at different stages of cell development. Within the *CsIF* gene family, high expression of *HvCsIF3* and *HvCsIF9* over *HvCsIF6* in the meristem and elongation zones were particularly interesting for investigating the relationships between cell wall synthesis and root tip development. In this Chapter, polysaccharide composition was also revealed. By using antibody-specific immunolabelling and glycosidic linkage analysis, the abundance and tissue specificity of (1,3;1,4)- β -glucan,

callose, and pectin as key non-cellulosic polysaccharides was revealed. The variation between the cell wall composition of the different tissues may reflect the unique functional characteristics of different cell types in barley root tips.

To further investigate the function of *Csl* genes in developing barley root tips, we focused on the *HvCslF3* and *HvCslF9* genes in Chapter 3. By analysing the phenotypic and cellular differences between wild-type and RNAi down-regulated *HvCslF3* and *HvCslF9* barley lines, we demonstrated the importance of these two genes in root tip development in seedlings. Significant reduction of the size of the elongation zone was observed in the *HvCslF3*-RNAi plants, and smaller meristem and elongation zone sizes were observed in the *HvCslF9*-RNAi plants. Consequently, slower growth rates and shorter seminal roots were observed in the transgenic plants. Furthermore, differences in cell wall composition were also observed, suggesting cell wall properties are essential to maintain the root tip. *HvCslF3* and *HvCslF9* are involved in the synthesis of different cell wall polysaccharides. Reduced (1,4)- β -linked glucoxytan amounts were determined in the *HvCslF3*-RNAi and *HvCslF9*-RNAi root tips. Although the regulatory machinery of (1,4)- β -linked glucoxytan synthesis remains unknown, the results suggest that these genes participate in (1,4)- β -linked glucoxytan biosynthesis. In addition, *HvCslF9* is also involved in (1,3;1,4)- β -glucan synthesis in the newly formed primary cell walls of the cells of the meristem and elongation zones. This challenges previous studies that reported *HvCslF6* to be the only determinant of (1,3;1,4)- β -glucan synthesis in barley. Despite this, the regulatory machinery influencing the expression of *HvCslF3* and *HvCslF9* genes, the potential interaction of their products, and the consequences for root cell elongation require further investigations. Our study provides insight into the role of *CslF* genes in the regulation of different cell wall polysaccharide biosynthesis in barley root tips and their key role in root development.

Phylogenetic studies have shown *CslF* and *CslD* gene families are sister clades,

although their evolutionary history remains to be fully resolved. The *CsIF* genes are absent in the Arabidopsis genome. This plant therefore provides an excellent heterologous expression system to study the functions of *HvCsIF* genes. In Chapter 4, the *HvCsIF3* gene was transformed into different Arabidopsis genotypes with the expression driven by a universal promoter and a root hair specific promoter. The functional redundancy between the *CsID* and *CsIF* gene families was demonstrated by the rescued phenotype of the *Atcsld5* mutant by *HvCsIF3* expression. Furthermore, a gain of function phenotype was identified in Arabidopsis plants expressing *HvCsIF3*; irregular root hairs formed from the epidermal cells in contact with one cortical cell. The regulatory pathway of *HvCsIF3* affecting root hair elongation and root hair cell file determination was hypothesised based on existing knowledge. In addition, the contrasting observations of (1,4)- β -linked glucoxytan accumulation in different heterologous expression systems (tobacco and Arabidopsis) suggest the mechanism behind the biosynthesis of this polysaccharide may be more complicated than predicted.

To assess the effects of *HvCsIF3* and *HvCsIF9* genes in later stages of plant development, plant morphologies and kinetics were obtained from glasshouse grown wild-type, *HvCsIF3-RNAi*, and *HvCsIF9-RNAi* barleys throughout the vegetative growth phase. The continuous restriction on root and shoot growth indicated the importance of *HvCsIF3* and *HvCsIF9* genes in maintaining proper plant development throughout the vegetative stages. More importantly, when the genes were down-regulated, plants exhibited a trend of reduced transpiration rate and stomata conductivity, but a normal photosynthetic rate. These data indicate that the transgenic plants likely suffer from limited water capture, which may also affect nutrient uptake. The computer mathematical model (OSR) that simulates plant growth in natural soil environments was employed to address root-soil interactions *in silico*. The quantitative simulations revealed the root systems of transgenic barleys contain traits beneficial to nutrient uptake. Less severe reduction of various physiological parameters in transgenic barleys was observed under different nutrient stresses. These findings suggest a new direction in plant breeding to generate

plants with more efficient root traits based on expression and regulation of cell wall related genes.

This thesis presents results obtained using a range of genetic, molecular, physiological and computational analyses, aiming to investigate the functions of the cell wall related genes, *HvCsIF3* and *HvCsIF9*, during barley root development and differentiation. This has revealed a number of determining factors, including gene expression regulation, cell wall polysaccharide heterogeneity, polysaccharide biosynthesis, root architecture and development. In summary, we have shown that: 1) The gene expression profiles differ in different root developmental zones, which revealed the specific role of the *HvCsIF3* and *HvCsIF9* genes in the cellular activities during cell division and elongation. 2) Complexity of the cell wall composition in different tissues of barley root tips reflected the unique functional characteristics of cell walls during root growth. 3) The synthesis of (1,3;1,4)- β -glucan is largely dependent on *HvCsIF6*, although *HvCsIF9* is also involved in this process, especially in the meristem and elongation zones where *HvCsIF9* is highly expressed in contrast to *HvCsIF6*. 4) Down regulation of *HvCsIF3* and *HvCsIF9* genes negatively affect root elongation and cortical cell proliferation, and consequently result in restricted size of the root system. The negative effects are continuous traits that affect both root and shoot development throughout the vegetative growth. 5) There is a direct impact of *HvCsIF3* gene expression on the accumulation of (1,4)- β -linked glucoxytan in the barley root tips. However, the *HvCsIF3* product was not able to synthesise (1,4)- β -linked glucoxytan in *Arabidopsis*, suggesting the regulatory pathway for (1,4)- β -linked glucoxytan is more complex and possibly involves other enzymes. 6) A functional redundancy between *CsIF* and *CsID* gene families in root hair elongation was revealed in *Arabidopsis*, with an additional function of *HvCsIF3* in the determination of the number of root hair cell files. In conclusion, the work presented in this thesis adds to the body of knowledge regarding the relationship between cell wall synthesis and root development in barley and *Arabidopsis*, and the results provide new perspectives for the manipulation of root development by influencing the

regulation of cell wall properties.

Future directions

Gene expression and network analysis at the cell type-specific level

In the present study, we only focused on the expression profile of *CsIF* and *CsID* genes in specific regions of the root samples. This allowed us to determine the role of candidate genes, *HvCsIF3* and *HvCsIF9*, in the control of root tip development. However, this analysis of gene expression was limited to relatively few genes. To gain a global view of gene networks, RNA sequencing is a more advanced tool to analyse entire transcriptomes. The publicly available barley genome database provides an excellent opportunity to map mRNA transcriptomes and construct a gene regulatory network in the root tips of wild-type barley, and also the transgenic lines. Furthermore, even though roots are relatively simple tissues in terms of cellular organisation, the existence of multiple cell types in different root development zones still involves complex genetic regulations. This could be resolved by employing the laser capture microdissection (LCM) technology. LCM allows the collection of specific cell types and the analysis of gene expression in specific cell types, which largely improves the resolution of the transcriptomic analysis.

Further characterisation of *HvCsIF3* and *HvCsIF9* knock-down mutants

RNAi transgenic lines targeting *HvCsIF3* and *HvCsIF9* gene expression in the barley root tips induced morphological alterations in cortical cell radial patterning and root hair growth. Although phenotypes were robustly observed in multiple independent transgenic lines, variations in mutant phenotypes between the transgenic lines led to difficulties on phenotypic assessment. The recent development of the precise gene editing and modification tool, CRISPR-Cas9, enables the knock-out of specific target genes. In a collaboration with the James Hutton Institute (UK) and the University of Melbourne, CRISPR-Cas9 lines targeting *HvCsIF3* and

HvCslF9 were generated (M. Tucker and K. Houston, unpublished). Successful gene edits were confirmed in the T0 plants, and the edits have been successfully maintained in the T1 plants. Edited sequences resulted in frame-shift mutations and premature termination of translation. To further analyse the knock-out mutants, selection of homozygous mutations and elimination of Cas9 gene sequence are required in the following generations. The CRISPR-Cas9 induced transgenic lines will be characterised at the genetic, molecular and phenotypic levels. The results will provide further information on root development in the absence of *HvCslF3* and *HvCslF9* gene expression, which may result in even more severe effects on root tip growth. By comparing the CRISPR-Cas9 and RNAi induced phenotypic changes, the data will further support the importance of *HvCslF3* and *HvCslF9* genes in barley root tip development.

How and why do *HvCslF3* and *HvCslF9* affect (1,4)- β -linked glucoxytan accumulation in barley root tips

Quantification of the oligosaccharides released from cellulase treated barley root tips revealed the presence of (1,4)- β -linked glucoxytan. A significant decrease of the (1,4)- β -linked glucoxytan content was observed in the root tips of *HvCslF3-RNAi* and *HvCslF9-RNAi* plants. A previous study on tobacco leaves expressing *HvCslF3* confirmed the direct involvement of this gene in the biosynthesis of (1,4)- β -linked glucoxytan. However, in Chapter 4, we failed to detect any (1,4)- β -linked glucoxytan accumulation in the *Arabidopsis* plants expressing *HvCslF3*, which raises the question of whether *HvCslF3*-directed (1,4)- β -linked glucoxytan biosynthesis requires different mechanisms in different expression systems. To address this question, the regulation pathway of the *HvCslF3* protein, and its potential interaction with other proteins need to be resolved. The synthesis of a cell wall polysaccharide is often a complex process that involves multiple enzymes. The cellulose synthase complex is a great example of how the different CesA proteins reformulate for the synthesis of cellulose. By investigating the regulatory mechanisms of *HvCslF9* we might better understand the reduction of (1,4)- β -linked

glucoxytan observed in the *HvCsIF9-RNAi* lines, and whether it is an indirect effect. The same study that revealed the role of *HvCsIF3* in (1,4)- β -linked glucoxytan biosynthesis in tobacco leaves, failed to find any evidence that *HvCsIF9* is also involved in this process. Therefore, the potential of *HvCsIF9* to affect (1,4)- β -linked glucoxytan accumulation downstream of *HvCsIF3* during barley root development needs to be investigated. To address this question, we addressed whether that the *HvCsIF3* and *HvCsIF9* proteins interact to form a heterodimer when co-expressed in onion epidermal cells. Preliminary data suggests that this is the case (data not shown). To further analyse the consequence of *HvCsIF3* and *HvCsIF9* co-expression and potential interaction, further experiments are needed, including transient co-expression in tobacco leaves, protein co-localisation using fluorescent tags, (1,4)- β -linked glucoxytan quantification, and yeast two hybrid analysis.

***HvCsIF9* directs (1,3;1,4)- β -glucan synthesis in barley root tips**

In the present study, we highlighted the predominant expression of *HvCsIF9* over *HvCsIF6* in the meristem and elongation zones of barley roots, and revealed the absence of (1,3;1,4)- β -glucan in the corresponding root regions by immunohistochemistry. *HvCsIF6* is well known to be the main determinant for (1,3;1,4)- β -glucan synthesis in various tissues in barley. Analysis of *HvCsIF9* knock-out mutants indicated that the (1,3;1,4)- β -glucan content in the grain was not affected (G. Garcia, M. Tucker, K Houston, *under review*). However, based on the gene expression profiles, it is likely that the effects of *HvCsIF9* on (1,3;1,4)- β -glucan content in the grain were diluted by the predominant expression of *HvCsIF6*. In order to assess the role of *HvCsIF9* in (1,3;1,4)- β -glucan synthesis, tissues such as root tips where *HvCsIF6* gene expression remains low should be analysed. Our preliminary results using an antibody specific to (1,3;1,4)- β -glucan indicated the absence of this polysaccharide in the *HvCsIF9-RNAi* barley root tips. To support this result, quantitative assays including (1,3;1,4)- β -glucan assays and glycosidic linkage analysis will need to be performed.

Why do both *HvCsIF6* mutant and *HvCsIF9* knockdown mutants show no (1,3;1,4)- β -glucan in root tips?

In Chapter 2 and 3, we showed no detectable (1,3;1,4)- β -glucan in the young root tips of the *bgl* mutant and *HvCsIF9-RNAi* lines by immunolabelling with the BG1 antibody. Both genotypes exhibited no (1,3;1,4)- β -glucan accumulation in the meristem and elongation zones of any cell type. However, in the *HvCsIF9-RNAi* plant, the (1,3;1,4)- β -glucan content recovered to wild-type level once the cells enter the maturation zone, whereas (1,3;1,4)- β -glucan remained undetectable in the *bgl* mutant. These results indicate the dominant role of *HvCsIF6* in the synthesis of (1,3;1,4)- β -glucan. However, with normal expression of *HvCsIF6* in the *HvCsIF9-RNAi* plants, and normal expression of *HvCsIF9* in the *bgl* mutant, the meristem and elongation zone lacking (1,3;1,4)- β -glucan suggest a potential enzyme cooperation for (1,3;1,4)- β -glucan synthesis in the root tips. The synthesis of cell wall polysaccharide is a complex process. For example, the cellulose synthase complex requires multiple *CesA* gene products to interact, and different isoforms are responsible for cellulose synthesis in different plant tissues. Therefore, we hypothesise that (1,3;1,4)- β -glucan synthesis may require different *CsIF* genes, and possibly involves the cooperation of different *CsIF* members in different tissues at different developmental stages. To test this hypothesis, experiments that reveal protein-protein interactions and regulation will need to be performed.

How does Arabidopsis respond to *HvCsIF9* expression?

In Chapter 4, *HvCsIF3* was transformed into multiple Arabidopsis genotypes. We successfully identified some functional redundancy between the *CsIF* and *CsID* genes during root hair elongation, and observed the potential function of *HvCsIF3* in the specification of root hair cells. However, due to the difficulty in cloning the *HvCsIF9* coding sequence, we were unable to express *HvCsIF9* in Arabidopsis. To further understand the function of *HvCsIF9* in a heterologous expression system, transformation of the *HvCsIF9* gene into different Arabidopsis

genotypes is required. Recently, we have successfully cloned the *HvCsIF9* coding sequence into an entry vector. This work will continue with the creation of the destination vectors with specific promoter sequences and transformation into *Arabidopsis* via *Agrobacterium*-mediated transformation. Once the homozygous transgenic lines are identified, sequential experiments will be performed to characterise the effect of *HvCsIF9* gene expression on *Arabidopsis* development.

Improvement of OpenSimRoot (OSR) models to simulate more realistic root development

The current OSR used for the simulations shown in Chapter 5 was optimized based on the Roseworthy (South Australia) field environment and the plant parameters measured in glasshouse grown barleys. The OSR is a functional-structural plant model that includes many modules to allow the simulation of root development and root-soil interactions. During the process of optimizing the OSR to fit Roseworthy's environments and specific barley genotypes, we faced great challenges in data collection for each OSR modules. Due to the limitation of available resources, some plant parameters were either adapted or estimated base on other studies, including root respiration of different root classes, nutrient uptake kinetics, minimal and optimal nutrient concentration requirements, cortical senescence, and hydraulic conductivities. To finalise the OSR parameters for the purpose of this project, details of the above parameters will need to be determined in Golden Promise, *HvCsIF3-RNAi*, and *HvCsIF9-RNAi* plants. Experiments on plant growth in a hydroponic environment allows easy access to root material for the purpose of measuring nutrient kinetics, nutrient stress factors, respiration, etc. In addition, we showed the decreased transpiration rate and stomata conductivity in the *HvCsIF3-RNAi* and *HvCsIF9-RNAi* plants grown in the glasshouse. This suggested potential water stress occurs in the transgenic plants. However, the water module of the current OSR version is simplistic and not fully developed for the prediction of plant-water interactions. Therefore, it was difficult to assess the water uptake kinetics and plant development under

drought stress. Recently, a more advanced water module has been successfully developed and used in the OSR rice model. The new water module will be optimised for different plant species including barley to allow the analysis of plant development under different drought conditions.

Appendix 1

Exploring the Role of Cell Wall-Related Genes and Polysaccharides during Plant Development



Appendix I – Published Manuscripts

Statement of Authorship

Title of Paper	Exploring the Role of Cell Wall-Related Genes and Polysaccharides during Plant Development
Publication Status	<input checked="" type="checkbox"/> Published <input type="checkbox"/> Accepted for Publication <input type="checkbox"/> Submitted for Publication <input type="checkbox"/> Unpublished and Unsubmitted work written in manuscript style
Publication Details	Matthew R. Tucker ^{1,*} , Haoyu Lou ^{1,2} , Matthew K. Aubert ^{1,2} , Laura G. Wilkinson ^{1,2} , Alan Little ¹ , Kelly Houston ³ , Sara C. Pinto ⁴ and Neil J. Shirley ^{1,2}


Principal Author

Name of Principal Author (Candidate)	Matthew R. Tucker		
Contribution to the Paper	Compiled information and wrote manuscript. I hereby certify that the statement of authorship is accurate.		
Overall percentage (%)	60%		
Certification:	This paper reports on original research I conducted during the period of my Higher Degree by Research candidature and is not subject to any obligations or contractual agreements with a third party that would constrain its inclusion in this thesis. I am the primary author of this paper.		
Signature		Date	22/11/2018

Co-Author Contributions

By signing the Statement of Authorship, each author certifies that:

- i. the candidate's stated contribution to the publication is accurate (as detailed above);
- ii. permission is granted for the candidate to include the publication in the thesis; and
- iii. the sum of all co-author contributions is equal to 100% less the candidate's stated contribution.

Name of Co-Author	Haoyu Lou		
Contribution to the Paper	Compiled information and contributed to the preparation of the manuscript. I hereby certify that the statement of authorship is accurate.		
Signature		Date	23/11/2018

Name of Co-Author	Matthew K. Aubert		
-------------------	-------------------	--	--

Appendix 1

Contribution to the Paper	Compiled information and contributed to the preparation of the manuscript. I hereby certify that the statement of authorship is accurate.		
Signature		Date	21/11/2018

Please cut and paste additional co-author panels here as required.

Name of Co-Author	Laura G. Wilkinson		
Contribution to the Paper	Compiled information and contributed to the preparation of the manuscript. I hereby certify that the statement of authorship is accurate.		
Signature		Date	22/11/2018

Name of Co-Author	Alan Little		
Contribution to the Paper	Compiled information and contributed to the preparation of the manuscript. I hereby certify that the statement of authorship is accurate.		
Signature		Date	22/11/18

Name of Co-Author	Kelly Houston		
Contribution to the Paper	Compiled information and contributed to the preparation of the manuscript. I hereby certify that the statement of authorship is accurate.		
Signature		Date	22/11/2018

Name of Co-Author	Sara C. Pinto		
Contribution to the Paper	Compiled information and contributed to the preparation of the manuscript. I hereby certify that the statement of authorship is accurate.		
Signature		Date	23/11/2018

Name of Co-Author	Neil J. Shirley		
-------------------	-----------------	--	--

Contribution to the Paper	Compiled information and contributed to the preparation of the manuscript. I hereby certify that the statement of authorship is accurate.		
Signature		Date	21/11/18

Review

Exploring the Role of Cell Wall-Related Genes and Polysaccharides during Plant Development

Matthew R. Tucker ^{1,*}, Haoyu Lou ^{1,2}, Matthew K. Aubert ^{1,2}, Laura G. Wilkinson ^{1,2}, Alan Little ¹, Kelly Houston ³, Sara C. Pinto ⁴ and Neil J. Shirley ^{1,2}

- ¹ School of Agriculture, Food and Wine, Waite Research Institute, The University of Adelaide, Glen Osmond, SA 5062, Australia; haoyu.lou@adelaide.edu.au (H.L.); matthew.aubert@adelaide.edu.au (M.K.A.); laura.g.wilkinson@adelaide.edu.au (L.G.W.); alan.little@adelaide.edu.au (A.L.); neil.shirley@adelaide.edu.au (N.J.S.)
- ² Australian Research Council Centre of Excellence in Plant Cell Walls, The University of Adelaide, Glen Osmond, SA 5062, Australia
- ³ Cell and Molecular Sciences, The James Hutton Institute, Dundee DD2 5DA, UK; Kelly.Houston@hutton.ac.uk
- ⁴ Departamento de Biologia, Faculdade de Ciências da Universidade do Porto, 4169-007 Porto, Portugal; sarapintomendes94@gmail.com
- * Correspondence: matthew.tucker@adelaide.edu.au; Tel.: +61-8313-9241

Received: 29 April 2018; Accepted: 29 May 2018; Published: 31 May 2018

Abstract: The majority of organs in plants are not established until after germination, when pluripotent stem cells in the growing apices give rise to daughter cells that proliferate and subsequently differentiate into new tissues and organ primordia. This remarkable capacity is not only restricted to the meristem, since maturing cells in many organs can also rapidly alter their identity depending on the cues they receive. One general feature of plant cell differentiation is a change in cell wall composition at the cell surface. Historically, this has been viewed as a downstream response to primary cues controlling differentiation, but a closer inspection of the wall suggests that it may play a much more active role. Specific polymers within the wall can act as substrates for modifications that impact receptor binding, signal mobility, and cell flexibility. Therefore, far from being a static barrier, the cell wall and its constituent polysaccharides can dictate signal transmission and perception, and directly contribute to a cell's capacity to differentiate. In this review, we re-visit the role of plant cell wall-related genes and polysaccharides during various stages of development, with a particular focus on how changes in cell wall machinery accompany the exit of cells from the stem cell niche.

Keywords: cell wall; polysaccharide; development; glycosyltransferase; glycosyl hydrolase; differentiation; shoot meristem; root meristem

1. Introduction

As plant cells divide away from apical meristems, their molecular and biochemical profiles change. At the molecular level, cells adopt identities through changes in their nuclear morphology, genomic landscape, and transcriptional signatures. Changes also occur at the periphery of the cell, most notably in the abundance and organization of cell wall components such as cellulose, non-cellulosic polysaccharides, phenolic acids, lipids, and proteins [1]. Sometimes this results in terminal differentiation, for example in vascular tissues such as lignified mature fibers [2]. Changes in wall composition influence the downstream function of cells as storage units, structural networks, and solute transporters [3]. In many cases, differentiation also influences the capacity of cells to respond to stresses imparted through pathogens and the environment [4].

Despite its importance for growth and reproduction, plant cell differentiation is infrequently irreversible [5]. Many plant cells, not only those located in the meristems, possess the remarkable ability to adopt new identities. This can be a simple switch in identity between adjoining cells; for example, in the developing maize seed (kernel), where aberrant inward (periclinal) divisions of aleurone cells at the periphery result in one daughter cell retaining aleurone identity and the other adopting inner starchy endosperm identity [6]. The same thing can occur in more complex systems such as apomictic (asexual) plants, where ovule cells that adjoin normal sexual cells can spontaneously adopt germline-like identity and initiate a form of gametophyte development [7,8]. However, the plant meristem remains the epitome of differentiation capacity; meristematic stem cells can give rise to many different cell types, often referred to as pluripotency (the ability to either give rise to all cells and tissues in an organ) or totipotency (the ability to give rise to the entire organism) [9]. At a fundamental level, this indicates that fate is not fixed, and plant cells must maintain flexible cellular properties compatible with differentiation.

Much of our knowledge regarding cell differentiation has come from *in vitro* studies involving tissue culture, during which plant cells can be induced to de-differentiate (essentially reverse differentiation and lose specialized characteristics [10]), forming protoplasts or callus [11]. Somewhat similar to pluripotent stem cells, these totipotent undifferentiated cells can be stimulated to give rise to entire new tissues and eventually whole plants, depending on the correct exogenous application of growth hormones and vitamin supplements. Importantly, one component of *in vitro* de-differentiation appears to be modification or removal of the cell wall from the progenitor cell [12,13]. Moreover, in some cell types, the over-accumulation of specific cell wall components even appears to prevent de-differentiation or regeneration [14,15]. Therefore, variation in cell wall composition may contribute to the maintenance of cellular identity in some cases, while promoting the capacity for differentiation in others. How this is determined has yet to be addressed in sufficient detail, since it requires a thorough qualitative and quantitative assessment of cell wall composition at the single cell level.

Prevailing models suggest that there are two types of walls in plants; primary cell walls are relatively thin and flexible and are synthesized during cell growth and division, while secondary cell walls provide strength and rigidity in tissues that are no longer growing [16,17]. In general, the plant cell wall comprises a framework of cellulose microfibrils coated in diverse non-cellulosic polysaccharides. Xyloglucan (XyG) is proposed to cross-link cellulosic microfibrils, while pectins such as homogalacturonan (HG) and rhamnogalacturonan (RG) form a structurally diverse glue that provides flexibility or stiffness depending on chemical modifications [18,19]. Other classes of polymers include 1,3- β -glucan, 1,3;1,4- β -glucan, mannan, arabinan, xylan, and phenolic compounds such as lignin, which vary depending on the cell type, species, and developmental age, and appear to fulfil diverse roles [20–23]. Figure 1 shows thin sections from a number of dicot and monocot tissues labelled with cell wall-related antibodies and/or viewed under UV light, highlighting the diversity of polysaccharides present in growing tissues, as well as specific differences between organs, tissues, and individual cell types. How the different polymers interact within the cell wall matrix is constantly being revisited; direct covalent connections have been reported between pectin and xylan [24], xylan and lignin [25], and xyloglucan and cellulose [26]. However, the nature of the cross-linkages and hydrophobic interactions within the wall are not fully understood, and present significant challenges for the prediction and modelling of cell wall physicochemical properties [27]. Additional complexity is conveyed through glycoproteins such as arabinogalactan proteins (Figure 1), and other cell wall proteins such as proline-rich proteins, extensins, and expansins [28].

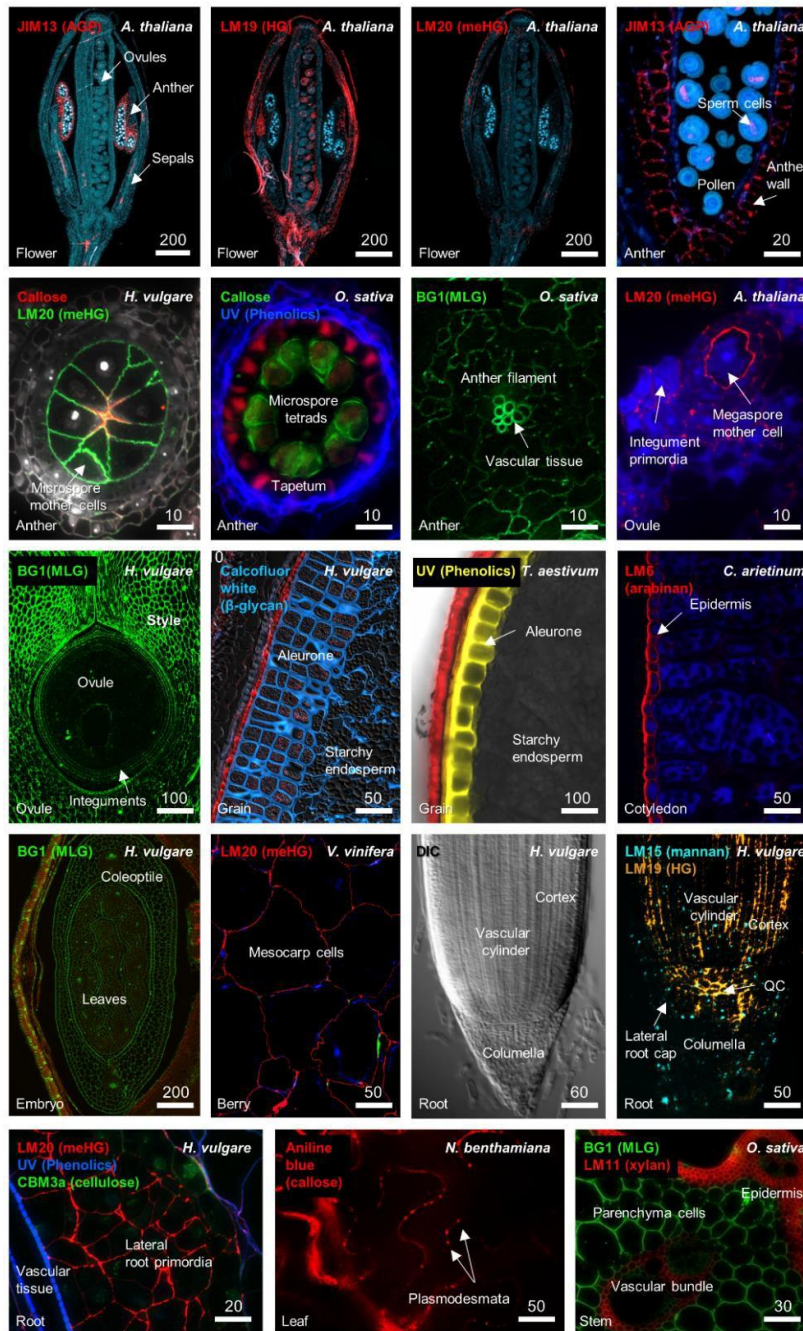


Figure 1. Detection of different cell wall components in distinct tissues of *Arabidopsis thaliana*, *Hordeum vulgare* (barley), *Oryza sativa* (rice), *Cicer arietinum* (chickpea), *Vitis vinifera* (grape), *Nicotiana benthamiana* (tobacco), and *Triticum aestivum* (bread wheat). The tissue origin of each section is indicated at the bottom left of each panel. The antibody or stain is indicated at the top left of each panel. Labelling of polymers was achieved through the use of diverse antibodies including BG1 (1,3;1,4-β-glucan), JIM13 (arabinogalactan proteins, AGP), LM19 (homogalacturonan, HG), LM20 (methylsterified homogalacturonan, meHG), callose (1,3-β-glucan), LM15 (mannan), LM6 (arabianan), LM11 (arabinoxylan), and CBM3a (cellulose), or stains such as aniline blue (1,3-β-glucan) and Calcofluor White (β-glycan), or UV autofluorescence. Differential contrast (DIC) microscopy was used to image the barley root tip and is shown as a reference for the adjoining immunolabelled sample. Images were generated for this review, but further details can be found in previous studies [23,29–32]. Scale bar dimensions are shown in μm.

Classical studies in two-celled embryos of the alga *Fucus* [33] showed that there is a direct role of the cell wall in maintaining cellular fate. Extending this hypothesis to examine the role of the cell wall during differentiation of specialized cells and tissues of higher plants has proved challenging, partially due to compositional complexity and the sub-epidermal location of cells [34]. Moreover, it remains technically challenging to view the cell wall in a high throughput manner, and with enough resolution, to identify specific quantitative and qualitative changes in composition that directly accompany or precede changes in cellular identity. Dogma suggests that as cells divide into new microenvironments they are exposed to new combinations of hormones and signals, which subsequently activate receptors at the plasma membrane to cue signal cascades and downstream transcriptional changes [35,36]. As a result of this feedback, the cell wall is remodeled to introduce new or modified polymers that exhibit different properties and contribute to new cellular identity. This almost certainly involves changes in biomechanical properties, which have been extensively reviewed in recent times [37–39]. However, in order to receive and process a particular differentiation signal, what basic structural or biochemical features are required? Do specific polysaccharides or cell wall proteins enable the preferential accumulation of receptors, transmission of signals or the synthesis of signaling molecules that potentiate differentiation? Is there an ideal wall composition required for cell differentiation? Studies in recent years provide some answers, hinting that the cell wall plays a dynamic role in development, and that cues to initiate remodeling may arise from and depend on the composition of the wall itself. As mentioned above, recent reviews have considered in detail the role of cell wall integrity and sensors in controlling plant growth [40,41]. In this review, we consider molecular and genetic evidence supporting a role for distinct cell wall polysaccharides during plant development, particularly in light of recent studies and technological advances in cell-type specific transcriptional profiling.

2. Cell Wall Modification during Growth, Differentiation, and Development

The molecular determinants of cell wall composition incorporate large families of enzymes including glycosyltransferases (GT), glycosylhydrolases (GH), methyltransferases, and acetyltransferases (see the Carbohydrate Active enZYme database; CAZy [42]). The location and presumed site of activity of these enzymes can vary between the Golgi, the plasma membrane or a combination of both [43]. The addition of new polymers to a wall through the action of glycosyltransferases can immediately lead to changes in the pH, providing substrates for de-acetylation [44], de-esterification [19], and transglycosylation [45], and even new binding sites for receptors [46,47]. Specific differences in cell wall composition can be observed at different stages of development, between adjoining cells and tissues, and between monocots and dicots (See Figure 1). Several polymers that are labeled in Figure 1, pectin and callose, have been implicated in key stages of plant development. In the following sections we consider these polysaccharides, in addition to several “structural” polymers, with a view to addressing how their synthesis and/or modification can influence differentiation and development.

2.1. Pectin

Pectin is an important polymer during development since it can undergo considerable modification once it is deposited in the cell wall [48]. Multiple types of pectin are detected in the primary walls of dicots and monocots, including homogalacturonan (HG), rhamnogalacturonan-I (RG-I), rhamnogalacturonan-II (RG-II), and xylogalacturonan (XGA) [48,49]. Immunolabelling shows that pectic polymers are particularly enriched in young flowers, ovules, fruits, and roots (Figure 1). RG-I is detected in a number of tissues and is particularly prominent in the *Arabidopsis* seed coat [50] and the transition zone of developing roots [51]. The tight developmental regulation of RG-I deposition in seedling roots suggests it may play a role in cell expansion [51], but its exact role and the details of its biosynthesis remain unclear [52]. HG is methylesterified (meHG) during synthesis in the Golgi, and this forms a substrate for pectin methylesterase (PME, CE8), which depending on the cellular context can lead to loosening or strengthening of cell walls [19]. Clear roles for PME have been demonstrated in meristem development, seed mucilage biosynthesis, and pollen tube growth [53–55]. In the shoot meristem, organ primordia initiation requires demethylesterification of HG in sub-epidermal layers through the action of PME [56], which reduces stiffness and promotes outgrowth (Figure 2). Negative regulation of *PME5* in the meristem dome by the *BELLRINGER* transcription factor ensures that the meHG substrate is only targeted by *PME5* at the flanks of the meristem, leading to correct positioning of organ primordia [37]. Similarly, in the root, alterations in PME activity and increased demethylesterification are associated with expansion of cell types in the root tip [57,58].

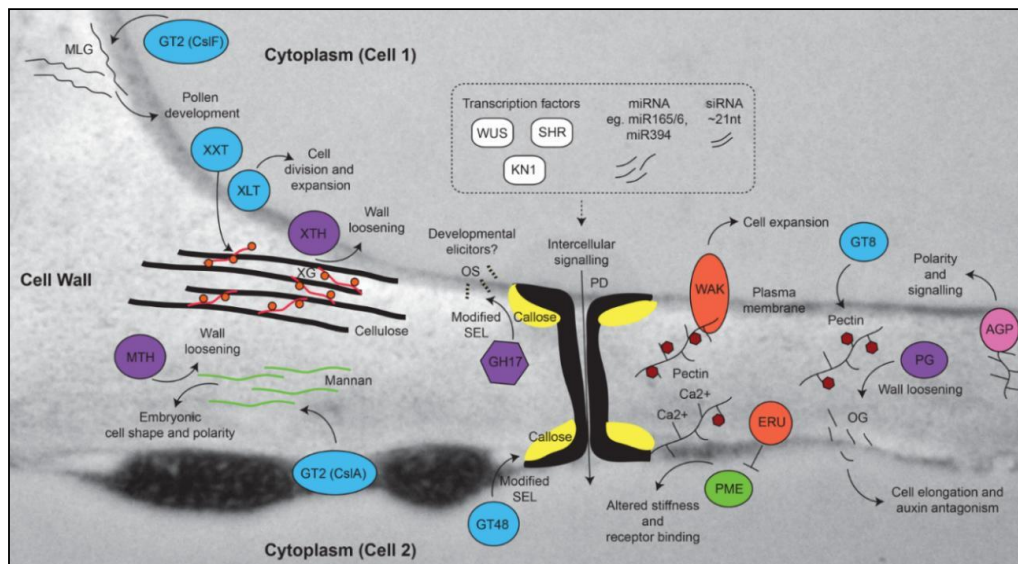


Figure 2. Cell wall components that contribute to growth, development, and differentiation. The model shows polymers superimposed on a TEM image of a leaf cell wall, including 1,3;1,4- β -glucan (MLG), cellulose, xyloglucan (XG), mannan, callose, and pectin. Enzymes that contribute to the biosynthesis or modification of these components are shown. The spatial separation of polymers is only shown for schematic purposes. Biosynthetic enzymes are shown in blue, hydrolytic enzymes are shown in purple, receptors are shown in orange, mobile transcription factors are shown in white, pectin methyltransferase (PME) is shown in green, and arabinogalactan protein (AGPs) in pink. Deposition and hydrolysis of callose at the neck of plasmodesmata (PD) can alter the size exclusion limit (SEL) of the PD, hence limiting the mobility of intercellular signaling molecules such as transcription factors (e.g., WUSCHEL [59], SHORT ROOT [60], and KNOTTED [61]), microRNAs (miRNAs [60,62]), and short interfering RNAs (siRNAs [63,64]). Hydrolysis of callose by GH17 enzymes leads to the release of stimulatory oligosaccharides (OS) from the glucan backbone in fungi, but it remains unclear if similar OS contribute to growth and development in plants. By contrast, release of oligogalacturonides (OG) from pectin by polygalacturonase (PG) has been implicated in plant development through antagonistic effects on auxin pathways. The small circles on XG indicate galactosyl residues present due to the activity of XLT2 (xyloglucan galactosyltransferase). GT8 family enzymes contribute to the biosynthesis of pectin, which is usually synthesized in a methylated form (e.g., methylated homogalacturonan; meHG). Removal of methyl groups (red hexagons) through the activity of PME can lead to calcium binding and subsequent cross-linking of pectin polysaccharides, which influences wall stiffness. GT, glycosyltransferase, XXT, xylosyltransferase, MTH, mannan transglycosylase/hydrolase, XTH, xyloglucan transglycosylase/hydrolase, CslF, cellulose synthase-like F, CslA, cellulose synthase-like A, GH, glycosyl hydrolase, WAK, wall-associated kinase, ERU, ERULUS receptor-like kinase.

Other factors that influence cell expansion are the Wall-Associated Kinases (WAKs), which directly bind pectin polymers in the cell wall in a way that is at least partially dependent upon the degree of methylation [65,66] (Figure 2). Mutations in several WAK genes suggest they play a role in mediating resistance against various pathogens [67,68], as well as in cell expansion during development [69]. Another putative receptor involved in the pectin pathway is the *Arabidopsis Catharanthus roseus* receptor-like kinase 1-like (CrRLK1) ERULUS (ERU) protein, which is required for correct root hair formation, and regulates cell wall composition through negative control of PME activity [70] (Figure 2). Interestingly, ERU transcription is downregulated in several mutants showing changes in cell wall composition related to pectin, suggesting a possible feedback mechanism from the wall to regulate pectin composition and root hair development. ERU is part of the FERONIA (FER) family of kinases [41,71] that are implicated in fertilization, cell wall sensing, and root growth. Defects in the FER signaling pathway lead to pronounced defects in pectin composition of pollen tubes and root hairs, and a recent report indicates that FER directly interacts with pectin *in vivo* and *in vitro* [72]. Curiously, the ability of cell walls to sense change may be restricted to components of the primary wall, since limited signaling and transcriptomic responses were observed in mutants showing altered secondary cell wall biosynthesis in *Arabidopsis* [73].

Finally, modification of pectin by hydrolytic enzymes can lead to the release of small fragments called oligogalacturonides, which are reported to effect plant growth and development [74]. These pectin fragments impact diverse physiological processes, including fruit ripening in tomato [48] and stem elongation in pea [75] via a mechanism that appears to involve antagonism with the plant hormone auxin [76]. In summary, these studies indicate that specific pectic polymers within the wall may predispose cells to respond to stimuli that influence growth and differentiation.

2.2. Callose and Plasmodesmata

Another polymer that influences cellular differentiation is callose. Comprised of a water-insoluble linear form of (1,3)- β -glucan, callose is an atypical cell wall polysaccharide in that it is not often co-extensive throughout cell walls with pectin and cellulose but has specific restricted occurrences and functions in locations such as the cell plate, reproductive tissues, and plasmodesmata (PD). Genes involved in callose biosynthesis and hydrolysis are well characterized and include the 1,3- β -glucan synthases (GT48 family) and 1,3- β -glucan hydrolases (GH17 family), respectively. These enzymes have historically been associated with roles in pathogen response, dormancy, cell division, and plant reproduction [21,77,78], but recent studies emphasize their general importance in controlling intercellular transport of developmental regulators through PD (Figures 1 and 2). PD are intercellular channels embedded in the cell wall that provide a cytoplasmic continuum between cells [79]. Different types of PD can be detected in the cell wall, which vary in terms of their structure and their arrangement within and between cell layers [80,81]. The formation of lateral roots in *Arabidopsis* depends upon restrictive callose deposits in the cell wall adjoining the PD [82], often referred to as the “neck” region. PD also regulate intercellular movement of transcription factors and microRNAs between the stele and endodermis to control xylem development [60]. Although the cues that drive PD formation are unknown, PD are present in many cell types and are accompanied by increased pectin and decreased cellulose deposits in flanking cell wall regions [83]. Enzymes regulating callose biosynthesis and turnover are enriched in the general PD proteome [84] in addition to several PMEs, polygalacturonases and diverse receptor kinases that likely influence PD function [85,86]. The biochemical analysis of PD highlights a potential relationship between pectin and callose that has yet to be explored in significant detail.

The removal of callose from PD and specialized cell walls in the anthers and ovule is mediated by GH17 enzymes, which form a large family found in archaea, bacteria, and eukaryotes [87]. In general, GH17 activity is likely to influence growth and development in several ways by (1) decreasing the size exclusion limit (SEL) of PD and allowing increased symplastic intercellular transport [88]; (2) removing apoplastic barriers that are proposed to insulate cells such as the megaspores or microspores against mobile signals [89,90] and (3) removing a transient matrix for deposition of secondary polymers during cytokinesis and cell division [91]. Consistent with a role in regulating the SEL of PD, studies in the shoot meristem have shown that mobile tracers are free to move between distinct “symplastic fields”, which incorporate different zones and layers [92,93]. This indicates that differential regulation of PD conductance is likely to be required for meristem cell identity and function. One key transcription factor involved in meristem maintenance, WUSCHEL, moves from the organizing centre (OC) of the meristem into above-lying stem cells through PD [59]. Therefore, the presence of PD and associated cell wall polymers is another example by which cells may be predisposed to be responsive to non-cell autonomous stimuli; in essence, the PD and adjoining regions of cell wall provide a substrate for receptor binding as well as for cell wall remodeling activities that can influence intercellular signaling and differentiation (Figure 2).

In addition to these developmental functions, GH17 enzymes also form a defensive barrier during pathogen attack that targets 1,3- β -glucan polymers in the fungal cell wall. A recent study showed that non-branched fungal 1,3- β -glucan oligosaccharides are able to trigger immune responses in *Arabidopsis* via CERK1 (chitin elicitor receptor kinase 1) [94]. It is tempting to speculate that similar to oligogalacturonides, cleavage of endogenous 1,3- β -glucan polymers might release backbone oligosaccharides that elicit responses during growth and development (Figure 2).

2.3. Roles for Other “Structural” Polymers in Growth and Development

1,3;1,4- β -glucan is predominantly found in monocots, particularly the *Poaceae*, where it accumulates in the primary and secondary walls of diverse tissues [95,96] (Figure 1). Evidence suggests that accumulation of 1,3;1,4- β -glucan is required for correct grain fill in barley and wheat [97,98]. However, genetic studies also reveal specific developmental abnormalities, such as male infertility, in rice plants lacking the primary biosynthetic enzyme controlling 1,3;1,4- β -glucan biosynthesis [99] (Cellulose synthase-like F6; CslF6). In barley, tissue-specific over-accumulation of 1,3;1,4- β -glucan appears to inhibit signal and/or solute transmission

[29,97] while barley *cslf6* mutants are shorter and show defects in leaf growth [100]. This is perhaps unsurprising given that *CsIF6* is expressed in a range of tissues [101], however, the specific role of 1,3;1,4- β -glucan and the *CsIF* gene family in plant development requires further investigation.

Unlike 1,3;1,4- β -glucan, xyloglucan (XyG) is a highly branched polysaccharide found in the primary cell wall of many plant tissues and is characterized as a structural cell wall component that binds to cellulose [102] (Figure 2). Remarkably, mutants lacking activity of three xylosyltransferase (*XXT*) genes (*XXT1*, 2 and 5) contain no detectable xyloglucan in their cell walls, yet develop relatively normally apart from defects in root hairs [103]. By contrast, *murus3* mutants that are deficient for a XyG-specific galactosyltransferase contain normal levels of xyloglucan, but in a form that is depleted of galactosyl substituents, and this results in extreme developmental defects including dwarfism [104]. Hence, while XyG is not required per se for *Arabidopsis* development, incorrect substitution of XyG may compromise interactions between different wall polymers, resulting in a cell wall composition that is incompatible with cell growth.

Similar to xyloglucan, several types of structurally diverse mannans are also linked to the cellulose network providing mechanical support [105], while others are involved in carbohydrate storage. Loss-of-function mutations in the *Cellulose synthase-like A* (*CsIA*) 2, 3, and 9 genes, encoding putative glucomannan synthases, result in no detectable glucomannan in stems but plants appear phenotypically normal [106]. However, mutants lacking function of the *CsIA7* gene show embryo lethality, suggesting that in some tissues glucomannan is a critical component for growth and differentiation [107]. Although the mechanistic basis for this lethality is unclear, the *csIA7* mutant embryos appear remarkably similar to those showing defects in developmental patterning and organ differentiation, such as double mutants of the *WUSCHEL-HOMEODOMAIN* 8/9 transcription factors [108] and *ARGONAUTE* 1/10 genes involved in post-transcriptional gene silencing [109,110]. This may indicate that targets of these transcriptional and post-transcriptional regulators converge at the cell wall, or that a distinct cell wall composition contributes to downstream function of these regulatory pathways. Interestingly, both mannan and xyloglucan are targets of transglycosylase enzymes activities, which essentially cleave the polysaccharide chain and attach it to a new chain to retain strength in the cell wall (Figure 2). Both mannan endotransglycosylases/hydrolases (MTH) and xyloglucan endotransglycosylases/hydrolases (XET/XTH) have been implicated in fruit development. LeMAN4a, an MTH from tomato, exhibits transglycosylase activity and is expressed in young floral buds where it is hypothesized to function in tissue softening [111]. Similarly, *XTH* genes are associated with fruit development in persimmon, apple, and tomato [112,113]. Therefore, even in the case of polysaccharides that have historically been associated with structural functions, there is evidence to suggest their presence in the wall may provide a substrate for remodeling enzymes that impact growth and differentiation during diverse stages of plant development.

1. Specific Cell Wall-Related Genes Accompany Differentiation in Meristematic Zones

Antibodies and glyco-arrays are an outstanding resource [114,115] to localize and identify specific cell wall-related epitopes, and this is highlighted by the distinct labelling patterns shown in Figure 1. The limitation of antibodies is that they only provide a limited view of the chemical complexity present in a cell wall at a particular time point. Technologies that enable local qualitative and quantitative assessments of wall complexity, particularly in the case of the shoot and root meristem and reproductive tissues, would provide a significant advantage in understanding cell wall changes during differentiation. Methods such as coherent anti-Stokes Raman scattering (CARS [1]) and FTIR microspectroscopy [116] may enable specific compositional changes to be identified, although they are yet to deliver the required precision for cell-type specific analysis during development. By contrast, at the molecular level, definition of the transcriptional programs underlying cell wall formation has recently become much more accessible. The analysis and identification of cell wall-related genes that define specific cell types and/or show altered expression during development remains a viable approach to assess the role of different cell wall components in facilitating differentiation.

In *Arabidopsis*, studies have utilized the elegant method of fluorescence-assisted cell sorting (FACS) to collect specific populations of cells from developing tissues [117–119]. This approach was used successfully in *Arabidopsis* roots [117,118] to profile RNA from, among others, cell types located in the meristematic zone including the quiescent centre (QC), the adjoining columella, and the lateral root cap (LRC). The QC is marked by the expression of *AGL42* and *WOX5* genes and contains slowly dividing, “undifferentiated” cells that stimulate the formation of adjoining stem cells [120] (Figure 1). Underlying the QC are the columella initials; stem cells that divide periclinally to give rise to one daughter that adopts columella fate and another that retains stem cell identity. Similarly, the LRC initial cells adjoin the QC and give rise to all cells in the lateral root cap. These cell types are in close proximity but assume different identities as soon as they divide away from the QC. Therefore, the cell-type specific transcriptional datasets provide an excellent resource to assess changes in the

cell wall machinery during differentiation.

Houston et al. [4] examined transcriptional datasets from *Arabidopsis* and other species to highlight cell wall gene families associated with cell wall remodeling during abiotic stress and pathogen attack. A similar survey of the *Arabidopsis* root cell-type specific RNA profiles [118] reveals a comprehensive set of cell wall genes potentially contributing to growth and differentiation (Figure 3). Relative to the QC (as an undifferentiated reference), cells that adopt LRC or columella fate express different gene families involved in polysaccharide biosynthesis and modification. Examples include the arabinogalactan proteins (AGPs), pectin methylesterases (CE8), glucuronyl/galacturonosyltransferases (GT8), and xylan 1,4- β -xylosyltransferases (GT43). Arabinogalactan proteins are cell wall proteins that have been implicated in many aspects of growth and development [30,31,121,122], while the other families are implicated in pectin and xylan biosynthesis and modification. The majority of these gene families are upregulated as cells adopt columella or LRC identity, consistent with the formation of new wall types compared to the relatively naïve wall in the undifferentiated QC. Notably, within the QC itself, representatives from the pectate lyase (PL1), expansin, 1,3- β -glucanase (GH17), and 1,3- β -glucan synthase (GT48) families are up-regulated, hinting at a key requirement for intercellular signaling and wall flexibility. This analysis exemplifies how transcriptomic studies can enable identification of cell wall-related genes and families that accompany changes in cell identity during differentiation. In many cases, these transcriptional changes directly relate to alterations in root cell wall composition [123] indicating a close link between transcript abundance and putative enzyme activity.

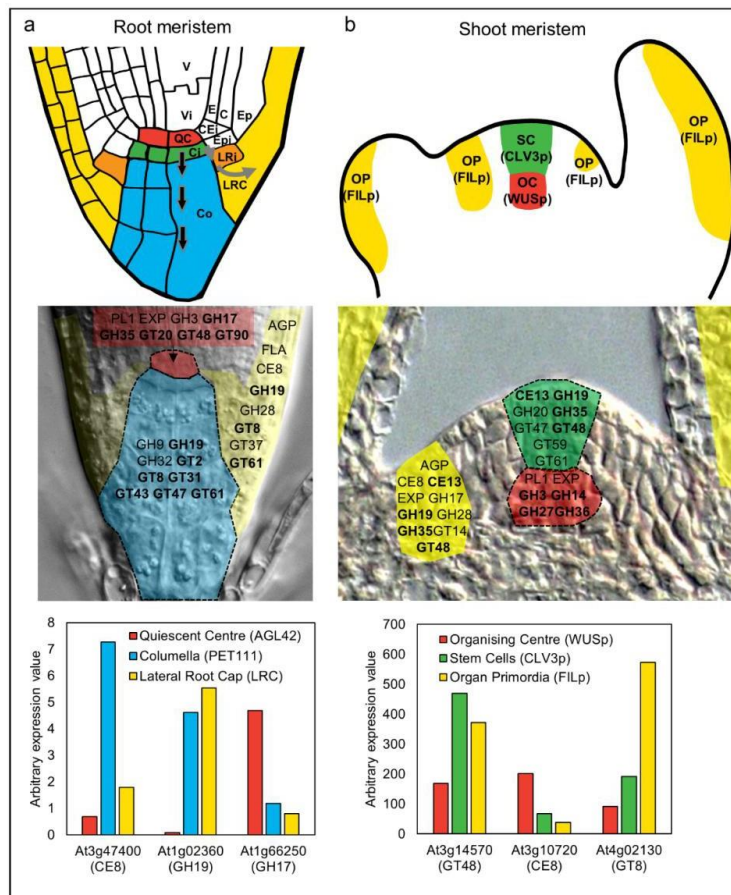


Figure 3. Analysis of cell wall-related gene expression during differentiation of stem cells in the root and shoot meristem of *Arabidopsis thaliana*. The upper panels in (a,b) show schematic representations of the root and shoot apical meristem [120]. (a) In the root meristem, initial cells (stem cells) directly adjoining the QC enter differentiation pathways as they divide away from the niche (shown by arrows for columella and lateral root cap). V, vasculature, Vi, vascular initial, QC, quiescent centre, E, endodermis, C, cortex, CEi, cortex/endodermis initials, Epi, epidermal initials, Ep, epidermis, LRI, lateral root cap initial, LRC, lateral root cap, Ci, columella initial, Co, columella. (b) In the shoot meristem, the organizing center (OC) functions via WUSCHEL (WUS) to maintain the stem cells (SC) in an undifferentiated state. The stem cells express the signal peptide CLAVATA3 (CLV3). Divisions of the stem cells provide daughters that enter differentiation pathways at the flanks of the meristem and become organ primordia (OP), which is marked by expression of genes such as *FILAMENTOUS FLOWER* (*FIL*). The second row of panels highlights gene families encoding CAZy carbohydrate-related enzymes [42] that are enriched in each meristem cell type according to FACS-mediated sorting and transcriptional profiling [118,119]. The genes are superimposed on sections of root and shoot meristem tissues. Family names in bold indicate that multiple members from the same family were up-regulated in the QC or OC (depending on the meristem) relative to both of the other cell types. GH, glycosyl hydrolase, GT, glycosyltransferase, PL, pectate lyase, AGP, arabinogalactan protein, EXP, expansin, CE, carbohydrate esterase, FLA, fasciclin-like arabinogalactan protein. See Table 1 for putative functions of enzyme families. The third row of panels shows expression patterns of selected CAZy family members in the different meristem cell types. Several of the individual genes reflect the behavior of the entire family. For example, At1g02360 is up-regulated in the columella and LRC relative to the OC, and this is a pattern shown for many GH19 family members. However, other genes such as At3g47400, At3g10720, and At4g02130 show unique patterns compared to other members of their families. The reason why multiple family members are recruited into some cell-type preferential expression pathways, while in others only individual members are expressed, remains to be elucidated.

In the shoot apical meristem (SAM), Yang et al. (2016) characterized changes in cell wall composition by immunolabelling, in addition to profiling cell wall-related gene expression in different meristematic regions [124]. Their results indicate that as cells divide through the meristem, different enzymes build new walls compared to those that build maturing walls. Complementing this, studies have examined transcriptional changes at the level of individual meristematic cell types (Figure 3). The organizing centre (OC) of the SAM is marked by expression of the *WUSCHEL* gene and is somewhat similar to the root QC, in that it is undifferentiated, slow to divide, and specifies adjoining cells as stem cells [120]. The shoot stem cells express the *CLAVATA3* gene, and as they divide anticlinally, they exit the control of the OC and enter organ differentiation pathways where expression of transcription factors such as *FILAMENTOUS FLOWER* are detected (Figure 3). Yadav et al. (2009) used these cell-type specific markers to isolate and transcriptionally profile shoot stem cell types [119]. Around half of the *Arabidopsis* CAZy cell wall families are up-regulated in organ primordia but downregulated in the stem cells relative to the OC; gene families include the expansins (EXP), fasciclin-like arabinogalactan proteins (FLAs), pectate lyases (PL1), pectin methylesterases (CE8), polygalacturonases (GH28), and endo-arabinanases (GH43). The lack of glycosyltransferases and abundance of cell wall modifying enzymes suggests that, similar to the root meristem, cell wall remodeling is the predominant feature of cell and organ differentiation in the shoot. Interestingly, gene families that are up-regulated in the stem cells relative to the OC and organ primordia include a number of key polysaccharide synthases and hydrolases such as 1,3- β -glucan synthase (GT48), arabinosyl/xylosyltransferase (GT61), and xylanase (GH10). As discussed above, the GT48 genes contribute to callose biosynthesis, and their up-regulation may relate to the formation of symplastic zones through altered PD conductance. Although a direct role for GT61 and GH10 genes during development has not been explicitly reported, GT61 enzymes have been implicated in substitution of polysaccharides to potentially influence wall polymer viscosity in seed-coat epidermal cells [125,126], and some GH10 xylanases are expressed during secondary wall synthesis in poplar [127].

In summary, these studies show that as cells exit the stem cell niche and start differentiating, clear trends are seen in the transcriptional behavior of CAZy families. The CAZy signatures of distinct cell-types within the shoot and root meristem are summarized in Figure 3. It is important to note that despite their grouping via functional domains and proposed carbohydrate-related activities, the vast majority of the CAZy genes remain uncharacterized. The transcriptional profiles of the meristematic cells are remarkably dynamic yet similar between the shoot and root meristems, identifying key activities whose role in differentiation might be addressed in more detail through further mutant and cell-type specific analyses.

3. Perspectives

The basis for this review was to consider the role of the plant cell wall in growth and development, and to assess how cell wall polysaccharides might predispose cells to undergo differentiation. We have focused our attention on polysaccharides including pectin, callose, xyloglucan, and mannan, which fulfil roles during different stages of growth and development. The presence and modification of these polymers correlates with changes in cell identity and function, and their depletion through mutagenesis or transgenic modification results in altered plant development. Callose and pectin in particular provide multiple avenues to influence differentiation, initially through deposition and subsequently through hydrolysis, chemical modification, and receptor binding. Consistent with the chemical complexity of the cell wall, the transcriptional machinery underlying cell wall polysaccharide deposition and modification is intricate. However, common activities are identified in cell types that exit from apical (shoot and root) stem cell niches and initiate differentiation. This overlap suggests that while the cellular context (i.e., roots vs. shoots) and specific gene family members might differ, early stages of differentiation likely depend on a similar wall composition that is compatible with remodeling. In this context, it seems prudent to consider the cell wall in the same light as other key factors, such as genomic and epigenetic modifications, that facilitate important steps of the cell differentiation process.

Table 1. Protein families potentially involved in polysaccharide biosynthesis and modification in *Arabidopsis*.

CAZy Family	Putative Polysaccharide Target	Gene ID	Enzyme Description
AGP			arabinogalactan protein *
CE13	Pectin		pectin acetyltransferase
CE8	Pectin	PME	pectin methylesterase
EXP			expansin
FLA			fasciclin-like arabinogalactan protein
GH3	Glucan/Xylan/Xyloglucan		β -D-glucosidase, α -L-arabinofuranosidase,
GH5	Mannan	MTH	β -D-xylopyranosidase endo- β -mannanase

Appendix 1

GH9	Cellulose		cellulase
GH10	Xylan		endo- β -xylanase
GH14	Starch		β -amylase
GH16	Xyloglucan	XTH/XET	xyloglucan:xyloglucosyltransferases
GH17	Callose	GLUC	glucan endo-1,3- β -glucosidase
GH19	Chitin		chitinase; lysozyme
GH20			beta-hexosaminidase
GH27			α -galactosidase
GH28	Pectin	PG	polygalacturonase
GH32			invertase
GH35	Pectin/Xyloglucan		β -galactosidase
GH36			α -galactosidase
GT2	Cellulose/Mannan/1,3;1,4- β -glucan	CsIA/CsIF	cellulose synthase/cellulose synthase-like
GT8	Pectin/Xylan		homogalacturonan 1,4- α galacturonosyltransferase
			UDP-GlcA: xylan α -glucuronosyltransferase
GT14	AGP		UDP-GlcA: [arabinogalactan] 1,3- β -/1,6- β -galactan
GT20			1,6- β -glucuronosyltransferase
GT31	AGP/Pectin		alpha,alpha-trehalose-phosphate synthase [UDP-forming]
GT34	Xyloglucan	XXT	1,3- β -glucuronosyltransferase
GT37	Xyloglucan		xyloglucan 1,6- α -xylosyltransferases
GT43	Xylan		xyloglucan 1,2- α -fucosyltransferase
GT47	Xylan/Xyloglucan	MUR3	glucuronoxylan glycosyltransferase
GT48	Callose	GSL	xylosyltransferase/xyloglucan galactosyltransferase
GT59			1,3- β -glucan synthase
GT61	Xylan/Xyloglucan		1,2- α -glucosyltransferase
GT90	Mannan		xylosyltransferase/arabinosyltransferase
PL1	Pectin		UDP-Xyl: (mannosyl) glucuronoxylomannan
			galactoxylomannan 1,2- β -xylosyltransferase
			pectate lyase

Note: * AGPs are not reported to exhibit enzymatic activity. Only families relevant to Figure 2 or the main text are included while genes that are referred to in the text are listed in the Gene ID column.

Author Contributions: All authors contributed to the Investigation, Visualization and Writing-Review & Editing of this review article.

Funding: This work was supported by the Australian Research Council grant numbers FT140100780 and CE110001007, the Grains Research and Development Corporation (GRDC) grant number GRS10938, the H2020- MSCA-RISE-2015 initiative "SEXSEED" and the Scottish Government via Rural Affairs Food and Environment Strategic Research (RESAS).

Acknowledgments: We wish to thank members of the Tucker lab for and four anonymous reviewers for helpful comments.

Conflicts of Interest: The authors declare no conflict of interest.

References

1. Zeng, Y.; Himmel, M.E.; Ding, S.Y. Visualizing chemical functionality in plant cell walls. *Biotechnol. Biofuels* **2017**, *10*, 1–16. [[CrossRef](#)] [[PubMed](#)]
2. Heo, J.O.; Blob, B.; Helariutta, Y. Differentiation of conductive cells: A matter of life and death. *Curr. Opin. Plant Biol.* **2017**, *35*, 23–29. [[CrossRef](#)] [[PubMed](#)]
3. Burton, R.A.; Gidley, M.J.; Fincher, G.B. Heterogeneity in the chemistry, structure and function of plant cell walls. *Nat. Chem. Biol.* **2010**, *6*, 724–732. [[CrossRef](#)] [[PubMed](#)]
4. Houston, K.; Tucker, M.R.; Chowdhury, J.; Shirley, N.; Little, A. The plant cell wall: A complex and dynamic structure as revealed by the responses of genes under stress conditions. *Front. Plant Sci.* **2016**, *7*, 984. [[CrossRef](#)] [[PubMed](#)]
5. Grafi, G.; Florentin, A.; Ransbotyn, V.; Morgenstern, Y. The stem cell state in plant development and in response to stress. *Front. Plant Sci.* **2011**, *2*, 53. [[CrossRef](#)] [[PubMed](#)]
6. Becraft, P.W.; Asuncion-Crabb, Y. Positional cues specify and maintain aleurone cell fate in maize endosperm development. *Development* **2000**, *127*, 4039–4048. [[PubMed](#)]
7. Tucker, M.R.; Araujo, A.C.; Paech, N.A.; Hecht, V.; Schmidt, E.D.; Rossell, J.B.; De Vries, S.C.; Koltunow, A.M. Sexual and apomictic reproduction in *Hieracium* subgenus *Pilosella* are closely interrelated developmental pathways. *Plant Cell* **2003**, *15*, 1524–1537. [[CrossRef](#)] [[PubMed](#)]
8. Tucker, M.R.; Okada, T.; Johnson, S.D.; Takaiwa, F.; Koltunow, A.M. Sporophytic ovule tissues modulate the initiation and progression of apomixis in *Hieracium*. *J. Exp. Bot.* **2012**, *63*, 3229–3241. [[CrossRef](#)] [[PubMed](#)]
9. Gailloch, C.; Lohmann, J.U. The never-ending story: From pluripotency to plant developmental plasticity. *Development* **2015**, *142*, 2237–2249. [[CrossRef](#)] [[PubMed](#)]
10. Verdeil, J.L.; Alemanno, L.; Niemenak, N.; Tranbarger, T.J. Pluripotent versus totipotent plant stem cells: Dependence versus autonomy? *Trends Plant Sci.* **2007**, *12*, 245–252. [[CrossRef](#)] [[PubMed](#)]
11. Fukuda, H.; Ito, M.; Sugiyama, M.; Komamine, A. Mechanisms of the proliferation and differentiation of plant cells in cell culture systems. *Int. J. Dev. Biol.* **1994**, *38*, 287–299. [[PubMed](#)]
12. Ikeuchi, M.; Ogawa, Y.; Iwase, A.; Sugimoto, K. Plant regeneration: Cellular origins and molecular mechanisms. *Development* **2016**, *143*, 1442–1451. [[CrossRef](#)] [[PubMed](#)]
13. Ikeuchi, M.; Sugimoto, K.; Iwase, A. Plant callus: Mechanisms of induction and repression. *Plant Cell* **2013**, *25*, 3159–3173. [[CrossRef](#)] [[PubMed](#)]
14. Lozovaya, V.; Gorshkova, T.; Yablokova, E.; Zabolotina, O.; Ageeva, M.; Rumyantseva, N.; Kolesnichenk, E.; Waranyuwat, A.; Widholm, J. Callus cell wall phenolics and plant regeneration ability. *J. Plant Physiol.* **1996**, *148*, 711–717. [[CrossRef](#)]
15. Chen, C.C.; Fu, S.F.; Lee, Y.I.; Lin, C.Y.; Lin, W.C.; Huang, H.J. Transcriptome analysis of age-related gain of callus-forming capacity in *Arabidopsis* hypocotyls. *Plant Cell Physiol.* **2012**, *53*, 1457–1469. [[CrossRef](#)] [[PubMed](#)]
16. Cosgrove, D.J.; Jarvis, M.C. Comparative structure and biomechanics of plant primary and secondary cell walls. *Front. Plant Sci.* **2012**, *3*, 204. [[CrossRef](#)] [[PubMed](#)]
17. Hofte, H.; Voxeur, A. Plant cell walls. *Curr. Biol.* **2017**, *27*, R865–R870. [[CrossRef](#)] [[PubMed](#)]
18. Park, Y.B.; Cosgrove, D.J. Xyloglucan and its interactions with other components of the growing cell wall. *Plant Cell Physiol.* **2015**, *56*, 180–194. [[CrossRef](#)] [[PubMed](#)]
19. Levesque-Tremblay, G.; Pelloux, J.; Braybrook, S.A.; Muller, K. Tuning of pectin methylesterification: Consequences for cell wall biomechanics and development. *Planta* **2015**, *242*, 791–811. [[CrossRef](#)] [[PubMed](#)]
20. Rancour, D.M.; Marita, J.M.; Hatfield, R.D. Cell wall composition throughout development for the model grass *Brachypodium distachyon*. *Front. Plant Sci.* **2012**, *3*, 266. [[CrossRef](#)] [[PubMed](#)]
21. Gibeault, D.M.; Pauly, M.; Bacic, A.; Fincher, G.B. Changes in cell wall polysaccharides in developing barley (*Hordeum vulgare*) coleoptiles. *Planta* **2005**, *221*, 729–738. [[CrossRef](#)] [[PubMed](#)]
22. Nunan, K.J.; Sims, I.M.; Bacic, A.; Robinson, S.P.; Fincher, G.B. Changes in cell wall composition during ripening of grape berries. *Plant Physiol.* **1998**, *118*, 783–792. [[CrossRef](#)] [[PubMed](#)]
23. Wood, J.A.; Tan, H.T.; Collins, H.M.; Yap, K.; Khor, S.; Lim, W.L.; Xing, X.; Bulone, V.; Burton, R.A.; Fincher, G.B.; et al. Genetic and environmental factors contribute to variation in cell wall composition in mature desi chickpea (*Cicer arietinum* L.) cotyledons. *Plant Cell Environ.* **2018**. [[CrossRef](#)] [[PubMed](#)]
24. Tan, L.; Eberhard, S.; Pattathil, S.; Warder, C.; Glushka, J.; Yuan, C.; Hao, Z.; Zhu, X.; Avci, U.; Miller, J.S.; et al. An *Arabidopsis* cell wall proteoglycan consists of pectin and arabinoxylan covalently linked to an arabinogalactan protein. *Plant Cell* **2013**, *25*, 270–287. [[CrossRef](#)] [[PubMed](#)]
25. Grabber, J.H.; Ralph, J.; Hatfield, R.D. Cross-linking of maize walls by ferulate dimerization and incorporation into lignin. *J. Agric. Food Chem.* **2000**, *48*, 6106–6113. [[CrossRef](#)] [[PubMed](#)]
26. Hrmova, M.; Farkas, V.; Lahnstein, J.; Fincher, G.B. A barley xyloglucan xyloglucosyl transferase covalently links xyloglucan, cellulosic substrates, and (1,3;1,4)- β -D-glucans. *J. Biol. Chem.* **2007**, *282*, 12951–12962. [[CrossRef](#)] [[PubMed](#)]
27. Cosgrove, D.J. Re-constructing our models of cellulose and primary cell wall assembly. *Curr. Opin. Plant Biol.* **2014**, *22*, 122–131. [[CrossRef](#)] [[PubMed](#)]
28. Jamet, E.; Canut, H.; Boudart, G.; Pont-Lezica, R.F. Cell wall proteins: A new insight through proteomics. *Trends*

- Plant Sci.* **2006**, *11*, 33–39. [[CrossRef](#)] [[PubMed](#)]
29. Aditya, J.; Lewis, J.; Shirley, N.J.; Tan, H.T.; Henderson, M.; Fincher, G.B.; Burton, R.A.; Mather, D.E.; Tucker, M.R. The dynamics of cereal cyst nematode infection differ between susceptible and resistant barley cultivars and lead to changes in (1,3;1,4)- β -glucan levels and *HvCslF* gene transcript abundance. *New Phytol.* **2015**, *207*, 135–147. [[CrossRef](#)] [[PubMed](#)]
 30. Lora, J.; Herrero, M.; Tucker, M.R.; Hormaza, J.I. The transition from somatic to germline identity shows conserved and specialized features during angiosperm evolution. *New Phytol.* **2017**, *216*, 495–509. [[CrossRef](#)] [[PubMed](#)]
 31. Coimbra, S.; Almeida, J.; Junqueira, V.; Costa, M.L.; Pereira, L.G. Arabinogalactan proteins as molecular markers in *Arabidopsis thaliana* sexual reproduction. *J. Exp. Bot.* **2007**, *58*, 4027–4035. [[CrossRef](#)] [[PubMed](#)]
 32. Yu, J.; Meng, Z.; Liang, W.; Behera, S.; Kudla, J.; Tucker, M.R.; Luo, Z.; Chen, M.; Xu, D.; Zhao, G.; et al. A rice Ca^{2+} binding protein is required for tapetum function and pollen formation. *Plant Physiol.* **2016**, *172*, 1772–1786. [[CrossRef](#)] [[PubMed](#)]
 33. Berger, F.; Taylor, A.; Brownlee, C. Cell fate determination by the cell wall in early *Fucus* development. *Science* **1994**, *263*, 1421–1423. [[CrossRef](#)] [[PubMed](#)]
 34. Fleming, A.J. The co-ordination of cell division, differentiation and morphogenesis in the shoot apical meristem: A perspective. *J. Exp. Bot.* **2006**, *57*, 25–32. [[CrossRef](#)] [[PubMed](#)]
 35. Torii, K.U. Stomatal differentiation: The beginning and the end. *Curr. Opin. Plant Biol.* **2015**, *28*, 16–22. [[CrossRef](#)] [[PubMed](#)]
 36. Benfey, P.N. Defining the path from stem cells to differentiated tissue. *Essays Dev. Biol. Part A* **2016**, *116*, 35–43.
 37. Vogler, H.; Felekis, D.; Nelson, B.J.; Grossniklaus, U. Measuring the mechanical properties of plant cell walls. *Plants* **2015**, *4*, 167–182. [[CrossRef](#)] [[PubMed](#)]
 38. Braybrook, S.A.; Jonsson, H. Shifting foundations: The mechanical cell wall and development. *Curr. Opin. Plant Biol.* **2016**, *29*, 115–120. [[CrossRef](#)] [[PubMed](#)]
 39. Cosgrove, D.J. Diffuse growth of plant cell walls. *Plant Physiol.* **2018**, *176*, 16–27. [[CrossRef](#)] [[PubMed](#)]
 40. Wolf, S.; Hematy, K.; Hofte, H. Growth control and cell wall signaling in plants. *Annu. Rev. Plant Biol.* **2012**, *63*, 381–407. [[CrossRef](#)] [[PubMed](#)]
 41. Franck, C.M.; Westermann, J.; Boisson-Dernier, A. Plant lectin-like receptor kinases: From cell wall integrity to immunity and beyond. *Annu. Rev. Plant Biol.* **2018**, *69*, 301–328. [[CrossRef](#)] [[PubMed](#)]
 42. Lombard, V.; Golaconda Ramulu, H.; Drula, E.; Coutinho, P.M.; Henrissat, B. The carbohydrate-active enzymes database (CAZy) in 2013. *Nucleic Acids Res.* **2014**, *42*, D490–D495. [[CrossRef](#)] [[PubMed](#)]
 43. Oikawa, A.; Lund, C.H.; Sakuragi, Y.; Scheller, H.V. Golgi-localized enzyme complexes for plant cell wall biosynthesis. *Trends Plant Sci.* **2013**, *18*, 49–58. [[CrossRef](#)] [[PubMed](#)]
 44. Gou, J.Y.; Miller, L.M.; Hou, G.C.; Yu, X.H.; Chen, X.Y.; Liu, C.J. Acetyltransferase-mediated deacetylation of pectin impairs cell elongation, pollen germination, and plant reproduction. *Plant Cell* **2012**, *24*, 50–65. [[CrossRef](#)] [[PubMed](#)]
 45. Bourquin, V.; Nishikubo, N.; Abe, H.; Brumer, H.; Denman, S.; Eklund, M.; Christiernin, M.; Teeri, T.T.; Sundberg, B.; Mellerowicz, E.J. Xyloglucan endotransglycosylases have a function during the formation of secondary cell walls of vascular tissues. *Plant Cell* **2002**, *14*, 3073–3088. [[CrossRef](#)] [[PubMed](#)]
 46. Kohorn, B.D.; Kobayashi, M.; Johansen, S.; Friedman, H.P.; Fischer, A.; Byers, N. Wall-associated kinase 1 (WAK1) is crosslinked in endomembranes, and transport to the cell surface requires correct cell-wall synthesis. *J. Cell Sci.* **2006**, *119*, 2282–2290. [[CrossRef](#)] [[PubMed](#)]
 47. Decreux, A.; Messiaen, J. Wall-associated kinase WAK1 interacts with cell wall pectins in a calcium-induced conformation. *Plant Cell Physiol.* **2005**, *46*, 268–278. [[CrossRef](#)] [[PubMed](#)]
 48. Wolf, S.; Greiner, S. Growth control by cell wall pectins. *Protoplasma* **2012**, *249* (Suppl. 2), S169–S175. [[CrossRef](#)] [[PubMed](#)]
 49. Sorieul, M.; Dickson, A.; Hill, S.J.; Pearson, H. Plant fibre: Molecular structure and biomechanical properties, of a complex living material, influencing its deconstruction towards a biobased composite. *Materials* **2016**, *9*, 618. [[CrossRef](#)] [[PubMed](#)]
 50. Griffiths, J.S.; Tsai, A.Y.; Xue, H.; Voiniciuc, C.; Sola, K.; Seifert, G.J.; Mansfield, S.D.; Haughn, G.W. SALT-OVERLY SENSITIVE5 mediates *Arabidopsis* seed coat mucilage adherence and organization through pectins. *Plant Physiol.* **2014**, *165*, 991–1004. [[CrossRef](#)] [[PubMed](#)]
 51. McCartney, L.; Steele-King, C.G.; Jordan, E.; Knox, J.P. Cell wall pectic (1→4)- β -D-galactan marks the acceleration of cell elongation in the *Arabidopsis* seedling root meristem. *Plant J.* **2003**, *33*, 447–454. [[CrossRef](#)] [[PubMed](#)]
 52. Harholt, J.; Suttangkakul, A.; Vibe Scheller, H. Biosynthesis of pectin. *Plant Physiol.* **2010**, *153*, 384–395. [[CrossRef](#)] [[PubMed](#)]
 53. Turbant, A.; Fournet, F.; Lequart, M.; Zabijak, L.; Pageau, K.; Bouton, S.; Van Wuytswinkel, O. Pme58 plays a role in pectin distribution during seed coat mucilage extrusion through homogalacturonan modification. *J. Exp. Bot.* **2016**, *67*, 2177–2190. [[CrossRef](#)] [[PubMed](#)]
 54. Jiang, L.; Yang, S.L.; Xie, L.F.; Puah, C.S.; Zhang, X.Q.; Yang, W.C.; Sundaresan, V.; Ye, D. Vanguard1 encodes a pectin methyltransferase that enhances pollen tube growth in the *Arabidopsis* style and transmitting tract. *Plant Cell* **2005**, *17*, 584–596. [[CrossRef](#)] [[PubMed](#)]

55. Etchells, J.P.; Moore, L.; Jiang, W.Z.; Prescott, H.; Capper, R.; Saunders, N.J.; Bhatt, A.M.; Dickinson, H.G. A role for *BELLRINGER* in cell wall development is supported by loss-of-function phenotypes. *BMC Plant Biol.* **2012**, *12*, 212. [[CrossRef](#)] [[PubMed](#)]
56. Peaucelle, A.; Braybrook, S.A.; Le Guillou, L.; Bron, E.; Kuhlemeier, C.; Hofte, H. Pectin-induced changes in cell wall mechanics underlie organ initiation in *Arabidopsis*. *Curr. Biol.* **2011**, *21*, 1720–1726. [[CrossRef](#)] [[PubMed](#)]
57. Xiong, J.; Yang, Y.; Fu, G.; Tao, L. Novel roles of hydrogen peroxide (H₂O₂) in regulating pectin synthesis and demethylesterification in the cell wall of rice (*Oryza sativa*) root tips. *New Phytol.* **2015**, *206*, 118–126. [[CrossRef](#)] [[PubMed](#)]
58. Lionetti, V.; Raiola, A.; Camardella, L.; Giovane, A.; Obel, N.; Pauly, M.; Favaron, F.; Cervone, F.; Bellincampi, D. Overexpression of pectin methylesterase inhibitors in *Arabidopsis* restricts fungal infection by *Botrytis cinerea*. *Plant Physiol.* **2007**, *143*, 1871–1880. [[CrossRef](#)] [[PubMed](#)]
59. Daum, G.; Medzihradzky, A.; Suzaki, T.; Lohmann, J.U. A mechanistic framework for noncell autonomous stem cell induction in *Arabidopsis*. *Proc. Natl. Acad. Sci. USA* **2014**, *111*, 14619–14624. [[CrossRef](#)] [[PubMed](#)]
60. Vaten, A.; Dettmer, J.; Wu, S.; Stierhof, Y.D.; Miyashima, S.; Yadav, S.R.; Roberts, C.J.; Campilho, A.; Bulone, V.; Lichtenberger, R.; et al. Callose biosynthesis regulates symplastic trafficking during root development. *Dev. Cell* **2011**, *21*, 1144–1155. [[CrossRef](#)] [[PubMed](#)]
61. Lucas, W.J.; Bouché-Pillon, S.; Jackson, D.P.; Nguyen, L.; Baker, L.; Ding, B.; Hake, S. Selective trafficking of KNOTTED1 homeodomain protein and its mRNA through plasmodesmata. *Science* **1995**, *270*, 1980–1983. [[CrossRef](#)] [[PubMed](#)]
62. Knauer, S.; Holt, A.L.; Rubio-Somoza, I.; Tucker, E.J.; Hinze, A.; Pisch, M.; Javelle, M.; Timmermans, M.C.; Tucker, M.R.; Laux, T. A protodermal miR394 signal defines a region of stem cell competence in the *Arabidopsis* shoot meristem. *Dev. Cell* **2013**, *24*, 125–132. [[CrossRef](#)] [[PubMed](#)]
63. Molnar, A.; Melnyk, C.; Baulcombe, D.C. Silencing signals in plants: A long journey for small rnas. *Genome Biol.* **2011**, *12*, 215. [[CrossRef](#)] [[PubMed](#)]
64. Taochy, C.; Gursansky, N.R.; Cao, J.; Fletcher, S.J.; Dressel, U.; Mitter, N.; Tucker, M.R.; Koltunow, A.M.G.; Bowman, J.L.; Vaucheret, H.; Carroll, B.J. A genetic screen for impaired systemic RNAi highlights the crucial role of *Dicer-like 2*. *Plant Physiol.* **2017**, *175*, 1424–1437. [[CrossRef](#)] [[PubMed](#)]
65. Kohorn, B.D.; Johansen, S.; Shishido, A.; Todorova, T.; Martinez, R.; Defeo, E.; Obregon, P. Pectin activation of MAP kinase and gene expression is WAK2 dependent. *Plant J.* **2009**, *60*, 974–982. [[CrossRef](#)] [[PubMed](#)]
66. Kohorn, B.D.; Kohorn, S.L.; Saba, N.J.; Martinez, V.M. Requirement for pectin methyl esterase and preference for fragmented over native pectins for wall-associated kinase-activated, EDS1/PAD4-dependent stress response in *Arabidopsis*. *J. Biol. Chem.* **2014**, *289*, 18978–18986. [[CrossRef](#)] [[PubMed](#)]
67. Saintenac, C.; Lee, W.S.; Cambon, F.; Rudd, J.J.; King, R.C.; Marande, W.; Powers, S.J.; Berges, H.; Phillips, A.L.; Uauy, C.; et al. Wheat receptor-kinase-like protein STB6 controls gene-for-gene resistance to fungal pathogen *Zymoseptoria tritici*. *Nat. Genet.* **2018**, *50*, 368–374. [[CrossRef](#)] [[PubMed](#)]
68. Zhang, N.; Zhang, B.; Zuo, W.; Xing, Y.; Konlasuk, S.; Tan, G.; Zhang, Q.; Ye, J.; Xu, M. Cytological and molecular characterization of *ZmWAK*-mediated head-smut resistance in maize. *Mol. Plant Microbe Interact.* **2017**, *30*, 455–465. [[CrossRef](#)] [[PubMed](#)]
69. Wagner, T.A.; Kohorn, B.D. Wall-associated kinases are expressed throughout plant development and are required for cell expansion. *Plant Cell* **2001**, *13*, 303–318. [[CrossRef](#)] [[PubMed](#)]
70. Schoenaers, S.; Balcerowicz, D.; Breen, G.; Hill, K.; Zdanio, M.; Mouille, G.; Holman, T.J.; Oh, J.; Wilson, M.H.; Nikonorova, N.; et al. The auxin-regulated CrRLK1L kinase *ERULUS* controls cell wall composition during root hair tip growth. *Curr. Biol.* **2018**, *28*, 722–732. [[CrossRef](#)] [[PubMed](#)]
71. Kessler, S.A.; Shimosato-Asano, H.; Keinath, N.F.; Wuest, S.E.; Ingram, G.; Panstruga, R.; Grossniklaus, U. Conserved molecular components for pollen tube reception and fungal invasion. *Science* **2010**, *330*, 968–971. [[CrossRef](#)] [[PubMed](#)]
72. Lin, W.; Tang, W.; Anderson, C.; Yang, Z. FERONIA's sensing of cell wall pectin activates ROP GTPase signaling in *Arabidopsis*. *bioRxiv* **2018**. [[CrossRef](#)]
73. Faria-Blanc, N.; Mortimer, J.C.; Dupree, P. A transcriptomic analysis of xylan mutants does not support the existence of a secondary cell wall integrity system in *Arabidopsis*. *Front. Plant Sci.* **2018**, *9*, 384. [[CrossRef](#)] [[PubMed](#)]
74. Ferrari, S.; Savatin, D.V.; Sicilia, F.; Gramegna, G.; Cervone, F.; Lorenzo, G.D. Oligogalacturonides: Plant damage-associated molecular patterns and regulators of growth and development. *Front. Plant Sci.* **2013**, *4*, 49. [[CrossRef](#)] [[PubMed](#)]
75. Branca, C.; Lorenzo, G.D.; Cervone, F. Competitive inhibition of the auxin-induced elongation by α -D-oligogalacturonides in pea stem segments. *Physiol. Plant.* **1988**, *72*, 499–504. [[CrossRef](#)]
76. Gramegna, G.; Modesti, V.; Savatin, D.V.; Sicilia, F.; Cervone, F.; De Lorenzo, G. GRP-3 and KAPP, encoding interactors of WAK1, negatively affect defense responses induced by oligogalacturonides and local response to wounding. *J. Exp. Bot.* **2016**, *67*, 1715–1729. [[CrossRef](#)] [[PubMed](#)]
77. Balasubramanian, V.; Vashisht, D.; Cletus, J.; Sakthivel, N. Plant β -1,3-glucanases: Their biological functions and transgenic expression against phytopathogenic fungi. *Biotechnol. Lett.* **2012**, *34*, 1983–1990. [[CrossRef](#)] [[PubMed](#)]

Appendix 1

78. van der Schoot, C.; Rinne, P.L.H. Dormancy cycling at the shoot apical meristem: Transitioning between self organization and self-arrest. *Plant Sci.* **2011**, *180*, 120–131. [[CrossRef](#)] [[PubMed](#)]
79. Seville, I.; Miyashima, S.; Helariutta, Y. Cell-to-cell communication via plasmodesmata in vascular plants. *Cell Adhes. Migr.* **2013**, *7*, 27–32. [[CrossRef](#)] [[PubMed](#)]
80. Kitagawa, M.; Jackson, D. Plasmodesmata-mediated cell-to-cell communication in the shoot apical meristem: How stem cells talk. *Plants* **2017**, *6*, 12. [[CrossRef](#)] [[PubMed](#)]
81. Amsbury, S.; Kirk, P.; Benitez-Alfonso, Y. Emerging models on the regulation of intercellular transport by plasmodesmata-associated callose. *J. Exp. Bot.* **2017**, *69*, 105–115. [[CrossRef](#)] [[PubMed](#)]
82. Benitez-Alfonso, Y.; Faulkner, C.; Pendle, A.; Miyashima, S.; Helariutta, Y.; Maule, A. Symplastic intercellular connectivity regulates lateral root patterning. *Dev. Cell* **2013**, *26*, 136–147. [[CrossRef](#)] [[PubMed](#)]
83. Faulkner, C.; Akman, O.E.; Bell, K.; Jeffree, C.; Oparka, K. Peeking into pit fields: A multiple twinning model of secondary plasmodesmata formation in tobacco. *Plant Cell* **2008**, *20*, 1504–1518. [[CrossRef](#)] [[PubMed](#)]
84. Fernandez-Calvino, L.; Faulkner, C.; Walshaw, J.; Saalbach, G.; Bayer, E.; Benitez-Alfonso, Y.; Maule, A. *Arabidopsis* plasmodesmal proteome. *PLoS ONE* **2011**, *6*, e18880. [[CrossRef](#)] [[PubMed](#)]
85. Knox, J.P.; Benitez-Alfonso, Y. Roles and regulation of plant cell walls surrounding plasmodesmata. *Curr. Opin. Plant Biol.* **2014**, *22*, 93–100. [[CrossRef](#)] [[PubMed](#)]
86. Stabolone, L.; Lionetti, V. Extracellular matrix in plants and animals: Hooks and locks for viruses. *Front. Microbiol.* **2017**, *8*, 1760. [[CrossRef](#)] [[PubMed](#)]
87. Doxey, A.C.; Yaish, M.W.; Moffatt, B.A.; Griffith, M.; McConkey, B.J. Functional divergence in the *Arabidopsis* β -1,3-glucanase gene family inferred by phylogenetic reconstruction of expression states. *Mol. Biol. Evol.* **2007**, *24*, 1045–1055. [[CrossRef](#)] [[PubMed](#)]
88. Maule, A.; Faulkner, C.; Benitez-Alfonso, Y. Plasmodesmata “in comunicado”. *Front. Plant Sci.* **2012**, *3*, 30. [[CrossRef](#)] [[PubMed](#)]
89. Bell, P.R. Megaspore abortion: A consequence of selective apoptosis. *Int. J. Plant Sci.* **1996**, *157*, 1–7. [[CrossRef](#)]
90. Buccigaglia, P.A.; Zimmermann, E.; Smith, A.G. Functional analysis of a β -1,3-glucanase gene (*Tag1*) with anther-specific RNA and protein accumulation using antisense RNA inhibition. *J. Plant Physiol.* **2003**, *160*, 1367–1373. [[CrossRef](#)] [[PubMed](#)]
91. Tucker, M.R.; Koltunow, A.M. Traffic monitors at the cell periphery: The role of cell walls during early female reproductive cell differentiation in plants. *Curr. Opin. Plant Biol.* **2014**, *17*, 137–145. [[CrossRef](#)] [[PubMed](#)]
92. Gisel, A.; Barella, S.; Hempel, F.D.; Zambryski, P.C. Temporal and spatial regulation of symplastic trafficking during development in *Arabidopsis thaliana* apices. *Development* **1999**, *126*, 1879–1889. [[PubMed](#)]
93. Kim, I.; Kobayashi, K.; Cho, E.; Zambryski, P.C. Subdomains for transport via plasmodesmata corresponding to the apical-basal axis are established during *Arabidopsis* embryogenesis. *Proc. Natl. Acad. Sci. USA* **2005**, *102*, 11945–11950. [[CrossRef](#)] [[PubMed](#)]
94. Melida, H.; Sopena-Torres, S.; Bacete, L.; Garrido-Arandia, M.; Jorda, L.; Lopez, G.; Munoz-Barrios, A.; Pacios, L.F.; Molina, A. Non-branched β -1,3-glucan oligosaccharides trigger immune responses in *Arabidopsis*. *Plant J.* **2018**, *93*, 34–49. [[CrossRef](#)] [[PubMed](#)]
95. Burton, R.A.; Fincher, G.B. (1, 3;1, 4)- β -D-glucans in cell walls of the *Poaceae*, lower plants, and fungi: A tale of two linkages. *Mol. Plant* **2009**, *2*, 873–882. [[CrossRef](#)] [[PubMed](#)]
96. Little, A.; Schwerdt, J.G.; Shirley, N.J.; Khor, S.-F.; Neumann, K.; O’Donovan, L.A.; Lahnstein, J.; Collins, H.C.; Henderson, M.; Fincher, G.B.; et al. Revised phylogeny of the cellulose synthase gene superfamily: New insights into cell wall evolution. *Plant Physiol.* **2018**. [[CrossRef](#)] [[PubMed](#)]
97. Burton, R.A.; Collins, H.M.; Kibble, N.A.; Smith, J.A.; Shirley, N.J.; Jobling, S.A.; Henderson, M.; Singh, R.R.; Pettolino, F.; Wilson, S.M.; et al. Over-expression of specific *HvCslF* cellulose synthase-like genes in transgenic barley increases the levels of cell wall (1, 3;1, 4)- β -D-glucans and alters their fine structure. *Plant Biotechnol. J.* **2011**, *9*, 117–135. [[CrossRef](#)] [[PubMed](#)]
98. Nemeth, C.; Freeman, J.; Jones, H.D.; Sparks, C.; Pellny, T.K.; Wilkinson, M.D.; Dunwell, J.; Andersson, A.A.M.; Aman, P.; Guillon, F.; et al. Down-regulation of the *CslF6* gene results in decreased (1,3;1,4)- β -D-glucan in endosperm of wheat. *Plant Physiol.* **2010**, *152*, 1209–1218. [[CrossRef](#)] [[PubMed](#)]
99. Vega-Sanchez, M.E.; Verherbruggen, Y.; Christensen, U.; Chen, X.W.; Sharma, V.; Varanasi, P.; Jobling, S.A.; Talbot, M.; White, R.G.; Joo, M.; et al. Loss of cellulose synthase-like f6 function affects mixed-linkage glucan deposition, cell wall mechanical properties, and defense responses in vegetative tissues of rice. *Plant Physiol.* **2012**, *159*, 56–69. [[CrossRef](#)] [[PubMed](#)]
100. Taketa, S.; Yuo, T.; Tonooka, T.; Tsumuraya, Y.; Inagaki, Y.; Haruyama, N.; Larroque, O.; Jobling, S.A. Functional characterization of barley betaglucanless mutants demonstrates a unique role for *CslF6* in (1,3;1,4)- β -D-glucan biosynthesis. *J. Exp. Bot.* **2012**, *63*, 381–392. [[CrossRef](#)] [[PubMed](#)]
101. Burton, R.A.; Jobling, S.A.; Harvey, A.J.; Shirley, N.J.; Mather, D.E.; Bacic, A.; Fincher, G.B. The genetics and transcriptional profiles of the cellulose synthase-like *HvCslF* gene family in barley. *Plant Physiol.* **2008**, *146*, 1821–1833. [[CrossRef](#)] [[PubMed](#)]
102. Zabolina, O. Xyloglucan and its biosynthesis. *Front. Plant Sci.* **2012**, *3*, 134. [[CrossRef](#)] [[PubMed](#)]
103. Zabolina, O.A.; Avci, U.; Cavalier, D.; Pattathil, S.; Chou, Y.H.; Eberhard, S.; Danhof, L.; Keegstra, K.; Hahn, M.G. Mutations in multiple *XXT* genes of *Arabidopsis* reveal the complexity of xyloglucan biosynthesis. *Plant Physiol.* **2012**,

- 159, 1367–1384. [[CrossRef](#)] [[PubMed](#)]
104. Kong, Y.; Pena, M.J.; Renna, L.; Avci, U.; Pattathil, S.; Tuomivaara, S.T.; Li, X.; Reiter, W.D.; Brandizzi, F.; Hahn, M.G.; et al. Galactose-depleted xyloglucan is dysfunctional and leads to dwarfism in *Arabidopsis*. *Plant Physiol.* **2015**, *167*, 1296–1306. [[CrossRef](#)] [[PubMed](#)]
 105. Schröder, R.; Atkinson, R.G.; Redgwell, R.J. Re-interpreting the role of endo- β -mannanases as mannan endotransglycosylase/hydrolases in the plant cell wall. *Ann. Bot.* **2009**, *104*, 197–204. [[CrossRef](#)] [[PubMed](#)]
 106. Goubet, F.; Barton, C.J.; Mortimer, J.C.; Yu, X.; Zhang, Z.; Miles, G.P.; Richens, J.; Liepman, A.H.; Seffen, K.; Dupree, P. Cell wall glucomannan in *Arabidopsis* is synthesised by *Csla* glycosyltransferases, and influences the progression of embryogenesis. *Plant J.* **2009**, *60*, 527–538. [[CrossRef](#)] [[PubMed](#)]
 107. Rodriguez-Gacio Mdel, C.; Iglesias-Fernandez, R.; Carbonero, P.; Matilla, A.J. Softening-up mannan-rich cell walls. *J. Exp. Bot.* **2012**, *63*, 3976–3988. [[CrossRef](#)] [[PubMed](#)]
 108. Ueda, M.; Zhang, Z.; Laux, T. Transcriptional activation of *Arabidopsis* axis patterning genes *WOX8/9* links zygote polarity to embryo development. *Dev. Cell* **2011**, *20*, 264–270. [[CrossRef](#)] [[PubMed](#)]
 109. Mallory, A.C.; Hinze, A.; Tucker, M.R.; Bouche, N.; Gascioli, V.; Elmayan, T.; Lauressegues, D.; Jauvion, V.; Vaucheret, H.; Laux, T. Redundant and specific roles of the ARGONAUTEe proteins AGO1 and ZLL in development and small RNA-directed gene silencing. *PLoS Genet.* **2009**, *5*, e1000646. [[CrossRef](#)] [[PubMed](#)]
 110. Bohmert, K.; Camus, I.; Bellini, C.; Bouchez, D.; Caboche, M.; Benning, C. *AGO1* defines a novel locus of *Arabidopsis* controlling leaf development. *EMBO J.* **1998**, *17*, 170–180. [[CrossRef](#)] [[PubMed](#)]
 111. Schröder, R.; Wegrzyn, T.F.; Sharma, N.N.; Atkinson, R.G. LeMAN4 endo- β -mannanase from ripe tomato fruit can act as a mannan transglycosylase or hydrolase. *Planta* **2006**, *224*, 1091–1102. [[CrossRef](#)] [[PubMed](#)]
 112. Han, Y.; Ban, Q.; Hou, Y.; Meng, K.; Suo, J.; Rao, J. Isolation and characterization of two persimmon xyloglucan endotransglycosylase/hydrolase (*XTH*) genes that have divergent functions in cell wall modification and fruit postharvest softening. *Front. Plant Sci.* **2016**, *7*, 624. [[CrossRef](#)] [[PubMed](#)]
 113. Muñoz-Bertomeu, J.; Miedes, E.; Lorences, E.P. Expression of xyloglucan endotransglycosylase/hydrolase (*XTH*) genes and XET activity in ethylene treated apple and tomato fruits. *J. Plant Physiol.* **2013**, *170*, 1194–1201. [[CrossRef](#)] [[PubMed](#)]
 114. Knox, J.P. The use of antibodies to study the architecture and developmental regulation of plant cell walls. *Int. Rev. Cytol.* **1997**, *171*, 79–120. [[PubMed](#)]
 115. Pedersen, H.L.; Fangel, J.U.; McCleary, B.; Ruzanski, C.; Rydahl, M.G.; Ralet, M.C.; Farkas, V.; von Schantz, L.; Marcus, S.E.; Andersen, M.C.; et al. Versatile high resolution oligosaccharide microarrays for plant glycobiology and cell wall research. *J. Biol. Chem.* **2012**, *287*, 39429–39438. [[CrossRef](#)] [[PubMed](#)]
 116. Gierlinger, N. New insights into plant cell walls by vibrational microspectroscopy. *Appl. Spectrosc. Rev.* **2017**. [[CrossRef](#)]
 117. Birnbaum, K.; Shasha, D.E.; Wang, J.Y.; Jung, J.W.; Lambert, G.M.; Galbraith, D.W.; Benfey, P.N. A gene expression map of the *Arabidopsis* root. *Science* **2003**, *302*, 1956–1960. [[CrossRef](#)] [[PubMed](#)]
 118. Brady, S.M.; Orlando, D.A.; Lee, J.-Y.; Wang, J.Y.; Koch, J.; Dinnyen, J.R.; Mace, D.; Ohler, U.; Benfey, P.N. A high-resolution root spatiotemporal map reveals dominant expression patterns. *Science* **2007**, *318*, 801–806. [[CrossRef](#)] [[PubMed](#)]
 119. Yadav, R.K.; Girke, T.; Pasala, S.; Xie, M.; Reddy, G.V. Gene expression map of the *Arabidopsis* shoot apical meristem stem cell niche. *Proc. Natl. Acad. Sci. USA* **2009**, *106*, 4941–4946. [[CrossRef](#)] [[PubMed](#)]
 120. Tucker, M.R.; Laux, T. Connecting the paths in plant stem cell regulation. *Trends Cell Biol.* **2007**, *17*, 403–410. [[CrossRef](#)] [[PubMed](#)]
 121. Nguema-Ona, E.; Coimbra, S.; Vire-Gibouin, M.; Mollet, J.C.; Driouich, A. Arabinogalactan proteins in root and pollen-tube cells: Distribution and functional aspects. *Ann. Bot.* **2012**, *110*, 383–404. [[CrossRef](#)] [[PubMed](#)]
 122. Lee, K.J.; Sakata, Y.; Mau, S.L.; Pettolino, F.; Bacic, A.; Quatrano, R.S.; Knight, C.D.; Knox, J.P. Arabinogalactan proteins are required for apical cell extension in the moss *Physcomitrella patens*. *Plant Cell* **2005**, *17*, 3051–3065. [[CrossRef](#)] [[PubMed](#)]
 123. Somssich, M.; Khan, G.A.; Persson, S. Cell wall heterogeneity in root development of *Arabidopsis*. *Front. Plant Sci.* **2016**, *7*, 1242. [[CrossRef](#)] [[PubMed](#)]
 124. Yang, W.; Schuster, C.; Beahan, C.T.; Charoensawan, V.; Peaucelle, A.; Bacic, A.; Doblin, M.S.; Wightman, R.; Meyerowitz, E.M. Regulation of meristem morphogenesis by cell wall synthases in *Arabidopsis*. *Curr. Biol.* **2016**, *26*, 1404–1415. [[CrossRef](#)] [[PubMed](#)]
 125. Tucker, M.R.; Ma, C.; Phan, J.; Neumann, K.; Shirley, N.J.; Hahn, M.G.; Cozzolino, D.; Burton, R.A. Dissecting the genetic basis for seed coat mucilage heteroxylan biosynthesis in *Plantago ovata* using gamma irradiation and infrared spectroscopy. *Front. Plant Sci.* **2017**, *8*, 326. [[CrossRef](#)] [[PubMed](#)]
 126. Phan, J.L.; Tucker, M.R.; Khor, S.F.; Shirley, N.; Lahnstein, J.; Beahan, C.; Bacic, A.; Burton, R.A. Differences in glycosyltransferase family 61 accompany variation in seed coat mucilage composition in *Plantago* spp. *J. Exp. Bot.* **2016**, *67*, 6481–6495. [[CrossRef](#)] [[PubMed](#)]
 127. Derba-Maceluch, M.; Awano, T.; Takahashi, J.; Lucenius, J.; Ratke, C.; Kontro, I.; Busse-Wicher, M.; Kosik, O.; Tanaka, R.; Winzél, A.; et al. Suppression of xylan endotransglycosylase *PtxtXyn10A* affects cellulose microfibril angle in

Appendix 1

secondary wall in aspen wood. *New Phytol.* **2015**, *205*, 666–681. [[CrossRef](#)] [[PubMed](#)]



© 2018 by the authors. Licensee MDPI, Basel, Switzerland. This article is an open access article distributed under the terms and conditions of the Creative Commons Attribution (CC BY) license (<http://creativecommons.org/licenses/by/4.0/>)

Appendix 2

Candidature Milestones



Date	Milestone
December 2015	Offered and Accepted a Beacon of Enlightenment PhD Scholarship - University of Nottingham Joint Award Admitted into PhD program at The University of Adelaide
February 2016	Started PhD
August 2016	Completed the “Core Component of the Structured Program”
September 2016	Volunteered with the School of Agriculture, Food and Wine at the Royal Adelaide Show
October 2016	Poster presentation at the ARC Centre of Excellence in Plant Cell Walls Centre Retreat. Adelaide, Australia
November 2016	Poster presentation at the 6 th Australia and New Zealand Society for Cell and Developmental Biology (ANZSCDB) Adelaide Meeting. Adelaide, Australia
February 2017	Completed the “Major Review of Progress for Doctoral Programs”
January 2017	Presentation at the ARC Centre of Excellence in Plant Cell Walls Centre Meeting. Melbourne, Australia
August 2017	Presentation at the ARC Centre of Excellence in Plant Cell Walls Centre Meeting. Brisbane, Australia
September 2017	Travel to Nottingham, UK starting the exchange program. Working at Sutton Bonington Campus, University of Nottingham, UK Attending UK multiscale biology summer school at University of Nottingham, University Park
April 2018	Poster presentation at the post graduate symposium at University of Nottingham, UK
June 2018	Poster presentation at 2 nd barley mutant workshop, University of Dundee, James Hutton Institute, Dundee, UK
October 2018	Presentation at the University of Nottingham-University of Adelaide-Joint PhD Workshop - UNMC, KL, Malaysia
November 2018	Completed the “Pre-Submission Review”
April 2019	Poster presentation at the RMS Botanical Microscopy meeting 2019, Oxford, UK Complete research at University of Nottingham, travel back to Adelaide, Australia.
September 2019	Presentation at the 12th Annual Postgraduate Symposium in the School of Agriculture, Food and Wine. Awarded the ARC Centre of Excellence in Plant Energy Biology prize for Best Presentation in Plant Cell Physiology
November 2019	Poster presentation at the Australian Society of Plant Scientists Conference, ASPS 2019, University of La Trobe, Australia
February 2020	Poster presentation at the Symposium Down Under: Mechanisms Controlling Plant Reproduction, University of Adelaide, Australia
February 2020	Submitted “Notification of Intention to Submit” to Adelaide

	Graduate Centre
February 2020	Submitted thesis to Adelaide Graduate Centre and University of Nottingham Graduate Centre
June 2020	Complete viva and thesis defence with examiners
July 2020	Thesis accepted and doctorate conferred